Comparative transcriptomic and proteomic investigation of host cell responses during *Toxoplasma gondii* and *Neospora caninum* invasion of human astrocytes

Thesis submitted in accordance with the requirements of the University of Liverpool for the degree of Doctor in Philosophy

by Sarah A Altwaim

October 2014

Acknowledgements

First, I would like to thank my supervisor, Professor Jonathan Wastling for all his constant guidance, advice and expertise throughout my PhD. I would also like to extend my thanks to the great post-doctoral researchers in Infection Biology; Dong Xia, Nadine Randle, Stuart Armstrong and Emma, who have taught me many techniques and have encouraged and supported me all the way through my thesis.

To the postgraduate students who I shared most of my journey (past and present); Corrado, Jenna Kit, Poomie, Mariwan, Sarah J, Kat, Achchuthan and everyone in Infection Biology (IC2 building), I thank you all for making my study an enjoyable experience.

I would also like to thank Dr. Glenn McConkey and Isra Alssady from the University of Leeds, in which one of the experiments in this thesis was done in collaboration with them, Professor Andrew Hemphill who has also generously provided us with the antibodies needed for one of the experiments. Also, thank you Gosia Wnek from the Brain Infection; for your advice on astrocyte culturing.

Special thanks to my parents, brother and sisters; Words cannot express how grateful I am to them. They have always been there for me in the good times and the bad times, thank you for all your blessings and prayers for me.

Finally last but not least, to my beloved husband Saleh for all the sacrifices you've made on my behalf; you have provided me with unending support, care and was always there for me. Not to forget my two sweethearts; Norah and Majed (my children), for your care, love and patience during my stressful days. I would like to apologize for all the days and events that I have not been able to be there for you and hope to make it up to you both in the future.

Abstract

Toxoplasma gondii and *Neospora caninum* are intracellular protozoan parasites from the phylum *Apicomplexa*. Both parasites share many morphological and genetic features, but have diverse host preferences. While *T. gondii* can infect any warm-blooded animal including humans, *N. caninum* does not. The basis of host preference in these two parasites is unknown, but could be due to differences in tropism to specific host cells. The discovery of differences between host cell responses could lead to a better understanding to why *T. gondii* can lead to disease in humans and *N. caninum* cannot, specifically related to infection of the CNS.

To investigate the differences in host cell response, the differential expression patterns of host-cell transcripts and proteins as well as protein secretions and dopamine level during the invasion of human astrocyte (HA) cells by both *Toxoplasma* and *Neospora* were investigated. Proteomic investigations were achieved by global proteomic profiling of human astrocytes during infection using two dimensional difference gel electrophoresis (2D-DIGE) and a quantitative label-free approach. Transcriptomic investigation of infected human astrocytes was carried out using an RNA-Seq approach.

A number of differences in host cell response genes/proteins were noted between *Toxoplasma* and *Neospora* infection. Transcriptome analysis revealed differential expression of host cells transcripts associated with cell adhesion and cytokine receptor interaction pathways. Differences were observed in cell adhesion molecules (such as VCAM1 and NCAM2) and chemokines (such as CCL2), which were up-regulated in *T. gondii* infected cells compared to *N. caninum* infection. Whereas up-regulation of neutrophil activation was identified in *N. caninum* infected cells compared to *T. gondii* infection. Host cell secretome analysis during infection identified significant changes in many secreted proteins such as cytokines chemokines and cell adhesion molecules (i.e. CXCL1, CXCL2, IL8 and ICAM1). This data suggested that the two parasites stimulate different host cell responses. Dopamine acts as a neurotransmitter in the brain and the induction of dopamine has been found to provoke behavioural changes in the host during infection by *T.*

gondii. Dopamine levels were measured in dopaminergic PC-12 cells during infection by *T. gondii* and *N. caninum* through tachyzoite conversion to the bradyzoite stage. Increased levels in dopamine production was observed in dopaminergic cells infected with *T. gondii*, compared to no changes in cells infected with *N. caninum*. This result suggested that *T. gondii* modifies the host's behaviour (rodents), whereas the successful vertical transmission of *N. caninum* in cattle has led the parasite to not need to alter changes in the host' brain.

Overall, differences were mostly observed in molecules associated with cell adhesion and cytokine receptor signalling pathway, which may suggest why *T. gondii* is more successful in host cell infection of the CNS compared to *N. caninum*. Dopamine measurements of host cells during infection has also confirmed that *T. gondii* induces significant production of dopamine in infected host cells compared to *N. caninum* infection, suggesting different modulation of the host cell between the parasites in the CNS.

Table of Contents

List of figures

List of Tables

List of abbreviations

° C	Degrees centigrade
1-DE	One-dimensional electrophoresis
2D-DIGE	Two dimensional difference in gel electrophoresis
2-DE	Two-dimensional electrophoresis
APS	Ammonium persulphate
BBB	Blood brain barrier
Bp	Base pairs
BSA	Bovine serum albumin
cDNA	Complementary DNA
CNS	Central nervous system
ddH_2O	Milli-Q grade water, resistivity 18.2 Ω.cm
DMEM-F12	Dulbecco's Modified Eagle Medium: Nutrient Mixture F-12
DPBS	Dulbecco's phosphate buffer saline
DTT	Dithiothreitol
EtOH	Ethanol
FPKM	Fragments per kilobase of exon per million fragments mapped
HA	Human astrocytes
HPLC	High performance liquid chromatography
IAA	Iodoacetemide
IL	Interleukin
IMDM	Iscove's-modified Dulbecco's medium
kDa	Kilo Dalton
LC-MS/MS	Liquid Chromatography - Tandem Mass Spectrometry

m/z	Mass-to-charge ratio
mM	Millimolar
mRNA	Messenger RNA
MS	Mass spectrometry
Nc	*Neospora caninum*
NcBAG1	*Neospora caninum* bradyzoite antigen 1
p.i.	Post infection
PAGE	Polyacrylamide gel electrophoresis
PBS	Phosphate buffer saline
Poly(A) RNA	Polyadenylated RNA
PV	Parasitophorous vacuole
PVM	Parasitophorous vacuole membrane
RNA	Ribonucleic acid
RNA-Seq	RNA sequencing
RP	Reverse phase
SDS	Sodium dodecyl sulphate
TE	Toxoplasmic encephalitis
TEMED	Tetramethylethylenediamine
TFA	Trifluoroacetic acid
Tg	*Toxoplasma gondii*
V	Voltage

1 Chapter one: Introduction

1.1 *Toxoplasma gondii* and *Neospora caninum*

Toxoplasma gondii and *Neospora caninum* are intracellular protozoan parasites of wide clinical and veterinary importance. They are members of the phylum Apicomplexa, class Sporozoa and subclass Coccidia. Other members of the Apicomplexa include *Plasmodium*, *Cryptosporidium*, *Theileria* and *Eimeria*. It was only in 1984 that *N. caninum* was distinguished from *T. gondii* as a separate species (Bjerkas et al. 1984), and later described and characterised by Dubey *et al.* in 1988. The parasite was identified in Norwegian dogs causing severe encephalomyelitis and had no antibodies to *T. gondii* (Bjerkas et al. 1984). The two parasites were distinguished based on three main differences. First was the clinical outcome of the disease where *N. caninum* causes paralysis especially in the hind limbs in dogs was not detected in *T. gondii* infected species. Differences in the tissue cysts were also distinct between the two parasites and antibodies of *T. gondii* were absent in the infected dogs (Dubey et al. 2002).

These two parasites are closely related and share many genetic, physiological and morphological similarities (Dubey 2009). Yet, there have been differences detected between *T. gondii* and *N. caninum* that resulted in their placement in separate genera (DeBarry & Kissinger 2011; Dubey et al. 1988a). The definitive host of *T. gondii* is the cat (felidae family) and in *N. caninum* is the dog (canidae family). While *T. gondii* can infect any warm blooded host including humans (Montoya & Liesenfeld 2004), *N. caninum* has not been found to be zoonotic and has a more restricted host range (Dubey et al. 2007), although it can infect human cells *in vitro*. Toxoplasmosis is a cosmopolitan disease of humans and animals (Dubey & Schares 2011); it is estimated that nearly one third of the world's population is infected with *T. gondii* (Montoya & Liesenfeld 2004). *N. caninum* is the causative agent of the Neosporosis; a disease mainly of cattle and dogs. It infects a more restricted range of animals as intermediate hosts, but mostly has a major impact as a pathogen of cattle causing abortions (Lindsay et al. 1999; McAllister et al. 1998). Whereas *T.*

gondii is the only known species in *Toxoplasma*; there are two known species in *Neospora*; *N. caninum* and *N. hughesi* (Hemphill & Gottstein 2000).

1.2 Life cycle of *T. gondii* and *N. caninum*

Both *T. gondii* and *N. caninum* have similar life cycles (Figure 1.1) but they differ in the definitive and intermediate hosts they can infect. They have complex life cycles which include a sexual cycle occurring in the definitive host and an asexual cycle in the intermediate host (Lindsay, Dubey & Duncan 1999; McAllister et al. 1998). Vertical transmission is of high importance in *N. caninum* infection, in which the disease is transmitted to the foetus via the placenta that can result from a newly acquired exogenous infection or reactivation of an endogenous infection (Trees & Williams 2005). Whereas in *T. gondii* infections; transmission mainly occurs through the horizontal route.

Three main parasitic stages are involved; tachyzoites, bradyzoites (tissue cysts) and the oocysts. The definitive host, which is the cat in *T. gondii* and dog in *N. caninum*, is infected through digestion of contaminated food or water, or from transplacental transmission of tachyzoites to developing foetuses (Barber & Trees 1998; Dubey et al. 1988b). The parasites are then liberated and the sexual stage occurs in the gut epithelium. When intermediate hosts ingest contaminated substances with oocysts, sporozoites are released from the oocysts and differentiate into tachyzoites, which spread through the circulatory system to different tissues and organs (Montoya & Liesenfeld 2004; Gibney et al. 2008; Williams et al. 2009). Tachyzoites multiply in parasitophorous vacuoles (PV) asexually in intermediate hosts through a process called endodyogeny, in which two progeny form within the parent parasite (Goldman, Carver & Sulzer 1958; Sheffield & Melton 1968). Unsporulated oocysts are excreted in the faeces of the definitive host and sporulate in the surrounding environment (Dubey et al. 2007). In the latent stage (chronic form) of infection, tachyzoites are converted into the cyst forming bradyzoite stages which are mostly localised in muscles and the central nervous system (CNS) (Nath & Sinai 2003).

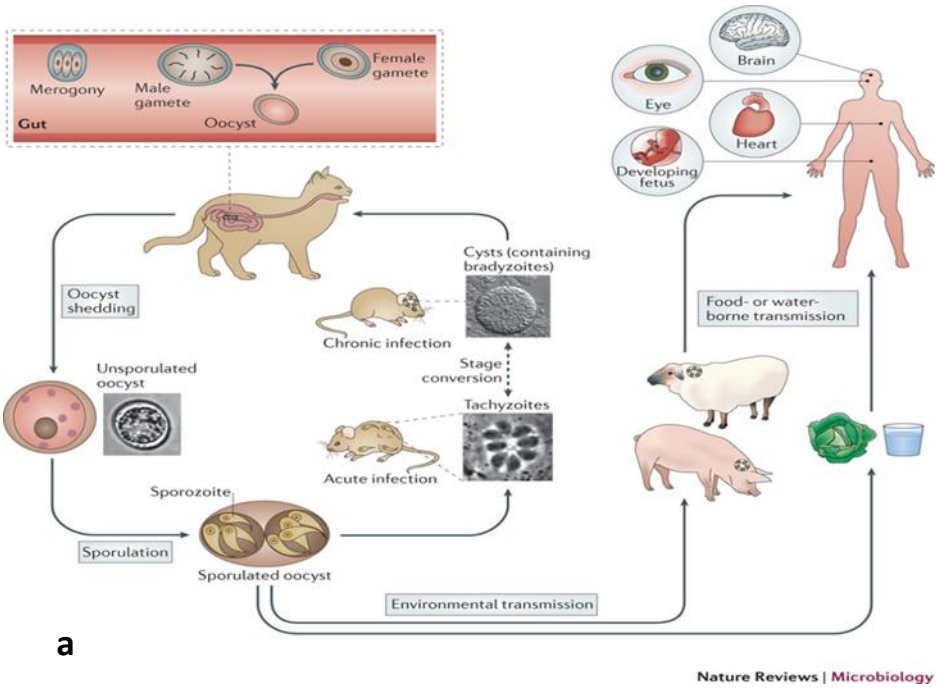

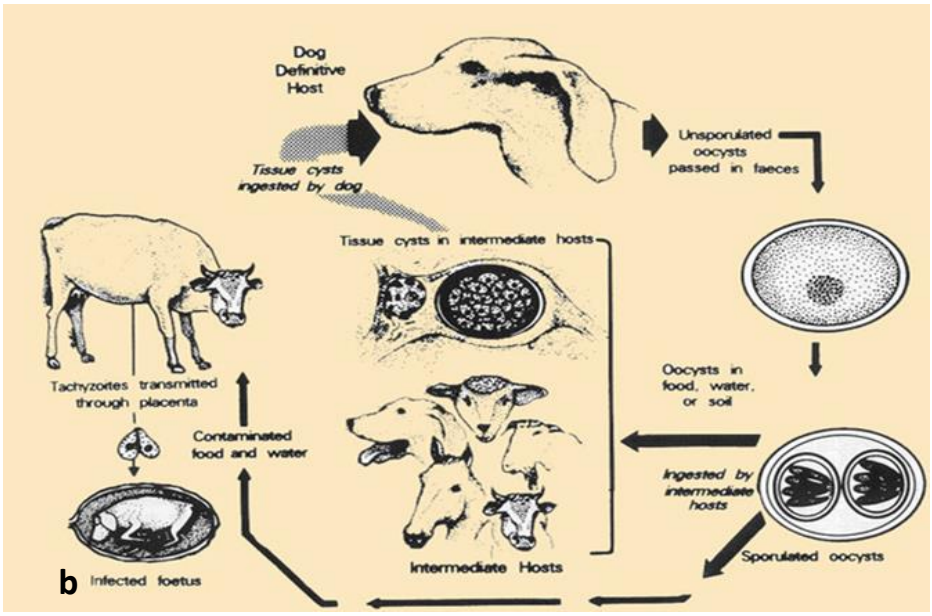

Figure 1.1: Life cycles of a) *T. gondii* and b) *N. caninum*. An oocyst, after being shed by the definitive host, sporulates and is ingested by an intermediate host; where sporozoites then invade cells lining the gut and form tachyzoites which then migrate to tissues. Infection transmission can then occur horizontally by a definitive host ingesting infected tissue and the cycle proceeding through the sexual stages, or vertically through the placenta of intermediate hosts. Tachyzoites can convert to tissue cysts and encyst in tissue such as the brain and muscles in *T. gondii* and *N. caninum* infections. Images taken from a) Hunter & Sibley 2012, and b) Dubey et al. 2007.

1.2.1 Tachyzoite stage of *T. gondii* and *N. caninum*

The tachyzoite is a motile fast multiplying form of the parasite; involved in the establishment of the acute stage of infection. Tachyzoites replicate every 6 to 8 hours within host cells in the parasitophorous vacuole (PV). Tachyzoites in *T. gondii* and *N. caninum* have similar structures; they are crescent shaped with a pointed anterior end and a rounded posterior end (Figure 1.2). Their sizes are usually 2 x 6 µm in *T. gondii* and slightly larger in *N. caninum* at 7.5 x 2 µm and contain numerous organelles. They contain a unique cytoskeleton (subpellicular microtubules, conoid, inner membrane complex), secretory organelles (rhoptries, micronemes, dense granules), mitochondrion, apicoplast, eukaryotic, nucleus, endoplasmic reticulum, Golgi apparatus and ribosomes, all surrounded by a complex membrane structure called the pellicle (Gustafson, Agar & Cramer 1954; Ferguson & Dubremetz 2007). They are able to invade host cells by penetrating the host cell membrane using their secretory organelles.

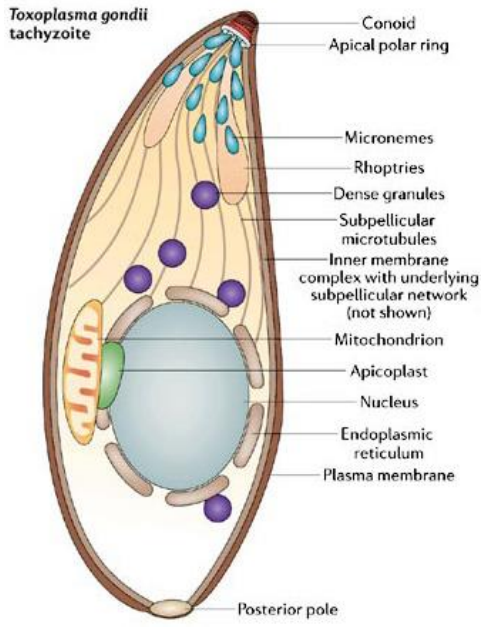

Figure 1.2: Diagram of a *T. gondii* tachyzoite, which also represents the same diagram in *N. caninum* tachyzoite. Organelles are as labelled (image taken from Baum et al. 2006).

1.2.2 Bradyzoite stage

Bradyzoites are intracellular, slow replicating, quiescent form of the parasites and are an indication of the chronic stage of the disease. Morphological features of this stage include the presence of a thick wall surrounding the cyst (Figure 1.3) containing parasite glycoproteins that may be associated with protection of the parasite from the host's immune defence (Zhang et al. 2001). When comparing bradyzoite with tachyzoite stage; bradyzoites are more slender, the nucleus is located more towards the posterior end of the parasite and bradyzoite replication does not cause the rupture of host cells (Dubey & Lindsay 2006; Zhang et al. 2001). In the CNS, *in vivo* studies demonstrated that *T. gondii* encysts in neurons and astrocytes (Ferguson & Hutchison 1987; Fischer et al. 1997). These cysts do not induce host inflammatory reactions and may persist throughout the host's life span (Hill & Dubey 2002). Tissue cysts of *T. gondii* are usually spherical shaped surrounded by elastic walls (0.5 um), the size of bradyzoites can reach up to 100 µm containing hundreds of parasites. In *N. caninum*, tissue cysts are round or oval shaped and can reach up to 107 µm in size, cyst walls thickness can reach up to 4 µm and contain fewer bradyzoites (Dubey et al. 1998).

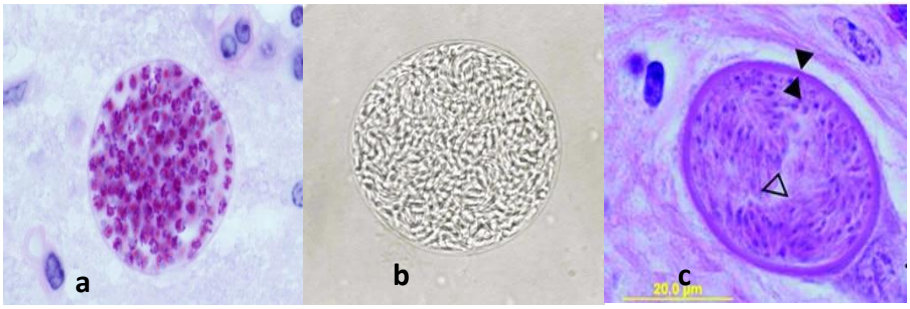

Figure 1.3: Bradyzoite cyst stage in host cells infected with *T. gondii* or *N. caninum*; a) *T. gondii* bradyzoite thin cyst wall stained with haematoxylin & eosin, b) *T. gondii* bradyzoite enclosing hundreds of bradyzoites (unstained), c) A thick walled (black arrow) *N. caninum* tissue cyst stained with haematoxylin & eosin, (taken from Dubey et al. 2007).

1.3 Secretory organelles of *T. gondii* and *N. caninum*

All members of the Apicomplexa comprise an apical complex in one or more stages of the life cycle, a collection of organelles involved in host-cell invasion process (Dubremetz et al. 1998). The organelles of the apical complex in both *T. gondii* and *N. caninum* include rhoptries, micronemes and dense granules. Rhoptries are secretory organelles essential in host cell invasion in *T. gondii* and *N. caninum* and are associated with virulence in *T. gondii* tachyzoites (Bradley et al. 2005). They include rhoptry neck proteins (RONs) that form elongated necks which function as ducts to discharge their contents, and rhoptry proteins (ROPs) that form large, club shaped secretory organelles (Bannister et al. 2003; Bradley et al. 2005). In *T. gondii*; ROP5, ROP16 and ROP18 have been associated with virulence (Reese et al. 2011; Saej et al. 2007; Peixoto et al. 2010). ROP18 destabilizes interferon gamma response of the host to prevent the rupture of the PV. Micronemes (MICs) are the smallest organelles that vary in their numbers in different Apicomplexa parasites and are involved in the early phase of the invasion process by attachment and penetration of the host's cell (Dubey & Lindsay 1996). Microneme proteins such as MIC1 enables the attachment to host cells through their adhesive domains and MIC1 also can form a complex with MIC4 and MIC6 that is associated with invasion (Garnett et al. 2009; Reiss et al. 2001). Dense granules (GRA) are involved in the establishment and maintenance of the PV during and after host cell invasion (Bannister et al. 2003; Speer et al. 1999). The conoid is a fibrous spiral-shaped structure which plays a role in invasion (Del Carmen et al. 2009) and the apicoplast is a non-photosynthetic plastid found in most Apicomplexa (Zhu et al. 2000).

1.4 Host cell invasion by *T. gondii* and *N. caninum*

The host cell invasion process takes place rapidly in a sequential series of events. Tachyzoites first move the host cell surface through an active actin-myosin driven motor called the gliding motility (Kappe et al. 2004). At first, the parasite must orientate itself in preparation for invasion so that it is vertical to the host cell

surface (Nichols, Chiappino & O'Connor 1983), followed by the formation of the 'moving junction' with the host cell membrane, using surface antigen proteins and proteins secreted from the micronemes and rhoptries (Besteiro et al. 2009). The parasite forms a parasitophorous vacuole (PV), where the membrane consists of host cell plasmalemma with integrated parasite proteins (Beckers et al. 1994). The mitochondria and endoplasmic reticulum (ER) of the host accumulate around the PV (de Melo et al. 1992); host transmembrane proteins are left out so that the vacuole is incapable to fuse with lysosomes and is shielded from host immune defences (Mordue et al. 1999).

1.4.1.1 Differences between *T. gondii* and *N. caninum*

There are ultrastructural differences between the two parasites (Speer & Dubey 1989). The size of *N. caninum* tachyzoite is slightly larger than *T. gondii*. Micronemes are more numerous in *N. caninum* (Speer et al. 1999) and the number of rhoptries in *N. caninum* is six to sixteen compared to four to ten in *T. gondii* (Speer et al. 1999). Electron-dense rhoptries of *N. caninum* tachyzoites are similar to the mature bradyzoites of both species, whereas in *T. gondii* are spongy and electron-lucent (Speer et al. 1999). Cyst walls of the bradyzoite stage in *T. gondii* are smooth and less than 0.5 µm thick and may contain hundreds of bradyzoites, whereas in *N. caninum* they tend to have irregular thick cyst walls (≤ 4 µm) but are smaller in size and contain fewer bradyzoites when compared to *T. gondii* tissue cysts (Figure 1.2) (Speer et al. 1999). Also, the number of oocysts shed in cats faeces are high and can reach up to millions of oocysts in comparison the dog which sheds less amounts of oocysts and can only reach up to 500.000 oocysts (Gondim et al. 2005).

Differences have been also associated with variances in surface antigens and secreted virulence factors; the number of surface antigen proteins were found to be increased in *N. caninum* (227) compared to *T. gondii* (109) (Reid et al. 2012; Wasmuth et al. 2009).

1.5 Pathogenesis and clinical outcome of *T. gondii* and *N. caninum* infection

Human infection with *T. gondii* can occur as a result of food or water contamination and organ transplantation or blood transfusion from individuals infected with *T. gondii* (Siegel et al. 1971). During pregnancy, a mother infected with *T. gondii* can transmit the parasites to the foetus; as these parasites can cross the placenta (Dubey & Jones 2008). As a result, severe congenital toxoplasmosis, hydrocephalus, abortion or death of the foetus inside the uterus may occur (Desmonts & Couvreur 1974; Holliman 1995). Other congenital clinical symptoms might include infection of the eyes (retinochoroiditis), which can lead to blindness and also mental abnormalities (Wilson et al. 1980; McAuley et al. 1994). *Toxoplasma* infection in immune supressed individuals, such as HIV/AIDS patients, may cause toxoplasmic encephalitis (TE) that can be fatal (Carruthers & Suzuki 2007).

Neosporosis can cause disease in dogs and more significantly in cattle. *N. caninum* transmission from mother to foetus in cattle is a major cause of abortion, stillbirth and clinical disease in new-born calves (Williams et al. 2000). In pregnant cattle, multiplication of the parasite can occur in the placenta through its entry to the foetal bloodstream, along with activation of pro-inflammatory cytokine and chemokines in the placenta can lead to tissue damage (Buxton et al. 2002; Innes et al. 2007). The parasite can cross endothelial barriers and reach the CNS of the foetus, in which it is purposed to reach the CNS through infection of dendritic cells (Collantes-Fernandez et al. 2012). In dogs, the disease manifests as neuromuscular dysfunction (Dubey 2005; Dubey et al. 2009). In severe cases in young, congenitally infected pups, hind limb paresis occurs and may progresses to paralysis. Additional symptoms in dogs include difficulty in swallowing, paralysis of the jaw, muscle flaccidity, muscle atrophy and even heart failure (Dubey 2003).

1.5.1 Economic impact of *T. gondii* and *N. caninum*

T. gondii causes toxoplasmosis in humans and animals. It is estimated that 16-40% of the population in the United States of America and the United Kingdom are infected with *T. gondii*. In Central and South America the infection rate is higher where it can reach from 50- 80% (Dubey et al. 1988). The socio-economic impact of the disease causes increase costs in healthcare, such as children with blindness (Roberts et al. 1990). In the United states, Toxoplasmosis was identified as the *second* primary cause of foodborne illness and around 4800 ocular infections are detected annually (Scallan et al. 2011; Jones & Holland 2010).

N. caninum has an economic impact especially in cattle and also causes pathology in dogs. Bovine neosporosis effects dairy and beef industries around the globe. In the United Kingdom, Neosporosis is the causative agent of abortion in cattle at an estimated number of 6000 abortions annually (Davison, Otter & Trees 1999b). A UK study into occurrence in cattle found that over 90 % of herds had at least one cow seropositive for *N. caninum* (Woodbine et al. 2008). Substantial economic losses result from abortion and stillbirths, reduced milk yield and reduced weight gain (Barling et al. 2000).

1.6 Host immune responses during *T. gondii* or *N. caninum* infection

During parasitic infection with *T .gondii* or *N. caninum* the host generates an immune response to the invading tachyzoites in order to control their spread and limit cell damage. Immune responses in hosts during *T. gondii* infection differ according to the parasite burden, type of parasitic strain and the host immune status (Suzuki & Remington, 1993). As *T. gondii* and *N. caninum* are closely related, similarities in host immune response have been detected. The host produces a Th1 immune response through up-regulation of interleukin-12 (IL12) by different cell types such as macrophages, neutrophils and dendritic cells leading to the induction of interferon gamma (IFN-γ) through T cells (Gazzinelli et al. 1993; Sher et al. 2003;

Wilson & hunter 2004; Innes et al. 1995). IFN-γ is a cytokine that is important in control of infection in both acute and chronic stage of disease (Suzuki et al. 1988; Gazzinelli et al. 1993; Innes et al. 2002). Under the protective immune response of the host, parasites are compelled to convert from tachyzoite to bradyzoites. These cysts can be found in different sites and organs but are mainly detected in muscle tissue and the CNS, persisting throughout the host's life (John, Weninger & Hunter 2010; Dubey & Lindsay 1996). In immunosuppressed hosts such as individuals with AIDS; the production of IFN-γ decreases as a result of the low level secretion of CD+4 T helper cells, thus reactivation of the parasitic infection in the brain reoccurs, where tachyzoites are reactivated from bradyzoite cysts and cause *Toxoplasma* encephalitis or even cause death (Luft & Chua 2000). In *N. caninum* infection, if tachyzoites reach the CNS, they can cause clinical signs of abortion of the foetus in cattle or neurological outcomes (Dubey & Lindsay 1996; Hemphill 1999). During pregnancy in infected cattle with *N. caninum*, Th1 immune responses as a result of infection may harm the foetus and therefore is reduced (Innes et al. 2001). In return, the Th2 response is elevated through the production of immune regulatory cytokines such as interleukin-10 (IL10) by the placental tissue (Quinn, Ellis & Smith 2004; Quinn, Miller & Ellis 2002; Innes et al. 2007).

1.7 The involvement of *T. gondii* in behavioural changes and neurological disorders

In recent years, there has been more interest in the possible involvement of *T. gondii* infection with neurological disorders (Torrey & Yolken 2003; Zhu 2009). It has been proposed that *T. gondii* infection in the CNS may cause behavioural changes in humans (Flegr 2007). *Toxoplasma* infection has been suggested to be connected to many neurological diseases; such Parkinson's disease through clinical observations of patients seropositive with *T. gondii* (Miman et al. 2010). There is evidence to indicate the possible involvement of *T. gondii* in modifying and increasing the hosts' dopaminergic signalling in the CNS (Gaskell et al. 2009; Prandovszky et al. 2011). Studies on infected rodents showed host behaviour

changes and increased levels of dopamine (Stibbs 1985; Flegr et al. 2003; Gaskell et al. 2009; Prandovszky et al. 2011). Elevated dopamine production was also found in patients with schizophrenia (Torrey & Yolken 2003; Carlsson 1988; Howes & Kapur 2009). Dopamine is a monoamine neurotransmitter formed in the brain by the decarboxylation of dopa and is needed for normal performance of the central nervous system. It is involved in important roles related to behaviour, cognition, voluntary movement and attention. Dopamine secretion is known to be involved in the modulation of neuronal activities linked to learning and memory functions in the hippocampus region of the brain (Backman et al. 2010).

Many factors play roles in the determination of neurological outcomes related to toxoplasmosis such as genetic and environmental factors, strain of *T. gondii* acquired, age of individual infected, severity of the acute stage of disease, the ability of the parasite to reach important parts of the body such as the CNS and the host's immune response (Murakami et al. 2000; Wilson & Hunter 2004). The parasite's localization to specific parts of the brain could play a role in the host's behavioural changes, especially in relation to fear responses (McConkey et al. 2013). There have also been reported cases linking disorders and diseases such as depression, anxiety and psychoses in patients with the chronic stage of disease (Arendt et al. 1999; Torrey & Yolken 2003).

1.8 Importance of astrocytes in the central nervous system

In the central nervous system (CNS), cells consist of neurons and glia cells. There are many types of glia cells such as astrocytes, microglia, oligodendrocytes and others: one of the most important glia cells are astrocytes (Figure 1.4). Astrocytes form the majority of the cells in the mammalian brain and are involved in the blood brain barrier (BBB) formation (Fields & Stevens-Graham, 2002). Moreover, they are important in cell-cell communication of neurons, defence against infectious organisms or traumatic injuries and provide homeostasis in the brain through neurite outgrowth and synaptic plasticity (Norenberg 1994; Pekny & Nilsson 2005; Fields & Stevens-Graham, 2002).

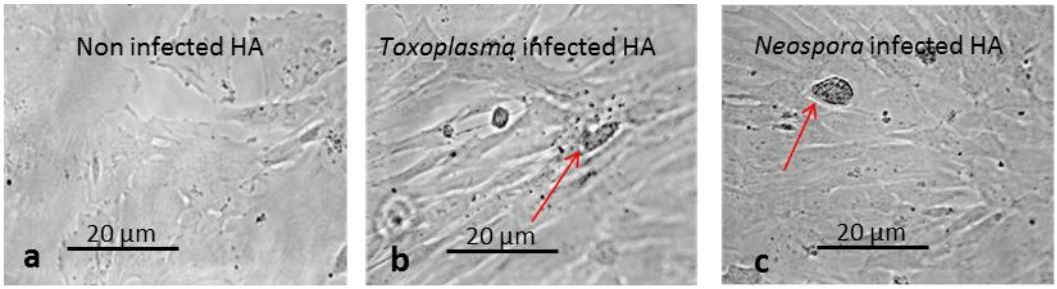

Figure 1.4: Images of human astrocytes *in vitro* using light microscopy and x40 magnification a) uninfected human astrocyte cells, b) cells infected with *T. gondii* and c) cells infected with *N. caninum* (red arrow indicated tachyzoite in parasitophorous vacuoles.

Any damage occurring to astrocytes can seriously effect neuron survival and have also been linked to pathological outcomes of many neurological diseases such as Alzheimer's disease and toxoplasmic encephalitis (TE) (Nedergaard et al. 2010; Drogemuller et al. 2008). In addition, astrocytes infected with *T. gondii* can decrease gap junctions between cells which may result in reduced communication between cells (Fischer et al. 1997). Astrocytes have been found to be infected to a higher extent with *T. gondii* compared to neurons and microglia cells in studies done both *in vivo* and *in vitro* (Halonen et al. 1996; Fagard et al. 1999; Luder et al. 1999).

IFN-γ induction of astrocytes can inhibit and limit immune pathological responses of parasitic infection in both *T. gondii* and *N. caninum* (Wilson & Hunter 2004; Halonen, Taylor & Weiss 2001). During inflammatory responses, these cells are capable of chemokine and cytokine production in addition to them acting as antigen processing cells (APC) to the T cells (Brenier-Pinchart et al. 2004; Strack et al. 2002; Wilson & Hunter 2004).

Human astrocytes used in this thesis were ethically approved for research purposes only and are a primary cell line that can be used up to five passages. There are some limitations associated with the use of these cells; such as the limitation of the number of passages used (five passages). *N. caninum* are arguably unlikely to infect human astrocytes *in vivo*, but have been found to infect human astrocytes *in vitro.*

Most of the comprehensive understanding about astrocytes has been achieved through *in vitro* studies. Therefore, *in vitro* cultures are an effective systems model for the study of pathological occurrence in the CNS, allowing a better understanding of host-parasite interactions. *T. gondii* and *N. caninum* have been found to infect astrocytes successfully *in vitro* (Pinheiro et al. 2006; Jesus et al. 2013). They are also responsible in information processing, learning and memory processing.

1.9 Methodologies for investigating host cell responses using proteomic and transcriptomic approaches

1.9.1 Quantitative proteomics in host cell investigations

Proteomic research deals with large scale profiling of protein expression levels, post-translational modifications (PTMs) and protein-protein interactions in many complex biological systems (Pandey & Mann 2000). Advances in mass spectrometry (MS) have broadened proteomic studies and enabled systems biology investigations that helped to solve important biological questions which were once considered a challenge (Aebersold & Mann 2003; Cravatt, Simon & Yates 2007). Generally, the classical way for many proteomic investigations include a protein separation step via gel based approaches and identification using MS, or a non-gel based approach by direct tryptic digestion of whole protein lysates into peptides before MS analysis. Protein or peptide fractionation is routinely utilised to increase proteome coverage and depth. Peptides are identified by MS then allocated to proteins by bioinformatic searching of predicted protein databases.

1.9.2 Gel based separation investigation methods

In order for complex protein samples to be separated, a classical approach is usually performed using a gel matrix along with the application of an electric field. One of the earliest separation methods to be established was Sodium dodecyl sulphate polyacrylamide gel electrophoresis (SDS-PAGE) (Shapiro, Vinuela & Maizel 1967). It enables the breakdown of interactions between proteins through solubilisation, denaturation and reduction steps followed by separation using a polyacrylamide gel along with a current, in which the proteins then migrate according to their molecular weight (Rabilloud 1996). Two dimensional electrophoresis (2-DE) separations consists of first separating the proteins according to their isoelectric point (pI) where the protein net charge is zero and in the second dimension according to its molecular weight (O'Farrell 1975). Then, gels are stained for protein visualization and proteins of interest are excised, digested into peptides using a proteolytic enzyme (usually trypsin) and finally proteins are identified using MS techniques. However, 2-DE methods are difficult to conduct on multiple comparative studies and are time-consuming and labour-intensive, in which the gels need to be run, analysed, and compared. They also suffer from poor reproducibility between gels which may cause variability (Zhou et al. 2002). Thus, two dimensional difference gel electrophoresis (2D-DIGE) was developed.

1.9.3 Two dimensional difference gel electrophoresis (2D-DIGE) investigations

Introduced in 1997, 2D-DIGE is a high performance proteomic tool used for separation of complex samples (Unlu et al. 1997). The development of 2D-DIGE enabled a more sensitive and reliable quantification method for the estimation of protein abundance compared to 2-DE, as samples are run altogether on the same gel, which minimizes potential gel-to-gel variation (Kondo 2008). Basically, steps involved in 2D-DIGE involve directly labelling proteins using the lysine groups on proteins with different fluorescent (cyanine) dyes (Cye™ dyes, GE healthcare) prior to protein separation according to their pI and then by molecular weight in the

second dimension through the application of an electrical field across a solid-based gel. Protein spots are then either directly scanned in the Cydye gels or stained first with a fluorescent stain for visualization of the proteins in the pick gel. Proteins of differential expression are selected using an appropriate software program such as Decyder 2D™ (GE Healthcare). Finally deferentially modulated proteins of interest are excised from the pick gel, digested into peptides and placed on a MS for protein identification followed by bioinformatic analysis (Westermeier & Gorg 2011).

1.9.4 Non-gel based proteomic investigations

There are numerous studies that have used 2D-DIGE for global proteomic profiling. Yet, this technique has many limitations; it requires a substantial level of skill, is time consuming, laborious and has many technical restrictions related to resolving proteins with high or low masses and has limited sensitivity (Zhu, Smith & Huang 2010; Old et al. 2005). Therefore; alternative proteomic approaches using non-gel based techniques have been developed for quantifying protein changes between samples of interest. This can be applied through two approaches; label-based and label-free proteomic analysis.

1.9.4.1 Label- based quantitative methods

In label based methods, such as stable isotope labelling, quantification is achieved by incorporating isotope labelled molecules into MS analysis as internal standards or relative references (Zhu, Smith & Huang 2010). This method involves the application of chemical and physical properties similar to the natural compounds of the samples to be investigated that enables the mass spectrometer to differentiate between identical proteins in separate samples. The labelled protein samples are then pooled together, digested, mixed and relative protein abundance changes are determined from ratios of intensities between the differentially labelled peptides (Gygi et al. 1999). Labelling approaches in 'shotgun' type experiments include stable isotope labelling by amino acids in cell culture (SILAC) (Ong 2002; Everley et al.

2004), tandem mass tags (TMT) (Thompson et al. 2003), isotope-coded affinity tags (ICAT) (Gygi et al. 1999; Smolka et al. 2001) and isobaric tags for relative and absolute quantification (iTRAQ) (Ross et al. 2004). These methods have enabled the identification and quantification of complex biological samples in systems biology approaches and in the reduction of variability between samples. However, most label-based quantification approaches have many limitations, including complex sample preparation, incomplete labelling and increased costs of these methods (Patel et al. 2009). Moreover, in the labelling approach, a higher sample concentration is needed and so far only TMT and iTRAQ methods can allow up to eight samples to be compared in a single experiment. Thus, non-labelled quantification procedures have been an interest for many researchers in the field of quantitative expression profiling of proteins (Panchaud 2008).

1.9.4.2 Label-free quantitative based methods

Label-free approaches use raw data directly from multiple mass spectrometry runs to enable the comparison of the relative protein abundances in different protein MS runs (Wastling et al. 2012). In contrast to label based approaches, each protein sample is separately prepared, then subjected to individual LC-MS/MS analysis. They have many advantages over labelling techniques including low cost, simplicity and a lower concentration of samples are required. Moreover, it has a higher proteome coverage and dynamic range and numerous protein samples can be compared in a single experiment. High resolution MS/MS instrumentation along with multiple sample preparations is recommended in label-free quantitative approaches. However, as every sample needs to be separately prepared and run on the LC–MS/MS, steps extending from sample preparation to MS analysis can introduce variations which may cause bias in the the quantitative analysis. Relative quantification offers calculation of abundance ratios between peptides and proteins by comparing their signals created from different samples. Usually this approach is used in non-targeted based experiments. It allows global quantitative profiling of tens of thousands of peptides from thousands of proteins within an experiment without prior information of these proteins. Absolute quantification can be used to

determine the amount (mass or copy number) of proteins in a mixture or complex and is generally performed at the peptide level. Currently, there are two different protein quantification schemes in label-free quantification: spectral counting (Liu, Sadygov & Yates 2004) and peak intensity measurements (Bondarenko, Chelius & Shaler 2002).

1.9.4.2.1 Spectral counting measurements

Spectral counting relies on the practical observation that more abundant peptides are more likely to be observed and detected in an MS experiment and involves the observation of possible linear correlation between MS/MS spectra of peptides acquired from a certain protein to the relative concentration of the protein (Zybailov et al. 2005). Calculation of relative quantification is done by comparing the number of spectra between the experiments. While spectral counting is a fairly simple technique and is easily applied, normalization and cautious statistical evaluation are still necessary for accurate quantification, which can decrease significantly for proteins with only a few recognisable peptides and when the quantitative changes between experiments are small (Mallick & Kuster 2010).This method is also controversial due to the fact that it does not take in account any measurement of direct physical property of a peptide, it relies on the quality of the spectra and low abundant peptides may not be detected and measured. It also does not measure any direct physical property of a peptide and assumes the same linearity response for every protein.

1.9.4.2.2 Peptide peak intensity measurements

Ion intensity based method is produced by obtaining an ion chromatogram for each peptide precursor from the MS data and also measuring the peak area over the chromatographic retention time. It aligns precursor ion spectra of the same peptide of a sample from parallel runs according to their retention times (RT) and protein quantification and identification is attained by summing ion intensities of all or top

three peptides that have been matched to peptides for a given protein. This is done by comparing intensity values for each peptide between one or more experiments for relative quantification purposes. This method allows peptide measurements with high accuracy and wide dynamic range, especially when high-resolution mass spectrometers are used and can differentiate distinct peptides sequences with interfering signals of similar masses (Nikolov, Schmidt & Urlaub 2012).

1.9.5 Liquid chromatography mass spectrometry (LC-MS)

Liquid chromatography–mass spectrometry (LC-MS) is a powerful analytical technique that enables the separation using liquid chromatography (LC) combined with the mass analysis of mass spectrometry (MS). LC-MS has very high sensitivity and selectivity used in the separation, detection and identification of molecules of particular masses found in complex mixtures.

1.9.5.1 Reverse-phase high performance liquid chromatography (RPLC)

During the investigation of complex biological systems, it is recommended to introduce additional steps of separation to allow better resolution of the peptides. High performance liquid chromatography (HPLC) is a procedure in which molecules contained within a liquid mobile phase are forced under pressure through a stationary phase within a closely-packed column. In the stationary phase, compounds bind to the column based upon their chemical properties. In reverse phase (RP) HPLC, non-polar molecules are recollected while polar molecules are first to elute. The mobile phase solvent is adjusted along a gradient by increasing the acetonitrile content gradually, to elute the more polar molecules by increasing hydrophobicity (Simpson 2003).

1.9.5.2 Tandem mass spectrometry (MS/MS)

Mass spectrometry determines the mass to charge ratio (m/z) of gas phase ions. Peptides are converted into the gas phase through an ionization source such as electrospray ionization source (ESI). The peptide mass (m/z) is measured by the detector followed by peptide fragmentation through collision with an inert gas. The mass (m/z) of the fragmented ions are then measured and used to determine the sequence of the peptide. Tandem mass spectrometry (MS/MS) includes multiple steps of MS selection in which fragmentation steps take place between the stages. Peptides are converted into the gas phase through an ionization source such as electrospray ionization source (ESI) as seen in a linear trap quadropole (LTQ) mass spectrometer. The three most abundant peptides identified from the gas phase by an initial spectrum search are fragmented by collision-induced dissociation (CID), followed by a second scan that measures mass to charge ratio (m/z) of the consequential fragments (MS/MS). Orbitrap mass spectrometer is a recent more accurate developed mass spectrometer instrument that has many advantages including high resolution of peptides, greater sensitivity and data acquisition that enables better identification and quantification of thousands of proteins during proteomic investigations (Makareov 2000; Beck et al. 2011). Basically in an Orbitrap, ions are trapped in an outer barrel like electrode, due to their attraction to the inner electrode through centrifugal force, ions end up cycling around the inner electrode and move back and forth in the central electrode in space which resembles a spiral form of movement.

1.10 Protein identification and bioinformatics analysis

Following mass spectrometry analysis, the tandem mass spectra data needs to be compared to an *in silico* database for protein identification. This is done to ensure that all possible peptides cleaved with the proteolytic enzyme are searched from predicted proteins of interest of the organism's genome. One of the major challenges in global proteomic expression profiling is processing large amount of data attained. Many database search tools have been developed for peptide/protein identification for MS/MS data such as MASCOT (Perkins et al.

1999), Sequest (Eng, McCormack & Yates 1994), X! Tandem (Craig & Beavis 2004) and PEAKs (Zhang et al. 2012). These search tools identify peptides using algorithms that match the precursor and MS/MS spectral data to those from an *in silico* digestion of a translated genome. As a result, a score unique to the spectra searched against theoretical spectra of the specific organism is given. Otherwise, *de novo* sequencing of individual MS/MS spectrum can be achieved using certain software such as PEAKS (Zhang et al. 2012). In order to guarantee that peptides identified do not contain any false positives, the false discovery rate (FDR) is needed. This is done by re-searching the data with a false database generated by reversing amino acid sequences of the actual database used for the protein search, usually around 1% or less is accepted. In addition, proteins identified from LC-MS/MS data analysis with only one peptide hit is excluded from the data search result.

1.11 Transcriptomics

Within a biological system, the analysis of messenger RNA (mRNA) provides information of the changes happening in the cell at the transcriptional level. The two methods commonly used to measure the expression profile of the transcriptome are hybridization and sequence based procedures. Hybridization approaches usually include incubating fluorescently labelled complementary DNA (cDNA) with custom-made or commercial oligonucleotide microarrays and measuring the intensity of the fluorescent dye used (Bammler et al. 2005). Sequence based approaches determine the cDNA sequence directly. These techniques include expressed sequence tag (EST) libraries that use relatively low throughput cDNA (Gerhard et al. 2004), tag-based methods such as serial analysis of gene expression (SAGE) (Velculescu et al. 1995); cap analysis of gene expression (CAGE) (Kodzius et al. 2006) and massively parallel signature sequencing (MPSS) (Brenner et al. 2000) and were produced to deliver quantitative expression profiles in a high throughput manner in a cell or tissue organism. Quantitative polymerase chain reaction (qPCR) is an accurate technique but is mostly used for smaller

numbers of sequences; therefore the development of RNA-Seq nowadays is the preferred technique.

1.11.1 RNA-Seq

RNA-Seq involves the sequencing of cDNA libraries generated from reverse transcription of mRNA. Sequencing techniques such as Sanger capillary sequencing is done through *in vivo* cloning of DNA in *E. coli* before sequencing with dye-labelled terminator dNTPs (Sanger et al. 1977). The application of next generation sequencing (NGS) has eased transcriptional investigations and eliminated the need of *in vivo* cloning. NGS requires either DNA synthesis, as used by the Illumina and 454 Life Sciences (Roche) sequencing platforms, or through ligation as in SOLiD (Applied Biosystems) sequencing. The 454 platform is also known as the *de novo* sequencing platform uses emulsion PCR for generating libraries to perform pyrosequensing; reads generated are around 500 base pairs and are similar in their lengths. This platform is widely used for DNA and RNA sequencing for organisms without any reference genome available (Margulies et al. 2005). SOLiD sequencing is done through a series of ligation runs of dinucleotides to adapters and each base is read twice (Shendure et al. 2005). Short reads produced from this platform are considered to be an accurate method but have a complex sample preparation and data processing procedure compared to other platforms such as Illumina. A new sequencing method developed by Helicos Biosciences is called 'single molecule sequencing' has been established (Harris et al. 2008), which requires only a small amount of mRNA material; but it is not yet widely accessible. Compared to microarray or cDNA sequencing, RNA-Seq is cheaper, involves less mRNA concentrations and has a high dynamic range for quantitation of transcripts with minimum background noise (Wang, Gerstein & Snyder 2009).

Illumina sequencing preparation involves the generation of a cDNA library from the sample mRNA. They are then amplified through PCR reaction and bridges are formed between oligonucleotide primer on a flow cell (Bennett et al. 2005; Bentley et al. 2008). Clusters of DNA are generated to which bases with fluorescent dye

attached are added to the flow cell is imaged then the dye removed and the next base is added and so on, until the whole sample has been sequenced. (Holt & Jones 2008). Illumina increases accuracy of sequencing, but read lengths are much shorter (50-100 base pairs) compared to other sequencing platforms, so a reference genome to align to is needed.

1.12 Systems biology in host-parasite interactions

Owing to advances in different genomic, transcriptomic and proteomic techniques; biological investigations in an organism is changing from components being examined individually, to a 'systems biology' approach. These advances have enabled the movement of studies focusing on single genes to broader integrative comprehensive studies (Wastling et al. 2012). In the last decade; systems biology has been of interest to many researchers, in which it allows deeper insight into genes and proteins involved in a complex cellular system and easing the investigation of the biomolecules roles, interaction and functions. Moreover, systems biology studies assisted in the integration of genomic, transcriptomic and MS based proteomic investigations of biological interactions that aided in the discovery of signalling pathways and networks of different organisms.

1.13 Current research in astrocytes proteome

Astrocytes play major roles in brain injury and pathogenesis, yet, only a few analyses of the whole-cell proteome and secretome in astrocytes have been performed (Mark et al. 1996). Proteome and secretome investigations on astrocytes were carried out to examine their roles in neurological diseases and disorders such as Alzheimer's disease, Huntington disease, schizophrenia and Parkinson's disease (Nedergaard, Rodriguez & Verkhratsky 2010; Sofroniew & Vinters 2010; Molofsky et al. 2012). An investigation was carried out on neurons, astrocytes, oligodendrocytes, and microglia in the human brain using fluorescence activated

nuclei sorting (FANS), in which a monoclonal antibody against the neuron specific splicing factor was applied. This approach identified 1755 cell-type-specific nuclear proteins that were involved in histone modifications, and regulation networks altered with normal brain aging or neurodegenerative disease (Dammer et al. 2013). In another study using a 2-DE based analysis of the proteome of mouse astrocytes, Yang *et al*. (2005) identified 191 individual proteins mostly involved in nucleic acid binding, cytoskeleton and signalling proteins and the proteasome. Using 2D-DIGE, investigation of specific protein modifications was carried out in the hippocampus region of rat brains following spatial learning. A total of 42 proteins were found significantly modulated after 24 hours associated with cellular structure and cellular metabolism compared to uninfected rat brains (controls) (Monopoli et al. 2011). In addition, Alzheimer's disease examination for biomarker detection and discovery in individuals was performed using 2D-DIGE, a putative indicator of neuroinflammation called YKL-40, was highly increased in Alzheimer patients and could be used as a biomarker for preclinical Alzheimer's (Craig-Schapiro et al. 2010). Yet, viral infection in astrocytes was explored by 2D-DIGE, polyriboinosinic-polyribocytidilic acid (polyI:C) was used to simulate immune activation by viral infections on mouse astrocyte conditioned medium (ACM). In total, 13 proteins were differentially expressed compared to uninfected ACM, among these proteins with significant expressions was matrix metalloproteinase-3 (MMP3), in which it can be associated with neurodevelopmental impairment (Yamada et al. 2014). Malignant mouse astrocyte cells were explored using 2D-DIGE to investigate metabolic programming in cancerous cells. Several changes were detected in isoenzymes associated with metabolic reprograming, such as the up-regulation of glycolytic enzymes to increase the use in glycolysis (Bentaib et al. 2014).

1.13.1.1 Proteomic investigations in host cells and parasitic infections

Several proteomic studies done on *T. gondii* have elucidated the specialized invasion organelles and their composition, as well as proteins associated with the cytoskeleton (Xia et al. 2008; Bradley et al. 2005; El Hajj et al. 2006). Shin *et al*. (2005) investigated the possible relationship between two distinct isolates of *N.*

caninum (KBA-2 and VMDL1) using 2-DE and found significant homology in the proteome and antigenic proteome profiles between them, though isolated from distinct geographical locations. In *T. gondii* investigation, tachyzoites of three different strains were compared using 2D-DIGE. Similar proteomic profiles were detected between type I (GT1 train) and type II (PTG strain) compared to type III (CTG strain). A total of 84 differentially expressed proteins were identified (Zhou et al. 2013).

In host cell response during *T. gondii* infection; Nelson *et al.* (2008) described the proteomic analysis (2D-DIGE) of human foreskin fibroblasts (HFFs) during infection *in vitro*, in which modulations of the host metabolic pathways, including glycolysis, lipid and sterol metabolism, mitosis, apoptosis and structural-protein expression were detected.

However, to date there have been no reported comparative proteomic studies of host astrocyte responses during *T. gondii* and *N. caninum* infection or any other cell type.

1.13.2 Current research in astrocytes and other host cells transcriptome

In relation to the use of RNA-Seq in exploring human astrocytes during parasitic infection, to date there have not been any studies published. The investigation of increased expression of astrocyte cell markers in schizophrenia and its association with neuroinflammation was done using RNA-Seq and has showed that patients with schizophrenia had increased expression of glial fibrillary acidic protein (GFAP) and hypertrophic astrocyte morphology (Catts et al. 2014). A study that localised Alzheimer's disease in the parietal cortex of the brain and its involvement in the early symptoms of the disease in humans was carried using RNA-Seq. The authors identified transcriptional profile changes related to lipid metabolism and concluded that astrocytes are associated with neurodegenerative disorders (Mills et al. 2013). Gail, Gross & Bohne (2001) explored transcriptional changes of human foreskin fibroblast (HFF) cells during *T. gondii* infection compared to *Salmonella typhimurium* and *Chlamydia trachomatis* using microarrays. They identified 13 genes (such as

Interluikin-6 (IL6) and tumour necrosis factor-inducible gene 6 (TNFAIP6)) up-regulated exclusively in infected cells with *Toxoplasma*. Another study examining the functional changes in the central nervous system (CNS) *in vivo* in mice during chronic *T. gondii* infection found that genes involved in immune responses and cell activation were up-regulated in the mouse brain after infection (Tanaka et al. 2013). In addition, host transcripts whose expression was reduced by infection were involved in small-GTPase-mediated signal transduction and vesicle mediated transport (Tanaka et al. 2013). Jia *et al*. (2013) examined transcriptional changes of brain tissues and peripheral lymphocytes of BALB/C mice infected with *T. gondii* RH and ME 49 strain along with uninfected mice through microarray hybridization and qPCR. Genes associated with immunity were up-regulated higher in ME49 strain infection, whereas up-regulated pathways associated with pathogenesis of the CNS was up-regulated significantly compared to ME49 infection.

1.13.2.1 RNA-Seq in *T. gondii* and *N. caninum* parasite investigation

In a comparative transcriptome study between *T. gondii* and *N. caninum* tachyzoites; an expansion in the number of surface antigens were identified in *N. caninum* compared to *T. gondii* tachyzoite stage using RNA-Seq. Furthermore, differences between the two parasites regarding secretory virulence factors found *in T. gondii*, specifically rhoptry kinase 18 (Rop18) which was found to be a pseudogene in *N. caninum* (Reid et al. 2012).

1.14 Secretome investigations in host cells

The secretome consists of proteins secreted or shed from the cells surface of an organism. Many of these proteins play essential roles in many physiological processes in a cell; such as cell signalling, communication, migration and tumour differentiation and invasion (Weston & Hood 2004). The word ‘secretome’ was first introduced by Tjalsma *et al*. (2000), in a genome based investigation of *Bacillus*

subtilis bacteria. Protein secretion is believed to be a balanced procedure essential for the normal physiological functions in host cells. In mammalian cells, secreted proteins are complex and closely regulated and have vital roles in physiological and pathological processes (Hathout 2007). Tissues in mammalian host such as the brain and muscle secrete several biological molecules. Any excess or enduring changes in the secretion of these secretory proteins may indicate a sign of abnormalities or pathological condition (Hathout 2007). Secretome analysis has been widely used in the many research fields, such as host-tumour communication, host-pathogen interaction and drug/vaccine development (Ochsenbein 2002; Sibbald et al. 2009; Brey 2005).

Challenges associated with secretome studies include; sample preparation, filtration, in which potential cytosolic protein contaminants in supernatant can be present and low protein concentrations of the secreted proteins.

1.14.1.1 Methods for secreted protein identification

While computer based genome analysis is an indirect approach for secreted protein identification using amino acid sequence information, proteomic based methods enabled a direct investigation of the secreted proteins in a different range of biological systems (Thouvenot et al. 2006). Label free quantitative proteomics is used nowadays widely; especially in neuroproteomic and secretome studies, owing to the advances and improvements in MS instrumentation (Findeisen & Neumaier 2009). An additional computational step can authenticate secreted proteins from other cytosolic proteins through peptide signal sequences database search tools such as SignalP and SecretomeP (Bendtsen et al. 2005; Petersen et al. 2011).

1.14.1.2 Astrocyte importance in secretome investigations

Astrocytes secrete proteins that are important for neuronal growth, neurogenesis, development and survival and synaptic development. These are mediated by the release of proteins and peptides such as extracellular matrix proteins, growth

factors and proteases (Bachoo et al. 2004). Also, astrocytes have been identified as a source for chemokine secretion and may participate in the infiltration process of leukocytes (Krumbholz et al. 2006)

Through studying secreted proteins *in vitro,* this can assist in understanding the biological processes happening in cells *in vivo*. Though *in vitro* investigations cannot exactly comprehend all cellular interactions under *in vivo* conditions, it is a valuable method for mapping quantified secreted proteins and enables metabolic pathway analysis in a biological system.

1.15 Current research in astrocytes secretome

While the first secretome studies were conducted on bacteria and fungi (Antelmann et al. 2001), there are now many investigations of the mammalian secretome. Major advances in the proteomic studies of the cells secretome have occurred during the past seven years, owing to the improvements in proteomic techniques and especially in MS (Brown et al. 2012). This has been applied in the systematic investigation of secreted proteins of astrocytes (Greenbaum et al. 2001; Dowell, Johnson & Li 2009), microglia (Liu et al. 2008) and other glial cells (Chen et al. 2012). Characterization of the whole cell proteome and secretome in astrocytes using label-free quantitative proteomics coupled with high resolution MS identified 6000 proteins (Han et al. 2104). In supernatants of astrocytes infected with *T. gondii*, induction of matrix metalloproteinase-2 and -9 lead to fibronectin degradation, which is associated with extracellular matrix degradation and was detected by western blot (Lu & Lai 2013). Moore *et al*. (2009) identified 133 secreted proteins involved in neuronal development in primary rat astrocytes using a label-free quantitative method. These included proteins of the extracellular matrix and protease systems that were induced by astrocyte cholinergic stimulation. Neuroinflammation of astrocyte-derived cytokines and chemokines play both neuroprotective and neurotoxic roles in brain lesions of human neurological diseases. A study done by Choi *et al*. (2014) looked at the cytokine secretome

profile of human astrocytes using a protein microarray approach. Results showed that astrocytes expressed a distinct set of NF-kB-target cytokines and chemokines, that may suggest that NF-kB signalling pathway, regulates gene expression of cytokines and chemokines in human astrocytes under physiological and inflammatory conditions.

1.16 Aims and objectives

The main aim of this thesis was to explore differences in host response (in HA cells) and host-parasite interactions that reflect the divergent evolutionary biology and life cycles between the closely related parasites *T. gondii* and *N. caninum*. This will be achieved by the investigation of differential transcriptional/proteomic and protein secretion expression changes during host cell responses to *T. gondii* infection compared to *N. caninum* infection. Examining *N. caninum* bradyzoite cysts involvement in neurotransmission induction through dopamine stimulation in neural cells compared to *T. gondii* cysts infection in cells will be achieved through dopamine concentration measurements using HPLC.

In order to compare differences of human astrocyte cell responses during infection with either *T. gondii* or *N. caninum* at the molecular level, both proteomic (2D-DIGE and label-free proteomic) and transcriptomic approaches were carried out. The analysis of host cell protein secretions during infection was also further investigated through global proteomic profile analysis using a label-free quantitative method. This was important as astrocytes are known to secrete signalling and inflammatory proteins during infection and injury and is associated with leukocyte trafficking. RNA-Seq provided a high-throughput platform from which to analyse and examine the differences in expression of key genes between host cell infections with *T. gondii* compared to *N. caninum*.

Although both parasites; *T. gondii* and *N. caninum* can infect and reach the CNS of the host, *T. gondii* causes more pathology and behaviour changes in the brain of infected hosts and has tropism for cells of the CNS. There was also little evidence in

relation to the pathology caused by *N. caninum* in the CNS found mainly in dogs and cattle that may suggest it may not cause severe pathogenesis of the CNS. Therefore, investigation of cells related to the CNS such as the use of astrocytes during infection with *T. gondii* and *N. caninum* will elucidate our understanding of differences that may be present between them. Astrocytes have been demonstrated to be good models for system biology investigations as both *T. gondii* and *N. caninum* can successfully infect these cells *in vitro* (Halonen et al. 1998; Pinheiro et al. 2006).

It has already been established that infection of *T. gondii* in the brain at the chronic stage increases dopamine secretion and was believed to be associated with behavioural changes in the intermediate host in mice to enable the transfer of the parasite to the cat through the cat mouse cycle (Gaskell et al. 2009; Prandovszky et al. 2011). However, it is not known if *N. caninum* can alter behaviour or other changes in the CNS host cells.

The current information on the cell biology and particularly the molecular aspects of host-parasite interactions, obtained from *T. gondii* were applied to *N. caninum*. Yet, in many cases this has been done without cautiously assessing potential differences between the two parasites. Therefore, it is important to elucidate what *Neospora* is doing differently compared to *Toxoplasma* in host cell of the CNS, and how we could exploit these differences to generate a better understanding of key differences between them that can result in the production of an efficient therapeutic or diagnostic tool of intervention in the future.

Overall, this thesis aimed to increase the knowledge of host biological responses in astrocytes during parasitic infection between these closely related parasites that would enable a broader understanding of changes occurring in the CNS intending to identify key differences in responses that will help explain the difference in the biology between the parasites.

2 Chapter two: Global proteomic investigation of host cells response during *T. gondii* and *N. caninum* infection

2.1 Introduction

T. gondii and *N. caninum* can both reach different sites in the host including the CNS and modulate changes in the host cells. These two parasites, although closely related, have distinct differences in their host range and definitive hosts. To understand the mechanisms of host cell modulation during parasitic infections, it is very important to consider the effects the parasite has upon the host cell machinery which often includes changes both at the gene and protein level. Technological advances in protein separation methods, mass spectrometry and bioinformatics analysis have facilitated the ability to study global proteomic profiles of cells and organisms (Aebersold & Mann 2003; Schrader & Klein 2004). These techniques are more useful to use for global proteomic profiling compared to traditional approaches such as western blot analysis or immuno-cytochemical methods, which only help to examine one or a few proteins at a time. Thousands of proteins can be examined in multiple samples in a quantitative manner through global proteome analysis which has become one of the preferred approaches (Tannu & Hemby 2006). Quantitative proteomic techniques have facilitated examination of intracellular parasite invasion revealing novel protein modulation of host-pathogen interactions (Nelson et al. 2008). It has also assisted in important advances in the measurement of protein expression changes between normal and disease conditions and conveys corresponding analysis of proteins within samples (Aebersold & Mann 2003).

2.1.1.1 2D-DIGE

One of the main advantages of 2D-DIGE over the conventional 2-D techniques is the ability to label two to three samples with different dyes and run them all on the same gel, thus reducing spot pattern variability, the number of gels used in an experiment and yielding accurate spot matching. As a result, the confidence that a difference between two samples in fluorescence intensity is due to biological rather than experimental variation is increased (Van den Bergh et al. 2003). This technique has demonstrated that it can generate statistically significant data using fewer 2D gels (Alban et al. 2003; Friedman, Hoving & Westermeier 2009). At the time of preparing this experiment; the combination of 2D-DIGE, mass spectrometry and bioinformatics approach was deemed to be a powerful tool for comparative proteomic investigations, but now has been superseded by the technological advances in the field. Mass spectrometry is needed for the identification of the proteins corresponding to any spots observed by 2D-DIGE; the data is then searched against the gene and literature database to interpret the proteomic data. Bioinformatics helps in determining the proteomic signatures responsible for the main pathological features and identifying key proteins, which could be candidates for disease markers and therapeutic targets (Hopf et al. 2011). The use of bioinformatics, together with the information of the individual proteins identified by 2D-DIGE, gives a clearer view host parasite interactions (Xi et al. 2011).

Using 2D-DIGE involves prelabelling two protein samples, using two fluorescent cyanine dyes (Cy3™ and Cy5™), in addition to a pooled sample of both proteins labelled with a third dye (Cy2™). Labelled samples can then be mixed and run on the same 2D gel where proteins are detected and visualised using fluorescence imaging. This enables the detection of differences between protein abundance and any post translational modifications taking place in the two samples. An overview of the 2D-DIGE workflow is outlined in Figure 2.1. Scanned gels are analysed using 2D DeCyder™ software containing ANOVA test and t-test to detect the fold change of the protein expression levels. The proteins of interest can then be excised from the gel and digested to generate peptides for analysis and identification by tandem

mass spectrometry (LC-MS/MS). Protein identification was performed using database search engines such as MASCOT along with bioinformatic analysis.

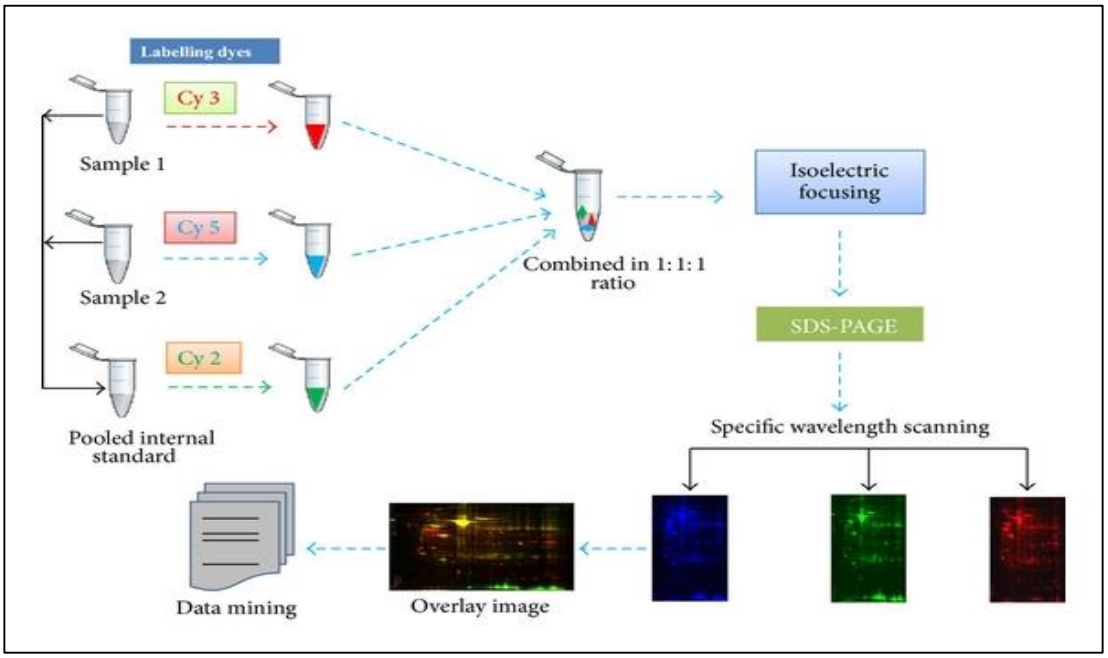

Figure2.1: Schematic of a typical 2D-DIGE experiment. Proteins from samples are first extracted, labelled with different fluorophores (Cy2, Cy3, and Cy5) and are resolved on the same 2D gel. Proteins spots are detected by scanning the gel with the appropriate wavelength for the Cy dyes; merging all of them yields an overlay image consisting of all three Cy dyes. The images are analysed using 2D DeCyder™ software and proteins of interest are identified, excised, digested and analysed on the MS followed by bioinformatic analysis (taken from Paul et al. 2013).

2.1.1.2 2D-DIGE studies in *Neospora*, *Toxoplasma* and host cells

Astrocytes are glia cells in the CNS that form the majority of the cells in the mammalian brain and are linked with all parts of neurons (Hatton 2002). Any damage to astrocytes can critically effect neuron survival and have been involved in the pathological processes of many neurological diseases such as Alzheimer's disease (Nedergaard, Rodriguez & Verkhratsky 2010). The understanding of astrocytes importance in nervous system functioning is increasing, especially in the modulation of neural activity (Nedergaard, Rodriguez & Verkhratsky 2010). Most of the current knowledge and comprehension of astrocytes is from the *in vitro* studies,

astrocyte cultures are continuing to provide a useful tool in exploring the diverse property of these cells (Halonen, Weiss & Chiu 1998; Pinheiro et al. 2006).

2.1.1.3 Parasite proteome investigations using 2-DE and 2D-DIGE

Several proteomic studies on *T. gondii* have elucidated the specialized invasion organelles and their composition, as well as proteins associated with the cytoskeleton (Bradley et al. 2005; El Hajj et al. 2006; Xia et al. 2008). For example; rhoptry proteomic investigation in *T. gondii* (RH strain) was carried out by Bradley *et al.* (2005) through the application of SDS-PAGE coupled with MS analysis. A total of 38 novel rhoptry proteins were discovered and the first *T. gondii* genes encoding rhoptry neck proteins were identified, along with novel proteases, phosphatase proteins that may be associated with the parasites invasion, survival and growth processes (Bradley et al. 2005). Xia *et al*. (2008) used 2-DE in combination with tandem mass spectrometry, and multidimensional protein identification technology (Mud-PIT) for characterizing the proteome of three different strains of *T. gondii* (GT1, ME49 and VEG), and 2252 proteins were identified.

Hill *et al*. (2011), characterised sporozoite specific antigen from *T. gondii* through the use of 2-DIGE in combination with tandem MS. Zhou *et al*. (2013), explored the proteomic profiles of three lineages in *T. gondii* (Type I, II and III) by 2D-DIGE along with MS. The total numbers of differentially expressed proteins were 84, in which similar protein profiles were detected between type I and II lineages of *T. gondii*, while type III was found with different protein profiles. Two different strains of *T. gondii* tachyzoites proteomic profile changes were also compared using 2D-DIGE. A total of 56 proteins matching to *T. gondii* were identified which included surface antigen (SAG1), heat shock protein 70 (HSP70), disulfide isomerase, coronin, heat shock protein 60 (HSP60), pyruvate kinase, receptor for activated C kinase 1, and peroxiredoxin. Most of the differentially expressed proteins were related to biological regulation, metabolic process, response to stress, binding, antioxidant activity, and transporter activity and glycolysis pathway (Zhou et al. 2014).

In *N. caninum* proteomic investigations; Shin *et al*. (2005) investigated the possible relationship between two distinct isolates of *N. caninum* (KBA-2 and VMDL1) using 2-DE and identified many proteins such as heat shock protein 70, subtilisin-like serine protease, nucleoside triphosphatase in the two isolates. Significant homology in the proteome and antigenic proteome profiles between the two *N. caninum* isolates were observed, though isolated from distinct geographical locations (Shin et al. 2005). Comparative investigation of two isolates of *N. caninum* (KBA-2 and JPA1) and RH strain of *T. gondii* were investigated through 2-DE by Lee *et al.* (2005). The study displayed increased similarities between *N. caninum* isolates (KBA-2 and JPA1), whereas differences in protein expressions between *N. caninum* and *T. gondii* were observed, as proteins NcSUB1, NcGRA2 and NcGRA7 are thought be species-specific proteins for *N. caninum* tachyzoites (Lee et al. 2005). However, there were no reported studies of the application of 2D-DIGE in the investigation of *N. caninum* parasites.

In other host cells investigation; Nelson *et al*. (2008) described the proteomic analysis of *T. gondii* infected human foreskin fibroblasts (HFFs) *in vitro* using 2D-DIGE which revealed that the proteome of host cell responded in a dramatic way to *T. gondii* invasion associated with modulations of the host metabolic pathways, including glycolysis, lipid and sterol metabolism, mitosis, apoptosis, and structural-protein expression.

2.1.2 Aims and objectives

In this chapter, the main aim was to investigate differential protein modulation of the host cell response to *T. gondii* and *N. caninum* infection. The hypothesis is that host responses during infection will reflect differences in the proteins being translated during infection between the two parasites. The investigation of global proteome profile changes during host infection will be carried out using 2D-DIGE, mass spectrometry (LC-MS/MS) and bioinformatic analysis. Human astrocytes are a good model system for CNS investigation *in vitro*. It is one of the most abundant

cells in the brain and can be successfully cultured *in vitro* compared to other cells of the CNS such as neurons. In addition, both parasites have been found to infect astrocytes at a higher rate compared to neurons and microglia cells (Pinheiro et al. 2006; Jesus et al. 2013; Halonen et al. 1996). In order to understand biological changes occurring in the hosts CNS during infection with tachyzoites of *T. gondii* compared to *N. caninum*; proteomic investigation of these cells will help to identify key differences between parasite infections in cells of the CNS. As *T. gondii* is found more frequently in intermediate host brain cells compared to *N. caninum* which was mainly detected in a low number of dogs and cattle.

2.2 Materials and methods

2.2.1 Cell culture

2.2.1.1 Human Astrocytes (HA)

Human astrocyte (HA) cells (ScienCell Research Laboratories, USA) are primary cell lines isolated from human brain cerebral cortex that have a limited lifespan and can only be maintained up to five passages. Prior to seeding HA cells, the flasks need to be coated with poly-L-lysine hydrobromide (mol. wt. 70,000-150,000, Sigma Aldrich) in order for the cells to attach on the surface. Poly L-lysine was (0.1 mg/ml) coated on surfaces of T75 cm^2 flasks for 5 minutes with 1 ml of the suspension, then flasks washed twice with ddH_2O and left to incubate for a minimum of 2 hours in the incubator. A total of 15 ml of Dulbecco's Modified Eagle's Medium/Ham's Nutrient Mixture F12 (DMEM-F12) (Sigma Aldrich, UK) was inserted in each flask prepared with 10 % (v/v) foetal bovine serum (FBS) (Sigma Aldrich), 100 U/ml penicillin and 100 µg/ml streptomycin sulphate (Sigma-Aldrich) and filtered prior to use. Flasks were seeded with HA cells incubated at 37°C and 5 % CO_2, and medium was changed every three days for cell maintenance, where they were left until they reached 80-90% confluence and were passaged into new coated flasks.

2.2.1.2 Human astrocyte cell passage

A total of 15 ml of fresh DMEM-F12 medium was added to the poly-L-lysine coated T75 flask. Confluent HA cells were first washed with 10 ml of Dulbecco's Phosphate Buffered Saline (DPBS), without calcium chloride and magnesium chloride (Sigma Aldrich), followed by incubation for 2-3 minutes in 2 ml Trypsin-Versene (EDTA) mixture (Lonza) in addition to 8 ml of DPBS, at 37°C and 5 % CO_2 until cells round up and detached. Detached cells were transferred to 5 ml filtered FBS in 50 ml centrifuge tubes. If some cells were still attached, flasks were gently tapped to dislodge cells and added to the tubes. Tubes containing the cells were centrifuged at 188 x g for 5 minutes, the supernatant was carefully discarded and cells were

resuspended in 5 ml DMEM-F12 medium. The numbers of cells were calculated using a haemocytometer; coated T75 cm^2 were seeded with 4 x 10^5 cells/flask and incubated at 37°C and 5 % CO_2. The medium was changed every three days until cells reached 80-90% confluency, then either passaged for maintenance or directly used for the experiment.

2.2.1.3 Vero cell passage

Vero cells are monolayer cells of African green monkey kidney fibroblasts. They were used to culture and grow the parasites. Confluent vero cells in 25 cm^2 tissue culture flasks were washed with 5 ml 1M HEPES Balanced Salt Solution (Sigma-Aldrich) before incubating the cells for 5 minutes in 5 ml Trypsin-Versene (EDTA) mixture, at 37°C and 5 % CO_2. The cell suspension was centrifuged for 5 minutes at 1500 x g, and then resuspended in 5 ml IMDM (Iscove's Modified Dulbecco's Medium, Lonza). The medium was supplemented with 10 % (v/v) foetal calf serum (Sigma Aldrich), 100 U/ ml penicillin and 100 µg/ml streptomycin sulphate (Sigma-Aldrich) and filtered prior to use. A haemocytometer was used for calculating the number of cells, before they were seeded at a ratio of 1 x 10^5 per 5 ml IMDM/ 25 cm^2 flask.

2.2.1.4 Parasite passage

Two different lineages of *T. gondii* parasites were used in this experiment; the virulent type I (RH strain) and a less virulent type III (VEG strain) and one strain of *N. caninum* (Liverpool isolate). At 24 hours post seeding, when vero cells reached 10-20 % confluency, they were infected with 4 x 10^5 tachyzoites through counting the parasites using a haemocytometer. *T. gondii* (type I strain (TgRH) and type III strain (TgVEG)) and *N. caninum* Liverpool isolate (NcLIV) tachyzoite stages were passaged twice weekly onto a layer of vero cells and parasites were maintained at 37°C and 5 % CO_2, which were then left to grow for 3-4 days before harvesting them with a

sterile cell scraper. Parasites were then either passaged into new cells, or isolated for use in experiments.

2.2.1.5 Parasite isolation

Tachyzoites of TgVEG, TgRH and NcLIV were isolated from host cells by filtration through 47 mm diameter 3 µm pore-sized Nucleopore™ polycarbonate membranes (Whatman). Then, they were washed twice in phosphate-buffered saline (PBS) pH 7.4 by centrifugation at 1500 x g for 10 minutes. The supernatant was discarded, and parasites were resuspended in DMEM-F12 and were used to infect either HA cells for the experiment or vero cells for parasite maintenance.

2.2.1.6 Human astrocyte cell infection

Purified tachyzoites were applied to confluent HA cells at an infection ratio of 10 parasites per cell through counting the cells and parasites using a haemocytometer. As a control (mock infection); uninfected HA cells were harvested and mixed with the same amount of parasites as added to the infected cells (*Neospora* and *Toxoplasma* RH), parasites were inserted directly prior to centrifugation to keep the proportion of host and parasite material the same for each sample. Two replicates of each flask (i.e. infected and uninfected) were collected at 24 hours post infection. Cells were harvested then washed twice with Dulbecco's Phosphate-Buffered Saline (DPBS) through centrifugation at 188 x g for 5 minutes. Afterwards, the numbers of cells were calculated and a final wash and centrifugation at 13000 x g was applied for 5 minutes, supernatant was discarded and pellets were collected and stored in -20°C.

2.2.2 2D-DIGE

2.2.2.1 Human astrocyte cell lysis

The cell pellets were lysed in 500 µl of lysis buffer (30mM Tris, 2M Thiourea, 7M Urea, 4% CHAPS) along with 10 µl DNases/RNases (100 mg) and 5 µl of protease inhibitors. The samples then were subjected to five cycles of freeze-thaw procedures (freezing in liquid nitrogen, thawing at 29°C and briefly vortexing) before centrifuging at 13000 x g for 10 minutes to remove any remaining cell debris.

2.2.2.2 2D Clean up

In order to remove any salts, detergents, lipids, nucleic acids and percipitate present in the samples a 2D-clean up kit (GE Healthcare) was used. All steps were carried out on ice unless stated otherwise according to the manufacturer's protocol. Briefly, 300 µl of precipitant was added to each sample and mixed by vortexing before being incubated on ice for 15 minutes. Then, 300 µl of co-precipitant was added to each sample and vortexed briefly before centrifugation at 13 000 x g for 5 minutes.

The supernatant was discarded and the tubes centrifuged once more to guarantee that any remaining supernatant was removed. Then, 40 µl of co-precipitant was carefully layered on top of the pellet, to avoid pellet disturbance and were incubated on ice for 5 minutes. Samples were centrifuged again and the supernatant was discarded. Next, 25 µl of ddH_2O was added to each pellet and vortexed until the pellet was dispersed but not completely dissolved in the solution. A total of 1 ml of chilled wash buffer was added together with 5 µl of wash additive and the tubes were incubated at -20°C for at least 30 minutes, making sure that the samples were vortexed for 20-30s every 10 minutes. Then, samples were centrifuged at 13 000 x g for 5 minutes and the supernatant was decanted before the pellet was left to air dry for a maximum of 5 minutes. Finally, the pellets were

resuspended in 40 µl of 2x sample buffer (2M Thiourea, 7M Urea, 2% CHAPS), followed by determining the protein concentration in each sample.

2.2.2.3 Bradford assay

In order to determine protein concentrations, a Pierce Coomassie plus (Bradford) protein assay (Thermo Scientific) was used for protein concentration measurements of the samples. Two replicates of protein standards ranging from 2.5-25 µg/ml BSA were prepared. A serial dilution of each sample was applied (1:100, 1:200 and 1:400) and two replicates per sample were used. Then, 150 µl of each standard and also samples were inserted on a 96 well plate; 150 µl of Coomassie plus reagent was added to all standards and afterwards left to incubate 10 minutes at room temperature. A multiskan Ascent microplate photometer was used at 595 nm to read the absorbance. A standard curve was formed from the absorbance of the standards and the sample concentrations were calculated and verified.

2.2.2.4 2D-DIGE labelling

Before starting the CyDye labelling, it is essential to optimize the concentrations and pH of the samples for efficient labelling with CyDyes. Samples were adjusted to 5 µg/µl and pH 8-9. The CyDyes were reconstituted with anhydrous dimethylformamide (DMF) and a working solution of 400 pmol/µl was prepared through mixing and vortexing, followed by centrifugation at 12 000 x g for 30 seconds. For each protein sample, a total of 50 µg was labelled with 1 µl of the appropriate CyDye and combined according to the gel they would be loaded onto (as stated in the experimental design (Table 2.1)) as well as 50 µg of the internal standard for each gel. The pick gel (gel 6); in which the proteins of interest will be excised from includes a gel containing an equal amount of pooled protein samples without labelling the proteins with CyDye's labelling (Table 2.1). All samples were mixed thoroughly and centrifuged briefly before incubating them for 30 minutes on ice in the dark. The reaction was brought to an end by adding 1 µl of 10 mM lysine

to each reaction before being further incubated on ice for 10 minutes in the dark. The internal standard, labelled with Cy2, was prepared by pooling 25 µg of each sample in each gel and was included on every gel. Therefore, a standard was available for every spot on the gel, and all gels could be quantitatively linked within the same experiment. The internal standard minimizes gel-to-gel variation, thus technical replicates were not essential for this experiment. In the experimental design (Table 2.1); dye-swapping approach was applied to control any dye-specific effects that may result from preferential labelling or different fluorescence characteristics of acrylamide at the different wavelengths of excitation for Cy2, 3 and 5, particularly at low protein spot volumes.

Table 2.1: 2D-DIGE experimental design performed on 24 hour p.i. HA cells infected with *Toxoplasma* RH, *Toxoplasma* VEG or *N. caninum* LIV along with controls (mock infections) were used in this experiment. For the internal standard; a total of 50 µg was needed/gel.

Gel number	Cye 2	Cye 3	Cye 5
1	Internal standard HA infected (TgRH 1 + mock NcLIV 1)	HA infected with TgRH 1	mock infected HA with NcLIV 1
2	Internal standard HA infected (NcLIV 1 + TgVEG 2)	HA Infected with NcLIV 1	HA infected with TgVEG 2
3	Internal standard HA infected (mock TgRH 2 + TgRH 2)	mock infected HA with TgRH 2	HA infected with TgRH 2
4	Internal standard HA infected (TgRH 2 + NcLIV 2)	HA infected with TgRH 2	HA infected with NcLIV 2
5	Internal standard HA infected (mock NcLIV 2 + mock TgRH 2)	mock infected HA with NcLIV 2	mock infected HA with TgRH 2
6 (Pick gel)	All 10 samples combined together (unlabelled) (TgRH 1, mock NcLIV 1, NcLIV 1, TgVEG 2, mock TgRH 2, TgRH 2, mock NcLIV 2, mock NcLIV 2 and mock TgRH 2)		

2.2.2.5 IPG strip rehydration

Each sample mixture was combined with 450 µl rehydration buffer (8M urea, 2% CHAPS, 0.002% bromophenol blue) including 40 mM Dithiothreitol (DTT) and 0.5% IPG buffer pH3-10 (GE Healthcare). The solution was then loaded to one reservoir slot of the immobiline DryStrip reswelling tray (GE Healthcare). A 24 cm pH 3-10 nonlinear NL IPG strip (GE Healthcare) was placed in the reservoir slot for each sample with the gel side down, was covered with cover fluid (GE Healthcare) and left to rehydrate in the dark overnight at room temperature. For the pick gel a total of 300 µg of protein (made from a combination of 30 ug of each sample, Table 2.1) was loaded onto the strip.

2.2.2.6 Isoelectric focussing (IEF)

First-dimension separations were carried by focussing the rehydrated strips using the Ettan IPGphor II (GE Healthcare) at 30V for 5hours, 500V for 1 hour, 100V for 1hour, 8000V for 2 hours and 8000V for 9 hours with current restricted to 50 µA/strip. The strips were either directly used or carefully stored at -20°C.

2.2.2.7 Second dimension SDS-Page

In the second dimension, proteins were separated using 12.5% precast acrylamide gels (size 255 x 196 x 1 mm) (GE Healthcare). For the pick gel, the IPG strip was applied on a 12.5% precast gel. The pick gel was prepared using low fluorescence glass plates (size 255 x 196 x 1 mm) treated with bind saline solution (80% (v/v) ethanol, 18% (v/v) ddH_2O, 2% (v/v) acetic acid, 0.1% (v/v) γ-methacryloxypropyltrimethoxysilane) and left to dry completely (minimum of 2 hours) before casting. Reference markers were inserted to each treated glass plate to allocate references to orientate the automated spot picker. A 12.5% acrylamide

gel was prepared (40% (v/v) bis-acrylamide, 25% (v/v) Tris-HCl, pH 8.8, 30% (v/v) ddH_2O and 10% SDS, 0.01% (w/v) ammonium persulphate APS and 0.001% (v/v) TEMED) and poured straight away into the casting unit before placing on top a 0.1% solution of SDS and leaving them to polymerise overnight at room temperature.

2.2.2.7.1 Strip equilibration

For strip equilibration; two steps were carried out. Firstly, IPG strips were incubated in equilibration buffer (2% (w/v) SDS, 50 mM Tris-HCl pH 8.8, 6M urea, 30% (v/v) glycerol and 0.002% (w/v) bromophenol blue) containing 100 µg of (10 mg/ml) DTT for 15 minutes at room temperature with shaking. The IPG strips were then transferred to equilibration buffer containing 250 µg (25 mg/ml) iodacetamide (IAA) and incubated for further 15 minutes to alkylate the cysteine residues.

2.2.2.7.2 2D gel electrophoresis

The equilibrated strips were assembled onto a DALT precast gel carefully and sealed in with an agarose sealing solution (25 mM Tris, 192 mM glycine, 0.1% (w/v) SDS, 0.5% (w/v) agarose, trace bromophenol blue). The gels were assembled in an Ettan Dalt six electrophoresis system (GE Healthcare) and the tank was filled with electrophoresis buffer (2.5 mM Tris-base, 19.2 mM glycine, 0.02% (w/v) SDS). The gels were run at 5W per gel for 30 minutes and afterwards adjusted to 17W per gel for 4 hours until the tracking dye reached the bottom of the plate. The same previous steps were also carried out on the precast gel for the pick gel.

2.2.2.8 Staining of pick gel with SYPRO™ Ruby

To visualize the proteins present on the pick gel, SYPRO™ Ruby protein gel stain (Sigma-Aldrich) was used. The gel was fixed in 40% (v/v) MeOH, 10% (v/v) acetic acid for one hour and stained with SYPRO™ Ruby gel stain overnight. The gel was

then washed in 10% (v/v) MeOH, 7% (v/v) acetic acid for one hour followed by two 5 minutes washes in ddH_2O prior to gel imaging.

2.2.2.9 Scanning the gels

The gels were scanned immediately after the electrophoresis step using an Ettan DIGE imager (GE Healthcare) that was set at 100 pixels and 0.800 exposures on all three CyDye channels (Cy2, Cy3 and Cy5) (Table 2.2). For the pick gel, SYPRO Ruby conditions were used at the settings as described in Table 2.2.

Table 2.2: Filter parameters for each Cydye as recommended by Ettan DIGE System (GE Healthcare) for scanning the gels.

Dye	Excitation filter (nm)	Emission filter (nm)
Cy2	480/30	530/40
Cy3	540/25	595/25
Cy5	635/30	680/30
SYPRO Ruby	540/25	595/25

2.2.2.10 Decyder-2D image analysis

The DeCyder-2D image analysis software (version 7.0) (GE Healthcare) was used for the analysis of DIGE images. A total of fifteen gel images produced from three channels of the five 2D-DIGE gels were loaded onto the DeCyder software and the differential in gel analysis (DIA) module was used to detect the number of spots on one gel (Figure 2.2). All spots in each gel were then identified using the batch processor and the output files were then opened in the Biological Variation Analysis section (BVA) module. Gel to gel matching of spots was carried out in the BVA module using the match detection algorithm allowing quantitative comparisons of protein expression across multiple gels (Figure 2.2). One of the Cy2 internal standard images was allocated as a master gel status and all other images were then matched to it either by automated Batch Processor or manual curation, sorting

common protein spots across the gels. The student's T-test was used to determine whether changes in volume of specific spots were significant between samples from different experimental groups. Protein spots which displayed a greater than 1.5 fold change ($p<0.05$) between the samples were reported. The pick gel was loaded onto the DeCyder-2D software and assigned as the pick gel in the BVA module. The protein spots of interest were matched onto the pick gel and a pick list was exported by DeCyder-2D software.

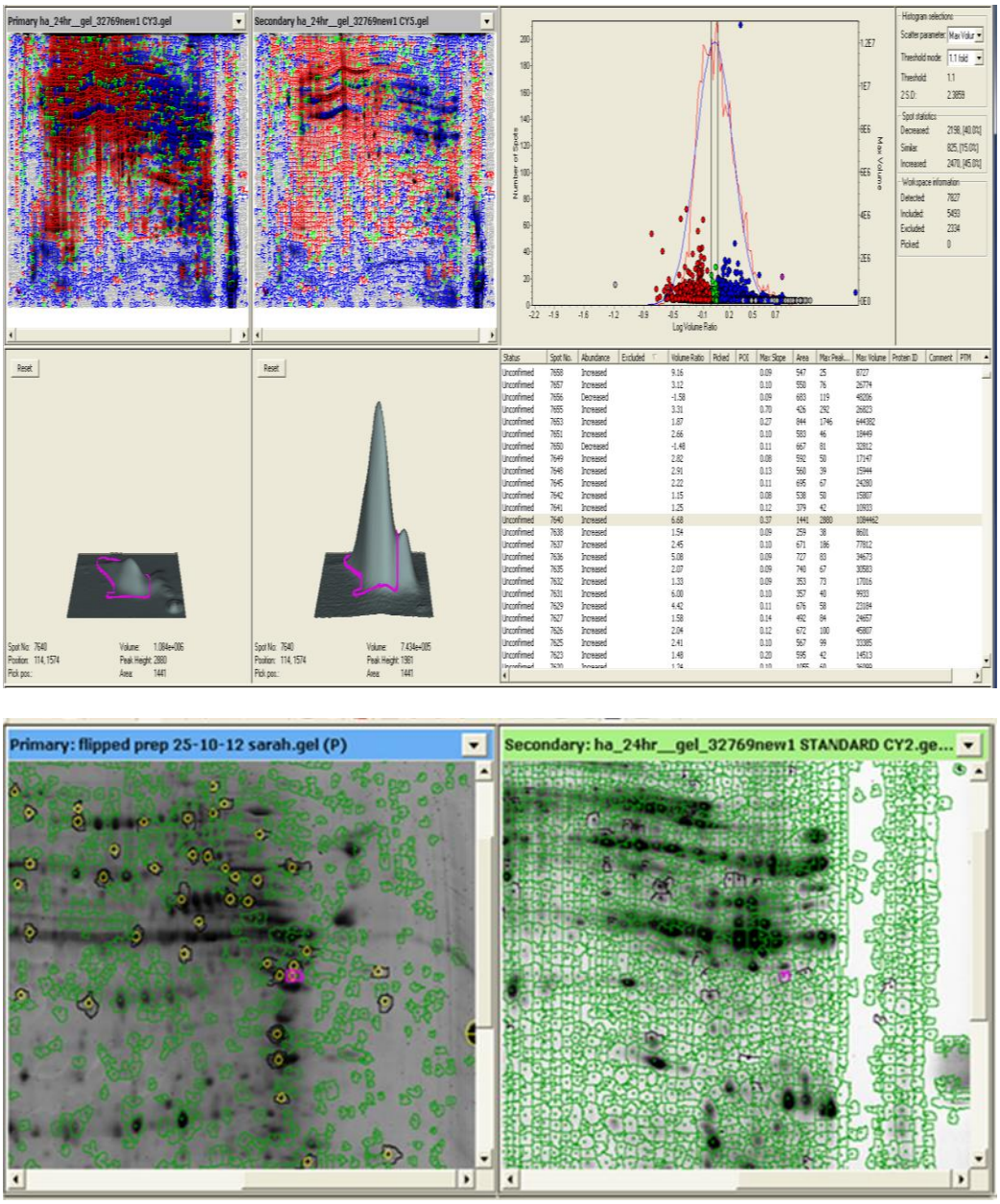

Figure 2.2: An example of DIA analysis in DeCyder showing total number of proteins increased, decreased or similar on the top right. On the top left corner; images of the gels that are being compared and on the bottom left corner an example of a protein spot decreased. BVA analysis in DeCyder showing on the top the internal standard image where the protein of interest were matched with the top left image of the pick gel and proteins were assigned to be picked (yellow).

2.2.2.11 Spot picking

The protein spots of interest were excised from the pick gel using an Ettan™ spot picker (GE Healthcare) that automatically calculates the locations of the selected spots through the identification of the reference markers positions attached to the glass plates.

2.2.3 Protein Identification

2.2.3.1 Trypsin digestion

The gel spots were digested using trypsin in order to generate peptides appropriate for analysis by mass spectrometry. To guarantee the removal of any stain from the plugs, each plug was incubated at 37°C for 10 minutes in 10 µl of 50 mM ammonium bicarbonate/50% acetonitrile (in HPLC grade water); the liquid was discarded and the step repeated. A dehydration step was then followed by adding 10 µl of 100% acetonitrile to each gel spot and incubated at 37°C for 15 minutes. After removing the solvent from the dehydrated gel plug, the tubes were left to incubate at 37°C until all traces of the solvent had evaporated for 10 minutes. Trypsin stock solution (0.1 µg/µl) was diluted 1 in 10 with 25 mM ammonium bicarbonate and 10 µl of this was inserted on each plug and incubated at 37°C for 1 hour. A further 10 µl of 25 mM ammonium bicarbonate was added and samples incubated overnight at 37°C. The reaction was stopped by storing the samples at -20°C.

2.2.3.2 Tandem mass spectrometry LC-MS/MS

Tandem mass spectrometry was performed by Dr. Stuart Armstrong and Dr. Dong Xia (Liverpool) as follows: peptide mixtures (1 µg) were analyzed by on-line nanoflow liquid chromatography using the nano ACQUITY-nLC system (Waters)

coupled to an LTQ-Orbitrap Velos (ThermoFisher Scientific) mass spectrometer equipped with the manufacturer's nanospray ion source. The analytical column (nanoACQUITY UPLCTM BEH130 C18 15 cm x 75 µm, 1.7 µm capillary columns) was maintained at 35 ^{o}C and a flow-rate of 300 nl/minute. The gradient consisted of 3-40 % acetonitrile in 0.1 % formic acid for 90 minutes then a ramp of 40-85 % acetonitrile in 0.1 % formic acid for 3 minutes. Full scan MS spectra (m/z range 300-2000) were acquired by the Orbitrap at a resolution of 30,000. Analysis was performed in data dependant mode. The top 20 most intense ions from MS1 scan (full MS) were selected for tandem MS by collision induced dissociation (CID) and all product spectra were acquired in the LTQ ion trap. Ion trap and orbitrap maximal injection times were set to 50 ms and 500 ms, respectively.

2.2.3.3 Protein identification using Mascot

The generated raw files were converted to mgf files (mascot generated files) in order to search for the proteins in MASCOT Daemon™ search engine Version 2.3.2 (Matrix Science). From the ESI-LTQ Orbitrap Velos, the monoisotopic peaks were extracted from the raw data, and searched against the relevant database (*Homo sapiens* in Uniprot database). The enzyme trypsin, fixed modification of Carbamidomethyl (C) and variable modification of oxidation (M), 1 missed cleavage site and charge states +1, +2, and +3 were all specified. Only identifications with scores of $p<0.05$ were accepted. The data was searched against a decoy database of reversed peptide sequences to attain a false discovery rate (FDR).

2.2.3.4 Bioinformatics analysis

Proteins that were identified were searched in Uniprot Protein knowledgebase (http://www.uniprot.org/) for their functions; gene ontology, cellular content and molecular functions. No further functional annotations or pathway analysis were carried out due to the low number of proteins identified and variations between the pick gel and the internal standard gels it was difficult to allocate each specific

protein of interest and this has led to the low number of proteins identified. Functional analysis of HA cell proteins that were statistically significant (p-value<0.05 and ≥2 hits) were also investigated using the functional analysis and clustering tool from the Database for Annotation, Visualisation, and Integrated Discovery (DAVID) (DAVID bioinformatics resources 6.7) (Huang et al. 2009). Proteins were searched in DAVID for metabolic pathway analysis (KEGG pathway) and functional annotations; for their GO biological processes, molecular function and cellular content.

2.3 Results

2.3.1 Identification of host cell proteins modulated at 24 hours post infection

2D-DIGE was used to compare proteomic differences in the host cell response to infection with *N. caninum* and *T. gondii*. After IEF and 2-DE, the analysis of the six gel scanned images were aligned and statistical analysis performed to differentially modulated protein detection using Decyder-2D. In order for a spot to be determined statistically significantly different, a t-test p-value of ≤ 0.05 and ≥1.5 fold change from the BVA analysis (In total, 55 spots were detected before assigning them on the pick gel) . The use of the mixed internal standard allowed the detection of significant abundance changes, based on the variance of the mean change within the cohort. Overall, a total of 26 spots were found statistically different of *Neospora* infected cells with *Toxoplasma* infected cells (VEG, RH), and infected cells (*N. caninum* or *T. gondii*) compared to uninfected HA cells (mock infected) (Appendix I). The spots were excised, digested and run on the LC-MS/MS. Raw data from the mass spectrometer was searched in MASCOT using human database search parameter, only proteins with a score> 40 and ≥2 peptide hits were selected. Due to technical difficulties the pick gel had to be re-run at a later date, therefore variations between the gels were likely to occur. Moreover, there was an amount of contaminants seen on the gel which makes it difficult to distinguish individual spots.

The spots identified and quantified in HA cells were as follow: nine spots identified as differentially modulated comparing TgRH2 with NcLIV2, four spots differentially modulated between NcLIV1 and TgVEG2, five spots identified between NcLIV and NcLIV control (mock infected), four spots between TgRH and TgVEG and four spots between TgRH and TgRH control (mock infected). Since the main aim was to investigate differences in host cells (HA) that occur between *T. gondii* and *N. caninum*, thus, only TgRH with NcLIV (nine spots) (Figure 2.3) and NcLIV with TgVEG (four spots) (Figure 2.4) were further analysed.

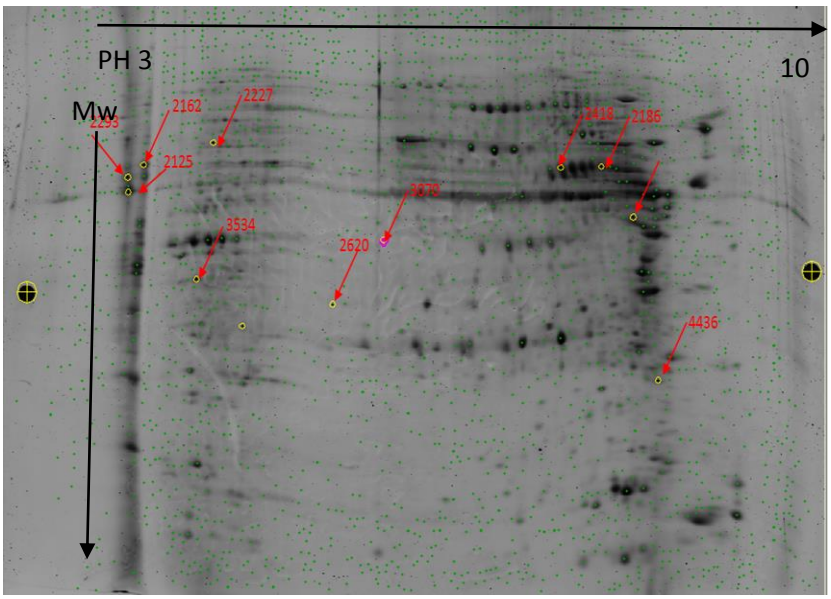

Figure 2.3: 2D-DIGE pick gel showing spots that were differentially modulated between TgRH and NcLIV either increased or decreased and assigned spot number (red arrows).

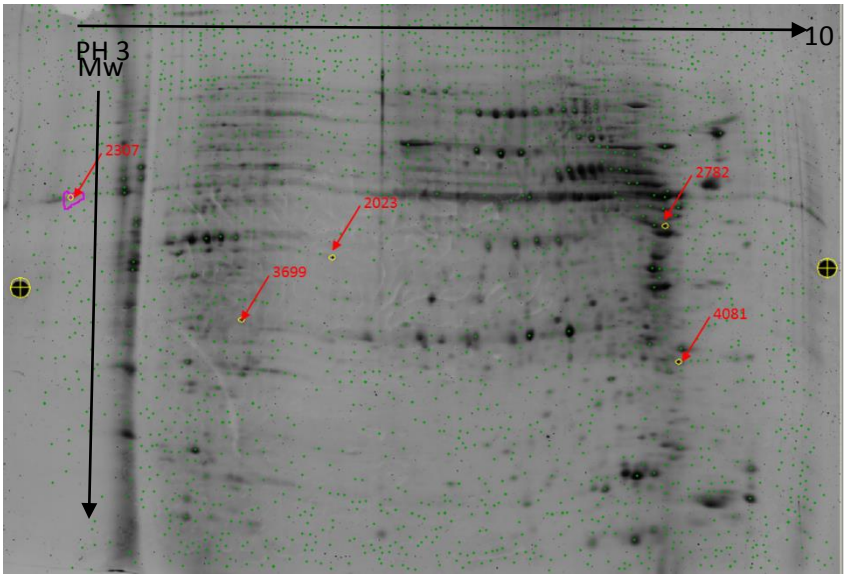

Figure 2.4: 2D-DIGE pick gel showing spots that were differentially modulated between TgVEG and NcLIV either increased or decreased and assigned spot number (red arrows).

Several protein identifications resulted from each digested spot (Appendix I) therefore the protein ID with the highest Mascot score and peptide count was

selected and others were excluded, in which each spot gave one ID as seen in Table 2.3. Most of the modulated proteins were identified at several different places on a single gel, indicating that multiple isoforms and/or post-translationally modified forms might be present for that protein. In these instances, it was not always possible to assign a simple increased or decreased modulation to the protein.

Proteins showing decreased modulation in HA cells infected with NcLIV when compared to TgRH infected cells were; ankyrin-3 (ANK3), L-lactate dehydrogenase A chain (LDHA), ribosome-releasing factor 2, mitochondrial (RRF2M), ATP synthase subunit alpha, mitochondrial (ATPA) and transgelin (TAGL) (Table 2.3). The four proteins that were increased in NcLIV compared to TgRH were: nesprin-2 (SYNE2), sodium/potassium-transporting ATPase subunit alpha-1 (AT1A1), creatine kinase B-type (KRCB) and heat shock protein 60 kDa (CH60) (Table 2.3).

In the comparison of modulated proteins between HA cells infected with NcLIV and cells infected with TgVEG; two proteins were decreased in cells infected with NcLIV compared to TgVEG (78 kDa glucose-regulated protein (GRP78) and actin, cytoplasmic 1 (ACTB); whereas vimentin (VIME) was increased in two different protein spots (Table 2.4).

Table 2.3: Host cell proteins differentially modulated in response to infection with *T. gondii* and *N. caninum* (HA cells infected with NcLIV compared to TgRH). Proteins were identified by mass spectrometry analysis and searched against the human database using MASCOT. Up-regulated proteins (fold changes) are highlighted in red, down-regulated proteins are highlighted in green. Spot numbers are as labelled on the pick gel (as seen in Figure 2.3 and 2.4)

Spot number	Accession number	Protein	Protein description	Protein score	Protein mass (Da)	Protein match	t-test	fold change (NcLIV/TgRH)
2418	Q12955	ANK3	Ankyrin-3	67	482394	19	0.045	-4.57
4436	P00338	LDHA	L-lactate dehydrogenase A chain	225	37061	6	0.026	-2.39
2638	Q969S9	RRF2M	Ribosome-releasing factor 2, mitochondrial	58	87512	4	0.004	-1.77
3534	P25705	ATPA	ATP synthase subunit alpha, mitochondrial	658	59939	16	0.036	-1.51
2293	Q01995	TAGL	Transgelin	348	22764	14	0.026	-1.51
2227	Q8WXH0	SYNE2	Nesprin-2	72	801817	18	0.013	2.67
2620	P05023	AT1A1	Sodium/potassium-transporting ATPase subunit alpha-1	353	114246	6	0.027	2.54

3070	P12277	KCRB	Creatine kinase B-type	319	43013	8	0.021	2.03
2125	P10809	CH60	60 kDa heat shock protein, mitochondrial	366	61298	13	0.045	1.53

Table 2.4: Host cell proteins differentially modulated in response to infection with *T. gondii* and *N. caninum* (HA cells infected with NcLIV compared to TgVEG). Proteins were identified by mass spectrometry analysis and searched against the human database using MASCOT. Up-regulated proteins (fold changes) are highlighted in red, down-regulated proteins are highlighted in green. Spot numbers are as labelled on the pick gel (as seen in Figure 2.3 and 2.4)

Spot number	Accession number	Protein	Protein description	Protein score	Protein Mass (Da)	Protein match	t-test (p-value)	fold change (NcLIV/ TgVEG)
2023	P11021	GRP78	78 kDa glucose-regulated protein	90	72513	3	0.0006	-2.07
2307	P60709	ACTB	Actin, cytoplasmic 1	221	42163	6	0.028	-1.89
2782	P08670	VIME	Vimentin	639	53787	16	0.02	1.68
4081	P08670	ViME	Vimentin	980	53787	29	0.045	1.54

2.3.2 Functional annotation of host cells proteins

In order to allocate functional information to the 12 proteins that were identified, Uniprot Protein knowledgebase (http://www.uniprot.org/) was used. Each protein was searched individually for their biological process, cellular content and molecular function as described in Table 2.4. Proteins that were found increased in cells infected with TgRH compared to NcLIV were involved in different biological processes such as axon guidance, glycolysis, cell adhesion and protein biosynthesis; whereas the proteins that were decreased were involved in cell migration, ATP biosynthetic process (Table 2.5).

Proteins that were increased in HA cells infected with TgVEG compared to cells infected with NcLIV were associated with astrocyte development and protein transport and translation; while the decreased infected cells were involved in metabolic processes and signalling pathways (Table 2.5).

Functional analysis of the modulated host proteins were also investigated using DAVID. Unfortunately, no metabolic pathways were identified and functional annotations; for their GO biological process were not significant and the number of proteins associated with each biological process were low (2 proteins). Cellular content was associated with cell projection and ER (Table 2.6).

Table 2.5: Proteins identified differentially modulated between cells infected with *T. gondii* compared to *N. caninum*, proteins were searched in Uniprot Protein knowledgebase. Cellular components, biological process and molecular functions were identified.

Protein	Accession number	Protein description	Cellular component	Biological process	Molecular function
ANK3	Q12955	Ankyrin-3	Cytoplasm Golgi apparatus	Axon guidance	Cadherin binding & protein binding
LDHA	P00338	L-lactate dehydrogenase A chain	Cytoplasm	Glycolysis cellular metabolic process	L-lactate dehydrogenase activity
RRF2M	Q969S9	Ribosome-releasing factor 2, mitochondrial	Mitochondrion	Protein biosynthesis GTP catabolic process	GTP binding
DPP4	P25705	Dipeptidyl peptidase 4	Cell membrane	Cell adhesion T cell activation	Aminopeptidase
TAGL	Q01995	Transgelin	Cytoplasm	epithelial cell differentiation	Muscle protein
SYNE2	Q8WXH0	Nesprin-2	Cytoplasm Mitochondrion	positive regulation of cell migration	actin binding
AT1A1	P05023	Sodium/potassium-transporting ATPase subunit alpha-1	Cell membrane	ATP biosynthetic process Sodium/potassium transport	ATP binding
KCRB	P12277	Creatine kinase B-type	Cytoplasm	cellular chloride ion	ATP binding

				homeostasis Creatine metabolic process	
CH60	P10809	60 kDa heat shock protein, mitochondrial	Mitochondrion	Host-virus interaction T and B cell activation	Chaperone
GRP78	P11021	78 kDa glucose-regulated protein (HSP70)	Cytoplasm Endoplasmic reticulum	ATP catabolic process Metabolic process	chaperone binding
ACTB	P60709	Actin, cytoplasmic 1	Cytoplasm	Fc-gamma receptor signaling pathway involved in phagocytosis innate immune response	ATP binding
VIME	P08670	Vimentin	Cytoplasm	Host-virus interaction apoptotic process astrocyte development	structural constituent of cytoskeleton

Table 2.6: DAVID analysis of differentially modulated proteins of astrocytes infected with TgVEG, TgrRH and NcLIV. Biological process, cellular components and molecular functions were identified.

Category	Term	Protein count	% of proteins inserted	P-Value
Biological process	axonogenesis	2	1.3	5.60E-02
	cell morphogenesis involved in neuron differentiation	2	1.3	6.00E-02
	neuron projection morphogenesis	2	1.3	6.20E-02
	cell morphogenesis involved in differentiation	2	1.3	7.00E-02
	cell projection morphogenesis	2	1.3	7.10E-02
	cell part morphogenesis	2	1.3	7.40E-02
	neuron projection development	2	1.3	7.40E-02
	neuron development	2	1.3	9.70E-02
Cellular component	cell projection	3	2	2.70E-02
	endoplasmic reticulum	3	2	4.80E-02
	intracellular non-membrane-bounded organelle	4	2.6	6.00E-02
	non-membrane-bounded organelle	4	2.6	6.00E-02
	cell fraction	3	2	6.00E-02
	axon	2	1.3	6.10E-02
	cytoskeleton	3	2	9.30E-02

2.4 Discussion

This chapter investigated proteomic profile changes in cells related to the CNS (human astrocytes) during infection with *T. gondii* compared to *N. caninum* infected cells. While *T. gondii* can infect a wide range of hosts including humans; *N. caninum* does not. Moreover, *T. gondii* is known to cause severe neurological pathogenesis in humans; especially in immune-deficient individuals, such as Toxoplasmic encephalitis whereas *N. caninum* can cause neuromuscular disease in dogs. Astrocytes are known to be involved in cell-cell communication of neurons, defence against infectious organisms and provide homeostasis in the brain (Norenberg 1994; Pekny & Nilsson 2005). Moreover, they enable the propagation of *T. gondii* and *N. caninum* (Halonen, Lyman & Chiu 1996; Fagard et al. 1999).

With conventional techniques, studies on proteins can only be conducted on a limited number of proteins. Advances in proteomic analysis nowadays help monitor global changes in protein expression and post-translational modifications. 2D-DIGE exploits mass and charge-matched spectrally resolvable fluorescent dyes (Cy3 and Cy5) to label two different protein samples before 2-DE.

The use of 2D-DIGE as a means to compare proteomes from different infection states gives an outcome of the differences in protein expression between the cellular proteomes; however, it is not a faultless technique. There are many concerns associated with 2D-DIGE analysis, it can be bias towards the most abundant proteins and cannot distinguish the precise protein in each differentially modified spot. Moreover, proteins with large masses along with insoluble proteins may not be detected using 2D-DIGE.

2.4.1 Increased protein expression of human astrocyte cells infected with *T. gondii*

Two different lineages of *T. gondii* parasites were used in this experiment; the virulent type I (RH strain) and a less virulent type III (VEG strain) and one strain of *N. caninum* (Liverpool isolate). It is known that different strains of *T. gondii* cause different host cell response and, as a consequence, pathogenesis of the infected host.

2.4.1.1 Host response to TgRH infection compared to NcLIV

Proteins showing increased modulation in HA cells infected with TgRH compared to NcLIV infected cells were; ANK3, LDHA, RRF2M, ATPA and TAGL (Table 2.3).

Ankyrin-3 (ANK-3), also known as ankyrin-G, is a protein from the ankyrin family that, in humans, is encoded by the ANK3 gene (Kapfhamer et al. 1995). It was up-modulted with more than four fold in cells infected with TgRH compared to cells infected with NcLIV. This protein was initially found at the axonal initial segment and nodes of Ranvier of neurons in the central and peripheral nervous systems participate in the maintenance/targeting of ion channels and cell adhesion molecules. The protein links the integral membrane proteins to the primary spectrin-actin cytoskeleton. The ankyrin protein family play major roles in activities such as cell motility, activation, proliferation and the maintenance of specialized membrane domains. This protein has an important function in axon guidance. This may indicate that TgRH parasites modify ANK3 to enable host invasion and establishment of infection, as ANK3 is associated with cytoskeletal anchoring at plasma membrane and protein targeting.

LDHA was up-modulated more than two fold in TgRH infected HA cells compared to cells infected with NcLIV. Lactate dehydrogenase (LDH) is a glycolytic enzyme that catalyses the conversion of pyruvate to lactate, and plays a crucial role in the glycolysis pathway; that is essential to provide energy to *T. gondii* parasites under anaerobic conditions (Kavanagh, Elling & Wilson 2004). The parasite itself encodes

two genes for lactate dehydrogenase; TgLDH1 and TgLDH2. A study done on knockout mice with LDH1 and LDH2 showed that LDH is essential for parasite differentiation, showed these parasites were unable to exhibit brain cysts in LDH1 & LDH2 knockout mice in the chronic stage of infection (Al-Anouti et al. 2004). Lee *et al*. (2003), identified lactate dehydrogenase as proteins conserved between *T. gondii* and *N. caninum* tachyzoites using 2-DE analysis. This protein is also associated with the glycolysis pathway (Denton et al. 1996), which may possibly be increased in TgRH infection due to the higher need for energy uptake by the fast replicating *Toxoplasma* strain (TgRH) compared to *N. caninum*.

RRF2M is a mitochondrial ribosome protein that mediates the disassembly of ribosomes from messenger RNA at the termination of mitochondrial protein biosynthesis. It is associated with GTP catabolic process in the cell. This protein was up-modulated (1.7 fold) in cells infected with TgRH compared to NcLIV infected cells. It has a role in the regulation of normal mitochondrial function which may indicate TgRH modification of RRF2M to enable nutritional uptake from the host cell mitochondria.

ATPA was only found increased (1.5 fold) in cells infected with TgRH. Mitochondrial membrane ATP synthase produces ATP from ADP in the presence of a proton gradient through the membrane which is produced by electron transport complexes of the respiratory chain. It is linked to cellular metabolic processes that may enable the establishment of TgRH parasitic infection in host cells.

TAGL was also up-modulated (1.5 fold) in cells infected with TgRH. Transgelin a protein found in humans is encoded by the TAGLN gene (Kobayashi, Kubota & Hidaka 1994). The protein encoded by this gene is a transformation and shape-change sensitive actin cross-linking/gelling protein found in fibroblasts and smooth muscles (Camoretti-Mercado et al. 1998). Proteomic analysis of host cells (HFF cells) infected with *T. gondii* by Nelson *et al.* (2008) found that TAGL was down-regulated during infection using a 2D-DIGE method, which contradicts the proteins found in this chapter. This protein is associated with calcium interactions and contractile

properties of the cell and epithelial cell differentiation, which may also be associated with TgRH parasite establishment in host cells.

2.4.1.2 Host response to TgVEG infection compared to NcLIV

Proteins that showed increased expression in cells infected with TgVEG compared to NcLIV infected cells were GRP78 and ACTB (Table 2.4).

GRP78, also called heat shock 70 kDa protein 5, was increased two fold; it is involved in facilitating the assembly of protein complexes inside the endoplasmic reticulum and in the correct folding of proteins and degradation of misfolded proteins through its interaction with DNAJC10. This protein inhibits key effectors of the apoptotic pathway and plays a role in the proteasome-mediated degradation of apoptosis-regulatory proteins (Garrido et al. 2003). Moreover, HSP70 protects cells from stress-induced caspase-dependent apoptosis, both upstream and downstream of the death-associated mitochondrial events (Garrido et al. 2003). Notably, host HSPs have been implicated in immunity to *T. gondii*; through host defence against infection (Hisaeda & Himeno 1997). Another regulatory cascade known to be comprised of HSPs is the stress hypoxia pathway induced in parasite-infected cells (Spear et al. 2006). This may propose that infected cells with TgVEG induce GRP78 to delay or inhibit apoptosis process in the cell compared to infected cells with NcLIV.

Microfilaments are generally made up of actins, microtubules consist of tubulins and intermediate fibres include vimentin and keratin (Sodeik 2000). ACTB was increased 1.89 fold in TgVEG infected cells compared to cells infected with NcLIV. Actins are essential cellular components involved in cellular motility, movement of vesicles and organelles around the cell, cellular division and maintenance of cellular shape. It is known that infection with *Toxoplasma* causes broad remodelling of the host cell at the level of the cytoskeleton (Nelson et al. 2008). Actin and actin-related (ACTB) proteins representing key components of microfilaments were increased in infected cells with TgVEG. Host actin may have a more elusive role during invasion

during the process of attachment and invasion, through the moving junction interaction of *T. gondii* parasite with the host cytoskeleton (Blader & Saeij 2009).

2.4.2 Increased protein expression of host cells infected with *N. caninum*

2.4.2.1 Host response to NcLIV infection compared to TgRH

Four proteins were up-modulated in NcLIV infected cells compared to cells infected with TgRH: nesprin-2 (SYNE2), sodium/potassium-transporting ATPase subunit alpha-1 (AT1A1), creatine kinase B-type (KRCB) and heat shock protein 60 kDa (CH60) (Table 2.3).

SYNE2 was up-modulated more than 2.5 fold in cells infected with NcLIV. Nesprin-2 is a protein which forms a linking network between organelles and the actin cytoskeleton to maintain the subcellular spatial organization. It is associated with the maintenance of nuclear organization and structural integrity. To our knowledge; there is no known function for this protein in relation to *T. gondii* or *N. caninum* invasion/infection process, but may be associated with establishment of *N. caninum* and parasite-host interaction.

AT1A1 was up-modulated more than 2.5 fold in cells infected with NcLIV compared to infected cells with TgRH. This protein is the catalytic component of the active enzyme, which catalyses the hydrolysis of ATP coupled with the exchange of sodium and potassium ions across the plasma membrane and provides energy for active transport. This may suggest that *N. caninum* increases energy production and ion transport to enable its nutrient uptake and enable growth in host cells as AT1A1 provides energy for active transport of various nutrients.

KRCB was increased two fold. It is important in energy transduction in tissues with large, unstable energy needs, such as skeletal muscle, heart and brain, which may also suggest nutrient uptake by *N. caninum*, especially in sites such as the brain.

Another heat shock protein found in this experiment was CH60. It was up-modulated in cells infected with NcLIV (1.5 fold) in comparison to TgRH infected cells (Table 2.3). Human astrocyte heat shock proteins (HSPs) were modulated during parasitic infection in this experiment, which may be linked to an increase in transcription and translation, since HSPs are important in protein processing (Garrido et al. 2003). They are commonly responsible for preventing damage to proteins in response to high levels of heat and are classified into six major families based on their molecular mass: small HSPs, HSP40, HSP60, HSP70, HSP90, and HSP110 (Wu 1995). Additional studies have associated HSP60 to diabetes, stress response, cancer and certain types of immunological disorders. They are present in all cells under normal conditions and during stress (e.g., heat/cold/oxygen deprivation) and can make up to 15% of the total cellular protein content (Pockley 2001). HSPs ensure the correct conformation of proteins and facilitate the degradation of selected proteins by the ubiquitin/proteasome system, as well as their own inherent activities (Garrido et al. 2003).

CH60 is associated with mitochondrial protein import and macromolecular assembly, facilitate the correct folding of imported proteins and prevent misfolding of proteins. This may suggest that the *N. caninum* increases this protein due to its involvement in mitochondrial protein import and macromolecular assembly which may facilitate host-parasite interaction.

2.4.2.2 Host response to NcLIV infection compared to TgVEG

In comparison of modulated proteins between HA cells infected with NcLIV and TgVEG infected cells; only one protein was increased in two different protein spots; vimentin (Table 2.4).

A class of cytoskeletal structures is the intermediate filaments, characterized by the protein vimentin (Wang & Stamenovic 2002). Vimentin has been associated with various functions, from structural roles, cell cycle and mitosis (Wang & Stamenovic 2002), as well as lipid metabolism (Schweitzer & Evans 1998), whose roles in lipid storage and metabolism are the likely link to energy metabolism and mitochondrial

function (Annunen-Rasila et al. 2007). More important, vimentin is known to be reorganized around the parasitophorous vacuole (PV) in *T. gondii*-infected cells (Coppens et al. 2006; Halonen & Weidner 1994). The slight increase in cells infected with *N. caninum* may not indicate notable differences in vimentin modulation by *N. caninum* compared to *T. gondii*. Nelson *et al*. (2008) found vimentin to be increased in *T. gondii* infected HFF cells, which contradicts the findings related to this protein. Another suggestion would be that vimentin is increased in *N. caninum* infected cells for its growth due to its involvement in energy, metabolism processes and mitochondrial function.

Host mitochondria and the endoplasmic reticulum (ER) have a close relationship with *Toxoplasma* and *Neospora* due to their recruitment to, and association with, the parasitophorous vacuole membrane (Sinai, Webster & Joiner 1997). The fundamental roles of both these organelle systems in nearly every aspect of cellular physiology points of remodelling established in the infected cell. From this data, most of the proteins identified were primarily found in these two organelles.

2.4.3 Limitations of 2D-DIGE in host proteome investigations

One of the main concerns with the proteins identified was whether their abundance was due to a contamination occurring on the 2D gels caused by a partial insolubility, or whether it is a true modification of cells responds to infection in protein expression. Each modulated protein spot contained multiple protein identifications, which made determining the exact protein causing differential changes challenging. Though calculating Mascot scores and peptide counts may help in estimating which protein is more dominant within a spot. In the analysis, differentially modulated protein spots that had high score and peptide number were selected from the total number of protein identifications. However, the results and analysis must be viewed with a degree of caution, due to incomplete protein resolution. Also, the numbers of identified protein spots modulated were very low and the dataset is small, both of which need to be taken in consideration when analysing the results. Therefore, an alternative approach in the investigation of proteome expression

profiles of host cell response is needed. Recurrently, the same proteins appeared in many spots across the gel, which complicates the analysis of the data.

In a gel spot from which numerous proteins can be identified it is difficult to define which protein has dominated the changes detected at the gel spot level. Also, a genuine protein change of a low abundance could be masked by a high abundance protein co-migrating that did not have any substantial changes.

A paper published in the Journal of Proteomics investigated the occurrence of individual differentially expressed human, mouse and rat proteins reported in 169 articles in 2-DE experiments between 2004 and 2006 (Petrak et al. 2008). This meta-analysis study has shown that among the most frequently identified differentially expressed proteins were heat shock proteins (HSP60, HSP70), Vimentin, ATP synthase and actins (Petrak et al. 2008) which have also been identified in this chapter. The fact that the most commonly identified proteins are highly abundant soluble proteins raised concerns as to whether their repeated identification represents a technical artefact (Petrak et al. 2008).

2.4.4 Conclusions and future directions

In this chapter, the application of the quantitative proteomic approach 2D-DIGE in understanding protein expression changes of human astrocytes during *Neospora* and *Toxoplasma* tachyzoites invasion was investigated and discussed. 2D-DIGE analysis can provide a large scale quantitative screening of protein expression changes. Proteins have been identified, such as enzyme L-lactate dehydrogenase A chain, that is involved in the glycolysis, as well as Ankyrin3 were found differentially modulated between the infected cells, in which were up-modulated in *T. gondii* infected cells. That may suggest *T. gondii* modulation of proteins for nutritional uptake and regulation of ion transport for the parasites propagation and establishment in cells. While proteins such as Vimentin and Syne2 were up-modulated in *N. caninum* infected cells compared to *T. gondii*, suggesting that *N. caninum* may modify the cytoskeleton of host cells for parasite invasion and entry. However, the results obtained need to be interpreted cautiously. Considerations

related to the separation limitations inherited from 2-DE, as well as the commonly observed occurrences of multiple proteins found at the same gel spot need to be taken in mind. There have been some suggestions that using 2D gels to separate proteins for identification of differentially expressed proteins can lead to similar proteins being found as modulated (Petrak et al. 2008). It is therefore important to ensure that the proteins identified as differentially expressed within a 2D-DIGE experiment are confirmed using alternative methods. Alternative methods for quantitating protein expression without using gels for separation are available such as label-free quantitative mass spectrometry. The whole cell lysate of samples are directly digested and run on a high resolution LC-MS/MS followed by bioinformatics analysis. This technique enables multiple samples to be compared and less concentrations of sample is needed. This kind of comparison should allow whole cell proteomes to be interrogated. While 2D-DIGE is a useful technique for exploring global proteomic changes and PTMs; it is time consuming, laborious and has numerous limitations. At the time this work was performed, this technique was a good approach for proteomic profiling analysis, but, with advances in MS, we are now able to use more sophisticated approaches. This will provide valuable insights into the dynamic changes of human astrocytes during infection with these two close relatives (*Toxoplasma* and *Neospora*). Thus, in chapter four quantitative proteomic in solution investigation was carried out using Label-free proteomic with the addition of three different time points to capture the changes occurring at the different time points.

3 Chapter three: Transcriptomic analysis of host cells response during *T. gondii* and *N. caninum* infection using RNA-Seq

3.1 Introduction

In the previous chapter, changes in the cellular proteome of human astrocytes in response to infection with *T. gondii* compared to *N. caninum* infection were investigated using 2D-DIGE. This chapter will focus on the changes of human astrocytes at the gene transcriptional level in response to infection with the two parasites. The transcriptome is the complete set of RNA molecules in a cell including coding and non-coding transcripts (Wang et al. 2009). In contrast to the genome which is stable for any given cell line, the external environment, physiological conditions and developmental stage can all cause variations to the transcriptome. Exploring the transcriptional changes enables us to explore the functional components of a genome and help to reveal changes in the molecular elements in cells and for understanding development and disease envolvement (Wang et al. 2009).

While both *T. gondii* and *N. caninum* parasites can reach the CNS and encyst in the brain, *T. gondii* is the parasite mostly known to cause tropism in neural cells. In order to understand molecular differences in astrocytes infected with *T. gondii* and *N. caninum*, it is vital to study these changes at the transcriptional level. This can be acheived through hybridization techniques such as microarrays or sequencing based approaches.

3.1.1 RNA-Seq

While mass spectrometry enables the identification and quantification of proteins, next generation sequencing (NGS) investigates the gene expression level profiles and is known as RNA sequencing (RNA-Seq) (Hall 2007). It allows rapid, in depth

sequencing which makes it easier to analyse whole transcriptomes in a very short period of time (Liu et al. 2014). It also has many advantages over other transcriptional approaches as discussed previously in chapter one (1.10.1).

The first publications on transcriptomic studies done using RNA-Seq were in 2008 (Nagalakshmi et al. 2008; Lister et al. 2008; Sultan et al. 2008). It was applied to analyse and explore human, yeast and *Arabidopsis* mRNA and has extended further to investigate other organisms, including apicomplexan species such as *T. gondii* and *Plasmodium spp*. (Sorber et al. 2011; Hassan et al. 2012).

3.1.1.1 Steps involved in RNA-Seq

RNA-Seq involves multiple stages that including sample preparation, amplification, fragmentation, purification and sequencing of the samples of interest (Mortazavi et al. 2008). Briefly, this technique begins with the conversion of RNA to a constructed library of cDNA fragments with adaptors attached to one end (single-end sequencing) or both ends (paired-end sequencing), which is then sequenced with a high-throughput sequencing platform to attain short sequences from one end or both ends (Wang et al., 2009); reads generated from the sequencing platforms are typically 30–400 bp in length (Figure 3.1). The resulting sequences can then be aligned to the organism's reference genome or transcriptome, or assembled *de novo* if no reference genome is available (Wang et al. 2009). In this chapter, Illumina platform was used for mRNA sequencing; details related to this platform including its advances have been described in chapter one (1.10.1)

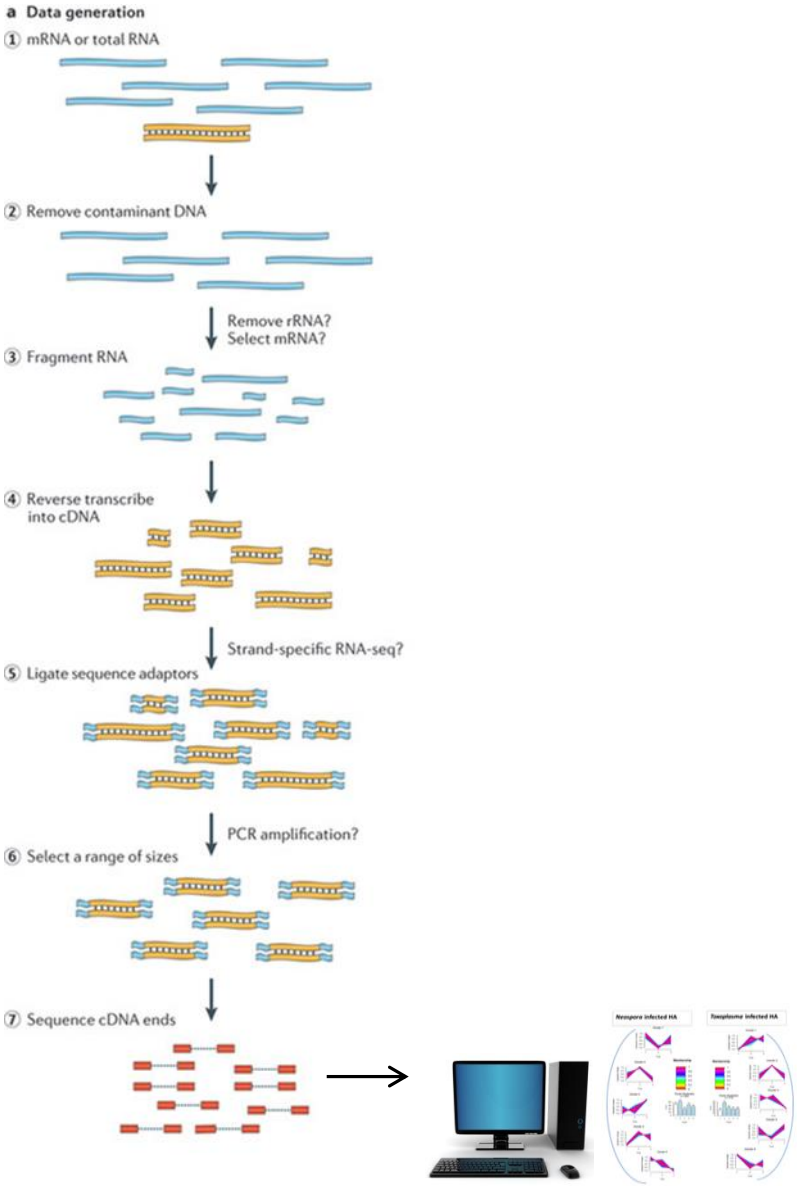

Figure 3.1: Illustrative scheme of RNA-Seq steps. RNA is first extracted, DNase treated, then fragmented into smaller pieces. Libraries are created from the fragments and sequenced at a high coverage. The sequenced reads are afterwards aligned to a reference genome and the results are analysed statistically and interpreted through bioinformatic approaches. (Image adapted from Martin & Wang 2011).

3.1.2 RNA-Seq in systems biology investigations

RNA-Seq enables the deep sequencing of the transcriptome with high resolution and without the need of a known reference genome to be included. It is known that mammalian cells are highly complex, RNA-Seq is a tool that aids in understanding different biological processes occurring in the cell at the transcriptional level (Westermann et al. 2012). The transcriptomes from different mouse tissues *in vivo* was first mapped and analysed using RNA-Seq, and novel transcripts were detected in the liver, skeletal muscle and brain tissue analysed from mice (Mortazavi et al. 2008). Human cell transcript analysis of an embryonic kidney cell line (Ramos B) was investigated *in vitro* through RNA-Sequencing; novel transcripts were identified and 25% more genes were detected when compared to a microarray-based approach (Sultan et al. 2008).

3.1.1.2 Transcriptomic studies in host cells and pathogens

There have been many studies that investigated the biological changes that occur to a cell or tissue during infection with different organisms in the same experiment. For example, a study done by Gail, Gross & Bohne (2001) explored transcriptional changes of the human foreskin fibroblast (HFF) cells during *T. gondii* infection compared to *Salmonella typhimurium* and *Chlamydia trachomatis* using microarrays. They identified 13 genes (such as IL6 and TNFAIP6) up-regulated exclusively in cells infected with *Toxoplasma* (Gail, Gross & Bohne 2001). Functional changes in the central nervous system (CNS) were examined during the chronic stage of *T. gondii* infection in mice, in which genes involved in immune responses and cell activation were up-regulated in mice brains after infection (Tanaka et al. 2013). In addition, host transcripts whose expressions were reduced by infection were involved in small-GTPase-mediated signal transduction and vesicle mediated transport (Tanaka et al. 2013).

Comparative genomic and transcriptomic analysis of *N. caninum* and *T. gondii* have shown that they have developed distinct collections of surface antigens and

secreted kinases. An expansion in the number of surface antigens were identified in *N. caninum* compared to *T. gondii* tachyzoite stage (Reid et al. 2012).

An investigation of host responses to infection in HFF cells between these two parasites through comparative microarray profiling demonstrated that *N. caninum* is a strong inducer of innate IFN-α/β responses, whereas *T. gondii* has developed the capability to suppress this response (Beiting et al. 2014). It was concluded that *N. caninum* parasites are potent activators of type a/β interferon pathways in mice macrophages *in vivo* and were dependent on the toll-like receptor TLR3 and the adapter protein Trif (Beiting et al. 2014).

3.1.1.3 RNA-Seq in human astrocyte investigations

The investigation of increased expression of astrocytes markers in schizophrenia and its association with neuroinflammation was done using RNA-Seq and showed that patients with schizophrenia had increased expression of glial fibrillary acidic protein (GFAP) and hypertrophic astrocyte morphology (Catts et al. 2014). Another study explored the localization of Alzheimer's disease in the parietal cortex of the brain and its involvement of the early symptoms of the disease in humans through a using Illumina RNA-Seq platform (Mills et al. 2013). This study identified transcriptional profile changes related to lipid metabolism and concluded that astrocytes were associated with neurodegenerative disorders (Mills et al. 2013). In a study of neuropathogenesis in HIV-1 subtype C (clade C), synaptic plasticity associated genes were examined in primary human astrocytes (Atluri et al. 2013). The findings suggest that severe neuropathogenesis as an outcome of infection may be related to the down-regulation of synaptic plasticity genes, decreased dendritic spine density and induction of apoptosis in astrocytes. To date, there have been no studies examining human astrocytes response during *T. gondii* and *N. caninum* using high-throughput sequencing (RNA-Seq).

3.1.3 Aims and RNA-Seq experimental design

In this chapter, the aim was to investigate transcriptional expression changes of host cells (human astrocytes) during infection with *T. gondii* in comparison with *N. caninum* infection. *Toxoplasma* successfully invades the CNS and establishes its chronic stage of infection through cyst formation in any warm blooded animal including humans, while *Neospora* has a more restricted host range and seems to infect mostly the CNS of its definitive host. The main hypothesis is that differences in human astrocytes response during infection will reflect on the genes being transcribed during infection.

In this study, high throughput sequencing (RNA-Seq) was used to compare the responses of human astrocytes to infection with *T. gondii* and *N. caninum*. Previous work by Dr. Dong Xia on *T. gondii* infected human foreskin fibroblast (HFF) cells showed that the majority of transcriptional changes occurred within the first 16 hours post infection. Thus, in this study, three different time points were chosen to examine the transcriptional change in human astrocytes during early stages of infection (0, 4 and 16 hours).

3.2 Materials and methods

3.2.1 Human astrocyte cell sample preparation and collection

HA cells, *T. gondii* (TgVEG strain) and *N. caninum* (NcLIV) were grown and maintained as previously described at chapter two (chapter 2.2.1). TgVEG was used throughout the thesis chapters, it is the less virulent strain and the cyst forming strain in the brain and other organs in the host compared to TgRH strain which is the virulent strain and was only used in chapter two (2D-DIGE) and does not form cysts compared to TgVEG. Due to time and cost limitation's in the experiments as the costs (RNA-Seq and LC-MS/MS). In addition, the aim of the experiments was to compare the biological changes occurring in the host cells during infection with *T. gondii* compared to *N. caninum*.Parasites were resuspended in DMEM-F12 and confluent HA cells were infected at a M.O.I. of 8 parasites per cell. Duplicate confluent flasks (2 x T75 cm^2 with 1 x 10^6 cells/flask) for both *T. gondii* and *N. caninum* HA infection were scraped and collected at (0, 4 and 16 hours p.i.) and were subjected to two washes with DPBS through centrifugation at 188 x g for 10 minutes and a final wash in a 1.5 ml tube at 13 000 x g for five minutes. Finally supernatants were carefully discarded and the samples were stored at -80°C.

In order to increase Total RNA yield in samples; the two flasks from each sample were pooled together at all three different time points for the cells infected with *Neospora* and *T. gondii*.

3.2.2 Total RNA extraction

Prior to isolation of total RNA(TRNA) , the samples were first resupended in 350 µl RLT buffer (Qiagen) to disrupt the cell, and processed with Qiashredder columns (Qiagen) to homogenize the cells and reduce viscosity caused by high-molecular-weight cellular components and cell debris. Total RNA was extracted using RNeasy mini kit (Qiagen) according to the manufacturer's protocol. Briefly, samples were loaded onto an RNeasy column and centrifuged at 8000 x g for 30 seconds. The

flow-through was discarded, and the column was washed in buffers RW1 (700 µl, 30 second centrifugation at 8000 x g) and RPE (500µl, 30 second centrifugation at 8000 x g) before a 2 minute centrifugation step at 8,000 x g using a new collection tube to remove any remaining buffer. After that, the column was inserted to another collection tube and the total RNA eluted in 30 µl RNase-free water, through incubation at room temperature for 1 minute followed by centrifugation at 8,000 x g for 1 minute. Finally, samples were stored at -80°C for subsequent isolation of Poly(A) RNA.

3.2.2.1 Quantification of RNA

The concentrations of the TRNA samples were verified using a Qubit assay (Life Technologies). The RNA buffer supplied in the kit was mixed with the RNA reagent at a dilution of 1:200 µl. The buffer was then added to 0.5 ml tubes and two RNA calibration standards were prepared. A total of 10 µl of each standard was added to each tube containing 190 µl of reagent. The tubes were then left for two minutes, and placed on the Qubit fluorometer 2.0 (Life Technologies) machine to determine the RNA concentration of each sample.

3.2.2.2 Quality Control

Samples were submitted to the Centre for Genomic Research (CGR), University of Liverpool for quality and quantity evaluation on a Bioanalyzer chip (Agilent). Total RNA traces were checked for the intactness of RNA and Poly(A) RNA was assessed to ensure that appropriate depletion of ribosomal RNA had occurred so it does not interfere with the analysis of mRNA. An illustration of a total RNA and mRNA sample can be seen in Figure 3.2.

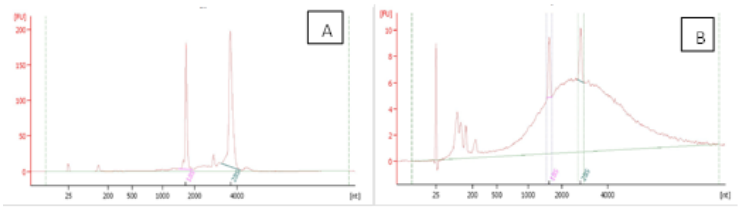

Figure 3.2: Bioanalyzer analysis (quality) of the samples which passed quality control. **A** displays total RNA, with two ribosomal peaks as shown (between 1500 and 4000 nt). **B** shows Poly(A) selection of RNA, ribosomal peaks can still be observed but they have been sufficiently depleted so as not to mask mRNA. The x axis shows the nucleotides and the fluorescence units are displayed on the y axis. Assessment of quality control was based on the appearance of the curve, and RNA quantitation was measured separately by Qubit Assay (Invitrogen).

3.2.3 Poly(A) selection

Isolation of messenger RNA (mRNA) from the samples was performed by the CGR. Poly-adenylated RNA was selected from total RNA samples using two rounds of selection with the Micropoly(A) purist kit (Ambion).

Briefly, mRNA enrichment of TRNA samples was performed as follows: samples were diluted to 250 µl with RNase-free water for mRNA selection using Micropoly(A) purist kit. All subsequent steps were performed according to the kit's protocol: samples were mixed with an equal volume of 2x binding solution, bound to oligo(dT) cellulose, heated to 70°C and then incubated with rocking for 1 hour at room temperature. The oligo(dT) cellulose was afterwards pelleted at 4 000 x g for 3 minutes at room temperature, washed twice with each of wash solutions 1 and 2, then eluted in 200 µl RNA storage solution preheated to 70°C, by centrifugation at 5000 x g for 2 minutes. The eluted Poly(A) RNA was left to precipitate overnight at 20^{o}C through the addition of 20 µl 5 M ammonium acetate, 1 µl glycogen and 550 µl 100 % (v/v) EtOH. It was recovered by 30 minutes of centrifugation at 12 000 x g at 4°C and resuspended in RNA storage solution, and quality and quantity evaluation of the samples were also checked using a Bioanalyzer chip (Agilent) and Qubit fluorometer at the CGR.

3.2.4 Sequencing

Library preparation, amplification and sequencing for six samples were done at the CGR. RNA Seq libraries were prepared from six HA cells infected with TgVEG/NcLIV enriched Poly(A)-RNA samples, and were subsequently sequenced on the Illumina HiSeq2000 platform in one lane to produce millions of paired-end reads per sample. Mapping to the human genome (GRCh37/Hg19) and also to the parasites (*T. gondii* and *N. caninum* genome (EuPathDB release 10.0)) was performed using TopHat version 2.0.10 (Trapnell et al. 2009; Kim et al. 2013) and generated FPKM (fragments per kilobase of exon per million fragments mapped) values which is a normalization step using Cufflinks.

3.2.5 Differential gene expression analysis

The experimental design contained no biological replicates due to the pooling of the samples together at the three different time points and the high cost of running an additional batch of samples. Therefore, the power to detect significantly differentially expressed genes was assumed to be low. However, it is still possible to estimate gene expression levels measured as fragments per kilobase per million mapped fragments (FPKM; a 'fragment' being a pair of reads, per kilobase being the gene length, so FPKM normalises for different gene lengths and total library size). The Cufflinks software package was used for normalization of the data (Trapnell et al. 2010). FPKM values were estimated across all six samples. At each time point post infection (0 hour, 4 hours and 16 hours); FPKM values from *T. gondii* infected human astrocytes were compared to those for *N. caninum* infected HA cells, using the Cufflinks package performed by the CGR.

3.2.6 Data analyses and functional annotation

A 20 percentile cut-off to the FPKM values was applied, together with ≥ 2 fold cut-off for the FPKM values for all datasets to define the most different expression levels among the compared samples.

The software package GProX (Rigbolt, Vanselow & Blagoev 2011) was used to perform cluster analyses, using a fuzzification value of 2 for 100 iterations. Additional functional annotations investigating their metabolic pathways including the cellular contents and molecular functions were analysed using the functional analysis and clustering tool from the Database for Annotation, Visualisation, and Integrated Discovery (DAVID) (DAVID bioinformatics resources 6.7) (Huang da et al. 2009).

Additional networks, functional analyses, and canonical pathways were produced through the use of Ingenuity Pathway Analysis (IPA) (Ingenuity Systems, www.ingenuity.com) to the list modulated transcripts with FPKM values ≥2 fold change. The functional analysis identified the biological functions and diseases along with canonical pathways that were most relevant and statistically significant to the data set.

3.3 Results

This project aimed to analyse the expression of transcripts of human astrocytes infected with *T. gondii* compared to *N. caninum* over three different time periods (0, 4 and 16 hours p.i.). In both infected cells (*T. gondii* and *N. caninum* infected cells) expression changes were compared between uninfected cells (0 hours) to infected cells (4 and 16 hours p.i.). This analysis was carried out as follows: sequence reads were aligned to reference sequence genomes of *H. sapiens* and *T. gondii* or *H. sapiens* and *N. caninum*. All samples submitted to the CGR for sequencing passed the quality control checks and gave the read counts shown in Table 3.1.

Table 3.1: Summary of reads and mapping to the human genome. Human astrocytes cells infected with *N. caninum* tachyzoites (Nc) and *T. gondii* VEG (Tg) tachyzoites were collected and sequenced at 0,4 and 16 hours post infection at the CGR.

Sample	Reads to align [1]	Aligned reads (%) [2]	Properly paired reads (%)[3]
Nc 0h	76,987,466	65,624,990 (85.24%)	40,330,564 (52.39%)
Tg 0h	64,597,110	49,443,284 (76.54%)	28,802,196 (44.59%)
Nc 4h	54,650,324	45,948,538 (84.08%)	28,672,092 (52.46%)
Tg 4h	75,787,490	64,778,431 (85.47%)	42,791,886 (56.46%)
Nc 16h	48,529,504	41,124,481 (84.74%)	22,730,728 (46.84%
Tg 16h	69,741,226	59,015,612 (84.62%)	37,426,250 (53.66%)

[1] Sum of reads used in the alignment.
[2] Reads that align to the reference genome (% of reads used in alignment).
[3] Properly paired reads (reads in correct relative orientation and within accepted distance from each other) (% of reads used in alignment).

Read pairs were aligned to the human cDNA reference. In general, more than 76% of reads were mapped, but for 5/6 samples >84% of reads were mapped to the reference sequence (Table 3.1).

The total human astrocyte FPKM value transcripts infected with either *T. gondii* or *N. caninum* were further filtered through a > 20 percentile cut-off and FPKM values that were ≥2 fold change. The total FPKM values identified in HA cells infected with *T. gondii* after the selection criteria were 1672 transcripts and in *N. caninum* infected cells were 1029 transcripts.

3.3.1 Cluster analysis and data visualization of host cell mRNA

Cluster analyses were carried out on FPKM values using GProX (Rigbolt, Vanselow & Blagoev 2011). These transcripts were clustered according to their transcriptional pattern changes in GProX (version 1.1.12) into five clusters which can be used to view the general trends in the data for FPKM values of TgVEG and NcLIV infected cells (Figure 3.3). Cluster analysis in *T. gondii* infected cells show transcripts identified to have a downward trend in expression over the time course (clusters 2 and 3) and cluster 4 has an upward trend in expression. *N. caninum* infected cells analysis show that the majority of genes identified have an upward trend in expression over the time course (clusters 1 and 5), whereas cluster 2 has a downward trend in expression (Figure 3.3). Visualization of the transcripts using the dendrogram heat map of infected HA cells showed clear differences in the hierarchical clustering. In *T. gondii* infected cells, the transcript expression is closely related at 0 and 4 hours compared to 16 hours p.i. (Figure 3.4 a). On the other hand, in *N. caninum* infected cells (Figure 3.4 b), 4 hours and 16 hours were closely correlated compared to 0 hours which may suggest a delay in the expression activation of the cells infected with *N. caninum*.

T. gondii infected human astrocytes

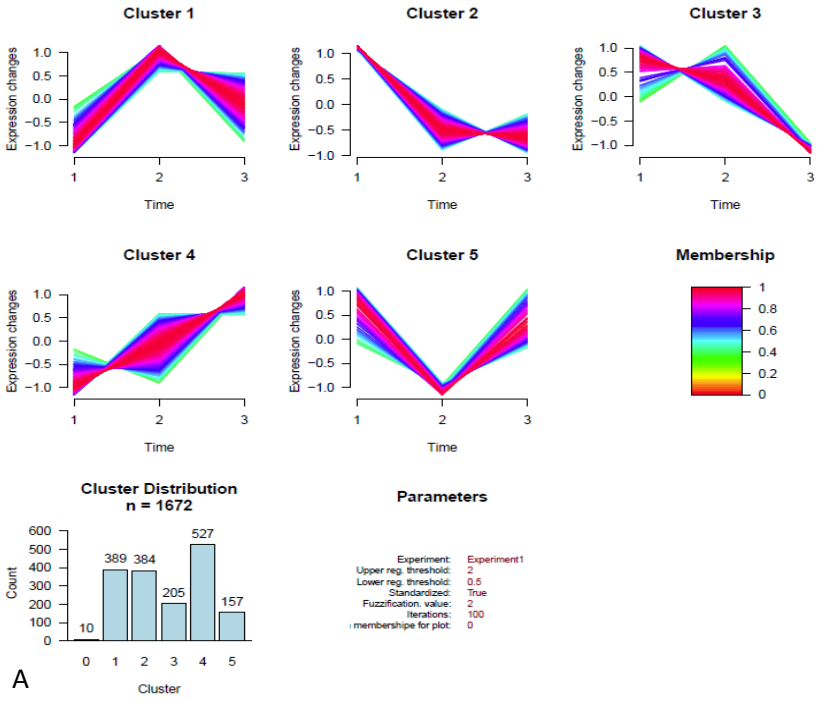

A

N. caninum infected human astrocytes

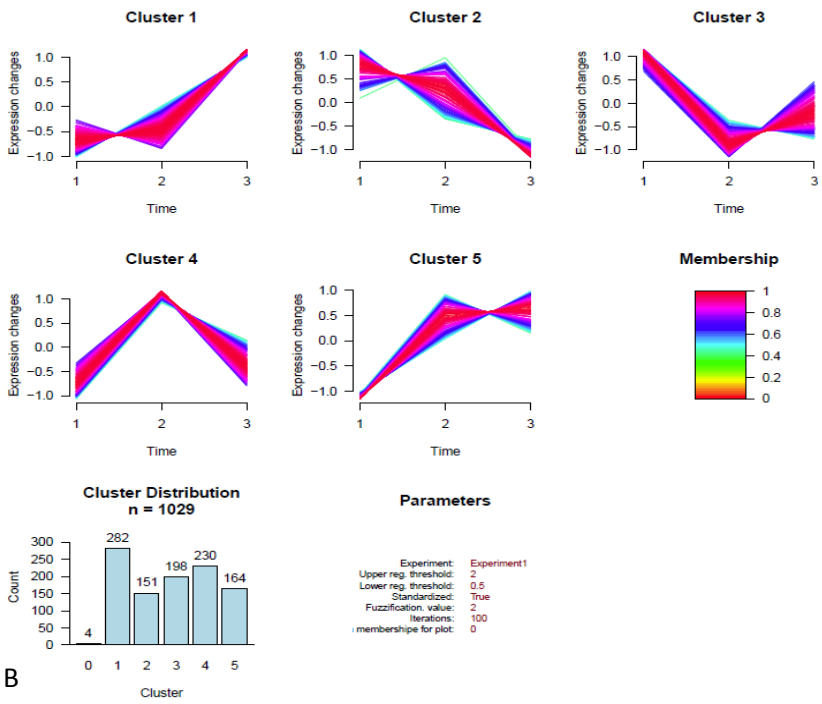

B

Figure 3.3: Cluster analyses of human astrocyte cells infected with *T. gondii* (VEG) and *N. caninum*. Transcripts were analysed in GProX using their FPKM values; 5 clusters were generated according to their transcript pattern expression across the time course for both *T. gondii* (A) and *N. caninum* (B). A total of 1672 transcripts were analysed for *T. gondii* and 1029 for *N. caninum* at all three time points. The x axis shows parasite post infection of cells at time points (0, 4 and 16 hours post infection) and the y axis the expression changes of host cells. Cluster analysis (A) show transcripts identified to have a downward trend in expression over the time course (clusters 2 and 3) and cluster 4 has an upward trend in expression. Cluster analysis (B) show that the majority of genes identified have an upward trend in expression over the time course (clusters 1 and 5), whereas cluster 2 has a downward trend in expression. Transcripts that didn't fall into any of the clusters were grouped in cluster 0.

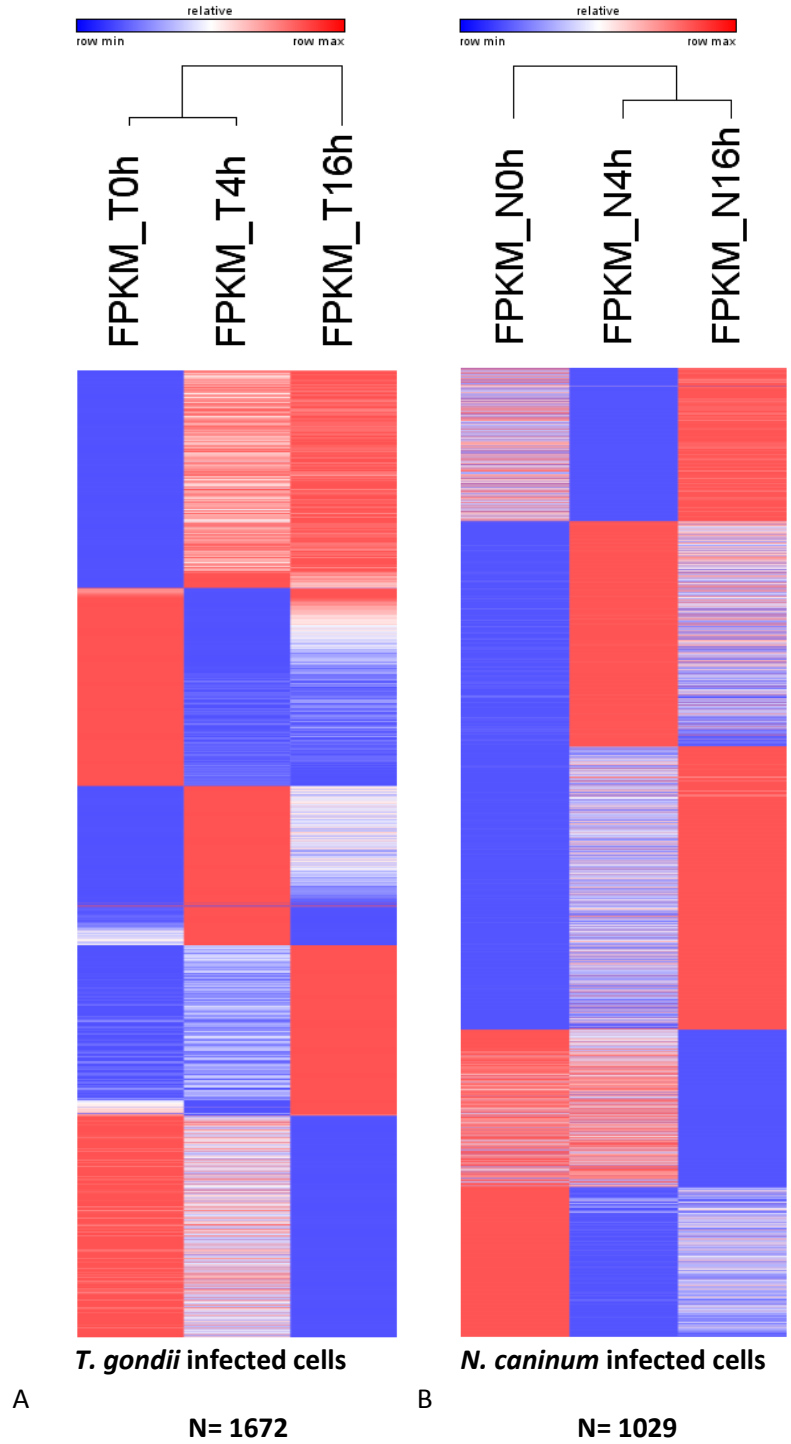

Figure 3.4: Dendrogram and heat map visualizing of human astrocyte cells infected with *T. gondii* and *N. caninum* using Gene-E software. In *T. gondii* infected cells (a); 0 and 4 hours p.i. were closely correlated compared to 16 hours p.i. On the other hand, *N. caninum* infected cells (b) showed that 4 and 16 hours p.i. were closely correlated compared to 0 hours.

3.3.2 Functional annotation of human astrocyte infected cells

For functional annotation and metabolic investigations of host transcriptional changes DAVID was used. A list of pathways for each cluster in both HA cells infected with *T. gondii* and cells infected with *N. caninum* were inserted into the search engine. Results involving metabolic pathways, gene ontology for biological process, cellular contents and molecular functions were delivered.

When generally comparing metabolic pathways between the two infections, it was necessary to look at differences and similarities between the cells infected. From the metabolic pathway analysis; a significant pathway showing differences in their trend of transcript patterns between *T. gondii* infected cells compared to *N. caninum* infected cells was the mitogen activated protein kinase pathway (MAPK pathway), in which showed opposite trends in expression changes throughout the three time points (Table 3.2). MAPK pathways are highly conserved cascades important in different aspects of the immune response (Dong, Davis & Flavell 2002). In *T. gondii* infected cells, eight genes were involved in the MAPK pathway and the pattern of their expression showed an increase at 4 hours followed by decreased expression at 16 hours post infection. On the other hand, in *N. caninum* infected cells, seven transcripts were involved in the MAPK pathway with a trend of decreased expression at 4 hours followed by an increased expression at 16 hours post infection (Table 3.2).

Table 3.2: Metabolic pathways identified within human astrocytes infected with *T. gondii* and *N. caninum*. Transcripts from *T. gondii* cluster 1 and *N. caninum* cluster 3 (see figure 3.3) were searched using DAVID. The MAPK pathway found in both infected cells with different transcriptional expression are highlighted in green.

Category	Term	Transcript count	% of transcripts	P-value	Cluster
T. gondii infected cells	Lipoic acid metabolism	2	0.6	4.40E-02	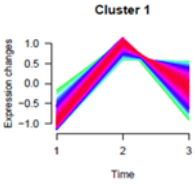
	Glycine, serine and threonine metabolism	3	0.9	7.60E-02	
	Long-term potentiation	4	1.1	7.80E-02	
	MAPK signalling pathway	8	2.3	9.70E-02	
N. caninum infected cells	MAPK signalling pathway	7	3.9	0.035	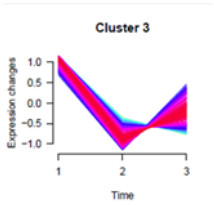
	TGF-beta signalling pathway	4	2.2	0.046	
	Purine metabolism	5	2.8	0.052	

3.3.2.1 Metabolic pathways of infected host cells

During the functional analysis of global expression profiles of host cells during infection; some notable pathways were detected. These pathways were the cytokine-cytokine receptor interaction and cell adhesion molecule pathways that are important in leukocyte migration and cell signalling processes in the cell.

The cytokine-cytokine receptor interaction pathway is associated with innate as well as adaptive inflammatory host defences, cell growth, differentiation, cell death, angiogenesis and development and repair processes directed at the re-establishment of homeostasis in the cell. Differences in host cell mRNA expressions were detected (Figure 3.5). Interleukin-8 (IL8), growth-regulated alpha protein (CXCL1) and C-X-C motif chemokine 3 (CXCL3) are chemotactic factors that attract mainly neutrophils and play roles in cellular inflammation. They were up-regulated in cells infected with *N. caninum* compared to cells infected with *T. gondii* at 16 hours p.i. (Table 3.3). Moreover, the chemokine CXCL2, also involved in neutrophil recruitment at sites of inflammation, was found up-regulated in *N. caninum* infected cells whereas, in *T. gondii* infected cells, it was decreased (Table 3.3). The chemokine CX3CL1, known as fractalkine, is a chemotactic for T-cells and monocytes, but not for neutrophils and is associated with regulating leukocyte adhesion and migration processes at the endothelium. It was found up-regulated in both infections with a higher fold change seen in *T. gondii* infected cells compared to *N. caninum* infected cells (Table 3.3). CXCL6, a chemotactic for neutrophil granulocytes that has strong antibacterial activity, was found up-regulated with an 8.3 fold change detected in *N. caninum* infected cells*;* whereas it in *T. gondii* infected cells it was below the cut-off value which was excluded during the 20 percentile cut off (Table 3.3). An illustration of the cytokine pathway and a descriptive table of the molecules associated with this pathway along with the expression changes (log2 fold change) can be seen in Figure 3.5 and Table 3.3.

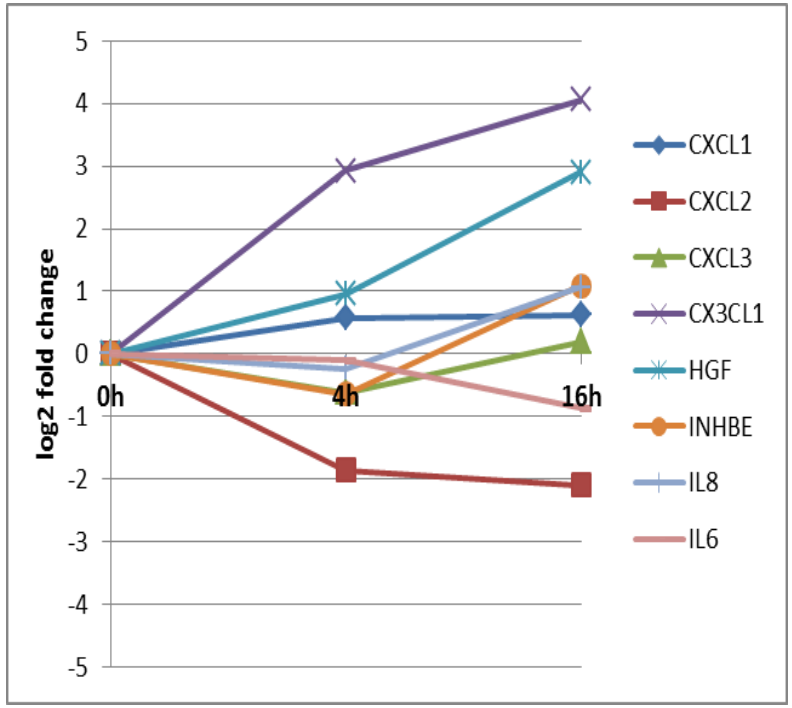

***T. gondii* infected human astrocytes**

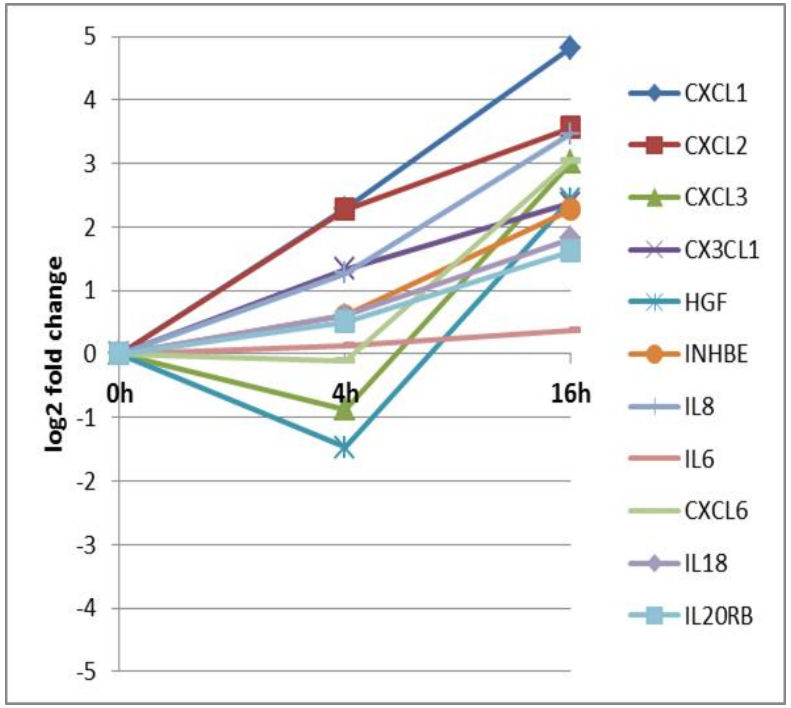

***N. caninum* infected human astrocytes**

Figure 3.5: Host transcripts involved in the cytokine-cytokine receptor interaction pathway in human astrocytes infected with *T. gondii* compared to *N. caninum* infected cells. CXCL1 shows an increased expression in cells infected with *N. caninum* compared to *T. gondii* infection and CXCL2 was also increased in *N. caninum* infection while showing the opposite trend of decreased expression in *T. gondii* infected cells. CX3CL1 was increased higher in *T. gondii* infected cells compared to cells infected with *N. caninum*.

Table 3.3: Differentially expressed host cell transcripts involved in cytokine-cytokine receptor interaction pathway in cells infected with *T. gondii* compared to cells infected with *N. caninum*. Log2 fold change in HA cells infected with *N. caninum* (Nc) and *T. gondii* (Tg) at 0, 4 and 16 hours p.i. are shown. Fold changes highlighted in red show up-regulated expression changes and fold changes highlighted in green show down-regulated transcript expressions.

Accession number	Gene name	Gene description	Log2 fold change					
			Nc 0h	Nc 4h	Nc 16 h	Tg 0h	Tg 4h	Tg 16h
ENSG00000163739	CXCL1	growth-regulated alpha protein	0	2.28	4.82	0	0.576	0.620
ENSG00000081041	CXCL2	C-X-C motif chemokine 2	0	2.27	3.561	0	-1.85	-2.086
ENSG00000163734	CXCL3	C-X-C motif chemokine 3	0	-0.87	3.018	0	-0.617	0.201
ENSG00000006210	CX3CL1	Fractalkine	0	1.342	2.37	0	2.92	4.05
ENSG00000019991	HGF	Hepatocyte growth factor	0	-1.46	2.43	0	0.95	2.89
ENSG00000139269	INHBE	Inhibin beta E chain	0	0.610	2.28	0	-0.63	1.089
ENSG00000169429	IL8	Interleukin-8	0	1.267	3.46	0	-0.22	1.064
ENSG00000136244	IL6	Interleukin-6	0	0.137	0.37	0	-0.10	-0.862
ENSG00000124875	CXCL6	C-X-C motif chemokine 6	0	-0.10	3.056	-	-	-
ENSG00000150782	IL18	Interleukin-18	0	0.602	1.814	-	-	-
ENSG00000174564	IL20RB	Interleukin-20 receptor subunit beta	0	0.512	1.619	-	-	-

The second pathway explored was the cell adhesion molecule pathway (CAM) (Figure 3.6). Cell adhesion molecules (CAMs) are glycoproteins found on the cell surface that are crucial to many biological processes in the cell that include immune responses, inflammation, haemostasis, embryogenesis, and development of neuronal tissue. Differences in their expression was detected between the two infections (Figure 3.6). Neural cell adhesion molecule 2 (NCAM 2) was significantly up-regulated in *T. gondii* infected cells whereas no change was detected in *N. caninum* infected cells (Table 3.4). An important molecule involved in blood brain barrier (BBB) permeability, vascular cell adhesion molecule 1 (VCAM1). It was up-regulated in cells infected with *T. gondii* compared to *N. caninum* (Figure 3.6 and Table 3.4). Claudin-22 (CLDN 22) had a significantly down-regulated fold change in *T. gondii* infected cells compared to *N. caninum*. HLA class I histocompatibility antigen, alpha chain F (HLA-F) was down-regulated in *T. gondii* infected cells and up-regulated in *N. caninum* infected cells (Figure 3.6 and Table 3.4). Cadherin-15 (CDH 15) was detected up-regulated in cells infected with *N. caninum*, while down-regulated in *T. gondii* infected cells (Figure 3.6 and Table 3.4). Intracellular cell adhesion molecule 1 (ICAM 1) was found with similar up-regulated expressions in both infections (Figure 3.6 and Table 3.4).

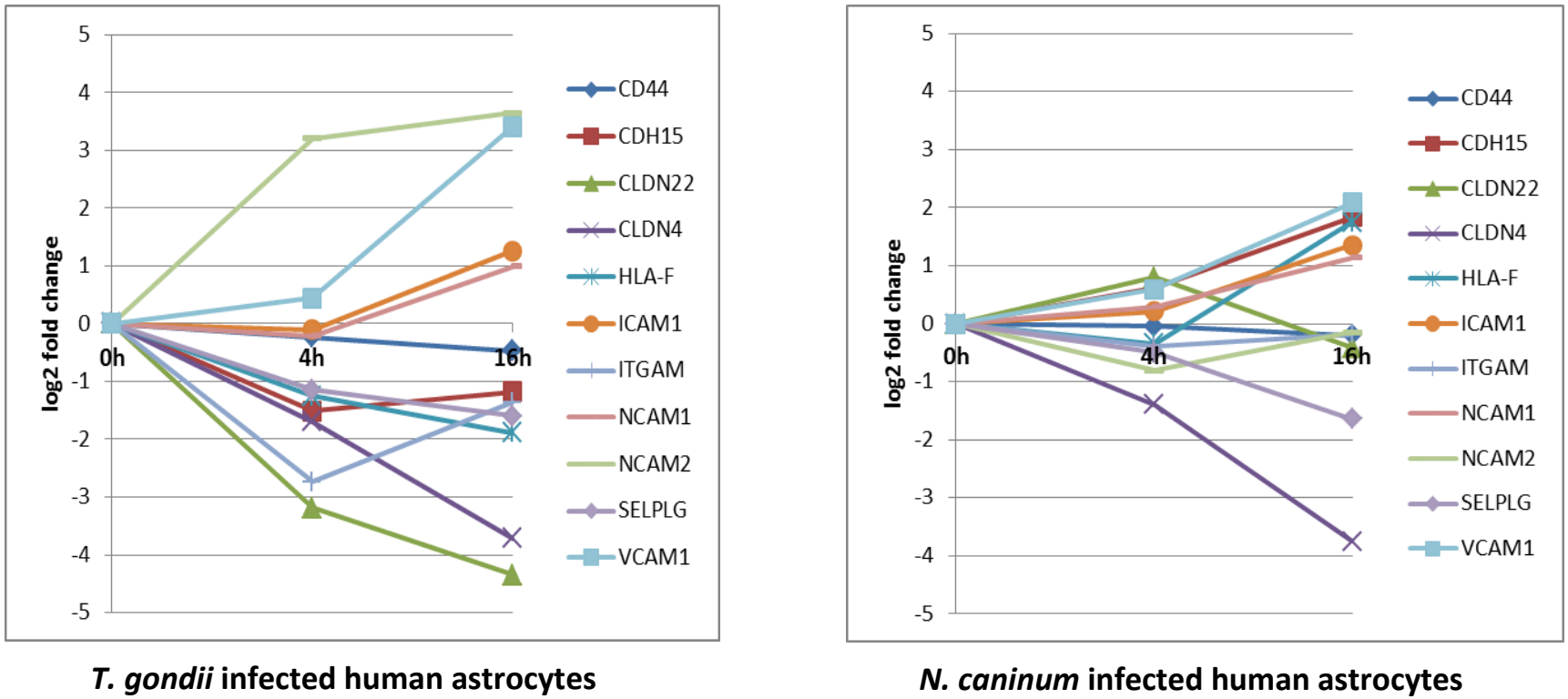

Figure 3.6: Host transcripts involved in the cell adhesion molecule pathway in human astrocytes infected with *T. gondii* compared to *N. caninum* infected cells. ICAM1 was up-regulated in a similar way andCLDN4 was down-regulated in both infected cells. On the other hand; NCAM2 was up-regulated in *T. gondii* infected cells compared to *N. caninum* infected cells.

Table 3.4: Differentially expressed host cell transcripts involved in cell adhesion pathway in cells infected with *T. gondii* compared to cells infected with *N. caninum*. Log2 fold change in HA cells infected with *N. caninum* (Nc) and *T. gondii* (Tg) at 0, 4 and 16 hours p.i. are shown. Fold changes highlighted in red show up-regulated expression changes and fold changes highlighted in green show down-regulated transcript expressions.

Accession number	Gene name	Gene description	Log2 fold change					
			Nc 0h	Nc 4h	Nc 16h	Tg 0h	Tg 4h	Tg 16h
ENSG00000026508	CD44	CD44 antigen	0	-0.043	-0.20	0	-0.23	-0.473
ENSG00000129910	CDH15	Cadherin-15	0	0.615	1.8336	0	-1.51	-1.184
ENSG00000177300	CLDN22	Claudin-22	0	0.802	-0.415	0	-3.18	-4.35
ENSG00000189143	CLDN4	Claudin-4	0	-1.39	-3.75	0	-1.68	-3.71
ENSG00000204642	HLA-F	HLA class I histocompatibility antigen, alpha chain F	0	-0.340	1.743	0	-1.25	-1.88
ENSG00000090339	ICAM1	Intercellular adhesion molecule 1	0	0.209	1.349	0	-0.10	1.254
ENSG00000169896	ITGAM	Integrin alpha-M	0	-0.39	-0.184	0	-2.73	-1.35
ENSG00000149294	NCAM1	Neural cell adhesion molecule 1	0	0.295	1.135	0	-0.21	0.992
ENSG00000154654	NCAM2	Neural cell adhesion molecule 2	0	-0.81	-0.152	0	3.207	3.648
ENSG00000110876	SELPLG	P-selectin glycoprotein ligand 1	0	-0.494	-1.64	0	-1.152	-1.59
ENSG00000162692	VCAM1	Vascular cell adhesion protein 1	0	0.591	2.0834	0	0.445	3.404

The data was also searched for molecules of interest in the CNS. One of the important cytokine molecule was C-C motif chemokine 2 (CCL2) that is associated with brain pathogenesis and toxoplasma encephalitis. It was down-regulated in *N. caninum* infected cells at 3.33 fold compared to an up-regulated expression (3.5 fold) in *T. gondii* infected cells at 16 hours post infection (Appendix II).

In both *T. gondii* infected cells and *N. caninum* infected cells, one of the most abundant transcripts (as shown by the FPKM values) with a down-regulation expression (3.33 fold) was plasminogen activator inhibitor 1 RNA-binding protein (SERPINE1) (Appendix II). SERPINE1 plays a role in the regulation of mRNA stability in the cell.

Matrix metalloproteases 1 (MMP1), a protease enzyme involved in proteolysis and extracellular matrix organization, was also one of the most abundant transcripts in both infected cells. It was found significantly down-regulated in cells infected with *T. gondii* at 16 hours p.i. (3.44 fold) compared to infected cells with *N. caninum* (1.6 fold) (Appendix II).

Neuronal pentraxin-1 (NPTX1) was up-regulated 3.8 fold in *N. caninum* infected cells higher, whereas in *T. gondii* infected cells was only up-regulated 1.4 fold. It is associated with the CNS development and synaptic transmission (Appendix II).

Interferon-induced protein with tetratricopeptide repeats 1 (IFIT1) and 2 (IFIT2) were only found in *N. caninum* infected cells with 25 fold in IFIT1 and 3.4 fold were up-regulated at 16 hours p.i., these molecules are involved in innate immunity, antiviral defence and type I interferon signalling pathway (Appendix II).

The molecular functions, cellular contents and biological process of individual host transcripts within the clusters of interest were determined in HA infected cells. Clusters that showed differential expression changes and contained a significant number of transcripts were chosen for functional annotations (Figures 3.3). Of these clusters, cluster 4 in cells infected with *T. gondii* contained the highest number of transcripts (527 transcripts) and showed an upward trend in expression (Figure 3.3a). Molecules associated within this cluster were involved in biological processes, including gland development, behaviour, chemokine activity, cell adhesion, forebrain development and leukocyte migration (Table 3.5). Cellular content was mainly found integral to membrane and the molecular functions were associated with chemokine activity (Table 3.5).

In cells infected with *N. caninum*, cluster 1 had the most abundant number of transcripts (282 transcripts) and showed an upward trend in expression (Figure 3.3b). The biological processes associated with these molecules were ion transport, chemotaxis and lipid transport (Table 3.6). The cellular content was related to the extracellular region part and the molecular function was involved in ion channel and chemokine activity (Table 3.6).

Table 3.5: Functional annotation of a subset of the transcripts identified in the analysis of human astrocyte infected with *T. gondii* using DAVID. A total of 527 transcripts (from cluster 4, Figure 3.3a) that showed an upward trend in expression were searched for their biological processes, cellular contents and molecular functions.

Category	Term	Transcript count	% of transcripts	P-value
Biological process	gland development	11	2.2	1.40E-03
	behaviour	23	4.7	2.00E-03
	mammary gland development	7	1.4	3.80E-03
	telencephalon development	7	1.4	4.40E-03
	taxis	11	2.2	5.00E-03
	chemotaxis	11	2.2	5.00E-03
	cell-substrate adhesion	8	1.6	8.80E-03
	cell-cell signalling	25	5.1	9.20E-03
	biological adhesion	28	5.7	9.40E-03
	forebrain development	10	2	1.10E-02
	leukocyte migration	6	1.2	1.10E-02
Cellular content	integral to membrane	163	33.3	2.30E-04
	intrinsic to membrane	167	34.2	3.10E-04
Molecular function	chemokine activity	6	1.2	4.50E-03
	chemokine receptor binding	6	1.2	5.90E-03
	ion channel activity	18	3.7	1.10E-02

Table 3.6: Functional annotation of a subset of the transcripts identified in the analysis of human astrocyte infected with *N. caninum* using DAVID. A total of 282 transcripts (from cluster 1, Figure 3.3b) that showed an upward trend in expression (Figure 3.3) were searched for their biological processes, cellular contents and molecular functions.

Category	Term	Transcript count	% of transcripts	P-value
Biological process	ion transport	21	8.3	0.0011
	chemotaxis	8	3.2	0.0035
	taxis	8	3.2	0.0035
	cation transport	15	5.9	0.0078
	lipid transport	7	2.8	0.0087
Cellular content	extracellular region part	24	9.5	1.50E-03
	extracellular space	18	7.1	4.50E-03
Molecular function	ion channel activity	16	6.3	1.40E-04
	substrate specific channel activity	16	6.3	1.90E-04
	channel activity	16	6.3	2.80E-04
	passive transmembrane transporter activity	16	6.3	2.90E-04
	chemokine activity	6	2.4	3.00E-04

3.3.2.2 Ingenuity Pathway analysis (IPA)

Previous analysis provided useful functional information for individual transcripts and pathways, but IPA can be used for a broader view of the transcripts especially in association with enriched pathways analysis. All the differentially expressed transcripts in *T. gondii* (n=1672) and *N. caninum* (n=1029) infected cells were searched using IPA pathway analysis. The top canonical pathway returned with the lowest p-values was mainly associated with the leukocyte extravasation signalling pathway. Astrocytes are known to cause migration of leukocytes during injury or infection. Therefore, the main pathway investigated was the leukocyte extravasation signalling pathway with a p-value of 1.89×10^{-4} and a total of 30 molecules involved in the pathway of *T. gondii* infected cells (Figure 3.7). In *N. caninum* infected cells a total of 20 molecules were involved in this pathway with a p-value of 9.7×10^{-4} (Figure 3.8).

The top enriched diseases in the *T. gondii* infected cells were associated with cancer (p-value of 1.32×10^{-6}) and neurological diseases (p-value of 1.44×10^{-5}). In *N. caninum* infected cells, they were associated with injury and abnormalities (p-value of 1.08×10^{-7}) and inflammatory diseases (p-value of 1.56×10^{-6}).

The main aim of this analysis was to look at the differences occurring in the host cells in response to different parasite infection at a molecular level. The leukocyte extravasation signalling pathway is the process by which leukocytes migrate from blood to tissues during inflammation (Figure 3.7 and 3.8). Some molecules were found to be specific to infection with a particular parasite. For example, matrix metalloproteases 1 (MMP1) was down-regulated (3.44 fold) in *T. gondii* infected cells at 16 hours. Also Integrin beta-3 (ITGB3) was down-regulated at 16 hours (2.77 fold) in *T. gondii* infected cells. In *N. caninum* infected cells, metalloproteinase inhibitor 4 (TIMP4) was up-regulated (3.2 fold) at 16 hours.

There were also differences between the two infections in the regulation of phosphoinositide phospholipase C-gamma-2 which was down-regulated in *T. gondii* infection (24 fold) and up-regulated in *N. caninum* infection (14.2 fold). Tyrosine-

protein kinase (TEC) was found down-regulated (6.25 fold) in *T. gondii* infected cells, while up-regulated (4 fold) in *N. caninum* infection. Both of these molecules are involved in innate immune response. Another molecule also showing differences between the two infections was Ras-related C3 botulinum toxin substrate 2 (RAC2) which is associated with axon guidance and platelet activation. It was down-regulated (1.8 fold) in cells infected with *T. gondii* and up-regulated (3.5 fold) in *N. caninum* infected cells. Claudin 14 (CLDN14) was up-regulated (2.9 fold) in *T. gondii* infected cells and down-regulated (3.7 fold) in *N. caninum* infected cells. This molecule is involved in tight junction assembly and calcium-independent cell-cell adhesion.

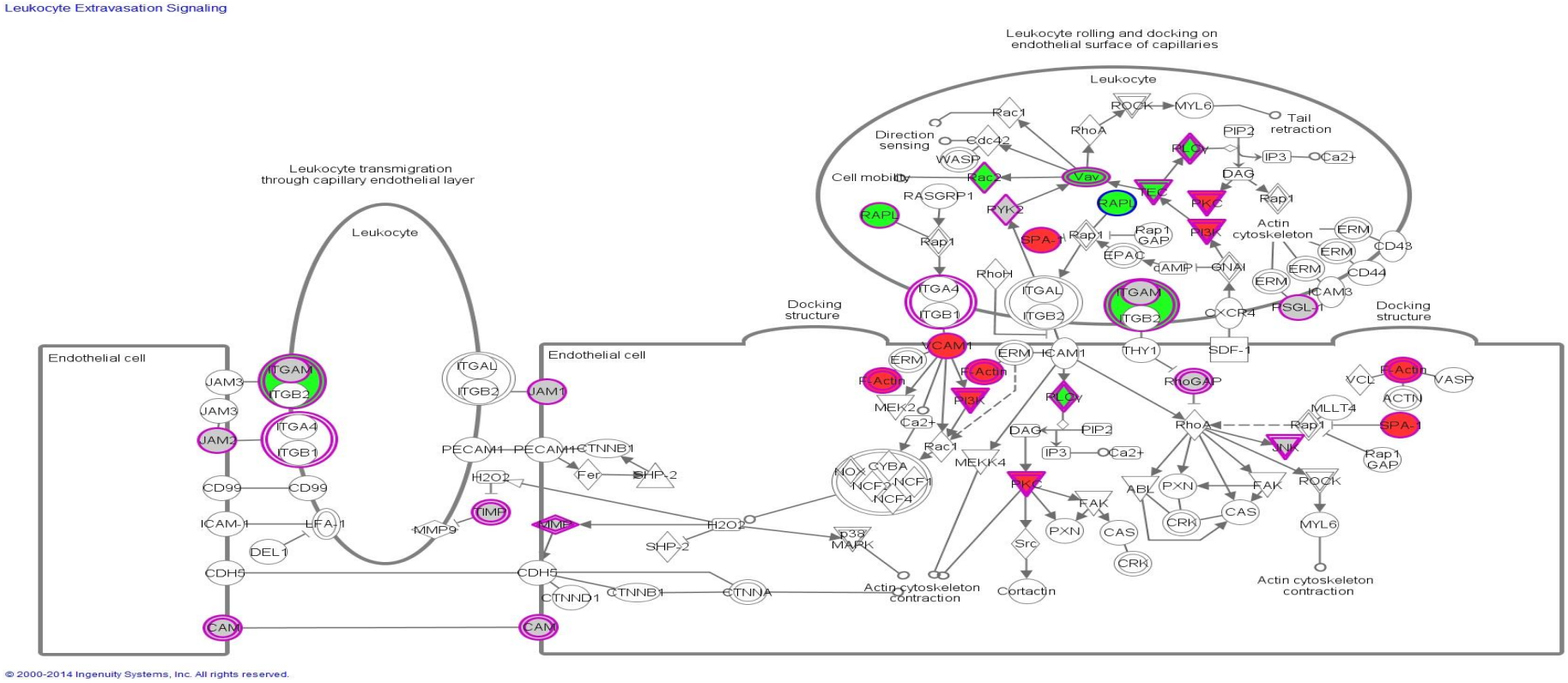

Figure 3.7: Leukocyte extravasation signalling pathway of human astrocyte cells infected with *T. gondii*. Expression data from the 1672 *T. gondii* transcripts were mapped onto pathways using Ingenuity pathway analysis. The molecules with up-regulated expression values were highlighted in red and the molecules with down-regulated expression values were highlighted in green. The molecules in grey shading indicate molecules associated with the pathway but were not found in the expressed transcripts inserted. Oolecules highlighted with purple lines without internal coloured shading are molecules detected in the pathway but show no significant (up-regulation or down-regulation) expressions.

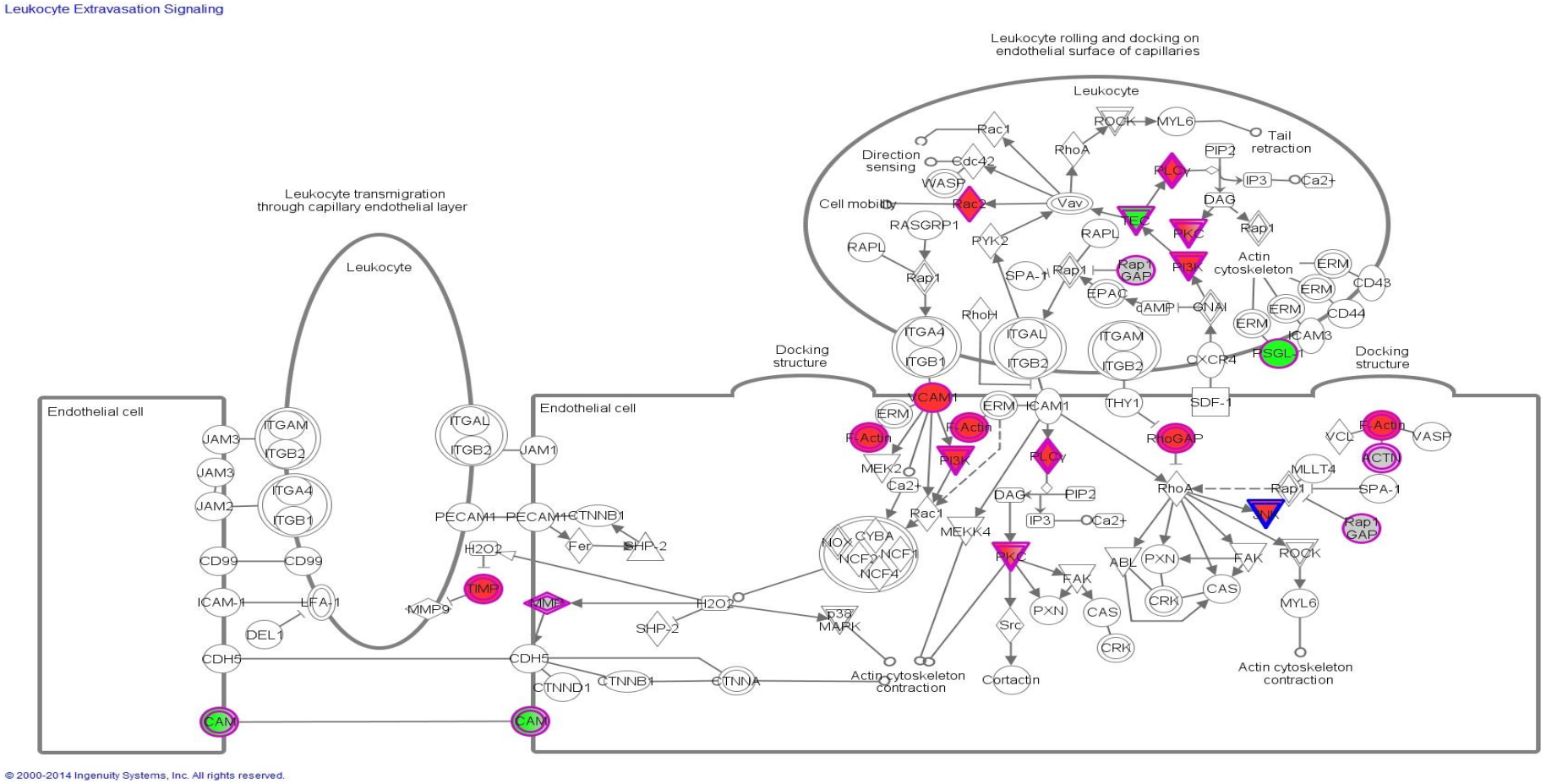

Figure 3.8: Leukocyte extravasation signalling pathway analysis of human astrocyte cells infected with *N. caninum*; it was generated using Ingenuity pathway analysis, the 1029 transcripts were all inserted to the IPA pathway. The molecules with increased expression values were highlighted in red and the molecules with decreased expression values were highlighted in green. The molecules in grey shading indicate molecules associated with the pathway but were not found in the expressed transcripts inserted. Molecules highlighted with purple lines are molecules detected in the pathway but show no significant (up-regulation or down-regulation) expressions.

3.4 Discussion

Understanding interactions of the intracellular apicomplexan pathogens with their host cells will help in identifying key differences between *T. gondii* and *N. caninum*. This can be achieved through information obtained of alterations occurring within the transcriptome and proteome of the host's responses during invasion. There are many factors that may affect the expression patterns of these transcripts such as the host cell type and biological status of the cell (Gail, Gross & Bohne 2001; McNicoll 2006).

The main aim of this experiment was to compare changes in the transcript profile expressions of human astrocytes during infection with *T. gondii* compared to *N. caninum*.

Initially, the experimental design was intended to include two biological replicates for the three time points in both infected cells. However, to ensure enough material was available for the experiment the two replicates were pooled together. Nevertheless, when looking into the literature; around 70% of the total published data was in fact using no replicates, through the application of RNA-Seq deep sequencing (e.g. Brawand et al. 2011; Graveley et al. 2011; Hah et al. 2011).

Overall, the main findings show differential expression of host cells in response to *T. gondii* infection compared to *N. caninum* infection. In order for the parasite to maintain its survival and proliferate in host cells, it must moderate the host's cell signalling pathways and scavenge nutrients needed from host cell organelles such as the mitochondria and ER. The RNA-Seq analysis presented here has identified key molecules associated with signalling pathways. For example, differences in the CAM receptor interaction pathway and cytokine-cytokine receptor interactions along with MAPK pathway were identified between *T. gondii* and *N. caninum* infected cells. Through IPA analysis, the leukocyte extravasation signalling pathway was identified as the top enriched pathway in both infected cells. This is in agreement with previous findings of the roles of astrocytes in leukocyte migration during infection (Jones, Bienz & Erb 1986; Fischer et al. 1997).

3.4.1.1 The cytokine-cytokine receptor interaction pathway

During infection with *T. gondii* or *N. caninum*, activation of innate and adaptive immune responses are induced through induction and migration of chemokines and cytokines. Chemokines are small secreted molecules that are divided into four subfamilies according to the position of the conserved cysteine residues (C, CC, CXC and CX3C), in which are associated with leukocyte migration of immune cells to sites of infection, immune homeostasis and angiogenesis (Zlotnik & Yoshie 2000; Adams & Lloyds 1997). There were reports demonstrating the roles of chemokines in the control of toxoplasamic encephalitis (TE), such as CCL2 (Amichay et al. 1996; Wen et al. 2010). It has been proven that chemokines can be secreted during *T. gondii* infection both *in vitro* and *in vivo* studies done on mice; for example CXCL1, CCL2 and IL8 (Brenier-Pinchart et al. 2000; Brenier-Pinchart et al. 2002).

In the cytokine-cytokine receptor interaction pathway (Figure 3.5) the general overall transcript expressions of cytokines and chemokines were up-regulated in cells infected with *N. caninum* compared to *T. gondii*. Of these molecules were: IL8, CXCL1, CXCL2, CXCL3 and CXCL6. While CX3CL1 was up-regulated in cells infected with *T. gondii* compared to *N. caninum* infected cells (Figure 3.5 and Table 3.4).

Interluikin8 (IL8) is a chemo attractant, mainly for neutrophils but also T cells, basophils and NK cells is stimulated during inflammatory responses (Burke et al. 2008). IL8 also induces phagocytosis and is known to be a potent promoter of angiogenesis. IL8 was significantly up-regulated in cells infected with *N. caninum* compared to a slight up-regulation in cells infected with *T. gondii*. In a comparative microarray study done by Beiting *et al*. (2014), fold changes of IL8 were higher in *N. caninum* infection in mice macrophages *in vivo* compared to the *T. gondii* VEG strain. Another study has also shown up-regulation of IL8 in *T. gondii* infected HFF and HeLa cells which were correlated with the findings in this chapter (Denney, Eckmann & Reed 1999).

During *Toxoplasma* infection, the innate immune response, in which neutrophils are recruited to areas of inflammation through the stimulation of chemokines such as

CXCL1 and CXCL2, helps in the control of *T. gondii* infection (Viola & Luster 2008; Denkers et al. 2004). CXCL1, CXCL2, CXCL3 and CXCL6 all belong to the same family of chemokines were highly increased in *N. caninum* infected cells compared to *T. gondii* infected astrocytes. Microarray investigations of *T. gondii* tachyzoite (RH strain) infection in HFF, dendritic cells, macrophage and retinal vascular endothelial cells was carried out in previous studies, and have detected an up-regulation of CXCL1, CXCL2, CCL2, MHC-I and IL8 through the analysis of immune cell responses to the infection (Blader, Manger & Boothroyd 2001; Chaussabel et al. 2003; Gail, Gross & Bohne 2001; Knight et al. 2005).

CXCL1, also known as growth-regulated alpha protein, is important in the processes of angiogenesis, inflammation, wound healing, and tumour genesis (Tsai et al. 2002). In a comparative microarray study done by Beiting *et al*. (2014), CXCL1 had an increased expression in *N. caninum* compared to TgVEG infected cells, which was in agreement with the RNA-Seq data analysis in this chapter. Furthermore, it was up-regulated in microglial cells after 24 hour p.i. with *T. gondii in vitro* and in brains and retina of infected mice in acute stage of infection independent from IFN-ϒ (Brenier-Pinchart et al. 2004 Kikumura et al. 2012). C-X-C motif chemokine 2 (CXCL2), also known as macrophage inflammatory protein 2-alpha, had up-regulated mRNA expression in cells infected with *N. caninum*, whereas it was down-regulated in *T. gondii* infection. It is involved in the activation of monocytes and neutrophils and is expressed at sites of inflammation. This contradicts findings that showed up-regulation of the CXCL2 in other studies; such as a study done by Kikumura *et al*. (2012), on the leukocyte migration during ocular toxoplasmosis in murine models and found up-regulated expression of CXCL2 and CCL2. However, there were no studies looking into the secretion of CXCL2 in *N. caninum* infected cells. Also, investigation of immune response at the transcriptional level were explored using human Muller cells in the retina. There findings also showed increase expression of CXCL2 in infected cells with two strains of *T. gondii* (Knight et al. 2006). This may suggest that *T. gondii* infection delays neutrophil recruitment more efficiently compared to *N. caninum* infection and as a result delays innate immune response. CXCL3 is also involved in neutrophil chemotaxis and was up-

regulated expression in astrocytes infected with *N. caninum* as mentioned earlier. Chemokine (C-X-C motif) ligand 6 (CXCL6) functions as a chemo-attractant for neutrophilic granulocytes and has strong antibacterial activity against gram-positive and gram-negative bacteria (Proost et al. 1993; Van Damme et al. 1997). Both CXCL6 and IL8 activate their immune responses through CXCR1 and CXCR2 receptors (Wuyts et al. 1998; Wolf et al. 1998). Investigation in gastrointestinal nematode infected cattle showed no differences between susceptible and resistance cattle in their secretion of CXCL6 (Li et al. 2007). CXCL6 has been linked to many inflammatory and pathological disorders such as inflammatory bowel disease and cancer (Zhu, Bagstaff & Woll 2006).

CX3CL1, also known as fractalkine, has three amino acids between the two cysteines and acts as a chemo-attractant and an adhesion molecule that enables the adhesion of cells to the endothelium (Goda et al. 2000). The CX3CL1 chemokine was up-regulated in *T. gondii* infected astrocytes compared to *N. caninum*. This was in agreement with other studies looking at the effect of *T. gondii* infection on host cells, in which they have found the up-regulation of chemokines including CCL2, CXCL1, CXCL2 and CX3CL1 (Lachenmaier et al. 2011; Stein & Nombela-Arrieta 2005).

CCL2 was up-regulated during astrocyte infection with *T. gondii* compared to a down-regulated expression in *N. caninum* infected cells. CCL2, also known as monocyte chemotactic protein-1 (MCP-1), is a member of the β-chemokine family. It functions as an attractant for monocyte/macrophages, CD4 and CD8 memory T lymphocytes (Adams & Lloyds 1997). This chemokine plays important roles in the CNS as neuroinflammatory mediators of leukocyte migration and has been associated with many neurological disorders (Bajetto et al. 2001; Zlotnik & Yoshie 2000). CCL2 has also been demonstrated to restrict *T. gondii* dissemination in human astrocytes and human fibroblastic cells (MRC5) and facilitate the recruitment of monocyte and lymphocytes to sites of inflammation (Brenier-Pinchart et al. 2002; Brenier-Pinchart et al. 2004). In addition, *in vivo* investigation on murine models with TE infections demonstrated that astrocytes were the main producers of CCL2 (MCP-1) (Strack et al. 2002; Knight et al. 2006). This is also

correlated with the findings presented here in human astrocytes infected with *T. gondii*. This may suggest that up-regulation of CCL2 by *T. gondii* can result in the migration of macrophages and activated T cells, NK and immature dendritic cells into the sites of infection in the brain and initiate adaptive immune responses through the migration across the blood brain barrier to enable the parasite to establish the chronic stage of infection in the brain and persist in the hosts brain.

A previous report has shown that neutrophils in peripheral blood increased in mice after *T. gondii* infection (Norose et al. 2008). Absence of IFN-γ function may cause neutrophil activation, as it is involved in the down regulation of IL8 production. Another cause of IL8 induction is the elevation of IL12 and TNFα found in human and mouse neutrophils *in vitro* (Denkers et al. 2003). From the mRNA data analysis; elevation of molecules related to TNFα have been detected suggesting that *N. caninum* may supress these genes which result in elevated production of neutrophil recruitment to sites of inflammation in cells infected with *N. caninum* compared to *T. gondii* infection. Most of the chemokines related to the induction of neutrophils were increased in *N. caninum* infected cells which may suggest that *T. gondii* attempts to supresses them in order to establish the chronic infection in the CNS and minimize inflammatory damage to the infected cells.

3.4.1.2 Cell adhesion molecule pathway

Many processes and interactions are important in the development and maintenance of the CNS; this includes formation of neuronal connections, synapse plasticity and guidance and the differentiation and migration of neural cells and other cells of the CNS (Basch, Garcia-Castro & Bronner-Fraser 2004; Tessier-Lavigne & Goodman 1996). Cell adhesion molecules (CAM) have been associated with the connection between cells through homophilic or heterophilic interactions (extracellular matrix (ECM)). These adhesion molecules are involved in many cellular processes such as homeostasis, inflammatory, immune responses and wound healing (Koukoulis, Patriarca & Gould 1998). They include four main families of immunoglobulins, integrins, selectins and cadherins (Chothia & Jones 1997). CAMs

are also associated with cytoskeleton organization and the alteration of signal transduction processes and are expressed in neurodegenerative disorders such as Alzheimer's disease (Bartsch 2003; Welzl & Stork 2003). Transcriptional changes in the peripheral lymphocytes of infected mice with type I and type II *T. gondii* were investigated by Jia *et al*. (2013), it was observed that in type I infected mice showed up-regulation of genes related to CAM, olfactory transduction and ribosome pathways, whereas in type II infected mice cytokine-cytokine pathway receptor interaction, chemokine signalling pathway, and toll-like receptor pathway were up-regulated (Jia et al. 2013). Cell adhesion molecules play vital roles in brain morphology and functions including learning and memory through neuron synapse formation of cell-cell adhesion with neighbouring cells.

Up-regulation of VCAM1 mRNA expression was found in HA cells infected with *T. gondii* compared to *N. caninum* and similar up-regulated expression was observed in ICAM1 (in both *T. gondii* and *N. caninum* infected cells). These are important adhesion molecules linked to parasitic infections of the CNS, such as cerebral malaria and TE. When inflammatory reactions take place in the CNS; cell adhesion molecules such as ICAM1, VCAM1 and selectins are induced through microvascular endothelial cells in addition to the secretion of many types of cytokine and chemokines (Kadl & Leitinger 2005; Coisne et al. 2006). Previous studies have demonstrated that both ICAM1 and VCAM1 are expressed on inflamed BBB endothelial cells and are critical for the transmigration of lymphocytes and monocytes (Carman & Springer 2004; Ifergan et al. 2006). ICAM1 is an endothelial and leukocyte-associated transmembrane protein related to the immunoglobulin family that is known for its importance in stabilizing cell-cell interactions and facilitating leukocyte endothelial transmigration. Increased expression of ICAM1 was reported to decrease the function of the BBB and permit transendothelial migration of infected immune cells through the parasites MIC2 adhesion in *T. gondii* infection (Rahman & Fazal 2008; Barragan, Brossier & Sibley 2005). Usually these proteins are secreted in low concentration; upon cytokine stimulus their concentrations increase (Dustin et al. 1986). VCAM1 is expressed on both large and small blood vessels after cytokine stimulation of the endothelial cells. It mediates

the adhesion of lymphocytes, monocytes, eosinophils and basophils to vascular endothelium and is involved in leukocyte-endothelial cell signal transduction. Transcriptional microarray profiles of infected retina cells (Muller cells) with two different strains of *T. gondii* (type I and II) demonstrated up-regulation of VCAM1, MHC-I (Knight et al. 2006). Siva *et al*. (2010), suggested that up-regulation of ICAM1, VCAM1 and increased BBB permeability participated in inflammatory cell infiltration into the CNS during *T. gondii* infection (Silva et al. 2010). This also correlates with the findings in this transcriptional analysis of human astrocytes.

Another cell adhesion molecule significantly up-regulated in cells infected with *T. gondii*, while no significant changes were observed in *N. caninum* infected cells was neural cell adhesion molecule-2 (NCAM2), which belongs to the immunoglobulin (Ig) superfamily. Both NCAM1 and NCAM2 are widely expressed in the CNS and may have similar functions. There have been no studies looking in the role of NCAM1 or NCAM2 during infection with protozoan parasites. NCAM2 may be a marker of certain types of neurological diseases and cancer such as breast cancer (Massaro, 2002). The sequence of NCAM1 has a high identity to NCAM2 and both are found abundant in the CNS suggesting that these two molecules share similarities (Paoloni-Giacobino, Chen & Antonarakis 1997). There has been limited research investigating the roles and functions of NCAM2 in the brain. Nevertheless, NCAM2 has been suggested to contribute to the establishment and maintenance of dendritic bundle in the region associated with learning and memory in the brain (the granular retrosplenial cortex) (Sutherland, Whishaw & Kolb 1988). NCAM's have also been associated with cell-cell adhesion (Zhang et al. 2003), which may indicate its role in increased permeability of the infected cells through the BBB.

Toxoplasma encephalitis (TE) involves strong activation of major histocompatibility complex (MHC) class I and II antigens as well as of the ICAM1 on cerebral endothelia, microglia and choroid plexus epithelium and VCAM1 on endothelial cells (Deckert-Schlüter et al. 1994). The major histocompatibility complex (MHC) consists of three subgroups: class I, class II and class III. HLA class I histocompatibility antigen, alpha chain F, is involved in the presentation of foreign antigens to the immune system and is expressed on the surface of activated lymphocytes. Usually

cells of the CNS do not express MHC-I, but astrocytes can up-regulate MHC-I expression through IFN-γ stimulation that is vital for controlling TE (Jarosinski & Massa 2002; Schluter et al. 1991). There is limited information of HLA-F function available, making it difficult to hypothesise possible roles in parasitic infections. One study examined the effect of *Leishmania major* infection on human monocyte cells and found no gene expressional changes in HLA-F secretion after 24 hours p.i. (Guerfali et al. 2008). HLA-F was down-regulated in astrocytes infected with *T. gondii*, whereas up-regulated in *N. caninum* infected cells. This could indicate that *T. gondii* down-regulates MHC-I expression at early stages of infection to invade and establish parasite infection in cells of the CNS.

Tight junction molecules are known for their importance in the BBB permeability through enabling the closure of spaces between adjacent endothelial cells and thereby only permitting the entry of small molecules to the brain (Zlokovic 2008). The down-regulation of claudins and cadherin in this data, such as CLDN-22, CLDN4 and CDH15 mainly in cells infected with *T. gondii* may be a result of a parasite-induced mechanism to support immune cell entry. Claudins play a role in sealing the tight junction (Ohtsuki et al. 2008; Krause et al. 2008). Most of the claudins and CDH15 were down-regulated in cells infected with *T. gondii*, with the exception of CLDN14 which was up-regulated in cells infected with *T. gondii* and down-regulated in *N. caninum* infected cells. Cadherins are involved in intracellular communication and homeostasis (Vleminckx & Kemler 1999). CDH15 is a calcium-dependent cell adhesion protein associated with cell junction assembly that was also found reduced in primary culture of mice skeletal muscle cells infected with *T. gondii* after 24 hours p.i. by Gomes *et al*. (2011). This may suggest that *T. gondii* down-regulates these molecules to loosen the tight junction and enhance its entry to the CNS.

Overall increased expression of cell adhesion molecules mostly in *T. gondii* infected cells may imply the ability of the parasite to increase its permeability through the BBB and loosen the tight junction through down-regulation of claudins and cadherin molecules in the CNS more efficiently compared to *N. caninum* infection in the brain and enables it to persist in the host.

3.4.1.3 MAPK pathway in host cells

The MAPK pathway consists of proteins that transfer a signal from a receptor on the cell surface to the nucleus DNA. The end product causes changes in the cell such as cell division. It has been suggested that the MAPK pathway is important during *T. gondii* infection, in which the parasite increases the regulation of this pathway (Brumlik et al. 2013). The MAPK pathway also functions in neutrophil activation during *T. gondii* infection (Sukhumavasi, Egan & Denkers 2007) and in controlling proinflammatory response during infection with *T. gondii* (Dong, Davis & Flavell 2002).

Differences in transcriptional expression patterns of molecules associated with the MAPK pathway was detected between astrocytes infected with *T. gondii* and *N. caninum* infected cells (Tables 3.2). While a total of eight transcripts associated with the pathway in *T. gondii* infected cells that were up-regulated at 4 hours and then down-regulated at 16 hours p.i., the opposite was detected in the seven transcripts in cells infected with *N. caninum*. However, the transcripts involved in each pathway in both infected cells differ and the only molecule found in both infected cells was the fibroblast growth factor receptor 2 (FGF2). Also, MAPK pathway was identified as statically significant in cells infected with *N. caninum*, whereas it was not significant in cells infected with *T. gondii* (Table 3.2). Therefore it is difficult to reach a definite conclusion related to the modifications found between the infected cells for this pathway.

3.4.1.4 Other functional annotations of host cell molecules

Analysis of individual significant transcripts included SERPINE1, MMP1 and NPTX1 (Appendix II). Plasminogen activator inhibitor 1 (SERPINE1) is a serine protease inhibitor involved in physiological and pathological processes in an organism such as angiogenesis, complement activation, coagulation and inflammatory responses. In the analysis presented here, SERPINE1 was down-regulated in astrocytes infected

with both parasites. In contrast, a previous study found SERPINE1 be up-regulated in *T. gondii* infected human neuron and microglial cells *in vitro* (Mammari et al. 2014). SERPINs have been proposed to reduce the parasite's duplication by obstructing the apoptosis process of the host cell. This has been associated to the increased production of SERPIN in microglial and neuron infected cells which may lead to the control of *T. gondii* replication and the inhibition of apoptosis of the nervous cells (Mammari et al. 2014).

MMP1 was only detected in *T. gondii* infected cells and was down-regulated. Matrix metalloproteases (MMPs) are major enzymes that are associated with the extracellular matrix (ECM) degradation, and may also be associated with cell migration, differentiation, growth and inflammatory processes in the cell. The parasites are able to control human monocytic cells through the degradation process using MMPs (Buache et al. 2007). A study done on astrocytes infected with *T. gondii* showed down-regulation of MMP2 and MMP9 during infection (Lu & Lai 2013). This correlates with the finding of MMP1. Thus, may suggest that the parasite may control inflammatory development in the host cells.

In *T. gondii* infection, the parasite alters leukocyte interactions, evade the hosts immune system and spread to important sites such as the CNS using different cells such as macrophages, monocytes, and dendritic cells (Da Gama et al. 2004; Lambert et al. 2006; Courret et al. 2006). Pentraxin-related proteins regulate innate resistance to pathogen and inflammatory reactions and the control of autoimmunity (Rovere et al. 2000). Pentraxins are highly abundant in many cell types, including mononuclear and phagocytic cells (Breviario et al. 1992). Neuronal pentraxin-1 (NPTX1) is mainly found in the CNS and is involved in the development and synaptic transmission and is found increased in glia cells and less in neurons that function in limiting brain tissue damage (Blasi et al. 1995; Mazzolla et al. 1996). It was found up-regulated in cells infected with *N. caninum* compared to cells infected with *T. gondii*. This may suggest that *N. caninum* parasites up-regulate NPTX1 to increase synaptic transmission between cells. Although this can also be assumed in cells infected with *T. gondii* as these parasites are able to delay apoptosis in cells.

Other molecules that were found up-regulated in one infection compared to the other and are related to cell signalling and immune responses were Interferon-induced protein with tetratricopeptide repeats 1 and 2 (IFIT1) and (IFIT2). Up-regulated mRNA expression of these two molecules was detected in cells infected with *N. caninum*. IFIT1 and IFIT2 are associated with innate immune responses, antiviral defence and type I interferon signalling pathway. This correlated with the microarray analysis performed by Beiting *et al*. (2014). This may suggest that *N. caninum* may act more as a virus during infection as type I interferon responses are highly associated with viral responses. Also, this may indicate that *T. gondii* supresses early innate immune responses in infected host cells.

3.4.2 Functional annotations of host cell transcripts

The biological processes and molecular functions of a subset of transcripts that showed up-regulation in host cells during infection across the three time points of infection were investigated. In both host cell infections (cluster 1 in *T. gondii* infected cells and cluster 4 in *N. caninum* infected cells, Table 3.6 and 3.7); the biological processes and molecular functions were mostly associated with chemotaxis and chemokine activity. In addition, cells infected with *T. gondii* showed biological processes related to behaviour and cell adhesion functions. This may suggest that *T. gondii* up-regulates host genes associated with behaviour and brain development, in which *T. gondii* manipulates its behaviour for its persistence as detected by previous studies (Gaskell et al. 2009; McConkey et al. 2013) compared to *N. caninum*, where no biological processes related to behaviour alteration was detected.

3.4.2.1 Leukocyte extravasation signalling pathway

The leukocyte extravasation signalling pathway was identified as the top enriched pathway in both infected cells through IPA analysis. This is in agreement with previous findings of the roles of astrocytes in leukocyte migration during infection

(Jones, Bienz & Erb 1986; Fischer et al. 1997). The transmigration of *T. gondii* through endothelial barriers differs according to strain type; type I strains have the highest ability to increase migration and dendritic cell activity (Lambert et al. 2009). With advances in culture techniques available, *in vitro* models have been established for deeper investigation of certain interactions between host-pathogen; such as the formation of 3D well models and transwell co-cultures. The investigation of CNS invasion by *T. gondii* and the involvement of leukocytes in this process were done using an *in vitro* model of the BBB of rat glia and endothelial cells (Veszelka et al. 2007). They have demonstrated the up-regulation of cytokines and chemokines, such as IL6, involved in the acute phase immune response and increased the transfer of *T. gondii* when compared to lymphocytes. This may suggest that APC are more likely to be involved in the parasites ability to cross the BBB (Veszelka et al. 2007). One of these molecules associated with this pathway was the tyrosine protein kinase (TEC). TEC was significantly down-regulated in cells infected with *T. gondii* while up-regulated in cells infected with *N. caninum*. The data related to this pathway proposes the role of these parasites in the migration of cytokines chemokines and other molecules during host astrocyte infection and especially in *T. gondii* infection.

3.4.3 Conclusions and future direction

In summary, transcriptional expression changes were observed between host cells infected with *T. gondii* compared to cells infected with *N. caninum*. These were mainly related to leukocyte migration through the BBB, which showed increased permeability of *T. gondii* infected cells compared to *N. caninum* infected cells. Neutrophil activation was found associated with *N. caninum* infection of cells compared to *T. gondii* infected cells. Functional annotations have also identified the up-regulation of biological processes such as behaviour changes in host cells infected with *T. gondii*, whereas both infected cells functional annotations were also associated with chemotaxis activities. In conclusion, *T. gondii* activates host cells to increase its establishment of the chronic stage in the host cell brain more successfully. Whereas inflammation and neutrophil recruitment is associated with

N. caninum infected cells suggesting that *N. caninum* initiates an earlier innate immune response and may lead to induction of apoptotic processes in infected cells.

It is known that not all identified transcripts are translated into proteins; therefore investigation of the host's global expression protein profiles during infection through a label-free quantitative method enables a comparison of the transcriptome and proteome. This would enhance our knowledge and understanding of similarities/ differences of the transcriptome and proteome expression analysis in host responses during *T. gondii* and *N. caninum* infection as discussed in the next chapter (chapter four).

4 Chapter four: Comparative proteomic profiles of host cells response during *T. gondii* and *N. caninum* infection using label-free analysis

4.1 Introduction

There are many apicomplexan parasites associated with CNS diseases that collectively have a huge impact on both human and animal health outcomes (Carruthers 2006). For example, one of the most successful parasites is *Plasmodium falciparum* that causes cerebral malaria due to the microvascular sequestration of the parasite and can lead to death in severe cases (Mackintosh, Beeson & Marsh 2004). *N. caninum* infection results in abortion in infected cattle and may cause neurological effects in congenitally infected calves. It can also result in limb paralysis in infected dogs (Dubey 2005). *T. gondii* infection in HIV/AIDS patients may lead to toxoplasmic encephalitis and may elicit severe cerebral damage in congenitally infected new-borns (Montoya & Liesenfeld 2004; Jones et al. 2001).

The biological properties of both *T. gondii* and *N. caninum* along with limitations in *N. caninum* investigations in the CNS has enhanced the need for investigating host-parasite interactions that may elucidate improvements in management of the diseases. In order for the parasite to successfully invade cells; modulation and alteration of host responses are required.

The availability of the genomic sequences of many organisms has facilitated the investigation of many biological aspects of functional annotations and metabolic pathways at the transcriptional level. Yet, genomic analysis alone is not enough to identify the resulting protein expressions profiles in biological systems under certain experimental conditions or during the complex life cycle of a particular parasite (Cuervo, Fernandes & de Jesus 2011; Walther & Mann 2010). Moreover, little or weak correlation between transcripts and protein expression have been found in

different protozoan analysis (McNicoll et al. 2006; Cohen-Freue et al. 2007). Thus, quantitative proteomic analysis enables the exploring of protein expression analysis in host biological systems during infection and determines protein functions (Aebersold & Mann 2003).

4.1.1 Label-free based quantitative investigations

Label-free approaches use raw data directly from parallel mass spectrometry runs to enable the comparison relative protein abundance in different protein runs (Wastling et al. 2012), and have many advantages over labelling techniques including low cost, simplicity and less concentrations of samples are required.

Currently, there are two different protein quantification schemes in label-free quantification: spectral counting and ion intensity measurements as discussed in detail in chapter one (1.9.4.2.1 and 1.9.4.2.2).

Throughout this thesis, ion intensity based strategy was used for label-free quantification. It is believed to be more robust compared to spectral counting which does not use retention time (Elliott et al. 2009). It can be biased towards abundant peptides, in which many low values are considered statistically unreliable due to high variability (Lundgren et al. 2010). Tandem mass spectrometers (MS/MS) coupled with liquid chromatography instruments such as Ion trap mass spectrometers (the LTQ Orbitrap Velos (Thermo)) were used for label-free proteomic quantification in this thesis. Furthermore, specialised software was required to generate normalised quantification values for each protein. There are open source programs available such as MZmine 2 (Pluskal et al. 2010) and commercially available software; such as SIEVE and Progenesis QI (http://www.nonlinear.com/progenesis/).

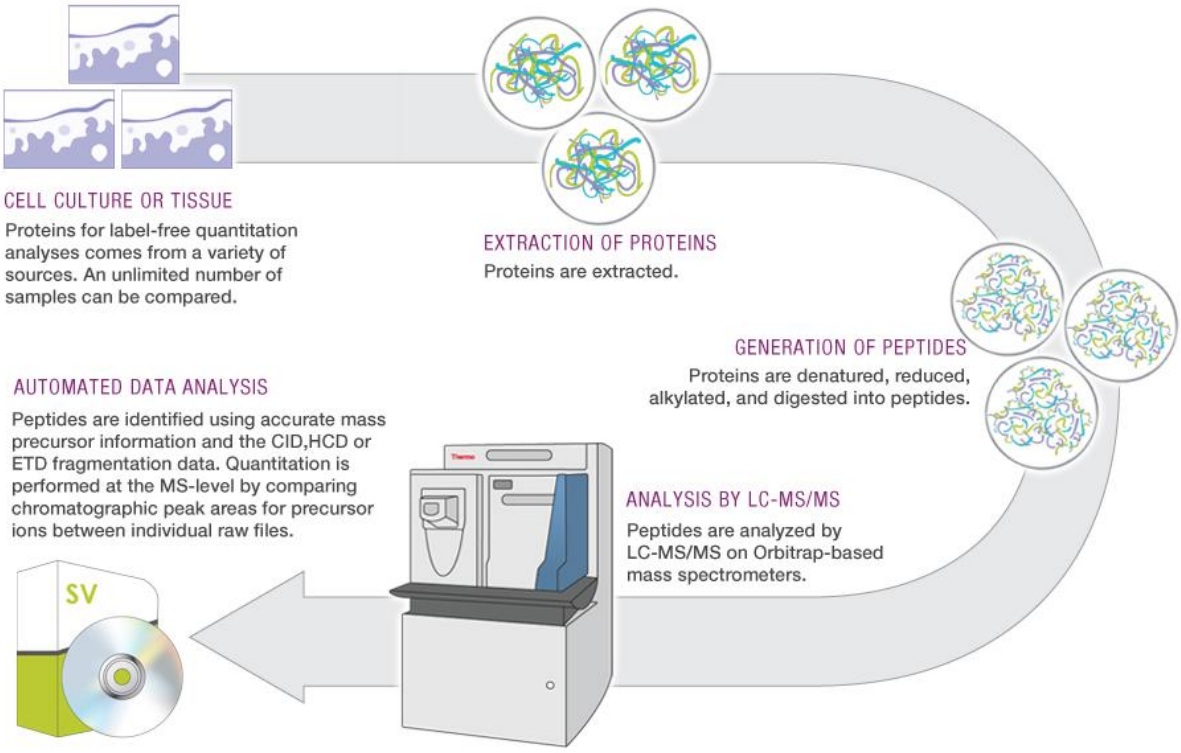

Figure 4.1: Overview of Label free workflow, samples are first prepared followed by protein extraction and digestion and later placed of the LC-MS/MS followed by protein identification and quantification using ion intensity generated by spectra or spectral counting, then analysed through an automated software (image taken from: http://planetorbitrap.com/label-free#.VBav7LFwaUk).

4.1.2 Research of astrocytes and parasites using label free quantitative proteomics

Limited investigations of the whole-cell proteome and secretome in astrocytes have been achieved (Skorupa et al. 2013; Yin et al. 2012). In particular, the whole-cell proteome of astrocytes has not been examined during parasitic invasion. An investigation done on neurons, astrocytes, oligodendrocytes and microglia in the human brain identified 1755 cell-type-specific nuclear proteins. These proteins are involved in histone modifications and the regulation of networks altered with normal brain aging or neurodegenerative disease (Dammer et al. 2013). Alzheimer's disease, a neurodegenerative disorder has been studied using label-free methods (Donovan et al. 2012; Ringman et al. 2012). A total of 13 proteins that were considerably altered from post-mortem brains of Alzheimer's disease patients compared to uninfected patients using spectral counting approach, such as Tau (MAPT), Ubiquitin carboxy-terminal hydrolase 1 (UCHL1), and syntaxin binding protein 1 (Munc-18) (Donovan et al. 2012). In a study done by Cutillas & Vanhaesebroeck, (2007); comparative proteomic profiling of five different mouse tissues (heart, brain, kidney, liver and lung) were analysed through label free ion intensity based method. A total of 1000 proteins were identified and biological processes in tissues were associated with transport, cell death, and development (Cutillas & Vanhaesebroeck 2007).

Label-free approach has also been applied to parasite studies. A study done by Bennuru *et al*. (2011) identified more than half of the predicted gene products in the filarial worm *Brugia malayi* from adult microfilaria and L3 larvae stages of the parasite through simple spectral counting. Also, different developmental stages of the parasite *S. japonicum* along with tissues of both host and parasites proteomes were characterised in parallel with transcriptomic data (Liu et al. 2006). Proteomics of the early gametocyte stage in the deadly malarial parasite *P. falciparum* determined the cellular proteome of 1427 proteins and discovered that the proteins involved in erythrocyte remodelling (Silvestrini et al. 2010).

In general, these quantitative label-free proteomic studies in both parasite and host cells have enabled a broader view of global proteomic expression changes to be identified, quantified and detect protein that were previously overlooked due to their low protein abundances with higher reproducibility and minimum variation detected between experimental samples.

To our knowledge, there have been no comparative studies investigating the host cell response in human astrocytes *in vitro* during infection with *T. gondii* and *N. caninum* through-label free quantitative method.

4.1.3 Aims and objectives

The main aim of this chapter was to compare proteomic changes occurring in human astrocytes during *T. gondii* to infected cells with *N. caninum* invasion using a label-free quantitative proteomics approach. In addition, the metabolic and functional annotations of the quantified proteins will be investigated which will enable a broader understanding of host-parasite interactions in the CNS.

4.2 Materials and methods

4.2.1 Cell culture

Human astrocytes (HA) primary cell lines were used as a model system. Cells were grown and maintained as mentioned previously in chapter two (2.2.1). TgVEG strain and NcLIV strain were used for infection; three time points (0, 4 and 16 hour's p.i) and three replicates per sample were selected for this experiment which is comparable to RNA-Seq chapter (3.2.1).

4.2.2 Label free sample preparation of HA cells

4.2.2.1 Lysis of HA cells

A total of 27 pellets of $1x10^7$ cells (three replicates each of HA cells infected with TgVEG, HA cells infected NcLIV and uninfected HA cells) were solubilised using 25 mM ammonium bicarbonate, followed by three cycles of the freeze/thaw/vortex method and two cycles of sonication in a sonicating water bath for 15 minutes each. The samples were centrifuged at 13,000 x g for 10 minutes at 4°C and the supernatant was collected. Protein concentration for each sample was determined by protein assay.

4.2.2.1.1 Protein Assay

Pierce Coomassie plus protein assay was used for protein concentration measurements of the 27 samples as mentioned previously in chapter two (2.2.2.3).

4.2.2.2 In-solution sample digestion

A total of 100 µg of each sample was further diluted in 25 mM ammonium bicarbonate to a volume of 160 µl, prior to the addition of 10 µl of 1 % Rapigest (Waters) (0.05 % (w/v) final concentration). The samples were heated to 80°C for 10 minutes and then 10 µl of 9.2 mg/ml DTT (3 mM final concentration) was added to

each sample, and incubated for 10 minutes at 60°C. A total of 10 µl of 33 mg/ml IAA (Iodoacetamide) was added to a final concentration of 9 mM and the samples were incubated in the dark for 30 minutes at room temperature. Trypsin was added at a 50:1 protein: trypsin ratio (10 µl/ 100 µg) using a 0.2µg/µl trypsin (Roche) solution and the digests were incubated overnight at 37°C. Trifluoroacetic acid (TFA) was added to a final concentration of 0.5 % (v/v) and the digest incubated for 45 minutes at 37°C. Finally, the samples were centrifuged for 15 minutes at 13000 x g at room temperature and the supernatant collected for subsequent mass spectrometric analysis (LC-MS/MS).

For quality control measures (QC), the digests and the proteins were run on a 1D-SDS PAGE to ensure complete digestion of the proteins to peptides prior to running them on the LC-MS/MS.

4.2.3 Protein identification and quantification

4.2.3.1 Label-free quantitative mass spectrometry analysis

The label-free quantitative mass spectrometry analysis of human astrocytes infected with TgVEG and NcLIV along with uninfected cells at three different time points was carried out by Dr. Dong Xia at the University of Liverpool using an Orbitrap Velos MS as described in chapter two (2.2.3.2).

4.2.3.2 Label-free peptide quantification of host cells

Raw data generated from the Orbitrap Velos was imported to Progenesis™ QI software (version 1, Nonlinear Dynamics) for label-free quantification. Two sets of analysis were performed on Progenesis; 1) HA cells infected with TgVEG vs. uninfected HA cells and 2) HA infected cells with NcLIV vs. uninfected HA cells. Profile data of the MS scans were transformed to peak lists, a sample was automatically selected as reference after checking the 2-D mapping (m/z versus retention time) for any LC variability. This is done to increase the reliability and

reproducibility of results and to produce combined data set. The retention times of the other samples within the experiment were aligned against the reference. Peptide maps created by peak picking were then applied to all replicates. Raw abundances were normalised to correct any experimental variation. Following peak picking the spectra produced for each feature were exported from Progenesis and used for peptide identification using Mascot (Matrix Science, version 2.3). against the UniProt reference and reviewed database for *H. sapiens* (Feb, 2014 version). Search parameters used were: 10ppm peptide mass tolerance (±10 ppm) and 0.8 Da fragment mass tolerance with one missed cleavage allowed. Fixed modification was set as carbamidomethylation while variable modification was set as methionine oxidation. Identified peptides with ion scores of > 13 ($p < 0.05$, FDR < 1%) were exported and re-imported into Progenesis™QI software. Statistical analysis was then performed on all detected features using normalized abundances for one-way analysis of variance (ANOVA). The results were further filtered to only include proteins ≥ 2 peptide hits and statistically significant (q value>0.05). Only the HA cells with infections at all three different time points (TgVEG infected and NcLIV infected) were used for the functional annotation analysis (a total of 18 samples).

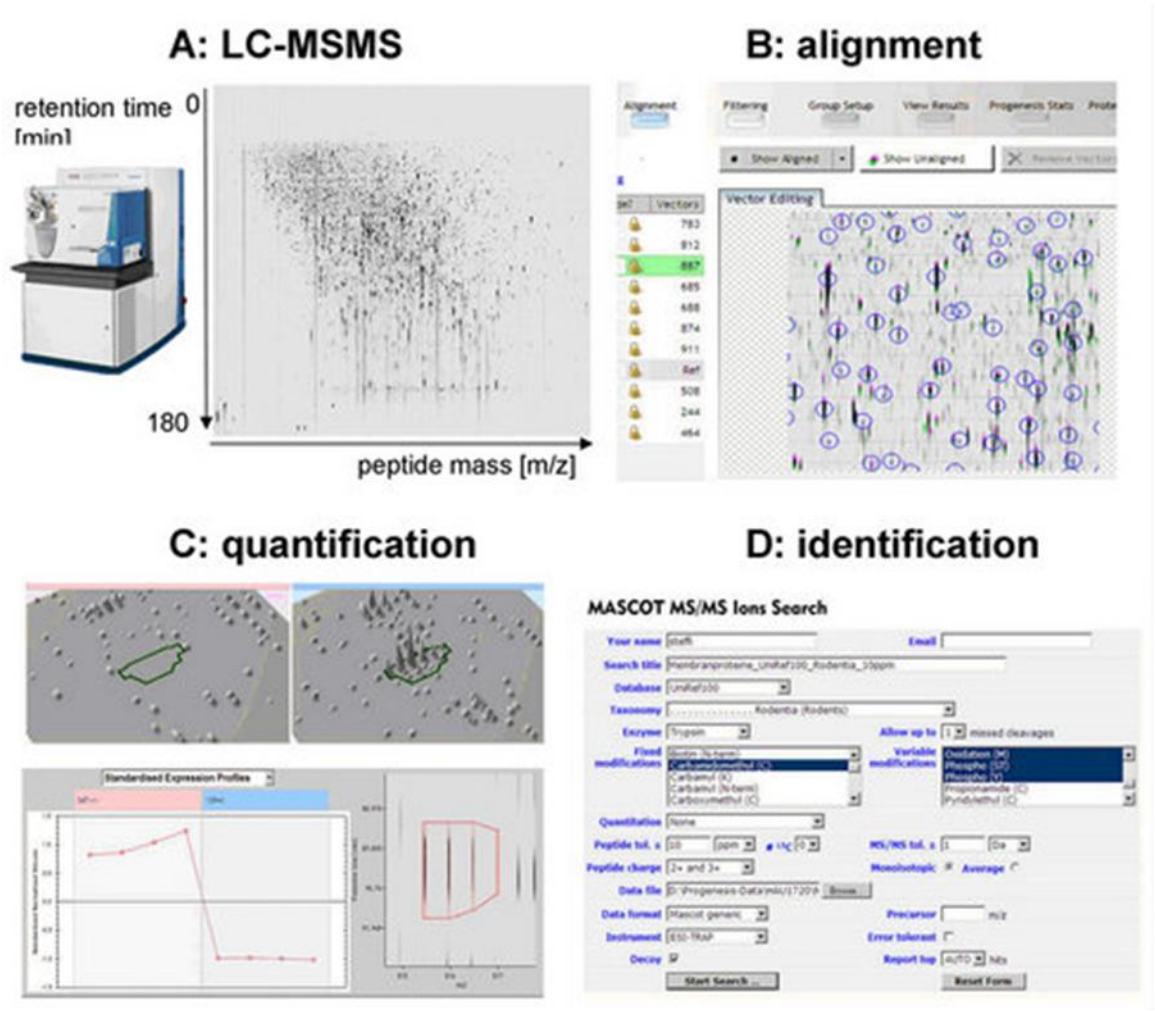

Figure 4.2: Workflow of label-free based protein quantification. Peptides that were digested from samples were inserted on Orbitrap (Thermo Fisher Scientific) (A).Raw peptide profiles were then aligned (B) and peptide intensities are quantified (C). Proteins are identified by MS/MS ion search in databases (Mascot) and peptide peak intensities assigned to each identified protein are accumulated (D). This figure was taken from http://www.helmholtz-muenchen.de/proteinscience/research/proteomics-technology-development/quantitative-proteomics/label-free-lc-msms-based-comparative-proteomics/overview/index.html.

4.2.4 Functional analysis and Annotation

Functional analysis of HA cell proteins that were found to be statistically significant were investigated using the functional analysis and clustering tool from the Database for Annotation, Visualisation, and Integrated Discovery (DAVID) (DAVID bioinformatics resources 6.7) (Huang et al. 2009). Proteins of HA cells infected with TgVEG and HA cells infected with NcLIV were searched in DAVID for metabolic pathway analysis (KEGG pathway) and functional annotations for their GO biological processes, molecular function and cellular components. The enriched metabolic pathways were compared to detect differences in the host's protein regulation and also the similarities between them.

4.2.4.1 Ingenuity Pathway Analysis (IPA)

Networks, functional analyses, and canonical pathways were produced through the use of the commercial software Ingenuity Pathway Analysis (IPA) (Ingenuity Systems, www.ingenuity.com). Functional analysis was used to identify the biological functions and diseases along with canonical pathways that were most relevant and statistically significant within the data set.

4.3 Results

A total of 1715 proteins were quantified and identified in the HA cells infected with *T. gondii*, while 1512 proteins were quantified in *N. caninum* infected HA cells. The proteins were then searched in DAVID for the enrichment of metabolic pathways, biological functions and cellular content.

4.3.1 DAVID analysis of host cells infected with TgVEG

Using DAVID analyses, a total of 30 statistically significant metabolic pathways were identified in infected HA cells with *T. gondii*. Pathways that were found with lower p-values and also differences in protein expressions between host cells infected with *T. gondii* and *N. caninum* were chosen (Table 4.1). Results from functional annotations of biological processes, cellular compartments and molecular functions are shown in table 4.2. Pathways selected with low p-values were ribosome, glycolysis, proteasome, focal adhesion and fatty acid metabolism (Table 4.1 and 4.3). The biological processes of host cells proteins infected with *T. gondii* were mainly associated with translation, intracellular transport and RNA processing. Cellular compartment was found mainly in mitochondrion and membrane-enclosed lumen, and molecular function was associated with RNA processing and structural molecule activity (Table 4.2).

Table 4.1: Metabolic pathways of human astrocytes infected with *T. gondii* searched using DAVID functional analysis.

Category	Term	Protein count	% of protein	P-Value	Benjamini
KEGG_PATHWAY	Ribosome	48	2.8	3.90E-18	7.00E-16
KEGG_PATHWAY	Spliceosome	58	3.4	4.70E-17	4.20E-15
KEGG_PATHWAY	Citrate cycle (TCA cycle)	25	1.5	6.20E-15	3.70E-13
KEGG_PATHWAY	Glycolysis / Gluconeogenesis	32	1.9	1.20E-11	5.40E-10
KEGG_PATHWAY	Fatty acid metabolism	23	1.3	2.60E-09	9.40E-08
KEGG_PATHWAY	Valine, leucine and isoleucine degradation	24	1.4	4.30E-09	1.30E-07
KEGG_PATHWAY	Oxidative phosphorylation	46	2.7	6.20E-09	1.60E-07
KEGG_PATHWAY	Proteasome	24	1.4	2.20E-08	4.90E-07
KEGG_PATHWAY	Huntington's disease	55	3.2	5.70E-08	1.10E-06
KEGG_PATHWAY	Pyruvate metabolism	21	1.2	1.20E-07	2.10E-06
KEGG_PATHWAY	Aminoacyl-tRNA biosynthesis	21	1.2	2.00E-07	3.20E-06
KEGG_PATHWAY	Parkinson's disease	42	2.4	3.40E-07	5.10E-06
KEGG_PATHWAY	Propanoate metabolism	18	1	3.50E-07	4.80E-06
KEGG_PATHWAY	Focal adhesion	57	3.3	5.10E-07	6.50E-06
KEGG_PATHWAY	Valine, leucine and isoleucine biosynthesis	9	0.5	2.20E-05	2.60E-04
KEGG_PATHWAY	Butanoate metabolism	16	0.9	3.20E-05	3.50E-04
KEGG_PATHWAY	Alzheimer's disease	44	2.6	4.80E-05	5.00E-04
KEGG_PATHWAY	Lysine degradation	18	1	7.50E-05	7.40E-04
KEGG_PATHWAY	Lysosome	34	2	9.00E-05	8.50E-04

Table 4.2: Functional annotations of human astrocytes infected with *T. gondii* protein; Biological processes (BP), cellular compartment (CC) and molecular function (MF).

Category	Term	Protein count	% of protein	P-Value	Benjamini
Biological process	translation	118	6.9	2.2E-33	7.8E-30
	translational elongation	58	3.4	2.4E-29	4.4E-26
	generation of precursor metabolites and energy	105	6.1	3.1E-27	3.7E-24
	intracellular transport	166	9.7	1.2E-26	1.1E-23
	RNA processing	144	8.4	5.3E-25	3.8E-22
Cellular compartment	ribonucleoprotein complex	188	11	2.7E-49	1.8E-46
	mitochondrion	287	16.7	3.2E-43	1.1E-40
	membrane-enclosed lumen	403	23.5	2.7E-39	6.1E-37
Molecular function	RNA binding	207	12.1	1.1E-41	1.4E-38
	nucleotide binding	423	24.7	1.4E-34	9.3E-32
	structural molecule activity	174	10.1	6.6E-32	2.8E-29
	structural constituent of ribosome	66	3.8	4E-21	1.3E-18
	actin binding	92	5.4	7.5E-18	1.9E-15

4.3.2 DAVID analysis of host cells infected with NcLIV

A total of 34 statistically significant metabolic pathways were identified in HA cells infected with *N. caninum*. Pathways that were found with low p-values and also differences in protein expressions between host cells infected with *T. gondii* and *N. caninum* were selected (Table 4.1 and 4.3). Functional annotations of biological processes, cellular compartment and molecular functions were searched (Table 4.4). The pathways with the lowest p-values were; ribosome, glycolysis, proteasome, focal adhesion and fatty acid metabolism pathways (Table 4.3). The biological processes of host cells infected with *N. caninum* were mostly related to translation, mRNA processing and oxidative reduction. Cellular compartment was mainly related to mitochondria and the molecular functions were associated with structural molecular activities (Table 4.4).

Table 4.3: KEGG metabolic pathways of human astrocytes infected with *N. caninum* searched using DAVID functional analysis.

Category	Term	Protein count	% of protein	P-Value	Benjamini
KEGG_PATHWAY	Ribosome	46	3	2E-18	3E-16
KEGG_PATHWAY	Spliceosome	48	3.2	2E-12	2E-10
KEGG_PATHWAY	Glycolysis / Gluconeogenesis	29	1.9	2E-10	1E-08
KEGG_PATHWAY	Fatty acid metabolism	23	1.5	3E-10	1E-08
KEGG_PATHWAY	Citrate cycle (TCA cycle)	20	1.3	4E-10	1E-08
KEGG_PATHWAY	Aminoacyl-tRNA biosynthesis	23	1.5	5E-10	2E-08
KEGG_PATHWAY	Valine, leucine and isoleucine degradation	23	1.5	3E-09	8E-08
KEGG_PATHWAY	Focal adhesion	53	3.5	4E-07	9E-06
KEGG_PATHWAY	Proteasome	21	1.4	5E-07	9E-06
KEGG_PATHWAY	Oxidative phosphorylation	39	2.6	6E-07	1E-05
KEGG_PATHWAY	Parkinson's disease	38	2.5	1E-06	2E-05
KEGG_PATHWAY	Propanoate metabolism	16	1.1	3E-06	5E-05
KEGG_PATHWAY	Pyruvate metabolism	17	1.1	2E-05	2E-04
KEGG_PATHWAY	Huntington's disease	44	2.9	4E-05	5E-04
KEGG_PATHWAY	Lysosome	32	2.1	6E-05	7E-04
KEGG_PATHWAY	Lysine degradation	17	1.1	7E-05	8E-04
KEGG_PATHWAY	ECM-receptor interaction	25	1.7	1E-04	0.001
KEGG_PATHWAY	Pathogenic Escherichia coli infection	18	1.2	6E-04	0.006
KEGG_PATHWAY	Pentose phosphate pathway	11	0.7	7E-04	0.006

Table 4.4: Functional annotation of human astrocytes infected with *N. caninum* proteins; Biological processes (BP), cellular compartment (CC) and molecular function (MF).

Category	Term	Protein count	% of protein	P-Value	Benjamini
Biological process	translation	113	7.5	6.2E-35	2.1E-31
	translational elongation	57	3.8	4.5E-31	7.6E-28
	generation of precursor metabolites and energy	97	6.4	2.6E-26	2.9E-23
	RNA processing	128	8.5	3.6E-22	3.1E-19
	intracellular transport	143	9.5	1.4E-21	9.7E-19
Cellular compartment	ribonucleoprotein complex	170	11.2	1.1E-45	7.4E-43
	mitochondrion	259	17.1	7.5E-41	2.5E-38
	mitochondrial part	174	11.5	7.4E-39	1.7E-36
Molecular function	structural molecule activity	164	10.8	9E-33	1.1E-29
	RNA binding	174	11.5	4.8E-31	2.9E-28
	nucleotide binding	378	25	7.1E-31	2.9E-28
	structural constituent of ribosome	65	4.3	4.5E-23	1.4E-20

4.3.3 Comparison of metabolic pathways of host cells response during infection

When investigating the differences in the metabolic pathways of HA cells infected with *T. gondii* and *N. caninum*, they generally had similar regulation patterns in their protein expressions; such as the citrate (TCA) cycle pathway, spliceosome and oxidation reduction pathway. The data was examined for differences between host cell protein expressions during TgVEG and NcLIV infection related to certain pathways; such as the ribosome (Figure 4.3), glycolysis (Figure 4.4), focal adhesion (Figure 4.5), fatty acid metabolism (Figure 4.6) and proteasome pathway (Figure 4.7).

In the ribosome pathway, four proteins showed differential expression between *T. gondii* and *N. caninum* infected cells. 60S ribosomal protein L14 (RL14) was up-regulated in cells infected with *T. gondii* at 4 hours followed by down-regulated expression at 16 hours p.i. compared to *N. caninum* infected cells, while 60S ribosomal protein L22 (RL22) showed the opposite trend in protein expression (Figure 4.3). 40S ribosomal protein S30 (RS30) was down-regulated at 4 hours followed by up-regulated expression at 16 hours p.i. in both infected cells with a higher rise in *T. gondii* infected cells (Figure 4.3). 60S ribosomal protein L21 (RL21) was only detected in cells infected with *N. caninum* and was significantly down-regulated (Figure 4.3). All the previous proteins are associated with RNA processing and translation.

Proteins involved in glycolysis pathway generally showed similar protein expression patterns between infections (Figure 4.4), with the exception of 4-trimethylaminobutyraldehyde dehydrogenase (AL9A1), which has roles in oxidation reduction and neurotransmitter biosynthetic process in the cell. AL9A1 was up-regulated in HA cells infected with *T. gondii* at 4 hours p.i. compared to *N. caninum* infected cells followed by down-regulation at 16 hours p.i. in both infections (Figure 4.4). ATP-dependent 6-phosphofructokinase, liver type (K6PL), involved in carbohydrate metabolic process was up-regulated in cells infected with *T. gondii*,

whereas down-regulated in HA cells infected with *N. caninum* at 4 hours p.i. (Figure 4.4).

In the focal adhesion pathway, serine/threonine-protein phosphatase PP1-gamma catalytic subunit enzyme (PP1G), and SHC-transforming protein 1 (SHC1) were both up-regulated in cells infected with *T. gondii* compared to cells infected with *N. caninum* (Figure 4.5). PP1G is a protein essential for cell division, glycogen metabolism and protein synthesis. SHC1 is a signalling adapter that couples activated growth factor receptors to signalling pathways. Growth factor receptor-bound protein 2 (GRB2) is associated with cell-cell signalling and axon guidance. It was up-regulated at 4hours in cells infected with *T. gondii* followed by down-regulation at 16 hours p.i. Mitogen-activated protein kinase 8 (MK08) was only detected in *N. caninum* infected cells and was significantly down-regulated at 4 hours and continued to decrease at 16 hours p.i. (Figure 4.5). MK08 is known to be associated with cell proliferation, differentiation, migration, transformation and programmed cell death.

Proteins associated with the fatty acid metabolism pathway; such as Peroxisomal acyl-coenzyme A oxidase 3 (ACOX3); is involved in cellular lipid metabolic processes. It was up-regulated in both infected cells, but at a slightly higher extent in cells infected with *N. caninum* (Figure 4.6). Peroxisomal bifunctional enzyme (ECHP); is an enzyme associated with receptor binding function and was down-regulated at 4 hours p.i followed by up-regulation at 16 hours p.i. in cells infected with *N. caninum*, while it was up-regulated in cells infected with *T. gondii* (Figure 4.6).

Proteasome pathway displayed similar pattern expressions in both infections with the exception of proteasome subunit beta type-6 (PSB6), which is linked to DNA damage response, signal transduction by p53 and cell cycle arrest. PSB6 was down-regulated in *T. gondii* infected cells and up-regulated in cells infected with *N. caninum*. 26S proteasome non-ATPase regulatory subunit 8 enzyme (PSMD8), which has similar functions as PSB6 was up-regulated at 4 hours followed by down-regulation at 16 hours p.i. in *T. gondii* infected cells (Figure 4.7).

HA cells infected with *T. gondii*

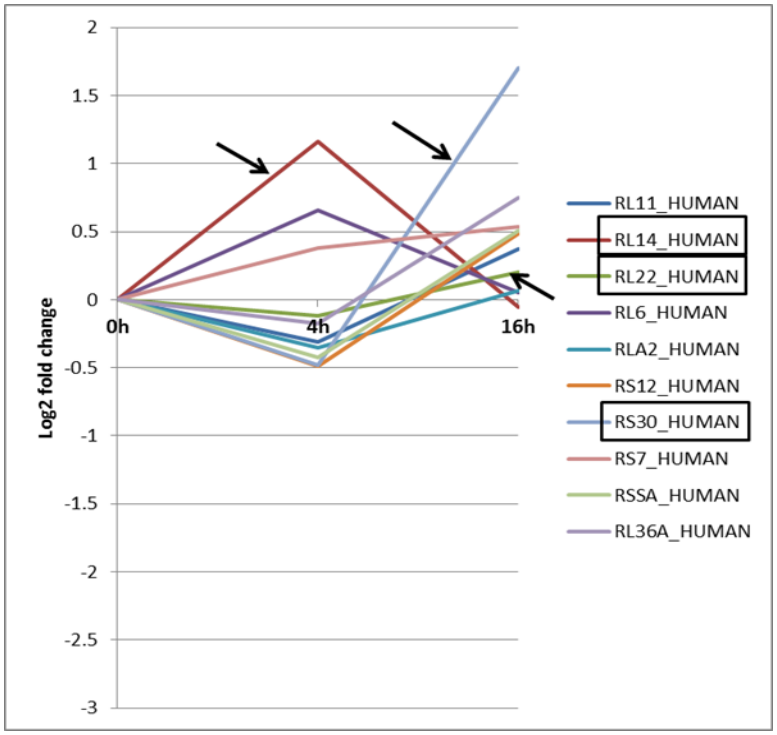

HA cells infected with *N. caninum*

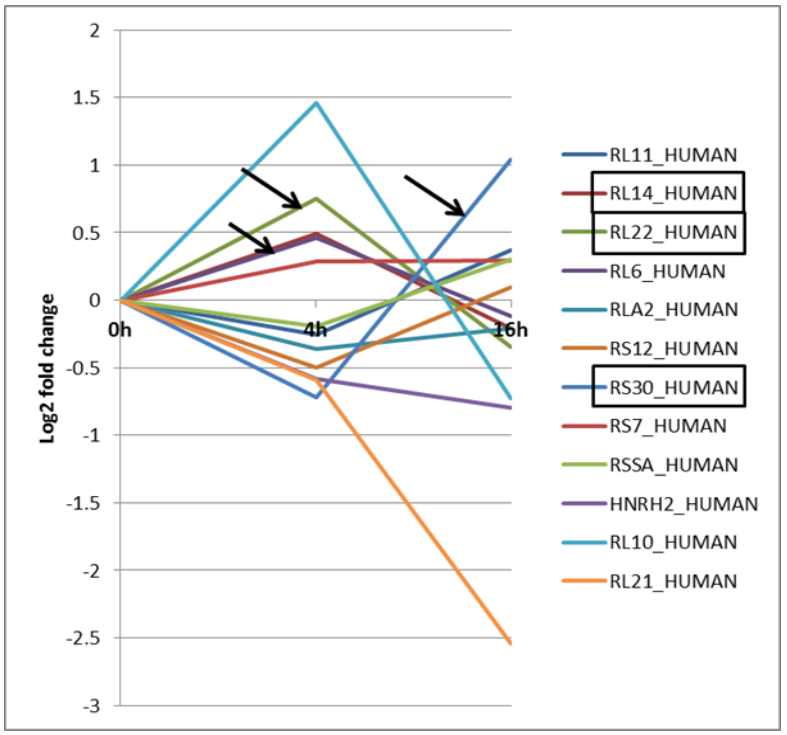

Figure 4.3: The ribosome pathway in HA cells infected with *T. gondii* and HA cells infected with *N. caninum*, RL14 (dark red line) was up regulated higher in HA cells infected with *T. gondii* at 4 hours then decreased at 16 hours p.i. compared to *N. caninum* infected cells. RL22 (dark green line) was decreased at 4 hours then slightly increased at 16 hours in HA cells infected with *T. gondii*, on the other hand it was increased at 4 hours then decreased at 16 hours p.i. in HA cells infected with *N. caninum*. RS30 (blue line) was found in both infections decreased at 4 hours followed by increased expression at 16 hours with a higher rise in *T. gondii* infected cells. RL21 (orange line) was only found in HA cells infected with *N. caninum* and was significantly decreased.

HA cells infected with *T. gondii*

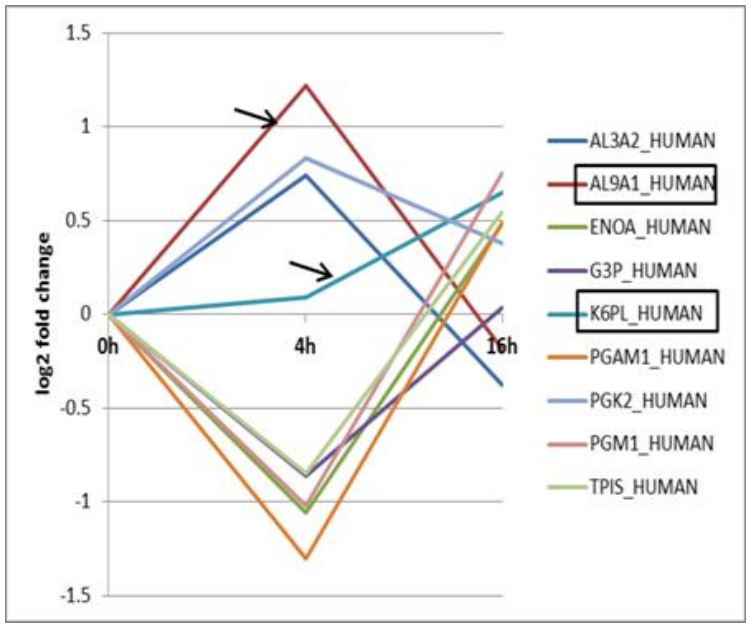

HA cells infected with *N. caninum*

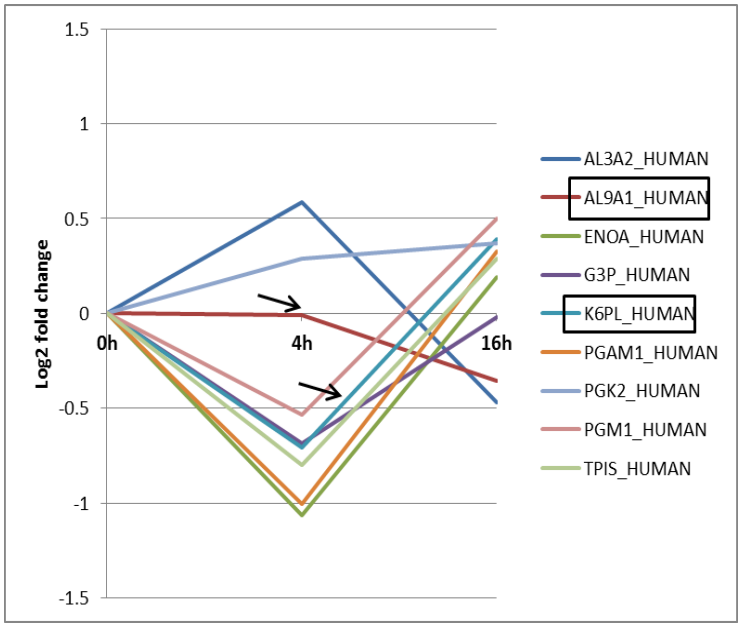

Figure 4.4: Proteins involved in glycolysis pathway in HA cells infected with *T. gondii* and HA cells infected with *N. caninum*. Most of the proteins showed similar protein expression patterns but AL9A1 (red line) was up regulated in *T. gondii* infected cell at 4 hours p.i. compared to *N. caninum* infected cells with no change in expression and down regulated in both infections. K6PL (blue line) was up regulated in *T. gondii* infected cells whereas down regulated in *N. caninum* infected cells at 4 hours and up regulated at 16 hours p.i.

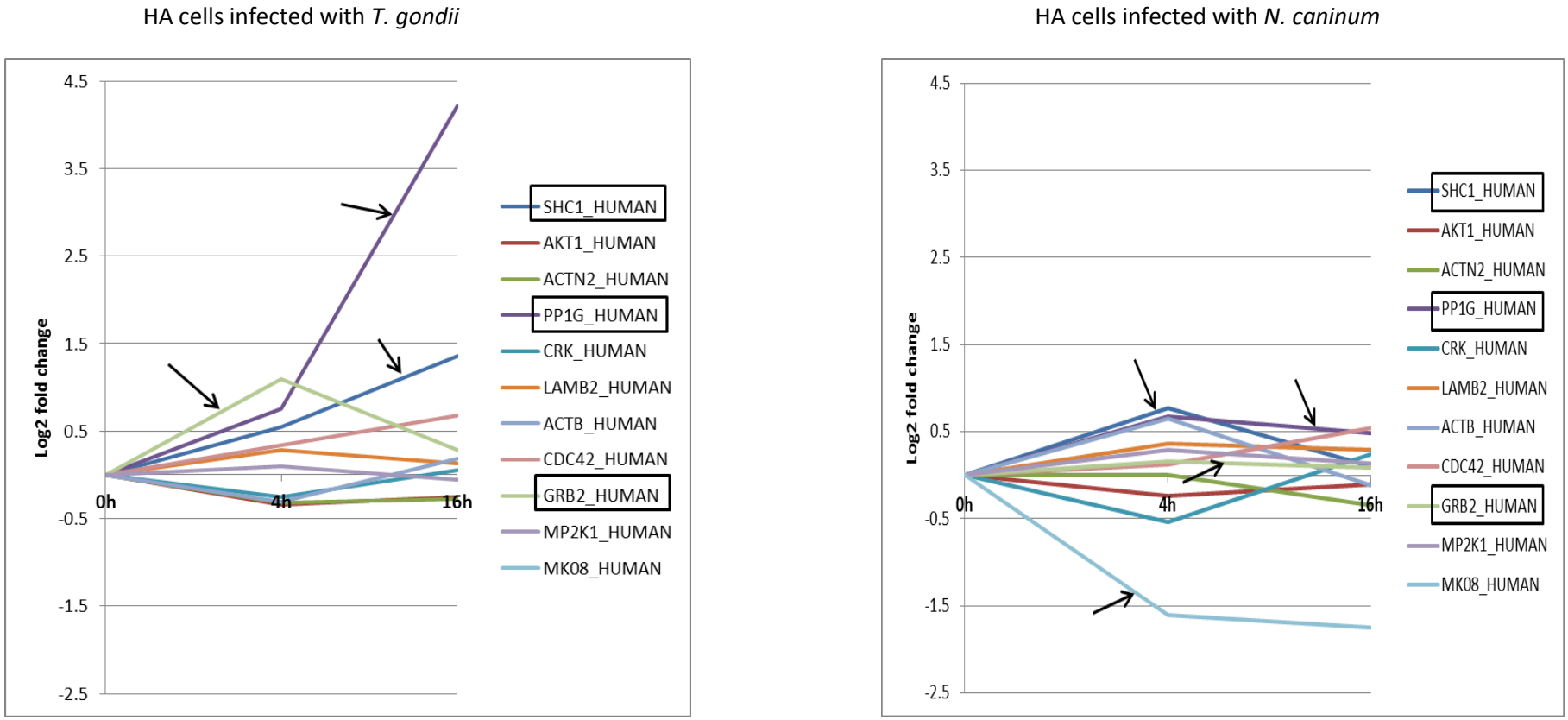

Figure 4.5: Focal adhesion molecule pathway comparison between HA cells infected with *T. gondii* and HA cells infected with *N. caninum*. PP1G (purple line) and SHC1 (blue line) proteins were found up-regulated higher in *T. gondii* infected cells compared to infected HA cells with *N. caninum*. GRB2 (light green line) was up-regulated at 4hours followed by a decrease at 16 hours p.i, whereas a slight increase of GRB2 was found in cells infected with *N. caninum*. MK08 (light blue line) protein was only found in HA cells infected with *N. caninum* and was significantly decreased at 4 hours and continued to decrease at 16 hours p.i.

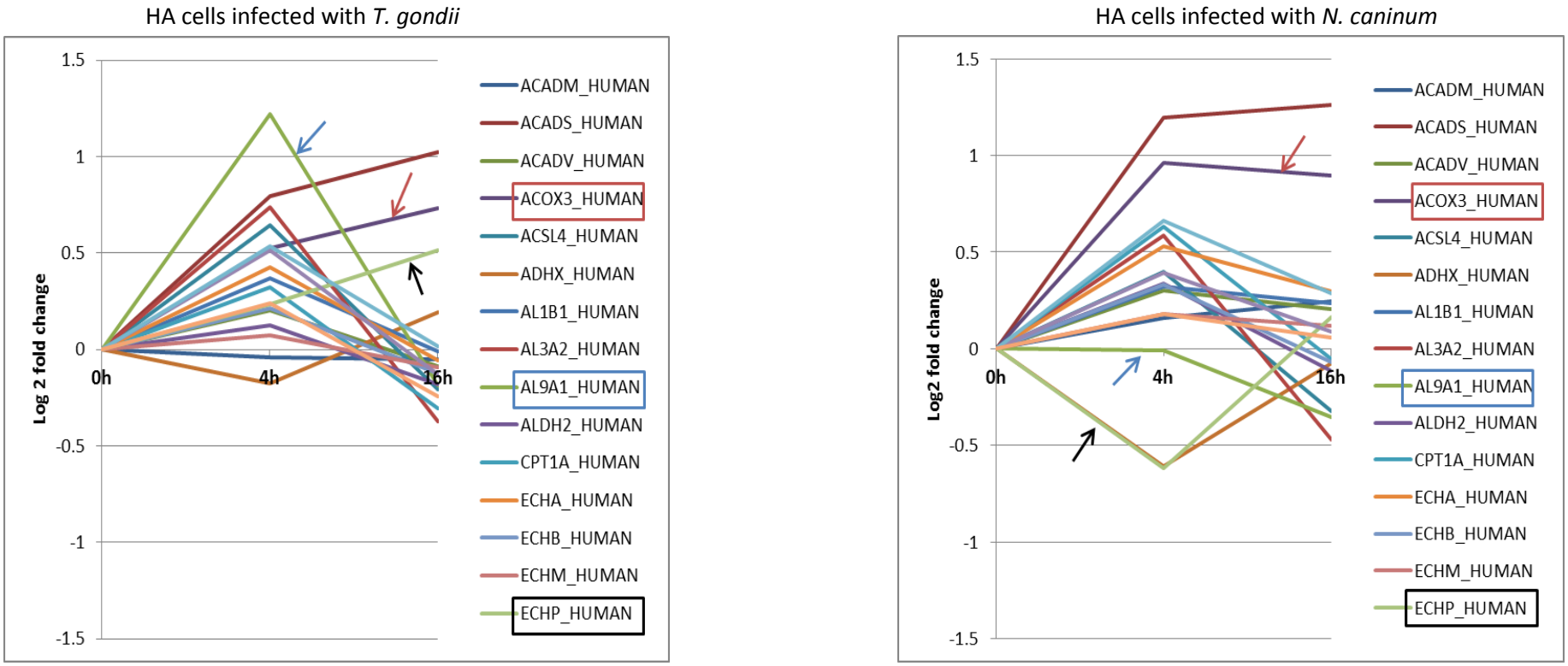

Figure 4.6: Fatty acid metabolism pathway comparison between HA cells infected with *T. gondii* and HA cells infected with *N. caninum*. ACOX3 (red arrow) and ECHP (black arrow) were found up-regulated in *T. gondii* infected cells, while ACOX3 was slightly higher up-regulated in *N. caninum* infected cells and ECHP was down regulated at 4 hours p.i then up regulated at 16 hours p.i. AL9A1 (blue arrow) also found in glycolysis pathway was up regulated at 4 hours then down regulated at 16 hours p.i in *T. gondii* infected cells, while no changes occurred in cells infected with *N. caninum* at 4 hours followed by slightly down regulation at 16 hours p.i.

HA cells infected with *T. gondii*

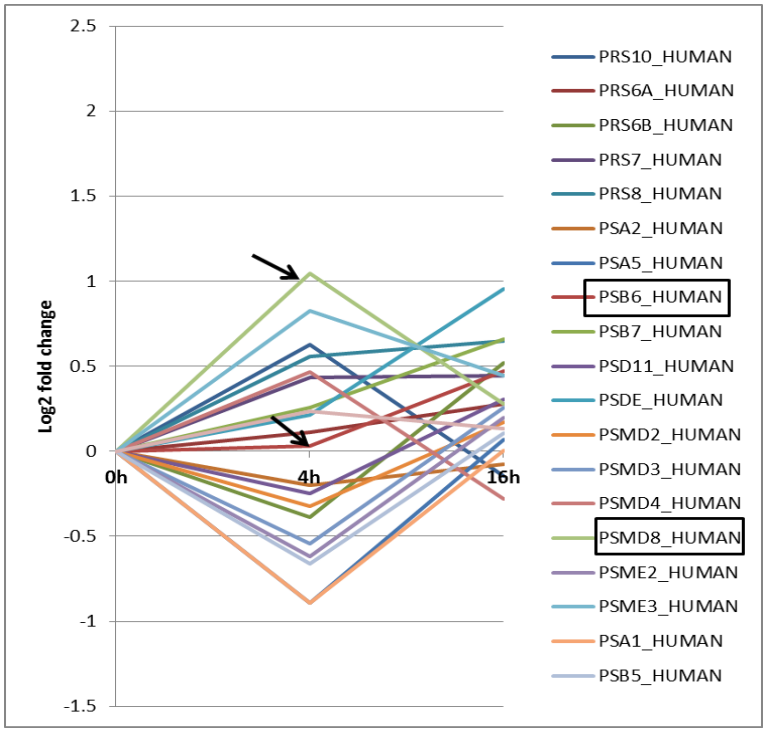

HA cells infected with *N. caninum*

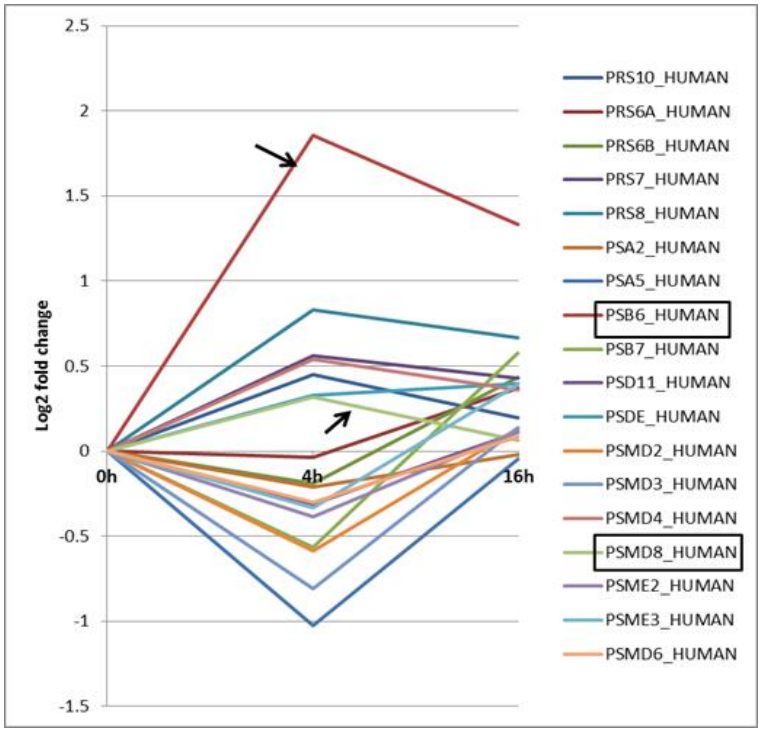

Figure 4.7: Proteasome pathway showing proteins clustered in both *T. gondii* infected cells and *N. caninum* infected cells. PSB6 (red line) was down-regulated in *T. gondii* infected cells and up-regulated in *N. caninum* infected cells. PSMD8 protein was showing increased (two times higher than *N. caninum* infected cells fold change) expression at 4 hours followed by down regulation at 16 hours p.i. in *T. gondii* infected cells.

4.3.4 Proteins with the highest fold changes during host cell infection

Another approach was carried out to investigate individual protein expression changes (at 4 hours and 16 hours p.i.) that were not associated with any individual pathways but had significantly increased expression changes (Figures 4.8, 4.9, 4.10 and 4.11).

The significantly up-regulated proteins identified in *T. gondii* infected cells at 4 hours p.i. were compared with proteins found in *N. caninum* infected cells (Figure 4.8). Proteins such as pannexin-1 (PANX1), which is associated with calcium ion transport and 28S ribosomal protein S29, mitochondrial (RT29), which is involved in mediating interferon-gamma-induced cell death were significantly increased. Proteins serine/arginine-rich splicing factor 8 (SRSF8) which is involved in mRNA processing and caskin-2 (CSKI2) were also increased in cells infected with *T. gondii* but not in *N. caninum* infected cells.

The significantly up-regulated protein expression changes in *N. caninum* infected cells compared to cells infected with *T. gondii* at 4 hours p.i. were 39S ribosomal protein L12, mitochondrial (RM12), which is involved in transcription and translation processes. DnaJ homolog subfamily C member 13 (DJC13), which is important in osteoblast differentiation, and histone H3.1 (H31), which is important in chromatin organization. Whereas other proteins were only found in *N. caninum* infection such as putative ATP-dependent RNA helicase DHX33 (DHX33), a protein involved in transcription, estradiol 17-beta-dehydrogenase 11 (DHB11), which is associated with lipid biosynthesis and lactotransferrin (TRFL) that has antimicrobial activity (Figure 4.9).

Significant up-regulated protein changes were also investigated at 16 hours p.i. There were certain individual proteins that were found in one infection and not detected in the other infection. For example; non-histone chromosomal protein HMG-17 (HMGN2) and helicase SRCAP (SRCAP) protein both associated with DNA binding were only identified in *T. gondii* infected cells (Figure 4.10). In *N. caninum* infected cells at 16 hours p.i.; asparagine-tRNA ligase (SYNC) is associated with catalytic activity in the cell. Fructose-bisphosphate aldolase C (ALDOC) involved in glucose metabolic process was up-regulated in *N. caninum* infection compared to *T. gondii* infected cells (Figure 4.11).

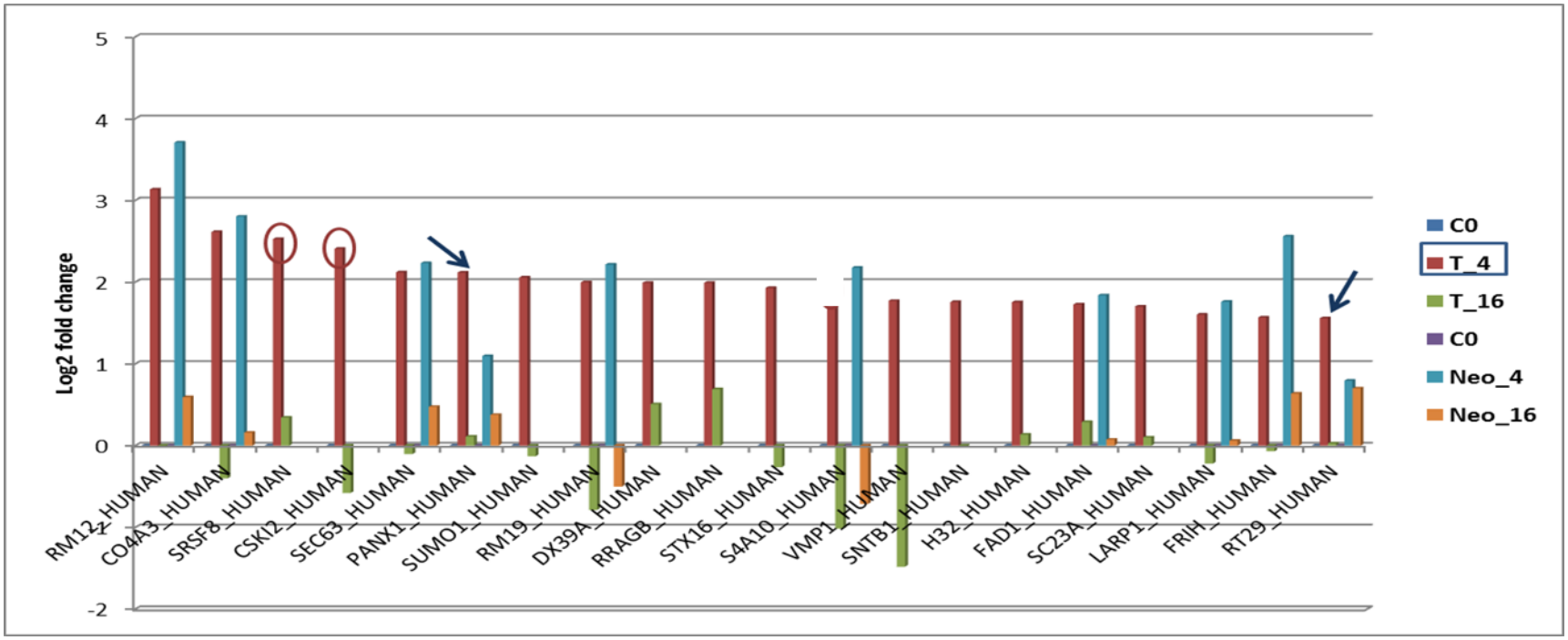

Figure 4.8: Significantly up-regulated fold changes at 4 hours p.i. in *T. gondii* infected HA cells comparing to *N. caninum* infected cells. Some proteins were found in both infected HA cells with higher increased expression in *T. gondii* infected cells; such as PANX1 and RT29 (arrows), whereas others were only found in cells infected with *T. gondii* such as SRSF8 and CSKI2 (red circles).

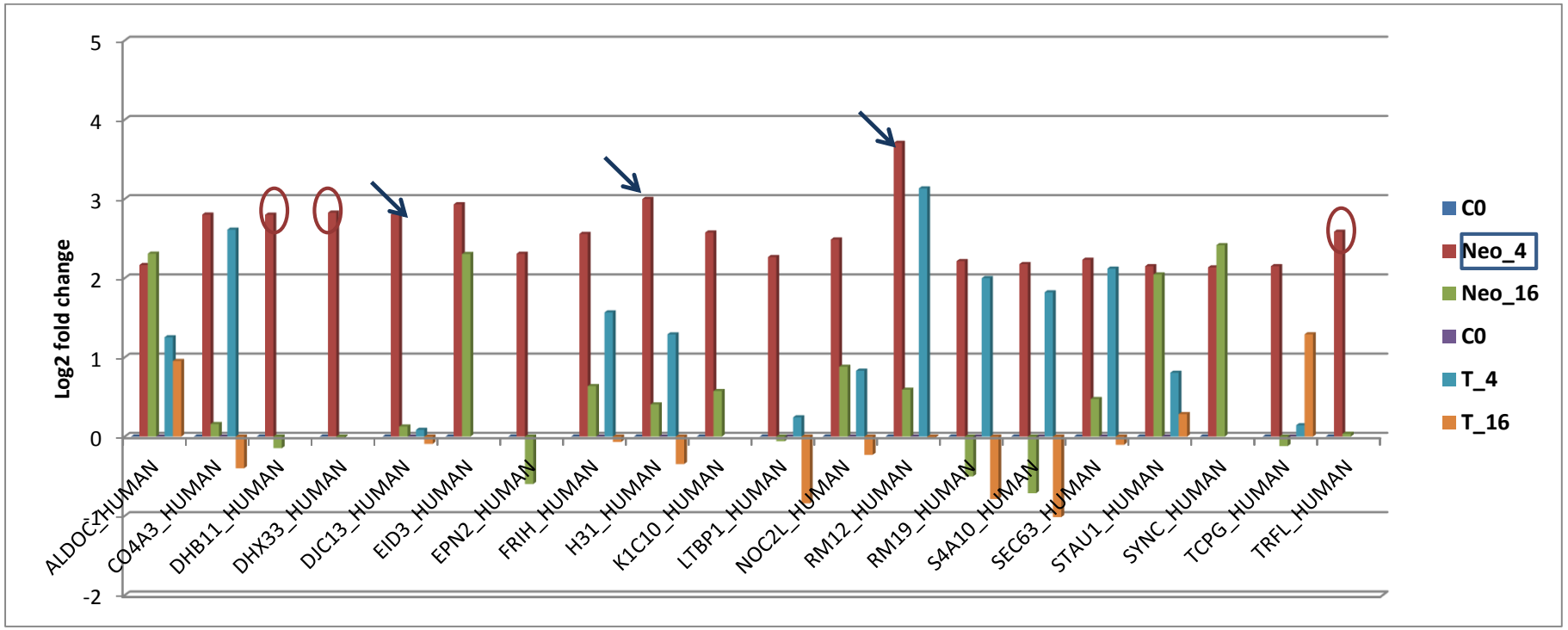

Figure 4.9: Significantly up-regulated protein changes in HA cells infected with *N. caninum* at 4 hours p.i. compared to proteins in HA cells infected with *T. gondii*. Some proteins were found in both HA cells infections with higher increased expression in cells infected with *N. caninum* such as DJC13, H31 and RM12 (arrows), whereas others were only found in HA cells infected with *N. caninum* such as DHX33, DHB11 and TRFL (red circles).

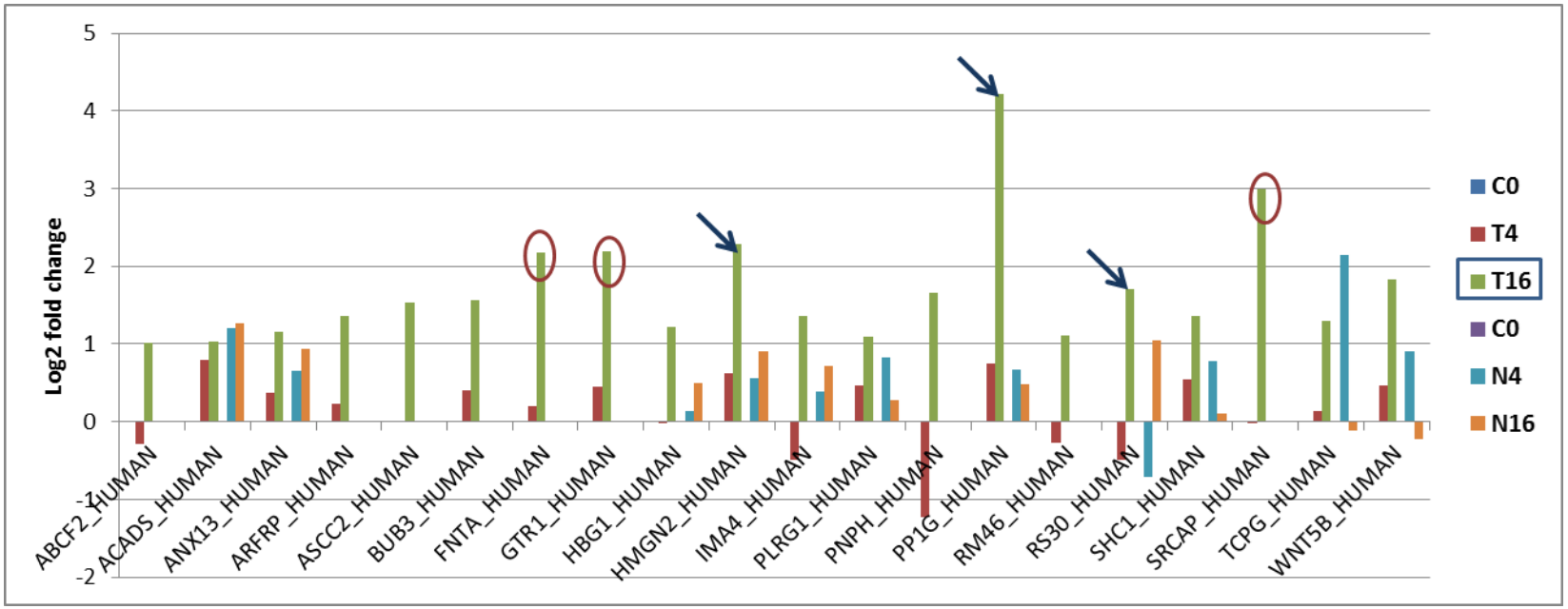

Figure 4.10: Significantly up-regulated protein changes in HA cells infected with *T. gondii* compared to HA cells infected with *N. caninum* at 16 hours p.i. Proteins found in both infected HA cells with higher increased expression in *T. gondii* infected cells included PP1G, HMGN2 and SRCAP (arrows), whereas others were only found in cells infected with *T. gondii* such as FNTA, GTR1 and SRCAP (red circles).

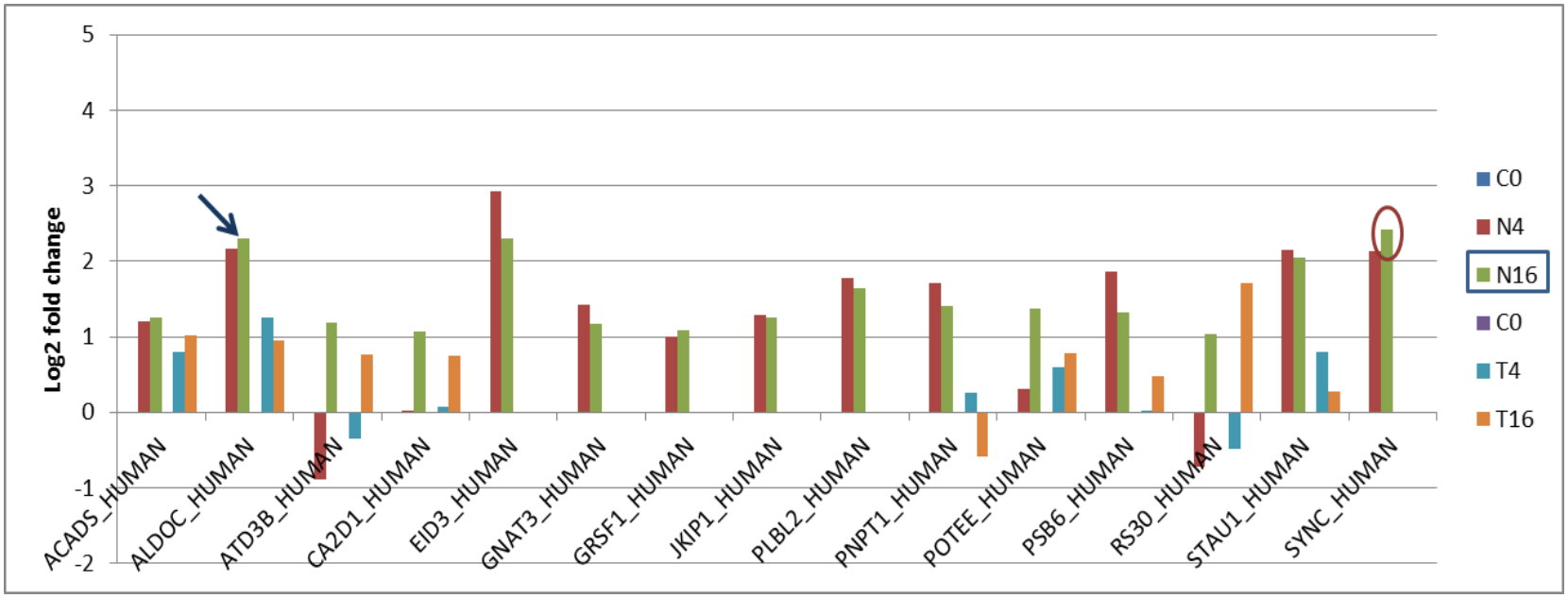

Figure 4.11: significantly up-regulated protein changes *N. caninum* infected cells compared to *T. gondii* infected cells at 16 hours p.i. Proteins found in with higher increased expression in cells infected with *N. caninum* such as ALDOC (arrow), whereas others were only found in cells infected with *N. caninum* such as SYNC (red circle).

4.3.5 Ingenuity Pathway Analysis of infected HA cells

The proteins quantified in both infected cells that have statistical significance (1715 in *T. gondii* infected cells and 1512 in *N. caninum* infected cells) were searched using Ingenuity Pathway Analysis (Qiagen). For the IPA mapping of the pathway, proteins with a ≥ 1.5 fold changes between the three time points were considered to be increased and were highlighted in red, proteins that were ≤ 0.66 fold change decreased were highlighted in green. The top enriched canonical pathway reported by IPA was the ERK/MAPK pathway in both *T. gondii* infected cells (Figure 4.12) and *N. caninum* infected cells (Figure 4.13), in which there were differences in some of the protein expressions in this pathway.

In the ERK/MAPK pathway, a total of six proteins showed differential expression between the infected cells including 1433B, 2ABA, GRB2, PP1G, SHC1 and RASH. A description of these proteins along with their expression changes at three different time points are shown in Table 4.5 in cells infected with *T. gondii* and Table 4.6 in cells infected with *N. caninum*.

Table 4.5: Proteins associated with the ERK/MAPK pathway in cells infected with *T. gondii* at three different time points (0, 4, and 16 hours p.i.).

Accession	Protein	Peptides used for quantitation	Confidence score	q Value	Description	C0_FC	T4_FC	T16_FC
P31946	1433B_HUMAN	4	914.27	9.71E-06	14-3-3 protein beta/alpha	1	0.494496	1.199595
P63151	2ABA_HUMAN	2	190.96	0.038746	Serine/threonine-protein phosphatase 2A 55 kDa regulatory subunit B alpha isoform	1	1.454835	1.111854
P62993	GRB2_HUMAN	3	25.03	0.01907	Growth factor receptor-bound protein 2	1	2.130628	1.219124
P36873	PP1G_HUMAN	2	990.98	0.007038	Serine/threonine-protein phosphatase PP1-gamma catalytic subunit	1	1.685766	18.57231
P01112	RASH_HUMAN	3	168.54	0.001976	GTPase HRas	1	1.793393	1.165845
P29353	SHC1_HUMAN	3	43.68	0.012909	SHC-transforming protein 1	1	1.455901	2.558603

Table 4.6: Proteins associated with the ERK/MAPK pathway in cells infected with *N. caninum* at three different time points (0, 4, and 16 hours p.i.).

Accession	Protein	Peptides used for quantitation	Confidence score	q Value	Description	C0_FC	Neo4_FC	Neo16_FC
P31946	1433B_HUMAN	7	744.21	0.001527	14-3-3 protein beta/alpha	1	0.677575	0.911362
P63151	2ABA_HUMAN	3	130.6	0.006356	Serine/threonine-protein phosphatase 2A 55 kDa regulatory subunit B alpha isoform	1	2.184887	1.236794
P62993	GRB2_HUMAN	4	24.25	0.022018	Growth factor receptor-bound protein 2	1	1.111681	1.064958
P36873	PP1G_HUMAN	2	619.8	0.04088	Serine/threonine-protein phosphatase PP1-gamma catalytic subunit	1	1.593644	1.393359
P01112	RASH_HUMAN	2	104.98	0.003716	GTPase HRas	1	1.805846	1.519057
P29353	SHC1_HUMAN	3	38.74	0.047089	SHC-transforming protein 1	1	1.708518	1.070796

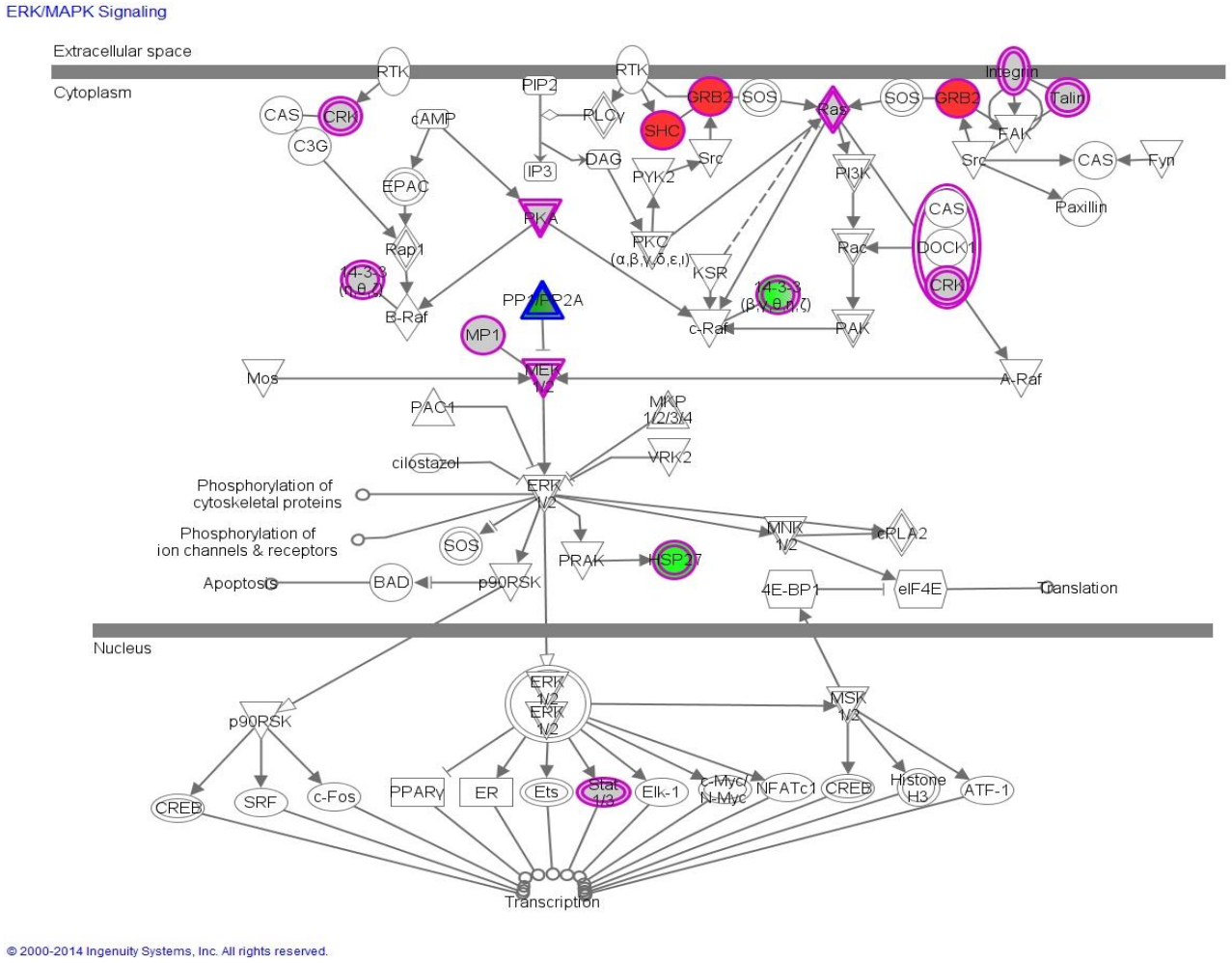

Figure 4.12: showing the **ERK/MAPK** pathway in **HA cells infected with *T. gondii*** at 4 hour p.i. using IPA analysis, the green colour indicates proteins that were down-regulated and the red colour indicated the proteins that were up-regulated, the proteins that were highlighted with purple and grey coloured shading are the proteins identified in this study but showed no significant fold changes.

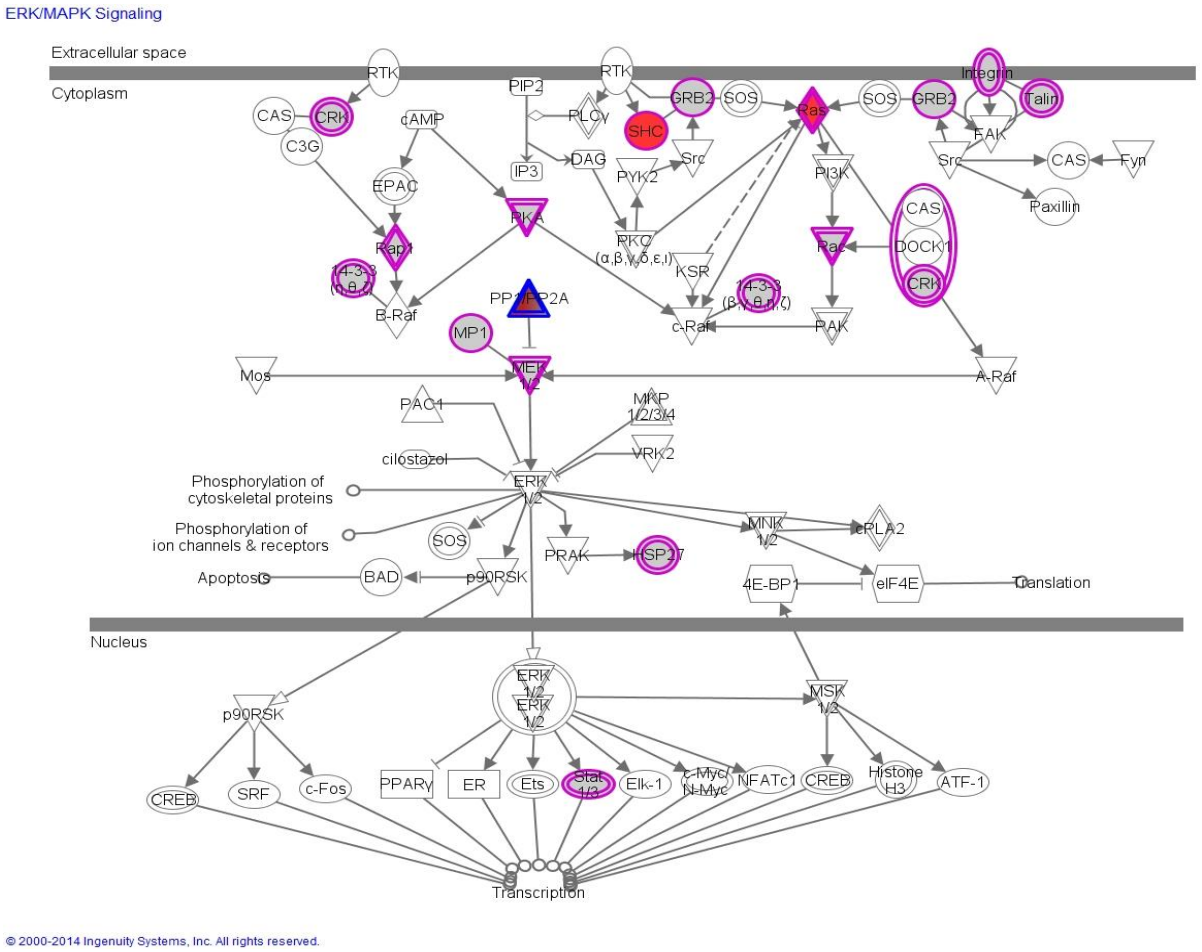

Figure 4.13: showing the **ERK/MAPK** pathway in **HA cells infected with *N. caninum*** at 4hours p.i. using IPA analysis, the green colour indicates proteins that were down-regulated and the red colour indicated the proteins that were up-regulated, the proteins that were highlighted with purple and grey coloured shading are the proteins identified in this study but showed no significant fold changes.

4.4 Discussion

In order for parasites to continue and multiply in host cells, they have evolved approaches to manipulate their hosts by modulating cell signalling pathways. In *T. gondii*; the parasite uses the host cells for proliferation through hijacking cells to disseminate in different areas of their hosts (Courret et al. 2006; Lambert & Barragan 2010). Tachyzoites of *T. gondii* have been proven to cross the blood brain barrier (BBB) and reach the brain.

The main aim of this investigation was to explore proteomic expression changes occurring in human astrocytes during infection with *T. gondii* or *N. caninum* at three different time points of infection correlating to the time points chosen for the host's transcriptomic analysis (Chapter three). Changes in transcriptional expressions between infections were observed and further confirmed through protein expression profile analysis between *T. gondii* and *N. caninum* carried out in this chapter. There was no correlation perceived between significant transcripts and differentially expressed proteins detected in this chapter. Most transcripts showing differential expression were linked to cytokine and cell signalling pathways, while in the proteomic expression profiles there were mostly related to metabolism (glycolysis and fatty acid metabolism).

Comparison of metabolic pathway analysis between the host cells infected by two parasites revealed that similar host responses were observed in many pathways, such as the spliceosome pathway and citrate TCA cycle pathways. Differences in protein expressions were also observed in some metabolic pathways including ribosome, focal adhesion, proteasome, glycolysis and fatty acid metabolism.

4.4.1.1 Ribosome metabolic pathway of infected human astrocytes

Ribosomes are complex molecules involved in the processing and biosynthesis of proteins, in which ribosome synthesis includes the assembly of two subunits, a large (60S) and small (40S) subunit. Nowadays, ribosomes are considered to play roles in

protein and transcript quality control (Kramer et al. 2009; Wilson & Beckmann 2011). They are also involved in cell stability, cellular response to different stimuli, cell proliferation, DNA repair, and apoptosis and are associated with the many diseases such as metabolic disease and cancer (Wang et al. 2014; Lindstrom & Zhang, 2008; Volarevic et al. 2000). Three proteins were found differentially expressed between the two infections; RL14, RL22 and RS30. RL14 was up-regulated in *T. gondii* infected cells at 4 hour p.i. compared to *N. caninum* followed by down-regulated expression at 16 hours p.i, whereas RL22 was up-regulated in HA cells infected with *N. caninum* at 4 hours p.i. compared to *T. gondii* infected cells. These differences were observed despite both RL14 and RL22 are 60S ribosomal proteins involved in gene expression and translation. RS30 was found up-regulated in both HA infected cells but at a higher extent in *T. gondii*. It is a 40S ribosomal protein associated with cellular metabolic process, gene expression and antibacterial humoral response. Previous investigations of the host global transcriptional expression profiles during *T. gondii* infection have found modulations taking place in host metabolic pathways such as the ribosome pathway (Blader et al. 2001). Transcriptional changes in the peripheral lymphocytes of mice infected with type I showed up regulation of genes related to CAM, olfactory transduction and ribosome pathways (Jia et al. 2013).

Although differences between proteins were observed in this pathway, they werea very low number of proteins. Moreover, other proteins related to this pathway showed similar expression which may suggest protein expression changes of host cells between these two parasites may in general behave in a similar manner related to the main metabolic pathwaysfound in the host cells (Figure 4.3). Furthermore, the use of the less virulent strain TgVEG may also have induced host responses closely related to *N. caninum* as demonstrated in a comparative transcriptional study by Beiting *et al*. (2014). As their asre strain differences in *T. gondii* parasites.

4.4.1.2 Glycolysis pathway of infected human astrocytes

Host cell induction of glycolysis supports the parasites growth and tachyzoites proliferation (Bohne & Roos, 1997; Dzierszinski et al. 2004). The preferred encystation sites for the parasite are the muscles and CNS are also tissues with increased glycolytic activities through increased lactate formation (Luft & Castro 1991; Brooks 2002). In addition, *T. gondii* expresses glycolytic enzymes (Dzierszinski et al. 1999; Pomel, Luk & Beckers 2008). Host mitochondrial recruitment to the *T. gondii* PVM is implicated to supply the tachyzoites with energy, but it is not clear the exact form of this nutrient (e.g. in glucose or glutamine source) (Sibley 2003; Polonais & Soldati-Favre 2010). A study done by Blume *et al*. (2009) on a mutant strain of *T. gondii* with impaired glucose transport ability showed a light effect on the parasites growth but showed impairment in the parasites extracellular motility.

Glycolysis metabolism is a 10-step process which produces ATP and pyruvate as the end product that may be linked to oxidative phosphorylation, and changes in the host metabolism can be a result of nutrient uptake by these parasites (Blader et al. 2001; Ainscow & Brand 1999). Only two proteins from the glycolysis metabolic pathway showed differential expression between infected cells with *T. gondii* and *N. caninum*; 4-trimethylaminobutyraldehyde dehydrogenase (AL9A1) and ATP-dependent 6-phosphofructokinase, liver type (K6PL). K6PL is from the initial steps of the glycolysis metabolism pathway, it catalyses the phosphorylation of D-fructose 6-phosphate to fructose 1, 6-bisphosphate using ATP (Yin et al. 2012). This glycolytic enzyme was up-regulated in cells infected with *T. gondii* whereas it was down-regulated at 4 hours followed by up-regulation at 16 hours post infection in cells infected with *N. caninum*. Due to the fact the parasite itself cannot produce the nutrients it needs, and obtains them directly from the host cells, the *T. gondii* PVM that surrounds and protects the parasites contains small pores that allow the exchange of nutrients, including glucose, iron, phospholipids and purines between the host cytoplasm and tachyzoites that enter through membrane transporters (Schwab et al. 1994, Charron & Sibley 2002; Blader & Saeij 2009). Host cells and specifically the mitochondria and ER are the main providers of essential products needed by the parasite (Sinai, Webster & Joiner 1997; Crawford et al. 2006). This

may suggest that *T. gondii* parasites have a higher need of glycolytic metabolism compared to cells infected with *N. caninum*. The AL9A1 enzyme causes oxidation of aldehyde in an NAD-dependent reaction and is associated with neurotransmitter synthesis and oxidation reduction (Vaz et al. 2000). This may suggest that *T. gondii* increases AL9A1 for neurotransmitter biosynthetic production to enable modification of host cell behavioural responses during infection. *T. gondii* has been indicated to change host behaviour during infection in mice (Prandovszky et al. 2011), in order to continue its life cycle by motivating the intermediate host to be ingested by the cat.

The proteomic analysis showed it was up-regulated at 4 hours p.i. then down-regulated at 16 hours p.i. in astrocytes infected with *T. gondii*, whereas no changes occurred in the first 4 hours of infection followed by decreased expression at 16 hour p.i. in cells infected with *N. caninum*.

4.4.1.3 Focal adhesion of infected human astrocytes

At the cell-extracellular matrix region, focal adhesion molecules are formed, where actin filaments are attached to transmembrane receptors of the integrin family. Focal adhesion molecules are macromolecule protein complexes that help to connect the cytoskeleton of a cell to the extracellular matrix (ECM) (Wozniak et al. 2004). They have essential roles such as cell motility, cell proliferation, cell differentiation, regulation of gene expression and cell survival. In the CNS, astrocytes have been shown to be key sources of ECM and adhesion proteins, that controls neurite outgrowth in relation to developmental or injury causes (Wang & Bordey 2008). Zhou et al. (2103), detected differences in regulation between the two strain infections, in which focal adhesion metabolism was up-regulated in TgRH infected brain tissue compared to TgME49 (Zhou et al. 2013).

Three proteins were found with increased fold change expressions in *T. gondii* infected cells compared to *N. caninum* infected cells; serine/threonine-protein phosphatase PP1-gamma catalytic subunit (PP1G), SHC-transforming protein 1 (SHC1) and growth factor receptor-bound protein 2 (GRB2) (Figure 4.4). PP1G is a

phosphatase that dephosphorylates biological targets and is involved in cell division, cell cycle, glycogen metabolism, protein synthesis and synaptic plasticity. SHC1 is a signalling adapter that links activated growth factor receptors to signalling pathways and is involved in signal transduction, apoptosis, cell migration, oxidative stress, and increased expression of this protein has been linked to cancer (Honda et al. 2008). GRB2 connects the cell surface growth factor receptors with the Ras signalling pathway that is involved in signal transduction and cell communication. Inhibition or dysfunction of GRB2 results in defects in developmental processes and impairs transformation and propagation of cells and may cause cell death. Up-regulation of PP1G may suggest that *T. gondii* increases this protein for protein binding processes. Also, the parasite might increase PP1G for glycogen production and synthesis to increase the parasite growth and proliferation in cells. SHC1 and GRB2 are both associated with MAPK cascade and regulation of cell proliferation and growth and were also detected in IPA analysis (Table 4.5). This may indicate that *T. gondii* enhances their production for its establishment in the cells. They are also involved in innate immune responses in cells, which may also suggest that *T. gondii* regulate immune responses to convert to the dormant stage of infection in the cells. One of the proteins that were only found in *N. caninum* infected cells was Mitogen-activated protein kinase 8 (MK08) and was significantly down-regulated at 16 hours post infection. Serine/threonine-protein kinase is involved in various processes such as cell proliferation, differentiation, migration, transformation and programmed cell death. The down-regulation of MK08 could enable the delay of cell death and apoptosis processes in the *N. caninum* infected cells.

4.4.1.4 Fatty acid metabolism of infected human astrocytes

Parasites can permit the entry of small molecules from the host cells through the pores on the PVM such as lipid and fatty acid proteins (Schwab, Beckers & Joiner 1994), which clearly indicates the necessity of tachyzoites to scavenge lipids and fatty acids from the host for parasite replication and growth (Charron & Sibley 2002). Three proteins in the fatty acid metabolism pathway showed difference in expressions between the infected cells; including peroxisomal acyl-coenzyme A

oxidase 3 (ACOX3), 4-trimethylaminobutyraldehyde dehydrogenase (AL9A1) and peroxisomal bifunctional enzyme (ECHP) (Figure 4.6). ACOX3 was up-regulated in cells infected with *N. caninum* at 4 hours post infection, while ECHP was down-regulated in *N. caninum* at 4 hours post infection compared to *T. gondii* infected cells. Both Enzymes (ACOX3 and ECHP) are associated with lipid metabolic process (Oppermann et al. 2009; Muzny et al. 2006), which may suggest that both *T. gondii* and *N. caninum* infection result in elevating host's fatty metabolism molecules. AL9A1 was up-regulated in *T. gondii* infected cells at 4 hours post infection. This enzyme is associated with cellular aldehyde metabolic and neurotransmitter biosynthetic processes (Kurys, Ambroziak & Pietruszko 1989). The fact that AL9A1 was increased in *T. gondii* infected cells may be involved in increasing neurotransmitter production that may suggest a role in host behavioural modification by *T. gondii* in the brain.

The organelles of the host are localized closely to the PVM, which may imply to direct protein transfer of lipids from the host mitochondria membrane to the PVM (Sinai & Joiner 2001). In addition, lipids created in the ER must transport to the mitochondria in order to enter the PVM (Sprong, van der Sluijs & van Meer 2001). The fact that only three proteins were found differentially expressed between both infected cells from a total of 18 proteins associated with this pathway, may indicate that *T. gondii* and *N. caninum* act in a similar way in the modification of cells related to fatty acid metabolism. The parasite therefore must satisfy its nutritional needs by scavenging essential nutrients from its host cells such as fatty acid and lipid nutrients for their growth process and development.

4.4.1.5 Proteasome pathway of infected human astrocytes

Proteasomes consist of protein complexes found in the nucleus and cytoplasm of cells. When there are damaged or unneeded proteins in a cell, proteasomes degrade them through disrupting the peptide bonds of those protein by photolytic enzymes. The proteins that are no longer needed in cells are labelled with ubiquitin, with result of attachment with other ubiquitin protein resulting in a chain that

attaches to a proteomic enzyme. This process is important in response to oxidative stress, gene expression and cell cycle processes (Hilt & Wolf 1996; Geng & Tansey 2012). Two proteins showed differential expression between the infected HA cells; 26S proteasome non-ATPase regulatory subunit 8 (PSMD8) and proteasome subunit beta type-6 (PSB6). PSMD8 was up-regulated in *T. gondii* infected cells at 4 hours post infection, while PSB6 was up-regulated in *N. caninum* infected cells (Figure 4.6). PSMD8 consists of 20S proteasome and 19S particles (Voges, Zwickl & Baumeister 1999), it is involved in the ATP-dependent degradation of ubiquitin marked proteins and participate in many biological processes in the cell including mitotic cell cycle, apoptotic process and antigen presentation through MHC class I. The exact function of PSMD8 is not known, but is suggested that it may cause deubiquitination (Stone et al. 2004). PSB6 is an ATP-dependent proteinase complex that can cleave peptides with Arg, Phe, Tyr, Leu, and Glu and has similar functions as PSMD8 (DeMartino et al. 1991). It is associated with apoptotic processes in cells, this may suggest that *N. caninum* infected cells induce apoptosis to a higher extend compared to *T. gondii* infected astrocytes.

4.4.2 Proteins with the highest fold changes during host cell infection

The significantly differentially expressed proteins in *T. gondii* and *N. caninum* infected cells were related to ribosomal proteins; 39S ribosomal protein L12, mitochondrial (RM12) and 39S ribosomal protein L19, mitochondrial (RM19). They are known to be associated with translation and biosynthesis of protein and are localised in the mitochondria. Mitochondrial ribosomes in mammalian hosts comprise of small (28S) and large (39S) subunits (Pel & Grivell 1994; O'Brien 2003). In addition to that the top biological processes in HA cells infected with *T. gondii* or *N. caninum* infected cells were associated with mRNA processing, translation and oxidative reduction. Also cellular compartments were mainly located in the mitochondria and ER, which indicates the importance of these organelles for the parasites survival and proliferation.

In general, similarity in metabolic pathway between the infected cells were quite close, though differences in a few proteins were detected. This may suggest that parasites might have similar modulation effects on host metabolic process related to nutrient and protein synthesis. Global transcriptional and proteomic analysis carried out on the tachyzoites of *T. gondii* and *N. caninum* found similar metabolic pathways in both parasites and were unable to distinguish differences between them (Reid et al. 2012). Moreover it is not known the exact function of the differentially expressed proteins in association with protozoan parasites or parasitic infections; such as GRB2 and SHC1 proteins that were found in both focal adhesion and MAPK pathway.

4.4.3 Conclusion and future direction

Although proteomic analysis of whole cell lysate enables the comparison of translated proteins expressed in a cell at a certain time and under certain conditions, the overall comparison of the HA cells during infection showed similar expression profiles in many pathways such as citrate (TCA) cycle and oxidative phosphorylation pathways. In addition, while some proteins were differentially expressed, the majority of proteins in many pathways explored shared similar protein expression patterns. This suggests that changes in metabolism may not play a large role in host restriction and zoonotic compatibility between *T. gondii* and *N. caninum*. This observation has inspired the investigation of secreted proteins of host cells, where key proteins secreted during infection can be identified. It has been found that astrocytes secrete many proteins outside the cell during injury or disease. Host cell secretome comparisons will be carried out in the following chapter using label-free quantitative proteomics.

5 Chapter five: Comparative secretome analysis of host cells during *T. gondii* and *N. caninum* infection

5.1 Introduction

After the investigation of the whole cell proteome of human astrocytes during infection with *T. gondii* and *N. caninum* in chapter four, further analysis of the host cells secreted proteins during infection between these parasites were applied in order to identify differences in host cells secretion during infection.

5.1.1 Secretome

The secretome (or "secretomics") can be defined as the global investigation of proteins secreted or shed from the cell surface and also proteins that are located in the extracellular matrix of the cells (Makridakis & Vlahou 2010). Protein secretion is believed to be a balanced procedure essential for the normal physiological functions in host cells. In mammalian cells, secreted proteins are complex and closely regulated and have vital roles in physiological and pathological processes (Hathout 2007). Tissues in the mammalian host such as the brain and muscle secrete several biological molecules. Any excess or enduring changes in the secretion of these secretory proteins may indicate signs of abnormalities or pathological conditions (Hathout 2007). During activation of a cell, different proteins may be secreted according to its response to the stimuli. For example; B cell activation causes the secretion of immunoglobulins (such as IgM or IgA) in response to the antigen presented to them (Askonas 1975). Therefore, a global analysis of host protein secretions during infection is a potent approach for diagnostic and biomarker discoveries.

Secreted proteins are encoded by approximately 10% of the human genome (Pavlou & Diamandis 2010). Typical secreted proteins include serum proteins; such as immunoglobulins, extracellular matrix proteins collagens, proteoglycans and

digestive enzymes. They are usually found in low concentration and include proteins such as growth factors, hormones and cytokines that are associated with cell regeneration and differentiation. In eukaryotic cells, there are two main ways for protein secretion by cells or tissues; classical and non-classical secretion pathways.

5.1.1.1 Classical Secretory Pathway

In the classical secretion pathway, intracellular signalling pathways are stimulated and activated, the storage granules or vesicles are released into the extracellular space. Synthesized proteins are then placed into the lumen of endoplasmic reticulum (ER), transported through the Golgi complex and finally released into the extracellular space (Mellman & Warren 2000). Signal peptides in proteins are important for determining interaction with the transport system, in which can define the endpoint of the protein to be delivered. However, not all proteins contain signalling regions; proteins without signals are retained in the cytoplasm. Signal peptide predictions and sequence comparisons have been typically used for the identification of potentially secreted proteins in an organism, through the application of database sequence investigation and the use of available software (Chen et al. 2003).

5.1.1.2 Non-classical Secretory Pathway

In the non-classical pathway, many proteins do not have a signal sequence and do not use the classical ER-Golgi pathway. There are four non-classical secretory pathways (Nickel & Seedorf 2008). These are; direct translocation of proteins through membrane transporters across the membrane, lysosomal secretion, blebbing and release through exosomes from multivescular bodies. Proteins can also be discharged from cells through mechanical wounding (McNeil & Steinhardt 2003). Many proteins associated with the immune response regulation, cell growth and cell differentiation are secreted through the non-classical pathway, such as interleukin-1 beta (IL1b).

5.1.2 Challenges in secretome investigations

There are many challenges associated with secretome analysis, this includes sample preparation, concentration and separation techniques (Dowling & Clynes 2011). Even with cautious sample preparation during cell culture secretome investigations; many non-secreted proteins can still be discovered during secretome analysis. One of the main challenges in culturing is eliminating traces of bovine serum and cellular debris that can contaminate the collection of secreted proteins used for analysis. The overlap between human and bovine protein sequences; such as fibronectin might cause a type of signal interference and identification of peptide sequences during quantitative measurements of secreted proteins as it has closely related homology to human fibronectin (Planque et al. 2009). The incubation period, along with the culture conditions, need to be optimized so that the metabolic stress does not affect secretomic analysis (Makridakis & Vlahou 2010). Moreover, many proteins are secreted in low concentrations in cells and then diluted further in the cell culture medium, making them difficult to detect and analyse. Secretomes can be concentrated by lyophilisation, speed vacuum centrifugation, precipitation by trichloroacetic acid (TCA) and ultrafiltration (Lim & Bodnar 2002).

5.1.3 Research on the astrocyte secretome

Major advances in the proteomic studies of the cells secretome have occurred during the past seven years, owing to the improvements in proteomic techniques and especially in mass spectrometry (Brown et al. 2012). Many studies of the secretome have been applied to different research areas and specifically in the clinical field of research. Studying the secreted proteins can enable the discovery of important biomarker therapeutic targets; especially in the area of cancer research (An et al. 2010; Formolo et al. 2011).

The applications of appropriate concepts of systems biology and proteomic technologies are essential in scientific research; this has been applied in the

systematic investigation of secreted proteins of astrocytes, microglia and other glial cells (Greenbaum et al. 2001, Dowell, Johnson & Li 2009; Liu et al. 2008). In recent years, the secretome of astrocytes has gained interest in the neuroscience field. It has been demonstrated to have roles in the development of the nervous system along with roles in neurodegenerative diseases such as Alzheimer's and multiple sclerosis (Cassina et al. 2005, Antony et al. 2004). During disease progression in the CNS, the blood brain barrier breaks down, allowing the entrance of immune cells, including macrophages and monocytes during chemokine production (Krumbholz et al. 2006). Although microglias are known to be a major source of chemokine secretion, astrocytes have also been identified as a source for chemokine secretion and may participate in this infiltration process (Krumbholz et al. 2006). A label-free study of the rat astrocyte secretome performed by Moore *et al*. (2009) identified many proteins involved in neuronal development, which included proteins of the extracellular matrix and protease systems induced by astrocyte cholinergic stimulation. Tarassishin *et al*. (2014) investigated glioma cells involvement in tumour development also through a label-free proteomic approach. A total of 190 proteins were detected that included cytokines, chemokines, growth factors, cell adhesion molecules and extracellular matrix proteins (Tarassishin et al. 2014). Another study done by Hur *et al*. (2010) on microglia and astrocyte cells *in vitro* examined ischemia-induced damage to the CNS. It showed that ischemia induced the activation of inflammatory cytokines, cytochrome c, reactive oxygen species (ROS) and NADPH oxidase resulting in neuronal cell death (Hur et al. 2010).

The damage caused by *N. caninum* in the CNS has been observed in congenitally infected young dogs and cattle (Dubey et al. 2004; Kobayashi et al. 2001). It has also been shown that *N. caninum* can successfully infect a wide range of host cell types *in vitro* (Dubey, Schares & Ortega-Mora 2007) and there still remains a potential concern whether it can be zoonotic (Tranas et al. 1996; Robert-Gangneux & Klein 2009). Human cell lines have been used to study *N. caninum* response and found that cytokine production was induced during infection (Carvalho et al. 2010). In cultured rat astrocytes infected with *N. caninum*, astrocyte reactivity, IL-10, IFN-γ

expression, and cell viability have been investigated at 24 and 72 hours post infection (Pinheiro et al. 2006). These studies have found astrocyte hypertrophy, gliofilament reorganization and metabolic changes occurred (Pinheiro et al. 2006). It has been demonstrated in a study done by Elsheikha *et al*. (2013) that *N. caninum* induced cellular death in an investigation in mitochondrial bioenergetics of brain microvascular endothelial cells (Elsheikha et al. 2013). Neuroinflammation of astrocyte-derived cytokines and chemokines play both neuroprotective and neurotoxic roles in brain lesions of human neurological diseases.

5.1.4 Aims and objectives

Further to the discoveries related to the global transcriptional and whole cell proteome expression analysis, secretome analysis was performed to explore differences in host protein secretions during *T. gondii* and *N. caninum* infection. This will help in the comprehensive understanding into why these parasites behave differently in host cells during infection in the CNS. As *T. gondii* seems to control its intermediate host more efficiently and has tropism for cells of the CNS while *N. caninum* has not been identified to induce any behaviour or neurological disorders in their hosts as efficient as *T. gondii*. The hypothesis is that host cells secretion during infection with *T. gondii* will differ from host cells secretion during *N. caninum* infection. Key proteins are constantly secreted outside the cells, and investigating these proteins can extend our understanding of the host-parasite interaction pathways involved.

5.2 Materials and methods

5.2.1 Cell culture

Human astrocyte (HA) cells, TgVEG and NcLIV strain were grown and maintained as mentioned previously in chapter two (2.2.1.).

5.2.1.1 Experimental infection and harvesting of host cells

Tachyzoites of TgVEG and NcLIV were isolated from host cells by filtration through 47mm diameter 3µm pore-sized Nucleopore™ polycarbonate membranes. Then they were washed twice in PBS pH 7.4 followed by centrifugation at 1,500 x g for 10 minutes. The supernatant was discarded, and parasites were resuspended in DMEM-F12. Three replicates of HA cells were required for *T. gondii* and *N. caninum* infection and also uninfected HA cells in this project (a total of 12 samples). Prior to infection, confluent cells were washed three times with DPBS and the medium was replaced with phenol red free DMEM-F12 (Gibco, life technologies) supplemented with 1% P/S (v/v) and excluding the addition of serum FBS. Afterwards, the number of HA cells were calculated and infected with NcLIV and TgVEG with a M.O.I. of 8 parasites per cell. The T75 cm^2 flasks (infected and uninfected) were incubated for 18-24 hours at 37^oC and 5% CO_2, astrocytes supernatant was collected and filtered using a 0.22 µm syringe filter units (Millex®, Sigma-Aldrich) to eliminate any debris, and the sample was concentrated using Vivaspin 20 ml centrifugal concentrator (Sigma-Aldrich) with a 5 kDa molecular weight (MW) cut-off. Samples were centrifuged following the manufacturer's instructions for 40 minutes at 4000 x g at 20^oC and samples were concentrated from 20 ml to 700 µl and stored at -80^oC until needed.

5.2.2 Protein extraction and tryptic digestion of host cell secretome

A total of 12 HA cell supernatants (three replicates each of HA cells infected with TgVEG, NcLIV and uninfected cells supernatants) proteins were extracted, and

digested through a label-free quantitative approach as mentioned previously in chapter four (4.2.2).

For peptide purification, concentration and high recovery from digests, samples were desalted and purified using C18 resin in the form of spin tips (Thermo Scientific) following the manufacturer's instructions. Samples were then speed vacuumed (Concentrator plus, Eppendorf) to near dryness, resuspended with 0.1 % TFA in 3% ACN and stored at -20^{o}C until later running the samples on the tandem mass spectrometer.

5.2.3 Protein identification and relative quantification

5.2.3.1 Mass spectrometry analysis

Mass spectrometry analysis of the samples was carried out by Dr. Dong Xia at the University of Liverpool. Peptide mixtures were analysed by on-line nanoflow liquid chromatography using the nanoACQUITY-nLC system (Waters MS technologies, Manchester, UK) coupled to an LTQ-Orbitrap Velos (ThermoFisher Scientific, Bremen, Germany) mass spectrometer equipped with the manufacturer's nanospray ion source. The analytical column (nanoACQUITY UPLCTM BEH130 C18 15cm x 75µm, 1.7µm capillary column) was maintained at 35^{o}C and a flow-rate of 300nl/min. The gradient consisted of 3-40% acetonitrile in 0.1% formic acid for 90min then a ramp of 40-85% acetonitrile in 0.1% formic acid for 3 min. Full scan MS spectra (m/z range 300-2000) were acquired by the Orbitrap at a resolution of 30,000. Analysis was performed in data dependant mode. The top 20 most intense ions from MS1 scan (full MS) were selected for tandem MS by collision induced dissociation (CID) and all product spectra were acquired in the LTQ ion trap. Ion trap and Orbitrap maximal injection times were set to 50ms and 500ms, respectively.

5.2.3.2 Label-free peptide quantification (Progenesis)

Raw data generated from the LTQ Orbitrap Velos was inputted directly into the Progenesis™ QI software (version 1.0, Nonlinear Dynamics) for label-free quantification as previously mentioned in chapter four (4.2.3.2). The secretome of HA infected cells (*N. caninum* or *T. gondii*) was compared to uninfected controls using Progenesis.

5.2.4 Functional analysis and annotation

Normalized protein abundance (proteins with ≥2 unique peptides and peptide score >30) of host secreted proteins were illustrated using volcano plots (Figure 5.2). DAVID (Database for Annotation, Visualisation, and Integrated Discovery, v 6.7, Huang et al. 2009) was used for functional annotation of differentially expressed proteins ($p < 0.05$, ± 1.5 fold change). Proteins accession numbers were searched against *Homo sapiens* genes background. An illustration of the overall label-free workflow in this experiment can be seen in Figure 5.1.

5.2.4.1 Predicted protein secretion

Identified proteins were searched against the Secreted Protein Database (http://spd.cbi.pku.edu.cn/) (Chen et al. 2005), SignalP database prediction server (4.1 server) (http://www.cbs.dtu.dk/services/SignalP/) and SecretomeP prediction server (v 2.0) (http://www.cbs.dtu.dk/services/SecretomeP/) (Bendtsen et al. 2004). All proteins were searched against mammalian database. The SignalP database was used for the investigation of the secreted proteins through the classical pathway of secretion. SecretomeP was used for identifying the secreted proteins through the non- classical pathway. Basically any proteins identified with a threshold of more the 0.5 was predicted to be a secreted protein in SecretomeP and SignalP.

5.2.4.2 Protein interaction analysis

Protein network analysis was carried out with STRING (Search Tool for Retrieval of Interacting Genes/Proteins v 9.1 (http://string-db.org/) (Jensen et al. 2009) on differentially expressed proteins ($p < 0.05$, ± 1.5 fold change). Statistically significant proteins accession numbers were inserted and searched against *Homo sapiens* proteins. The protein interaction maps were created by allowing for experimental evidence. Protein interaction maps were generated by enabling experimental evidence along with predicted functional links between the proteins; co-occurrence, co-expression, gene fusion, databases and text-mining. The minimum required confidence was set at 0.7 (hi confidence) search for the software.

5.2.4.3 Pathway analysis

Networks, functional analyses, and canonical pathways were produced through the use of the commercial software Ingenuity pathway analysis (IPA) (Ingenuity Systems, www.ingenuity.com). Settings included the search against a human database of the differentially expressed proteins ($p < 0.05$, ± 1.5 fold changes). The functional analysis managed to identify the biological functions and diseases along with canonical pathways that were most relevant and statistically significant to the data set.

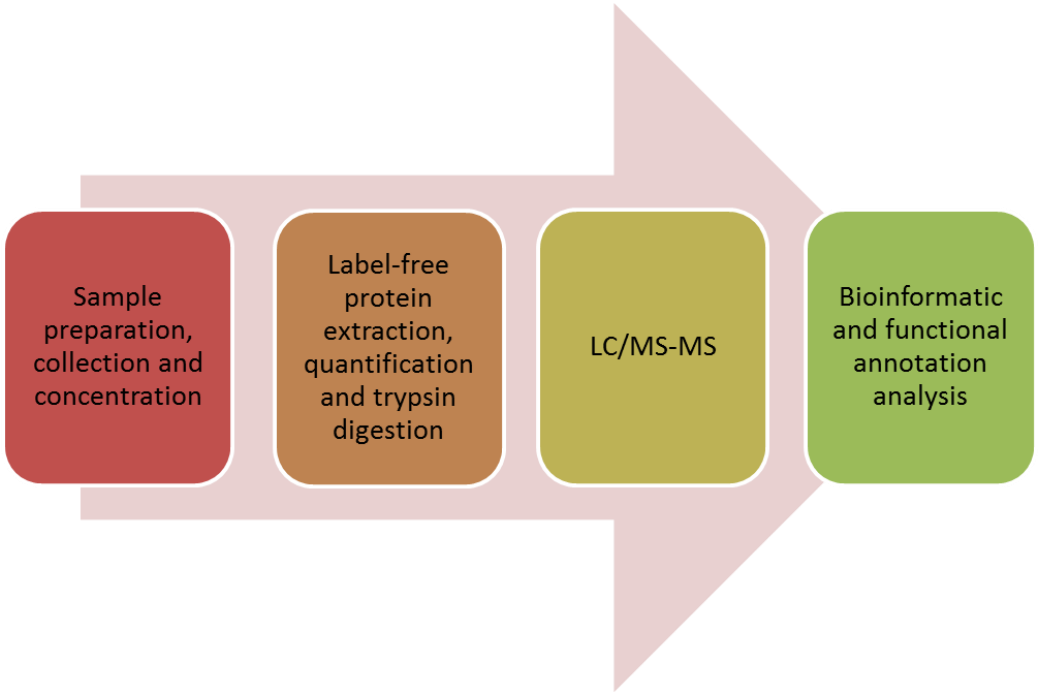

Figue5.1: Overview of label-free workflow of human astrocyte secretome. Cells were grown until confluent followed by infection of the cells with either *T. gondii*/ *N. caninum* or left uninfected as controls. Supernatants were carefully collected at 18-24 hours p.i. followed by filtration, concentration, protein extraction and digestion and later were placed on the LC-MS/MS. Protein identification and quantification was done using Progenesis along with Mascot. Functional annotations and metabolic pathways were afterwards determined.

5.3 Results

Mass spectra for the proteins secreted from HA cells infected with *T. gondii* or *N. caninum* and uninfected cells were analysed using Progenesis to identify and quantify proteins. The total number of human astrocyte proteins in *T. gondii* infected HA cells were 667 and in *N. caninum* infected HA cells 973 proteins (≥ 2 unique peptides) (Appendix V).

The secretomes of HA cells infected with either *T. gondii* or *N. caninum* compared to uninfected controls are displayed as volcano plots (Figure 5.2). The y-axis is the log10 of p-values (a lower value indicates greater significance) and the x-axis is the difference in secreted protein expression between the infected and non-infected cells measured in log2 fold change. Tables below the volcano plots indicate examples of significant up-regulated and down-regulated proteins, which are highlighted in different colours in the volcano plot. In *T. gondii* infected cells; examples of up-regulated proteins were CCL2, ICAM1, CXCL1 and MMP10 and down-regulated were VIME, RS28 and CALU (Figure 5.2). In cells infected with *N. caninum*, examples of significant up-regulated secreted proteins compared to uninfected cells were LOXL1, IL8, CXCL2 and IL6, whereas the down-regulated secreted proteins were CALD1, ITGBL and ROA3 (Figure 5.2).

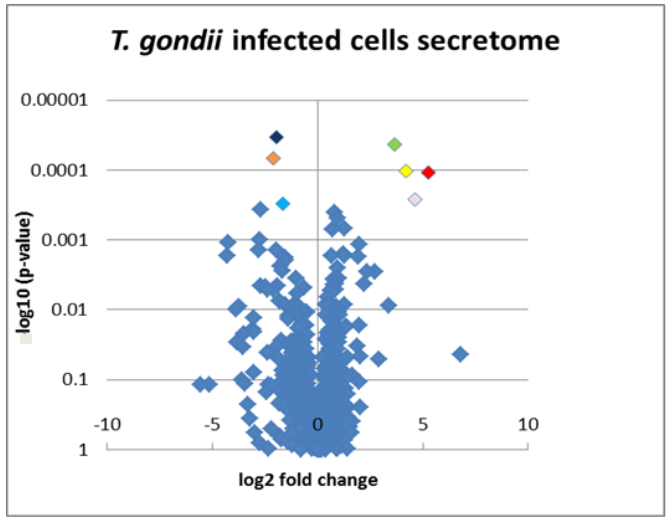

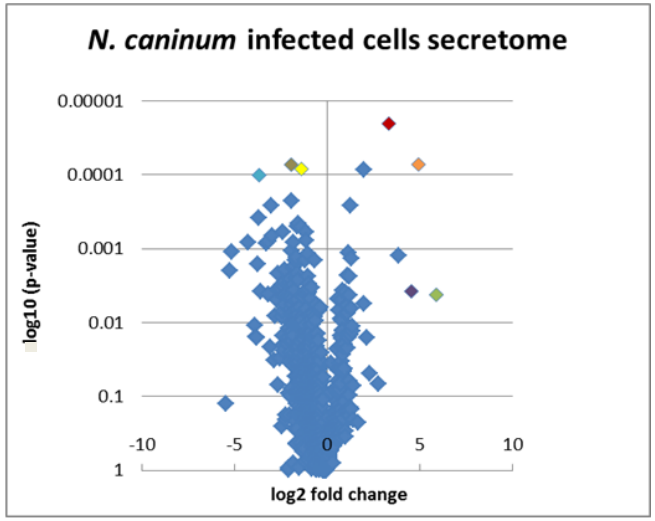

Down-regulated secreted proteins	up-regulated secreted proteins
VIME (dark blue)- R28 (orange)- CALU (light blue)	CCL2 (light green)- ICAM1 (yellow)- CXCL1 (red)- MMP10 (pink)

Down-regulated secreted proteins	up-regulated secreted proteins
CALD1 (brown)- ITGBL (yellow)- ROA3 (light blue)	LOXL1 (red)- IL8 (orange)- CXCL2 (light green)- IL6 (purple)

Figure 5.2: Volcano plots of the secreted proteins in HA cells infected with *T. gondii* (left) compared to uninfected cells, and cells infected with *N. caninum* compared to uninfected cells (right). These proteins were identified and quantified using Progenesis. The volcano plot displays the relationship between fold-change and significance between the infected and non-infected cells. The y-axis is the reverse log10 of p-values (a higher value indicates greater significance) and the x-axis is the difference in secreted protein expression between the infected and non-infected cells measured in log2 fold change. Tables below the volcano plots indicate the top significant up-regulated and down-regulated proteins (in p-value terms), which are highlighted in different colours in the volcano plot.

5.3.1 Predication of host protein secretions

In order to confirm that the proteins identified were predicted to be secreted proteins, protein ID's were searched against SPD, SignalP and SecretomeP using protein sequences (fasta) of the secreted proteins. Only statistical significant proteins were included in the search (p-value< 0.05 and ±1.5 fold change) resulting in a total of 132 proteins identified in *T. gondii* infected cells (out of 667 proteins) and 252 proteins (out of 973 proteins) in *N. caninum* infected cells. Out of the identified proteins 64% was predicted to be secreted in *T. gondii* infected cells and 56% in cells infected with *N. caninum*. In the Secreted Protein Database, 40 predicted proteins were identified as secreted proteins in cells infected with *T. gondii* and 56 proteins in *N. caninum* infected cells. This is likely to be an underrepresentation of the secreted proteins as the database was last updated in 2006. SignalP database identified 53 proteins predicted to be secreted through the classical-pathway in cells infected with *T. gondii* and 68 predicted secreted proteins in *N. caninum* infected cells. The secreted proteins through non- classical pathway was searched using SecretomeP; 80 proteins were predicted to be secreted in *T. gondii* infected cells and 123 predicted secreted proteins in *N. caninum* infected cells. A Venn diagram of the overall number of predicted secreted proteins and the overlapping proteins identified in cells infected with *T. gondii* and cells infected with *N. caninum* can be seen in Figure 5.3.

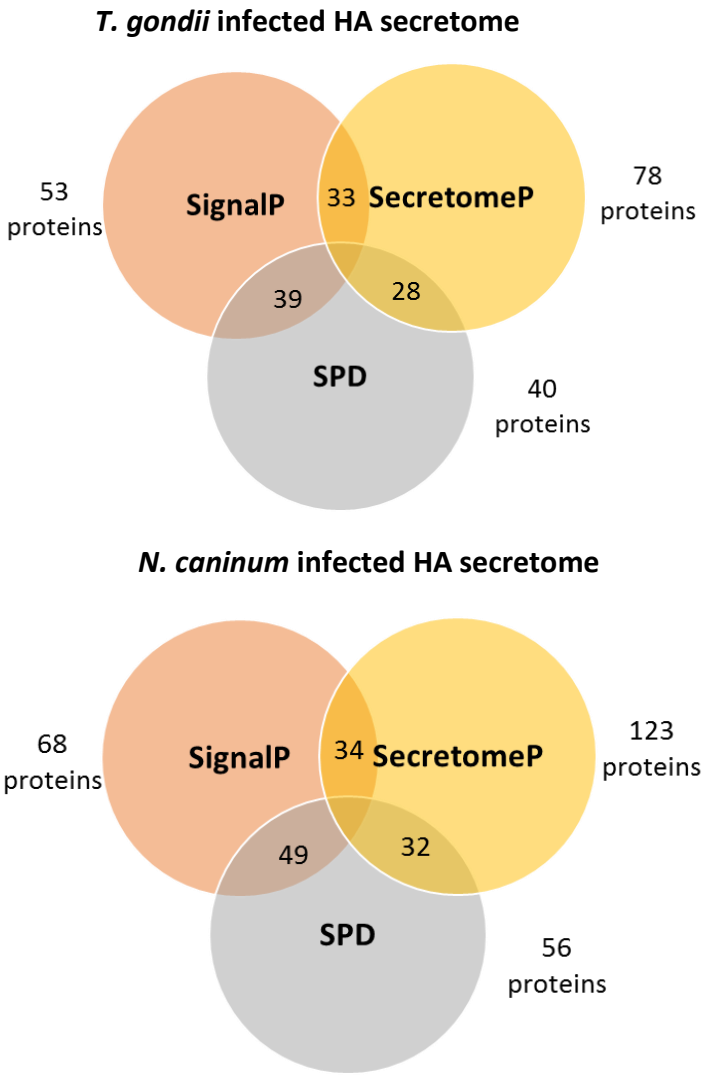

Figure 5.3: Venn diagram of the secreted proteins of *T. gondii* infected cells (top) and *N. caninum* infected cells (bottom). Proteins were searched against the Secreted protein database and the online prediction tools, SignalP and SecretomeP.

5.3.1.1 Key differences in the astrocyte secretome in response to *T. gondii* or *N. caninum* infection

The significant up-regulated proteins between host cells infected with *T. gondii* compared to *N. caninum* showed differences in key cytokines and other secreted proteins (Figure 5.4). CXCL1 (GROA); involved in inflammatory responses and chemokine CCL2 was up-regulated higher in *T. gondii* infected cells compared to *N. caninum* infected cells (Figure 5.4 and Table 5.1, 5.2). Other secreted proteins that were up-regulated in *T. gondii* infected cells and not detected in *N. caninum* infected cells included proteins such as; MMP10, ICAM1 and VCAM1 (Figure5.4 and Table 5.1).

Secreted proteins that were up-regulated in cells infected with *N. caninum* compared to *T. gondii* include proteins such as; chemokine CXCL2, (60 fold) that was found not to be statistically significant in *T. gondii* infected cells, interluikin-6 (IL6), lysyl oxidase homolog 1 (LOXL1), latent-transforming growth factor beta-binding protein 2 (LTBP2) and Interluekin-8 (IL8). IL8 was detected in infected cells with *T. gondii* but was not significant (p-value=0.33 and 1.5 fold increase) (Figure 5.4 and Table 5.1, 5.2).

Pentraxin-related protein-3 (PTX3); that plays a role in the regulation of innate resistance to pathogens and inflammatory reactions was up-regulated 4 fold in *T. gondii* infection but was found with no change in the *N. caninum* infected cells secretions (not statistically significant).

Table 5.1: A subset of statistically significant differentially expressed human astrocyte secreted proteins during *T. gondii* infection (with greatest fold changes). A total of 132 secreted proteins were identified ($p<0.05$ and ±1.5 fold change). Proteins showing up-regulation are highlighted in red and proteins showing down-regulation are highlighted in green (all proteins in table are predicted to be secreted).

Accession no	Protein	Description	Anova (p)	Log2 FC Toxo
P09341	GROA_HUMAN	Growth-regulated alpha protein	0.000108	5.25
P09238	MMP10_HUMAN	Stromelysin-2	0.000263	4.62
P05362	ICAM1_HUMAN	Intercellular adhesion molecule 1	0.000103	4.19
P13500	CCL2_HUMAN	C-C motif chemokine 2	4.31E-05	3.65
Q08397	LOXL1_HUMAN	Lysyl oxidase homolog 1	0.002837	2.72
P19320	VCAM1_HUMAN	Vascular cell adhesion protein 1	0.002893	2.36
P05231	IL6_HUMAN	Interleukin-6	0.016789	1.99
P26022	PTX3_HUMAN	Pentraxin-related protein PTX3	0.001155	1.97
Q14767	LTBP2_HUMAN	Latent-transforming growth factor beta-binding protein 2	0.02889	1.01
P16949	STMN1_HUMAN	Stathmin	0.028402	-1.27
Q13443	ADAM9_HUMAN	Disintegrin and metalloproteinase domain-containing protein 9	0.007574	-1.79
Q6NZI2	PTRF_HUMAN	Polymerase I and transcript release factor	0.00886	-3.73
Q93063	EXT2_HUMAN	Exostosin-2	0.009943	-3.85
P15502	ELN_HUMAN	Elastin	0.001098	-4.24
O75787	RENR_HUMAN	Renin receptor	0.001684	-4.29

Table 5.2: A subset of statistically significant human astrocyte secreted proteins during *N. caninum* infection (with greatest fold changes). A total of 252 secreted proteins were identified ($p<0.05$ and ±1.5 fold change). Proteins showing up-regulation are highlighted in red and proteins showing down-regulation are highlighted in green (all proteins in table are predicted to be secreted).

Accession no	Protein	Description	Anova (p)	Log2 Neo
P19875	CXCL2_HUMAN	C-X-C motif chemokine 2	0.004193	5.89
P10145	IL8_HUMAN	Interleukin-8	7.23E-05	4.93
P05231	IL6_HUMAN	Interleukin-6	0.003763	4.54
Q08397	LOXL1_HUMAN	Lysyl oxidase homolog 1	2.02E-05	3.32
P09341	GROA_HUMAN	Growth-regulated alpha protein	0.048183	2.31
P13500	CCL2_HUMAN	C-C motif chemokine 2	0.016222	2.11
Q14767	LTBP2_HUMAN	Latent-transforming growth factor beta-binding protein 2	8.47E-05	1.99
P30048	PRDX3_HUMAN	Thioredoxin-dependent peroxide reductase, mitochondrial	0.005613	1.98
Q93063	EXT2_HUMAN	Exostosin-2	0.009555	-0.60
Q6NZI2	PTRF_HUMAN	Polymerase I and transcript release factor	0.002841	-2.28
P16949	STMN1_HUMAN	Stathmin	0.000838	-3.27
O75787	RENR_HUMAN	Renin receptor	0.015457	-3.85
Q13443	ADAM9_HUMAN	Disintegrin and metalloproteinase domain-containing protein 9	0.001098	-5.16
O95450	ATS2_HUMAN	A disintegrin and metalloproteinase with thrombospondin motifs 2	0.001968	-5.24

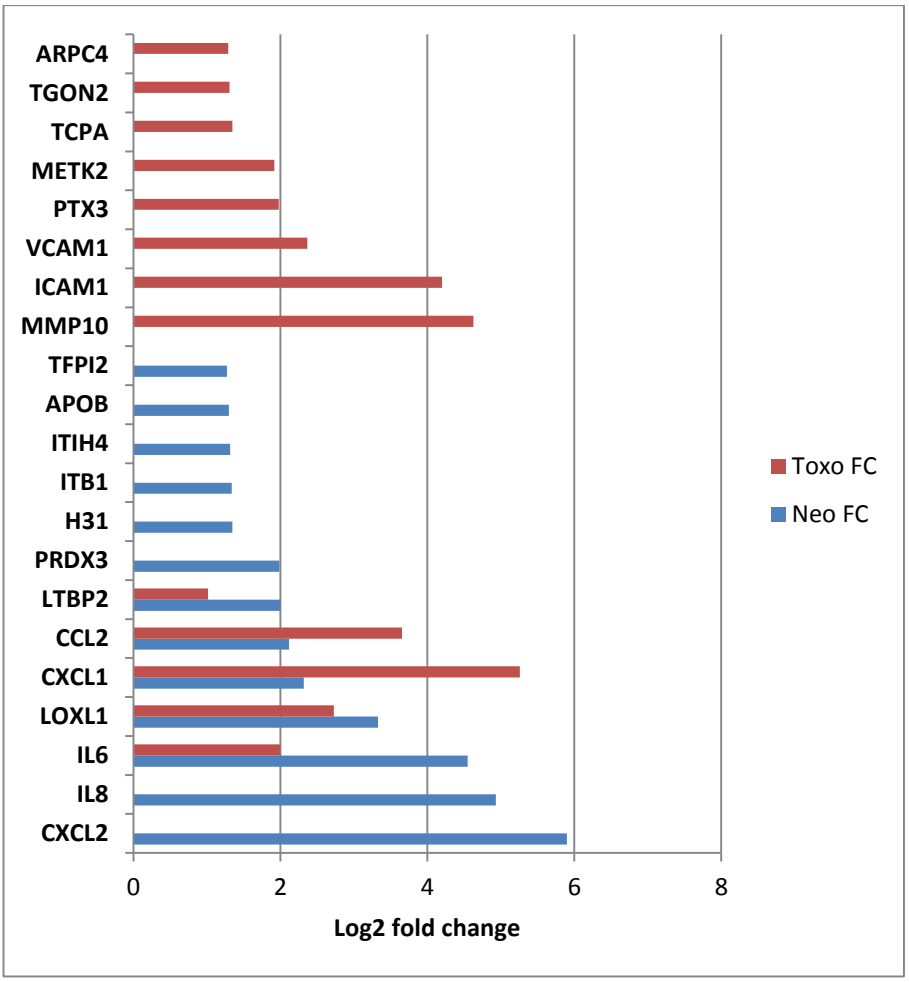

Figure 5.4: The secreted proteins significantly up-regulated (log2 fold changes) in infected HA cells with *T. gondii* (red) and *N. caninum* (blue). Increased secreted protein expressions in *T. gondii* infected cells were found in chemokines such as CCL2 and CXCL1; whereas IL6 and LTBP2 were increased in cells infected with *N. caninum*. Some secreted proteins were only found in one infection and not detected in the other; such as VCAM1 and ICAM1 found secreted in cells infected with *T. gondii* and not detected in *N. caninum* infected cells.

5.3.1.2 Down-regulated secreted proteins of astrocytes in response to *T. gondii* or *N .caninum* infection

The investigation of the significant down-regulated proteins secreted in HA cells infected with *T. gondii* and *N. caninum* was carried out. Secreted proteins that were down-regulated in *T. gondii* infected cells included proteins such as; the renin receptor (RENR), Elastin (ELN) and Exostosin-2 (EXT2); a protein involved in carbohydrate metabolic process and cell differentiation (Figure 5.5 and Table 5.1, 5.2).

Secreted proteins found significantly down-regulated in cells infected with *N. caninum* compared to *T. gondii* infected cells are proteins including; polymerase I and transcript release factor (PTRF), disintegrin and metalloproteinase domain-containing protein 9 (ADAM9) and stathmin (STMN1) (Figure 5.5 and Table 5.1, 5.2). In relation to proteases secretion, A disintegrin and metalloproteinase with thrombospondin motifs 2 (ATS2) that is associated with collagen degradation was only detected in *N. caninum* infected cells with a 38 decreased fold change (Figure 5.5 and Table 5.2).

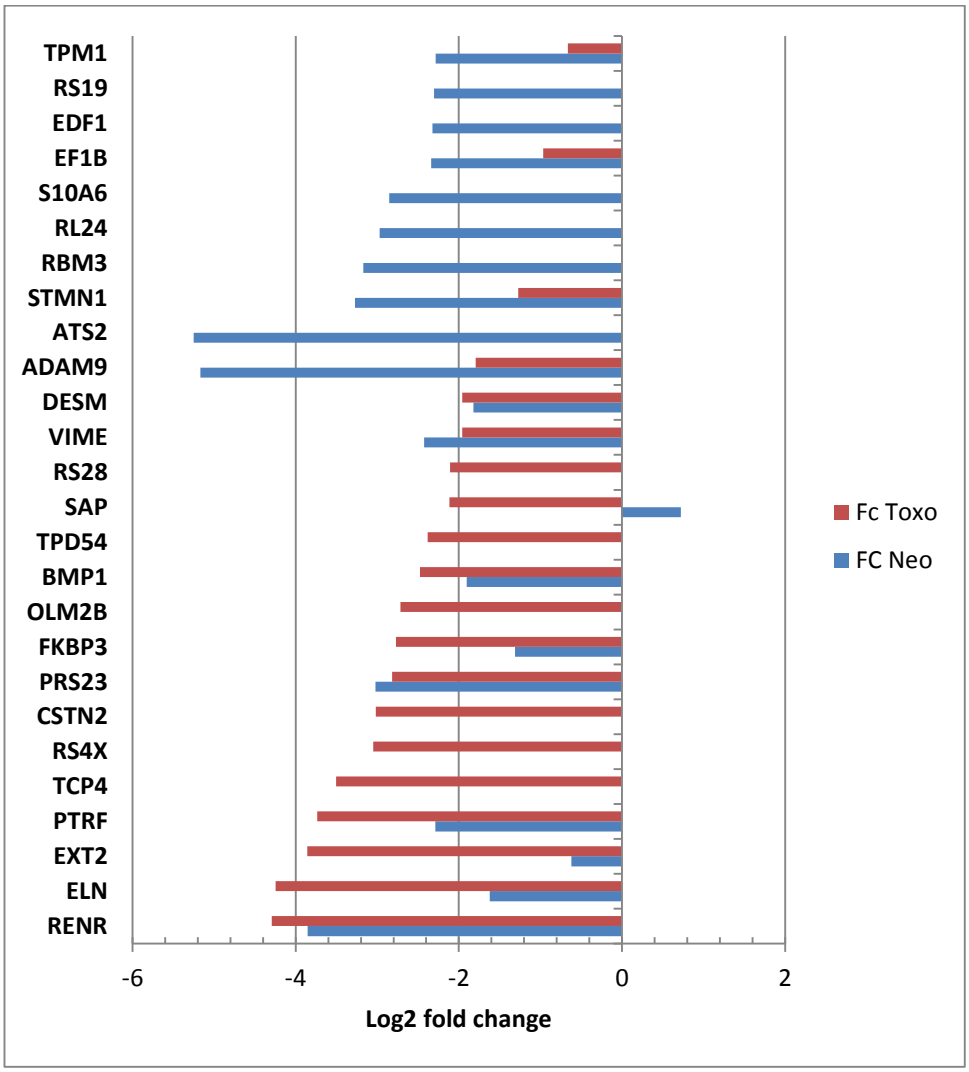

Figure 5.5: The secreted proteins significantly down-regulated (log2 fold changes) detected in HA cells infected with *T. gondii* (red) compared to cells infected with *N. caninum* secretions (blue). ADAM9 and STMN1 proteins were significantly decreased in cells infected with *N. caninum* compared to *T. gondii* infected cells. Some secreted proteins were only found in one infection and not detected in the other; such as ATS2 found secreted in cells infected with *N. caninum* and not detected in *T. gondii* infected cells.

5.3.2 Functional analysis of infected human astrocytes secretome

Proteins predicted to be secreted by SignalP, SPD and SecretomeP tools were combined together and only proteins with more than ±1.5 fold changes were searched. Using DAVID enabled the identification of metabolic pathways of the HA cells secreted proteins during infection with *T. gondii* (Table 5.1) or *N. caninum* (Table 5.2). In addition, functional annotation of the top biological functions, cellular contents and molecular functions were searched.

5.3.2.1 Functional annotation of *T. gondii* infected cells secretome

In the supernatant of HA cells infected with *T. gondii*, KEGG pathway analysis showed that the NOD-like receptor signalling pathway (containing CCL2 with 12.5 fold increase, CXCL1 with 38.2 fold increase and IL6 with a 4 fold increase), also Ribosome and Leukocyte transendothelial migration (Table 5.3), in which the latter pathway contains adhesion molecules with significant fold changes (ICAM-1 with 18 fold change increased and VCAM-1 with 5 fold change). The significant biological processes showed functions related to cell migration, cell communication and extracellular matrix orginization. The cellular content demonstrated also that the proteins were found in the extracellular region and molecular functions showed their involvement in extracellular matrix binding, cytokine activity and calcium ion binding (Table 5.4).

Table 5.3: Metabolic pathway analysis identified of human astrocytes infected with *T. gondii* secretome, proteins identified as secreted using SPD, SignalP and SecretomeP were only searched in DAVID with ±1.5 fold changes.

Category	Term	Protein count	% of proteins	P-value
KEGG_PATHWAY	NOD-like receptor signalling pathway	4	4.7	8.60E-03
	Ribosome	4	4.7	2.10E-02
	Leukocyte transendothelial migration	4	4.7	4.70E-02

Table 5.4: Functional annotations of the secreted human astrocytes infected with *T. gondii*. The significantly differentially expressed proteins biological processes, cellular content and molecular functions were identified using DAVID annotation tool.

Category	Term	Protein count	% of proteins	P-value
Biological process	negative regulation of signal transduction	10	11.6	5.40E-06
	negative regulation of cell communication	10	11.6	1.40E-05
	regulation of cell migration	8	9.3	5.70E-05
	regulation of locomotion	8	9.3	1.30E-04
	regulation of cell motion	8	9.3	1.30E-04
	regulation of actin cytoskeleton organization	6	7	1.70E-04
	regulation of actin filament-based process	6	7	2.00E-04
	regulation of leukocyte migration	4	4.7	2.00E-04
	actin cytoskeleton organization	8	9.3	3.50E-04
	extracellular matrix organization	6	7	3.50E-04
Cellular content	extracellular region part	36	41.9	4.80E-19
	extracellular region	43	50	2.40E-14
Molecular function	extracellular matrix binding	5	5.8	1.90E-05
	structural molecule activity	14	16.3	9.30E-05
	cytokine activity	8	9.3	1.70E-04
	calcium ion binding	16	18.6	3.20E-04

5.3.2.2 Functional annotation of *N. caninum* infected cells secretome

The metabolic pathways associated with the secreted proteins of human astrocytes during *N. caninum* infection were; ribosome, complement and coagulation cascades and NOD-like receptor signalling pathway (Table 5.5). The NOD-like pathway contained chemokines with significant fold changes (CCL2, CXCL1, CXCL2, IL6 and IL8). The biological processes were related to translation and inflammatory responses. The cellular content demonstrated that these proteins were in the extracellular region part and molecular functions showed their involvement in structural activities in the cells (Table 5.6).

Table 5.5: Metabolic pathway analysis of the secreted human astrocyte proteins infected with *N. caninum*, proteins identified as secreted using SPD, SignalP and SecretomeP were only searched in DAVID with ±1.5 fold changes.

Category	Term	Protein count	% of proteins	P-value
KEGG_PATHWAY	Ribosome	15	10.6	5.80E-13
	Complement and coagulation cascades	8	5.7	1.40E-05
	NOD-like receptor signalling pathway	5	3.5	5.90E-03
	Hypertrophic cardiomyopathy (HCM)	5	3.5	1.70E-02
	Dilated cardiomyopathy	4	2.8	9.40E-02

Table 5.6: Functional annotation of the secreted human astrocyte proteins infected with *N. caninum*. The biological processes, cellular content and molecular functions of proteins identified as secreted using SPD, SignalP and SecretomeP were only included in DAVID with ±1.5 fold changes.

Category	Term	Protein count	% of proteins	P-value
Biological process	translation	20	14.2	2.50E-10
	response to wounding	24	17	6.90E-10
	inflammatory response	18	12.8	9.50E-09
	acute inflammatory response	11	7.8	2.60E-08
	defence response	21	14.9	1.10E-06
	protein maturation by peptide bond cleavage	9	6.4	1.40E-06
	regulation of response to external stimulus	11	7.8	2.40E-06
	humoral immune response	8	5.7	9.00E-06
	protein processing	9	6.4	1.00E-05
	protein maturation	9	6.4	1.90E-05
	acute-phase response	6	4.3	3.40E-05
Cellular content	extracellular region part	42	29.8	5.00E-16
	extracellular region	55	39	9.20E-13
Molecular function	structural molecule activity	28	19.9	5.50E-11
	structural constituent of ribosome	16	11.3	7.60E-11
	endopeptidase inhibitor activity	14	9.9	1.40E-09

5.3.3 Protein interaction analysis of infected host secretome

Protein network analysis was carried out (Proteins with fold change >± 1.5 fold) using STRING (version 9.1). The up-regulated and down-regulated proteins were searched separately for their protein interactions in both infected cells secretions. In *T. gondii* infected cells; the total number of proteins inserted were 87 with ±1.5 fold changes or more increased and decreased expressions and in *N. caninum* HA cell infection; the total number of proteins were 138. . Proteins showingincreased fold changes in *T. gondii* infected cells were clustered together (cytokines, proteases, cell adhesion molecules and heat shock proteins), these included secreted proteins such as CCL2, CXCL1, IL6, MMP1, ICAM1 and VCAM1 (Figure 5.6). The down-regulated secreted proteins did not show connected network interactions and were clustered in five small groups of only three to five proteins involved in each cluster in cells infected with *T. gondii* (Figure 5.7).

N. caninum up-regulated secreted proteins (>1.5 fold) were grouped into one large cluster, which included cytokines, chemokines and other proteins such as CXCL1, CXCL2, IL6 and IL8 (Figure5.8). Decreased expression of *N. caninum* infection (Figure 5.8) were mainly clustered into one large cluster involved in ribosome pathway and three other small clusters (Figure 5.9).

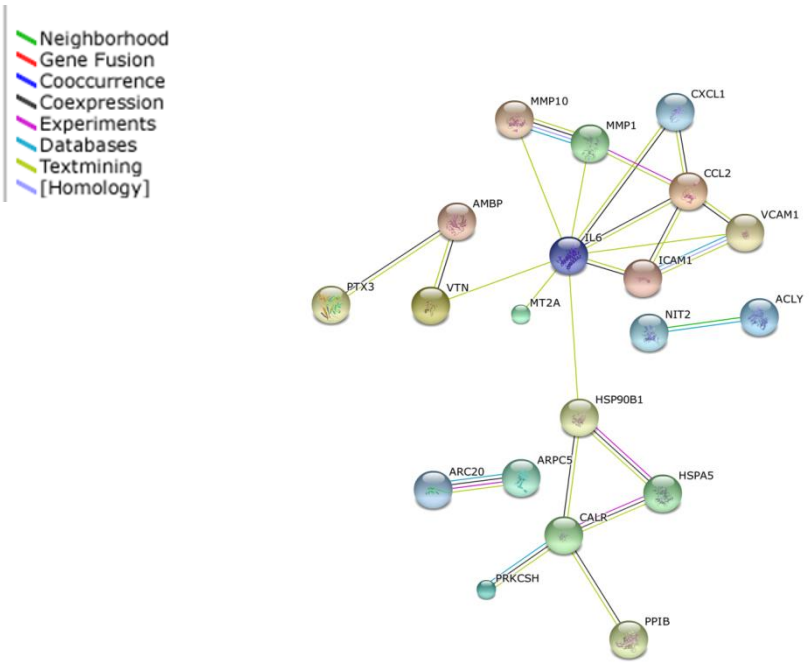

Figure 5.6: STRING generated protein-protein network interactions of significantly up-regulated secreted proteins in cells infected with *T. gondii* (>+1.5 fold,p<0.05). Protein search parameter was set at high confidence (0.7) in STRING. The cytokines and chemokines (CCL2, CXCL1, IL6) were clustered together with matrix metalloproteinases (MMP1 and MMP10) and cell adhesion molecules (ICAM1 and VCAM1), indicating protein-protein interactions between these molecules.

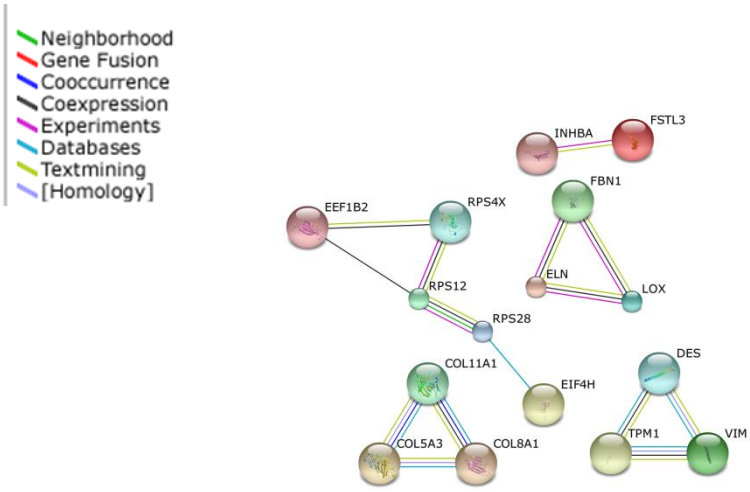

Figure 5.7: STRING generated protein-protein network interactions of significantly down-regulated secreted proteins in cells infected with *T. gondii*. Basically, the top decreased fold changes were inserted with -1.5 fold change or more. Five small grouped proteins were grouped. Protein search parameter was set at high confidence (0.7) in STRING.

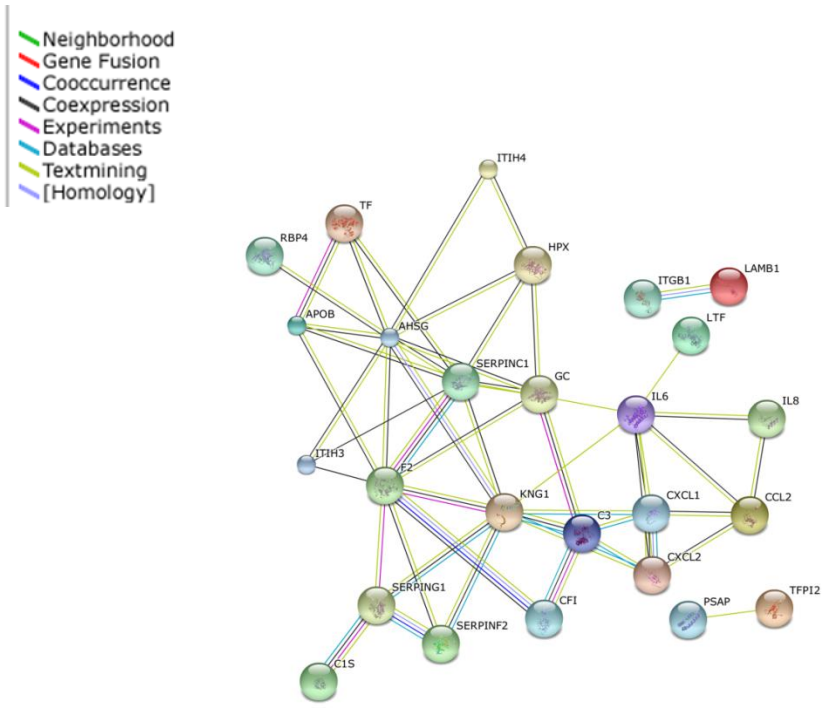

Figure 5.8: STRING generated protein-protein network interactions of significantly up-regulated secreted proteins in cells infected with *N. caninum*. Basically, the top increased fold changes were inserted with more than 1.5 fold change. Mainly one large cluster of proteins was grouped. Cytokines and chemokines were grouped together, including CXCL1, CXCL2, IL6 and IL8. Protein search parameter was set at high confidence (0.7) in STRING.

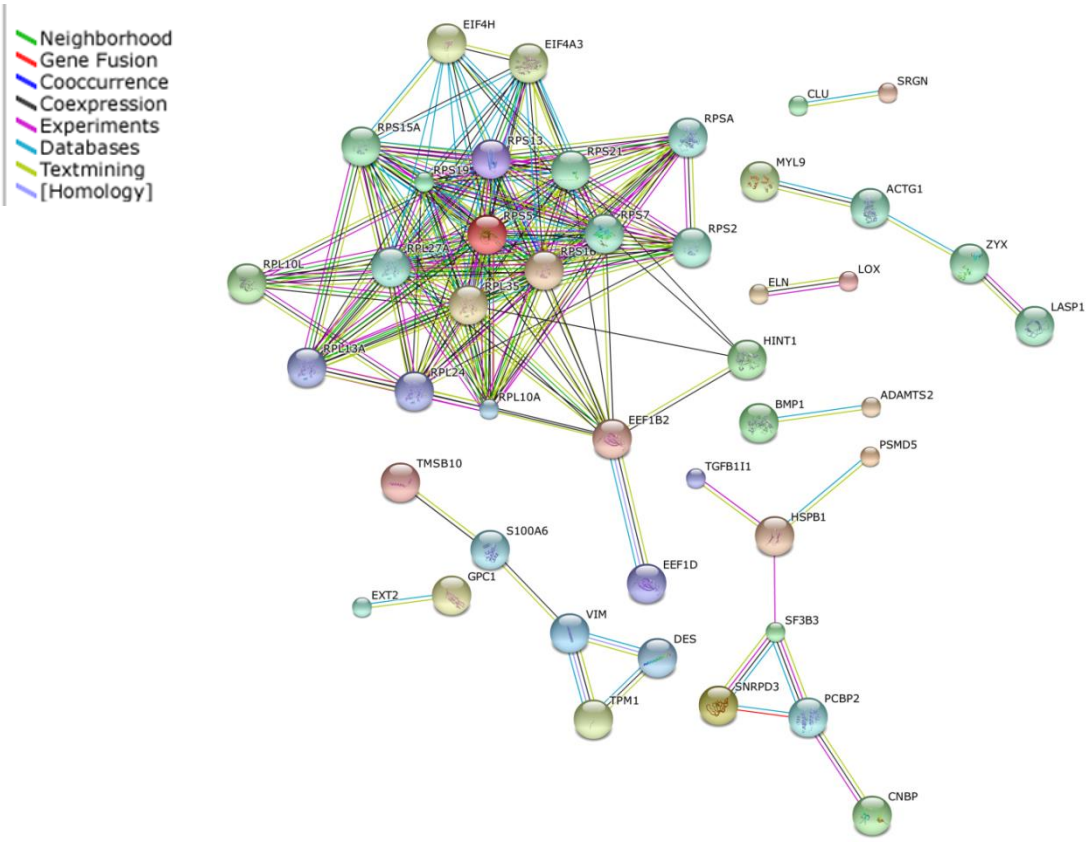

Figure 5.9: STRING generated protein-protein network interactions of significantly down-regulated secreted proteins in cells infected with *N. caninum*. Basically, the top decreased fold changes were inserted with more than -1.5 fold change. Mainly one large and three small clusters of proteins was grouped. Protein search parameter was set at high confidence (0.7) in STRING.

5.3.4 Ingenuity pathway analysis

Pathway analysis using IPA enables the identification of significant proteins from an enriched p-value. It also predicts if canonical pathways are increased or decreased based on differentially expressed proteins inserted. The host cell secreted proteins were also investigated using IPA analysis. Only secreted proteins identified using SPD, SignalP and SecretomeP were imported in the software with secreted proteins containing ± 1.5 fold changes. *T. gondii* infected cells compared with the uninfected cells secretions were searched separately and the same was applied to *N. caninum* infected cells.

The enriched canonical pathways, diseases and disorders and molecular functions returned from IPA analysis in both infected cell secretions can be seen in Table 5.7. In *T. gondii* infected HA cells; an example of the enriched canonical pathways was the agranulocyte adhesion and diapedesis (Figure 5.10), involved in the migration of leukocytes from the vascular system to sites of pathogenic exposure during inflammation. An example of enriched canonical pathway detected in *N. caninum* infected cells secretions was the acute phase response signalling pathway (Figure 5.11). Molecular and cellular functions included in both infected cell secretions were associated with cell movements (Figures 5.12 and 5.13).

Table 5.7: Canonical pathways, diseases and disorder and molecular function detected using IPA pathway analysis in host cells infected with *T. gondii* and cell infected with *N. caninum* protein secretions (p-value and number of proteins detected (no. of proteins)

Type of infection	Category	Name	P-value	No. of proteins
T. gondii infected cells	Canonical pathway	Agranulocyte Adhesion and Diapedesis	5.93E-06	7
		Differential Regulation of Cytokine Production in Macrophages and T Helper Cells by IL17A and IL17F	4.68E-05	3
		Granulocyte Adhesion and Diapedesis	4.89E-05	6
	Diseases and disorders	Neurological disease	1.23E-09	34
	Molecular and cellular function	Cellular Growth and Proliferation	7.17E-11	37
		Cellular Movement	1.57E-08	24
N. caninum infected cells	Canonical pathway	EIF2 Signaling	2.40E-13	15
		Acute Phase Response Signalling	9.24E-09	11
		Regulation of eIF4 and p70S6K Signalling	2.25E-08	10
	Diseases and disorders	Cancer	1.04E-10	47
	Molecular and cellular function	Cell-To-Cell Signaling and Interaction	5.48E-07	27
		Cellular Movement	1.09E-06	30

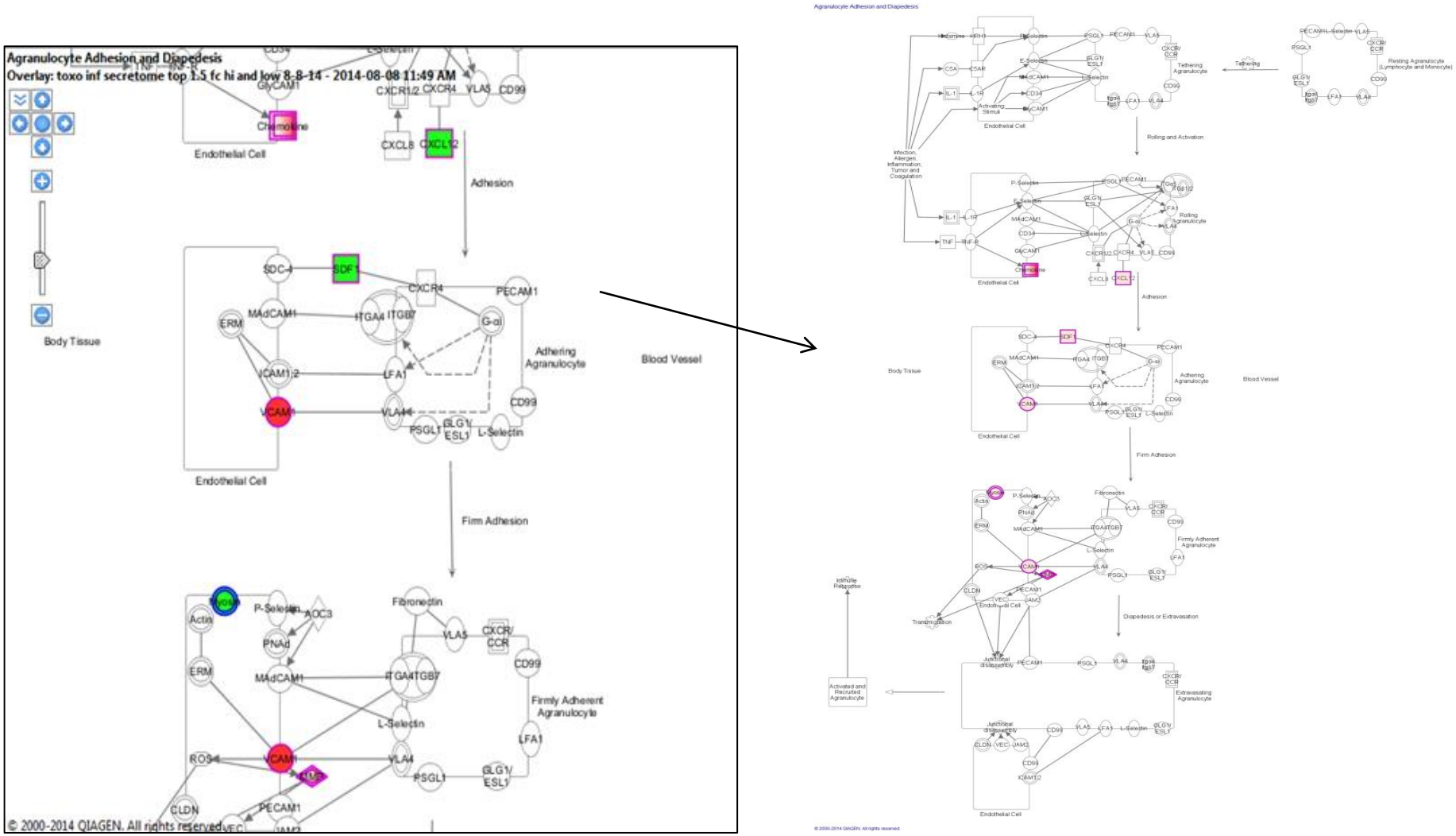

Figure 5.10: *T. gondii* infected human astrocyte secretome pathway analysis using IPA. On the left there are the proteins found in the agranulocyte adhesion and diapedesis pathway with red indicating the increased protein expression and green decreased expression. Proteins with grey shading were proteins not detected in the differentially expressed inserted data.

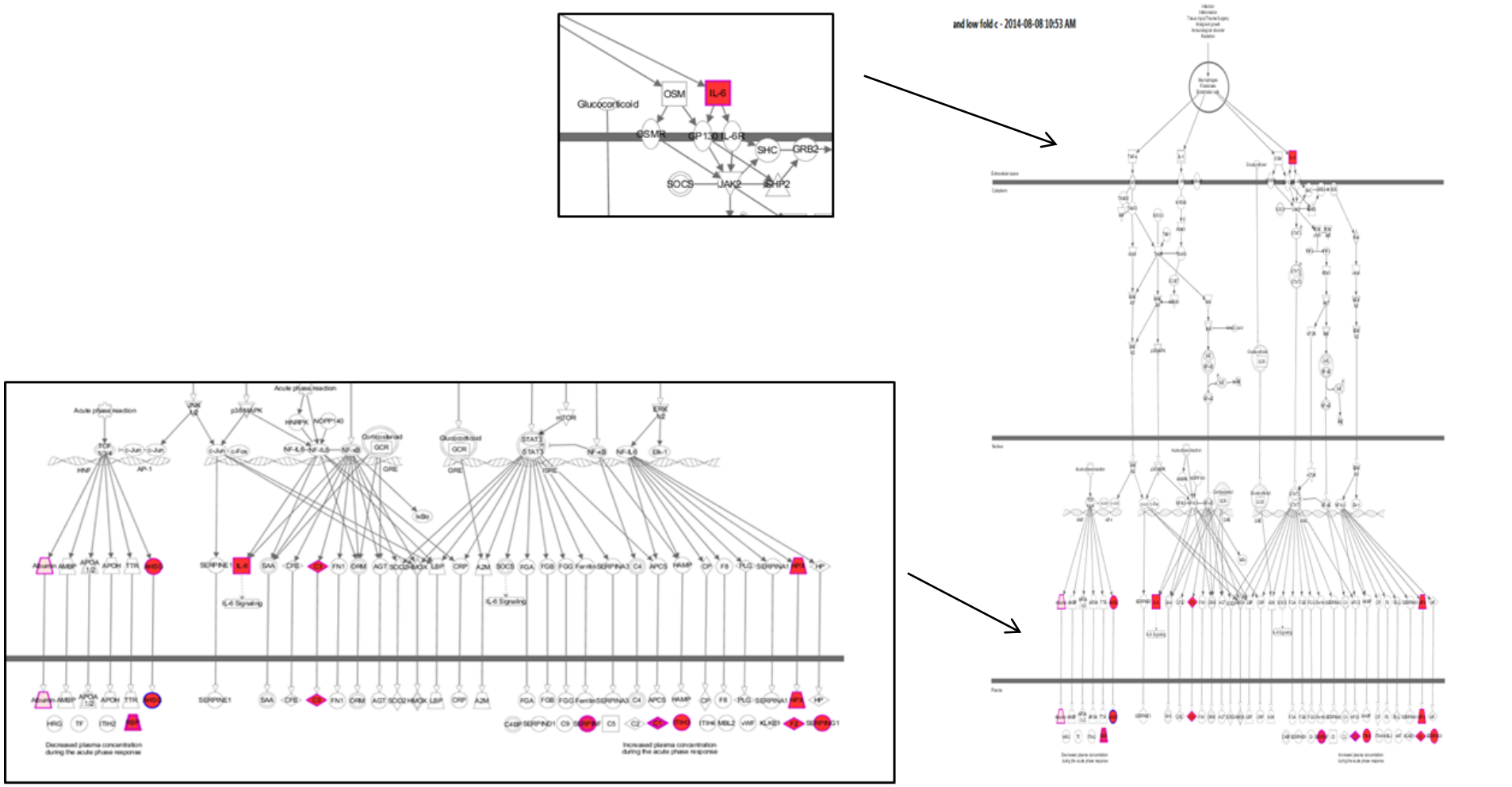

Figure 5.11: showing the acute phase response signalling pathway in HA cells secreted proteins infected with *N. caninum.* Proteins highlighted in red indicate increased expression. Proteins with grey shading were not proteins not detected in the differentially expressed inserted data.

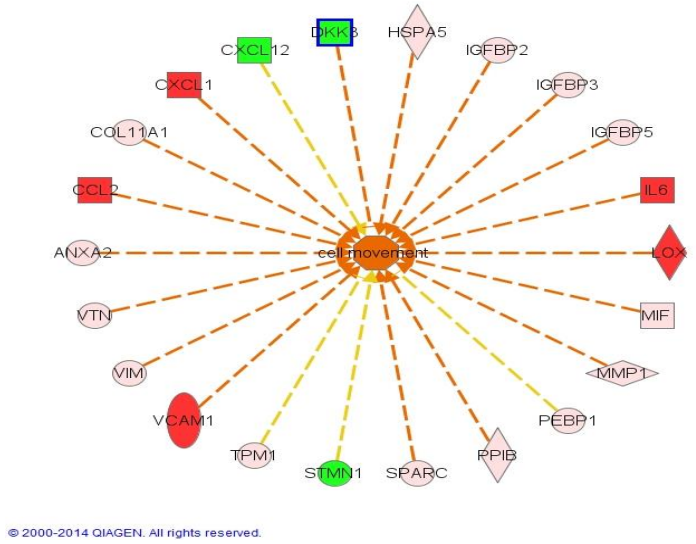

Figure 5.12: Functional annotation of host cells infected with *T. gondii* secretions involved in migration of cells. Secreted proteins highlighted in red show increased expression and in green decreased expression. Orange dashed lines connecting the protein to the function (cell movement) indicate activation of proteins relationship and yellow lines between the proteins indicate findings that were inconsistent with downstream application.

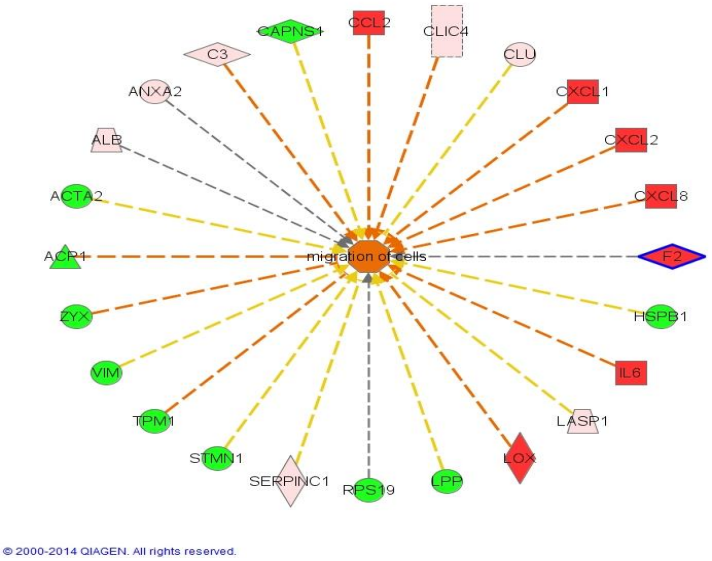

Figure 5.13: Functional annotation of host cells infected with *N. caninum* involved in migration of cells. Proteins highlighted in red indicate increased expression and with green indicate decreased expression of proteins. Orange dashed lines indicate activation of proteins relationship; yellow disconnected lines indicate findings inconsistent with downstream application and grey lines show effect relationship not predicted.

5.4 Discussion

Comparative investigation of the secreted proteins of host cells, especially cells relating to the CNS during infection with *T. gondii* and *N. caninum* was the main aim in this chapter.

There are many reported studies in the investigation and identification of the mouse astrocyte secretome (Perera et al. 2008; Dowell, Johnson & Li 2009; Delcourt et al. 2005). Astrocytes secrete proteins that are important for neuronal growth, neurogenesis, development and survival and synaptic development. These are mediated by the release of proteins and peptides, such as extracellular matrix proteins, growth factors and proteases (Bachoo et al. 2004). Astrocytes have an important role in the control of the immune response against *T. gondii* within the CNS; they activate and produce inflammatory cytokines such as IL1β, IL6 and TNFα in response to infection (Fischer et al. 1997).

Chemokines are involved in inflammatory responses and are essential for the recruitment and leukocyte activation. Secreted proteins, such as cytokines, chemokines, hormones, digestive enzymes, antibodies and components of the extra-cellular matrix are secreted from the cell into the extracellular media and play essential biological roles and are important foundations for protein therapeutics, these proteins are referred to as secretome. In recent years, some groups began to study secreted proteins from a genomic angle and helped to create publicly available databases for secreted proteins (Clark et al. 2003; Klee et al. 2004; Chen et al. 2005). There are many essential roles that secreted proteins may be involved in and it was necessary not only to look at the expression of the proteomic profiles of the infected cells, but also to explore the proteomic profiles of proteins secreted outside the cells, which can help in our understanding of the host-parasite interaction pathways involved. Up to date, there have been no studies looking into the differences of astrocyte proteomic responses during infection with *T. gondii* and *N. caninum*. The total number of secreted proteins in cells infected with *N. caninum*

(973 proteins) was higher than the number of proteins identified in cells infected with *T. gondii* (666 proteins), which might suggest elevated responses of astrocytes during *N. caninum* infection compared to *T. gondii*. Nevertheless, differences in the total number of proteins between infections could be related also to technical variations during culturing condition, sample preparation or through LC-MS/MS procedure. After identification and quantification of differentially expressed proteins of HA cells infected with either *T. gondii* or *N. caninum* and compared to uninfected controls, further analysis was used to highlight predicted secreted proteins were applied using online search databases such as SPD, SignalP and SecretomeP for functional annotation and network analysis.

5.4.1.1 Significant up-regulation differences between cells infected with *T. gondii* and *N. caninum*

Chemokines are key regulators of leukocyte trafficking (Adams & Lloyds, 1997). It has been established that chemokines can be secreted during *T. gondii* infection both *in vitro* and *in vivo* (Brenier-Pinchart et al. 2000; Brenier-Pinchart et al. 2002; Kim et al. 2001). Significant differences were noticed in chemokine expression between *T. gondii* and *N. caninum* infected cells. The C-X-C motif chemokine 2 (CXCL2), is produced by activated monocytes and neutrophils and expressed at sites of inflammation. A 60 fold up-regulation of CXCL2 was observed in the secretome of *N. caninum* infected HA cells compared to uninfected controls. No significant changes were observed in the secretome of *T. gondii* infected HA cells. This contradicts earlier studies that showed increased expression of CXCL2 in *T. gondii* infected cells secretome done by Kikumura, Ishikawa & Norose (2012), which explored leukocyte migration during ocular toxoplasmosis in murine models and found increased expression of CXCL2 and CCL2. But there were no investigations looking into the secretion of CXCL2 in *N. caninum* infected cells. Immune response during *T. gondii* infection at the transcriptional level were explored using human Muller cells, which also showed increase expression of CXCL2 in infected cells with two strains of *T. gondii* (Knight et al. 2006). On the other hand, other findings by

Knight *et al*., (2006) study were comparable to the results obtained from this experiment, in which increased expression level of cytokine and chemokines such as CCL2, IL6 were also detected in human astrocyte infections (Knight et al. 2006).

CXCL1; is also involved in inflammatory responses and has a chemotactic activity for neutrophils. Although, it would be expected that the secretion of CXCL1 chemokine would be similar to CXCL2 as both of them are involved in the recruitment of neutrophils to sites of inflammation; CXCL1 was significantly up-regulated in astrocytes infected with *T. gondii* with more than 38 fold compared to only 5 fold up-regulation in *N. caninum* infected cells. CXCL1 is involved in the processes of angiogenesis, inflammation, wound healing, and tumorigenesis (Tsai et al. 2002). The innate immune response of neutrophils has been shown to be critical for the successful resolution of *T. gondii* infection (Sayles & Johnson 1996). CXCL1 has also been found increased in ocular cells infected with *T. gondii* and in the brain in the acute stage of infection independent from IFN-Ɣ (Kikumura et al. 2012). Another cytokine involved in neutrophil recruitment to sites of inflammation was IL8; it induces chemotaxis in target cells, primarily neutrophils but also other granulocytes, causing them to migrate toward the site of infection. IL8 also induces phagocytosis and is known to be a potent promoter of angiogenesis (Muller et al. 2006). IL8 was significantly up-regulated in *N. caninum* infected cells compared to *T. gondii* infected cells (that was not detected significant). An up-regulated expression of IL8 in *T. gondii* infected HFF and HeLa cells was reported by Denney, Eckmann & Reed (1999), which do not correlate with the findings from this experiment. It has been previously reported that neutrophils in peripheral blood increased in mice after *T. gondii* infection (Norose et al. 2008). Absence of IFN-γ function may cause neutrophil activation, as it is involved in the down-regulation of IL8 production. Neutrophils have been shown to be involved in the dissemination of the parasite *in vivo* in susceptible mice. Dunay *et al*. (2010) reported that neutrophils are not protective against *T. gondii* infection but contribute to the pathology outcome. However, up to date, no investigations of IL8 secretion in *N. caninum* infected cells have been found in the literature, thus no comparable studies either *in vivo* or *in vitro* on IL8 cytokine secretion has been established on cells infected with these

closely related parasites. Many studies done on the involvement of IL6 secretion in the pathogenesis of different bacterial, viral and parasitic diseases have been investigated (van der Poll et al. 1997; Banks, Kastin & Gutierrez 1994). IL6 was up-regulated in both infected cells, but with to a higher extent in *N. caninum* infected cells (six times higher) compared to *T. gondii*. IL6 is secreted by T cells and macrophages to stimulate immune response and has vital roles in fighting infection, as demonstrated in mice that IL6 was required for resistance against bacterium *Streptococcus pneumonia* (van der Poll et al. 1997). IL6 can also cross the blood brain barrier (BBB) which explains its secretion in CNS cells as in astrocytes. IL6's role as an anti-inflammatory cytokine is mediated through its inhibitory effects on TNF-alpha and IL1, and activation of IL1ra and IL10. It was found to stimulate inflammatory and auto-immune processes in many diseases such as depression and Alzheimer's disease (Dowlati et al. 2010; Swardfager et al. 2010). IL6 in the CNS may have protective effects, stimulating neuroregeneration and neuronal growth factor (NGF) production in astrocytes (Otten et al. 2000), which parasites can benefit from during infection. Abe *et al*. (2014) also demonstrated increased secretion of IL6 in murine macrophages infected with *N. caninum* suggested that macrophages play an immunity protective role during *Neospora* infection. Moreover, activation of astrocytes and microglial cells was associated with the production of IL6 and IL10 in in rat mixed glial cells infected with *N. caninum in vitro* which may suggest a protective action by these glial cell types in the CNS (Pinheiro et al. 2010).

Astrocytes secrete IL6 as a protective action against infection that may suggest that the acute phase response to infection in astrocytes is induced higher in cells infected with *N. caninum* compared to *T. gondii* as IL6 is associated with the acute phase response during infection. This could also indicate that *T. gondii* may supresses the host innate response at early stage of infection for a better establishment of infection in cells compared to *N. caninum* infected cells.

Proteins associated with the cell adhesion molecule pathway; ICAM1 and VCAM1 were both found in *T. gondii* infected cells secretome and not in *N. caninum*. Interestingly, ICAM1 was found to increase with 18 fold change and VCAM1 with a 5 fold change. ICAM1 is a member of the immunoglobulins, including antibodies and

T-cell receptors. It is an endothelial- and leukocyte-associated transmembrane protein possessing an amino-terminus at the extracellular domain and known for its importance in stabilizing cell-cell interactions and facilitating leukocyte endothelial transmigration. Usually these proteins are secreted in low concentration; upon cytokine stimulus their concentrations increase (Dustin et al. 1986; Rothlein et al. 1986). ICAM1 also became recognized for its involvement in plasmodium falciparum-infected erythrocytes pathogenesis (Turner et al. 1994). VCAM1 is expressed on both large and small blood vessels after cytokine stimulation of the endothelial cells. It mediates the adhesion of lymphocytes, monocytes, eosinophils, and basophils to vascular endothelium and is involved in leukocyte-endothelial cell signal transduction (Schmitz et al. 2013).

Both ICAM1 and VCAM1 are expressed on inflamed BBB endothelial cells and are critical for the transmigration of lymphocytes and monocytes (Carman & Springer 2004; Ifergan et al. 2006). *Toxoplasma* encephalitis (TE) involves strong activation of major histocompatibility complex (MHC) class I and II antigens as well as of the ICAM1 on cerebral endothelia, microglia and choroid plexus epithelium and VCAM1 on endothelial cells (Deckert-Schluter et al. 1994). The up-regulation of ICAM1 and VCAM1 in secreted cells infected with *T. gondii* could indicate increased permeability of inflammatory cell migration through the BBB, in which infected cells with *T. gondii* could successfully enter and establish infection in the CNS.

One of the chemokines that has been extensively explored during cells infection with *T. gondii* is CCL2. This chemokine was up-regulated in *T. gondii* infected cells compared to cells infected with *N. caninum* secretions. CCL2, is an attractant for monocyte/ macrophages, CD4 and CD8 memory T lymphocytes (Adams & Lloyds 1997; Luther & Cyster 2001). It plays an important role in the CNS as a neuroinflammation mediator of leukocyte infiltration and has been associated with many neurological disorders (Bajetto et al. 2001). It has been illustrated that Hff and HeLa cells secreted CCL2. In addition, investigations done on murine models *in vivo*, showed that chemokines expressed by microglia, neurons and astrocytes may be involved in the leukocyte migration in the CNS (Schluter et al. 2001; Strack et al. 2002). It was demonstrated in mice with TE that astrocytes are the main producers

of CCL2 (MCP-1) (Strack et al. 2002). This also correlates to the findings in human astrocytes infected with *T. gondii* analysis. Chemokine secretion causes enhanced neuro-invasion of leukocytes, and astrocyte derived CCL2 monocytes can migrate across an *in vitro* model of the BBB (Weiss et al. 1998). This may suggest that up-regulation of CCL2 during human astrocyte infection with *T. gondii* enables successful migration of *T. gondii* parasites through the BBB and establishment and localization of the parasites in the CNS.

Key mediators of tissue remodelling after brain injury or disease include the MMPs (matrix metalloproteinases). MMP10 was only found in *T. gondii* infected cells with an increased expression of 25 fold change. MMP10 also known as Stromelysin-2 is an enzyme from the matrix metalloproteinase (MMP) family involved in the breakdown of extracellular matrix in both normal and disease processes and enables the degradation of proteoglycans and fibronectin. Increased expression of MMPs has been associated in diverse processes during disease; such as cancer and infectious pathologies (Ethell & Ethell 2007). During *Toxoplasma* infection, increased expression of MMP8 and MMP10 was observed in the brain, CD4+ and CD8+ T-cells are involved in MMP8 and MMP10 production (Clark et al. 2011). This may indicate the importance of the MMP in the trafficking of infiltrating cells into sites of infection with *T. gondii* in the CNS. Furthermore, regulation of metalloproteinases is vital for the immune populations to access infected CNS tissues that may be key to the balanced immune response that is related to the establishment of chronic infection with *T. gondii*.

Pentraxin-related protein PTX3; also known as TNF-inducible gene 14 protein, regulates innate resistance to pathogen and inflammatory reaction, control of autoimmunity and is produced in a variety of tissues during inflammation (Rovere et al. 2000; Christersdottir Bjorklund et al. 2013). It was found up-regulated in *T. gondii* infected cells and no changes were found in *N. caninum* infected cells. PTX3 acts as an acute phase response protein, as the blood levels of PTX3 are low in normal conditions and increases during inflammatory and infectious conditions. The secretome of mixed glial cells stimulated with lipopolysaccharide and IFN-γ were screened using LC-MS/MS (Jeon et al. 2010). Among the proteins identified was

Pentraxin-3 (PTX3), which is involved in the phagocytic activity of microglia and may serve as a potential diagnostic biomarker of inflammatory brain disorders. This may propose PTX3 to be a marker of malignancy in infected cells that increases in cells infected with *T. gondii* to signal immune responses that in response to immune stresses by the host will lead to the conversion of the dormant stage of the parasites in the CNS.

5.4.1.2 Protein down-regulation in astrocyte infected secretome

In *T. gondii* and *N. caninum* infected cells secretome, the renin receptor (RENR) was down-regulated compared to uninfected cells in *T. gondii* infected cells. RENR is expressed in the brain and functions as a renin and prorenin cellular receptor, cell death and the regulation of MAPK cascade. Exostosin-2 (EXT2) is a glycosyltransferase required for the biosynthesis of heparan-sulfate. It acts as a tumour suppressor and is also involved in carbohydrate metabolic process and cell differentiation. EXT2 was found significantly down-regulated in cells infected with *T. gondii* compared to *N. caninum* infected cells secretion with only 1.5 fold decrease. Down-regulation of RENR and EXT2 in cells infected with *T. gondii* secretion could suggest that the parasite delays apoptosis in infected cells compared to *N. caninum*.

Stathmin STMN1, also called Leukemia-associated phosphoprotein p18, is a highly conserved 17 kDa protein involved in the regulation of the microtubule filament system and may be required for axon formation during neurogenesis. STMN1 was down-regulated in cells infected with *N. caninum* (10 fold decrease) compared to *T. gondii* infected cells secretion. It is found in the brain, spinal cord and cerebellum and is involved in intracellular signal transduction.

In relation to protease secretions, A disintegrin and metalloproteinase with thrombospondin motifs 2 (ATS2) was only detected in *N. caninum* infected cells with a 38 decrease reverse fold change. This enzyme is found weakly expressed in the brain and is associated with collagen degradation and extracellular matrix organization. This might suggest that *N. caninum* supresses the production of the enzyme and procollagen cannot be processed correctly without this enzyme. As a

result, collagen fibrils are not assembled properly; chemical interactions, between collagen fibrils are also affected which as a result, weakens the connective tissue. Disintegrin and metalloproteinase domain-containing protein 9 (ADAM9), mediates cell-matrix interactions and is involved in cell adhesion and monocyte activation. ADAM9 was down-regulated with 36 fold change in *N. caninum* infected astrocytes compared to only 3 fold decrease in *T. gondii* infected cells. Decreased protease protein secretions in *N. caninum* infected cells may suggest that *N. caninum* does not establish successful cell adhesion signalling interactions and ECM organization as *T. gondii* parasites and could be implicated in down-regulation of neurogenesis.

5.4.2 Pathway analysis of host secretome

It was essential to look at the metabolic pathways in order to have a more comprehensive view of the host-parasite interaction. Secreted proteins of both infections were investigated for their involvement in metabolic pathways. Agranulocyte adhesion and diapedesis pathway (IPA analysis in Figure 5.10) was associated with *T. gondii* infected cells secretome. This pathway is associated with leukocyte migration of cells during inflammation which is also correlated with previous findings of the transcriptome analysis. The other significant enriched pathway in *N. caninum* infected cells secretome was the acute phase response pathway (IPA analysis Figure 5.11). This pathway is also correlated with previous findings associated with the up-regulation of molecules related to acute infection response in the transcriptome analysis. Both infected astrocytes with *T. gondii* and *N. caninum* secretions were involved in the NOD-like receptor (NLR) signalling pathway in DAVID analysis (Tables 5.3 and 5.5). Proteins involved in this pathway were up-regulated and include cytokines and chemokines such as CCL2, CXCL1, CXCL2, IL6 and IL8. This pathway involves specific families of pattern recognition receptors that are in charge of detecting various pathogens and producing innate immune responses. This family of proteins contain more than 20 members in mammals and plays essential roles in the recognition of intracellular ligands. NOD1 and NOD2, sense the presence of the bacterial peptidoglycan fragments that escaped from endosomal parts, causing the activation of NF-kappaB and MAPK,

cytokine production and apoptosis. In contrast, a different set of NLRs induces caspase-1 activation through the assembly of multi protein complexes called inflammasomes that are critical for causing mature proinflammatory cytokines along with Toll-like receptor signalling pathway. Secreted proteins identified in this pathway are mainly involved in neutrophil recruitment, T cell differentiation and antigen T and B cell responses. Functional annotations of infected astrocytes were also related to inflammatory responses and regulation of cell migration, which was also correlated to previous findings (Norose et al. 2011; Murdoch & Finn 2000). Moreover the cellular content investigations of both infected cells also demonstrated that proteins were of extracellular secretion.

5.4.3 Protein network analysis of host cell secretome during infection

Supporting evidence of protein-protein interactions were perceived through functional protein network analysis, although not all proteins showed connectivity between molecules during up-regulation or down-regulation expression changes. Cytokine, chemokine, cell adhesion molecules and proteases were clustered together in up-regulated expressed cells during *T. gondii* infection (Figure 5.6) (such as CCL2, IL6, CXCL1, ICAM1 and MMP10). Secreted host proteins up-regulated during *N. caninum* infection (Figure 5.8) also clustered cytokines and chemokines (such as IL6, IL8 and CXCL2), suggesting that predicted functional associations between grouped proteins are related to evidence of homology and text-mining. Down-regulated secreted proteins of both *T. gondii* and *N. caninum* infected cells (Figures 5.7 and 5.9) had proteins that constitute to the ribosome pathway, with a greater number of molecules associated with *N. caninum* infected cells. Proteins are synthesized in ribosomes which remain in the cytosol. The presence of high number of ribosomes in the secreted cells may indicate the presence cell lysis and cytosol contamination that could have occurred during cell secretome preparation and collection. This may also suggest potential involvement of exosomes. Exosomes are small membrane vesicles that are discharged in normal and diseased conditions in

different types of cells (Pan & Johnstone 1983). They are formed through inward budding of endosomal membranes in a cell that result in the intiation of intraluminal vesicles (Sotelo 1959). Exosomes can be considered as a non-classical secretion process of proteins and is involved in the transfer of RNA and proteins (Amzallag et al. 2004 Valadi et al. 2007). Mammalian cell types have been illustrated to discharge exosomes into culture medium *in vitro*; such as murine microglial and neural cells (Fevrier et al. 2004; Potolicchio et al. 2005).

5.4.4 Comparative analysis of transcriptome and secretome results of host cells

Compared to the proteomic study of HA cells at three different time points (chapter four), changes in secreted expression of these cells during infection showed obvious differences in both increased and decreased expression changes. The main findings in the transcriptome chapter (chapter three) were compared with the results of the secretome analysis. The proteome data was not included in the comparison due to similarities found in most metabolic pathways and functional annotations of the host expression profiles analysis (chapter four). In illustration of the key findings of similarities and differences in host cells transcriptional and secreted proteome expression levels can be seen in Table 5.8. Some molecules in the transcriptome analysis correlated with the findings in the secretome analysis of the host cells, proteins such as CXCL2, IL8 and CCL2 (Table 5.8). CXCL2 is a chemoattractant mainly for neutrophils was up-regulated in both *N. caninum* infected cells RNA and secretome analysis while down-regulated in *T. gondii* infected cells. IL8 is also associated with neutrophil recruitment to sites of inflammation was up-regulated in both sets of analysis. CXCL1 is also involved in neutrophil recruitment was up-regulated in *N. caninum* infected cells compared to *T. gondii* in RNA-Seq analysis, while up-regulated in *T. gondii* infected cell secretome analysis. Differences

observed in neutrophil recruitment during host infection do not clearly indicate the parasites association with neutrophil migration to sites of inflammation. But the RNA-Seq analysis does show a strong association of *N. caninum* infection to recruit molecules such as CXCL1, IL8, CXCL2 and CXCL3 to sites of infection. This may suggest that both parasites are able to trigger neutrophil migration to sites of inflammation but might be at a higher induction in *N. caninum* infection. IL6 cytokine was down-regulated in *T. gondii* infected cells while moderately up-regulated in *N. caninum* transcript analysis. This did not relate to the secretome analysis in which both infected cells showed up-regulation of IL6 secretion in cells infected with *N. caninum* (Table 5.8).

CCL2 was up-regulated in *T. gondii* infected cells transcript analysis and detected up-regulated in the secretome analysis. CCL2 has been associated with the pathology of the CNS and has been linked to the establishment of toxoplasma encephalitis in the brain (Sukhumavasi, Egan & Denkers 2007). Results from both RNA and secretome analysis propose that *T. gondii* increase the regulation of CCL2 in order to establish host cell infection and persist in host cell of the CNS. Cell adhesion molecules ICAM1 and VCAM1 were up-regulated in RNA analysis in both infected cells, but VCAM1 was up-regulated in cells infected with *T. gondii*. In the secreted cells protein expressions; ICAM1 and VCAM1 were only detected in cells infected with *T. gondii* and were found significantly up-regulated. Cell adhesion molecules have been linked to the ability of pathogens to cross the BBB and enter the brain. Increased expression of cytokines, chemokines and cell adhesion molecules all together suggest that the parasite uses these cells to migrate and filtrate through the tight junction and BBB in order to reach the CNS.

MMP10 was down-regulated in *N. caninum* infected cells transcript analysis, whereas it was only detected in *T. gondii* infected cell secretions with an increased expression. This may indicate that MMP10 enables the trafficking of infiltrating cells into sites of infection with *T. gondii* in the CNS.

Other molecules showing no association between the RNA and secretome analysis were ATS2 and EXT2. These molecules were up-regulated in cells infected with *N. caninum* RNA analysis but were down-regulated in the secretome analysis.

In conclusion, some results correlated between RNA and secretome analysis such as IL8, while other molecules did not such as ATS2. The lack of correlation might be related to the imbalanced association between transcriptome and secretome analysis along with the different time points associated with the comparison. Therefore, a clear conclusion cannot be obtained. Nevertheless, comparative analysis highlighted the importance of key molecules involvement in cell migration during infection and its association with the pathology of the parasites in the CNS.

Table 5.8: Comparative analysis of host cell transcripts involved in cell adhesion pathway and cytokine receptor interaction pathway compared to the differentially expressed secretome analysis of host cells during *T. gondii* and *N. caninum* infection. Three different time points (0h, 4h and 16h p.i.) were used in the transcriptomic analysis in both infected cells (TgVEG infected cells and NcLIV infected cells), whereas secreted protein of infected cells (secretome) were collected from (18-24 hour p.i.) Log2 fold changes highlighted in red indicate increased expression changes and fold changes highlighted in green show decreased transcript expressions.

Gene Acc. No.	Gene name	Protein Acc. No.	Gene description	Transcriptome Log2 FC						Secretome Log2 FC	
				N 0h	N 4h	N 16h	T 0h	T 4h	T 16h	Neo inf	Toxo inf
ENSG00000163739	CXCL1	P09341	growth-regulated alpha protein	0	2.28	4.82	0	0.576	0.620	2.31	5.257
ENSG00000081041	CXCL2	P19875	C-X-C motif chemokine 2	0	2.27	3.561	0	-1.85	-2.086	5.89	-0.08 *
ENSG00000169429	IL8	P10145	Interleukin-8	0	1.267	3.46	0	-0.22	1.064	4.93	0.713*
ENSG00000136244	IL6	P05231	Interleukin-6	0	0.137	0.37	0	-0.10	-0.862	4.54	1.99
ENSG00000108691	CCL2	P13500	C-C motif chemokine 2	0	0.061	0.716	0	0.60	1.82	2.11	3.65
ENSG00000090339	ICAM1	P05362	Intercellular adhesion molecule 1	0	0.209	1.349	0	-0.10	1.254	-	4.19
ENSG00000182220	ATP6AP2	O75787	Renin receptor (RENR)	0	0.374	0.044	0	-0.114	-0.463	-3.855	-4.29
ENSG00000166670	MMP10	P09238	Stromelysin-2	0	0.355	-2.63	0	-0.58	-1.64	-	4.624
ENSG00000129038	LOXL1	Q08397	Lysyl oxidase homolog 1	0	0.46	0.562	0	0.008	-0.165	3.327	2.72
ENSG00000168615	ADAM9	Q13443	Disintegrin and metalloproteinase domain-containing	0	0.364	0.44	0	0.082	-0.279	-5.24	1.79

			protein 9								
ENSG00000119681	LTBP2	Q14767	Latent-transforming growth factor beta-binding protein 2	0	0.121	0.017	0	0.182	-0.069	1.99	1.017
ENSG00000151348	EXT2	Q93063	Exostosin-2	0	1.021	0.948	0	0.0016	-0.037	-0.60	-3.85
ENSG00000087116	ADAMTS2	O95450	A disintegrin and metalloproteinase with thrombospondin motifs 2 (ATS2)	0	0.032	0.458	0	0.221	0.116	-5.24	-
ENSG00000163661	PTX3	P26022	Pentraxin-related protein PTX3	0	0.040	0.837	0	-1.068	-1.068	0.04*	1.97
ENSG00000162692	VCAM1	P19320	Vascular cell adhesion protein 1	0	0.591	2.083	0	0.445	3.404	-	2.36

* indicates proteins not significant (p-value<0.05).

5.4.5 Conclusions and future direction

In summary, differentially expressed secreted proteins; cytokines chemokines (such as CCL2 and CXCL1), proteases (MMP10) and cell adhesion molecules (ICAM1 and VCAM1) were up-regulated in secretome analysis of human astrocytes infected with *T. gondii*. That may indicate the parasites involvement in the modulation of cells relating to increase permeability and filtration of the infected cells through the BBB to the CNS more efficiently compared to *N. caninum* infection of cells. This may answer the question to why *T. gondii* is found more frequently in intermediate host cells CNS compared to *N. caninum* infection. On the other hand, *N. caninum* increases more efficiently neutrophil recruitment to infected cells compared to *T. gondii* (such as IL8 and CXCL2) which initiates an innate immune response and may lead to a more limited outcome of infection in cells.

Further immune-based investigations should be carried out; such as immunohistochemistry assays and transmigration assays, which will enable further confirmation of the differentially expressed cytokines and cell adhesion secreted proteins along with the other interesting findings in this chapter. Moreover, other experimental investigations can be carried out as supportive evidence of these secreted molecules. Cell migration assays and immunohistochemistry assays with specific antibodies to these secreted molecules (such as IL8, ICAM1 and VCAM1) can establish firm evidence of the involvement of these proteins in pathological pathways.

6 Chapter six: Comparative analysis of dopamine measurements in host cells during infection with *T. gondii* and *N. caninum* bradyzoites

6.1 Introduction

The behavioural manipulation hypothesis proposed that a parasite such as *T. gondii* manipulates host behaviours needed for its own success and survival (Barnard 1990; Berdoy, Webster & Macdonald 1995; Webster 2007). Since the sexual cycle of *T. gondii* can only occur in the cat, there is the need for the parasite to evolve ways for its transmission to the definitive host (Webster et al. 2006). Localization of the parasite in important parts of the body such as the brain of the intermediate host can enable it to manipulate its host (Werner, Masihi & Senk 1981). It has been suggested that the chronic stage of *T. gondii* infection in the central nervous system (CNS) may also modify behavioural changes in humans (Flegr 2007).

6.1.1 Dopamine changes during *T. gondii* infection

Dopamine is a monoamine neurotransmitter formed in the brain by the decarboxylation of dopa and is needed for normal performance of the central nervous system. It is involved in important roles related to behaviour, cognition, voluntary movement and attention. Dopamine secretion is known to be associated with the modulation of neuronal activities linked to learning and memory functions in the hippocampus region of the brain (Backman et al. 2010).

Remarkably, *T. gondii* infection has shown evidence to increase dopamine secretion. A study done on the chronic stage of *T. gondii* infection proved that parasites can control the hippocampus that may result in decreased memory functions (Berenreiterova et al. 2011). Modulation in the brain can be accomplished through modulation in neurotransmitter levels such as dopamine signalling. In

chronically infected mice, dopamine levels were 114% (1.14 fold) higher compared to their controls, and no changes were detected in other neurotransmitters (Stibbs 1985). In addition, Prandovsky *et al*. (2011) also found high concentrations of dopamine in neural cells infected with *T. gondii* in an *in vitro* experiment. The parasite itself was found to synthesize tyrosine hydroxylase and transforms to L-DOPA amino acid, which is a precursor of dopamine. From the *T. gondii* genome (http://www.toxodb.org), two tyrosine hydroxylase genes were identified (TgAaaH1 and TgAaaH2) (Whitaker et al. 2009). Tyrosine hydroxylase are enzymes belonging to the aromatic amino acid hydroxylases family. Moreover, tyrosine hydroxylase was also found in *N. caninum* but was not detected in *P. falciparum* or *Eimeria* (McConkey et al. 2013). In brain cells infected with *T. gondii* tissue cysts, cells contained tyrosine hydroxylase secreted by the parasite and is localised with the parasitophorous vacuoles (Gaskell et al. 2009; Prandovsky et al. 2011). Gaskell *et al.* (2009) revealed that *T. gondii* TgAaaH1 and TgAaaH2 genes are switched on during parasite conversion from tachyzoite to bradyzoite stage. Host genes may also be associated with the complex interaction between parasite and neurochemical alterations in the brain (Carter 2009).

6.1.2 *N. caninum* infections in hosts

There have been no studies investigating the secretion of dopamine in cells infected with *N. caninum*. *N. caninum* is known to infect animals, such as sheep, deer, goats and cattle. When a host is infected, parasites can cross the intestinal epithelium and reach the circulating blood and infect cells such as macrophages and lymphocytes. Tachyzoites convert to the cyst stage through stress caused by the hosts' immune responses (Buxton, McAllister & Dubey 2002) and are detected in the CNS (Peters et al. 2001). Although tissue cysts have not yet been detected in histological sections of infected adult cattle, it is thought that *N. caninum* can encyst in the tissues of adult cattle. It has been observed in the brains of two normal cows that gave birth to infected offspring (Sawada et al., 2000; Okeoma et al. 2004). A study

investigated a total of 82 foetuses of cattle infected with *N. caninum* in California, USA and found clinical symptoms including encephalitis, myocarditis and adrenalitis accompanied with the disease (Barr et al. 1991a; Barr et al. 1991b). Invasion by *N. caninum* and cyst formation in the CNS and damage caused by this parasite has been detected, which leads to abortion in cattle or neurological diseases in dogs (Dubey & Lindsay 1996; Hemphill, Gottstein & Kaufmann 1996).

6.1.3 Importance of parasite strain used in cyst stage investigations

When studying behaviour changes in hosts, the type of parasite strain used for the investigation is important. Most *T. gondii* strains found in North America and Europe can be categorized into three typical lineages, type; I, II and III (Howe et al. 1997). Type I strains are the most virulent, type II and III strains are the less virulent which can form cysts and initiate the chronic stage of infection. This can cause motor and behavioural changes in infected rodents. Type I parasites are typically highly lethal in mice and are mainly associated with the acute stage of infection and also cause ocular toxoplasmosis (Saeij et al. 2006; Reese & Boothroyd 2011). While type III can cause encystation and brain inflammation, it results in fewer cyst numbers and causes less pathology in the brain (Suzuki & Joh 1994). Therefore, most studies investigating the behavioural changes in hosts have used Type II strains, due to its high parasite-cyst burden found in the brains of mice in which result in elevated immune mediated responses in the brain (Hermes et al. 2008; Gulinello et al. 2010; Gatkowska et al. 2012). And also have higher expression of tyrosine hydroxylase and thereby establish the chronic infection (Howe, Summers & Sibley 1996; Sibley & Boothroyd 1992; Sibley et al. 2002; Gaskell et al. 2009).

6.1.4 Bradyzoite formation *in vitro* methods

Investigation of the tissue cyst of *T. gondii* during chronic infection should provide essential information on the mechanisms of reactivation, neurophysiological

changes and neuropathology of the disease. The importance of understanding host-parasite interactions *in vitro* and specifically in the chronic stage of the infection has led to the development of different methods for studying the tissue formation of *T. gondii* and *N. caninum*. In order to study the effect of dopamine levels secreted during *T. gondii* and *N. caninum* infection in cells of the brain, parasite conversion to bradyzoite stage *in vitro* is essential. Bradyzoite stage induction in *T. gondii* and *N. caninum* can be achieved using various methods such as alkaline induction, heat shock and chemical induction; such as the use of sodium nitroprusside (Skariah, McIntyre & Mordue 2010; Soete, Camus & Dubremetz 1994; Tobin, Pollard & Knoll 2010; Vonlaufen et al. 2004). Increasing the pH in culture media was found to be an effective method for tachyzoite to bradyzoite conversion *in vitro* (Soete, Camus & Dubremetz 1994; Tobin, Pollard & Knoll 2010). A study done by AlKuraishi et al. (2011), found that *N. caninum* transformation from tachyzoite to bradyzoite was enabled through pH alkaline method. For *in vitro* bradyzoite formation in *N. caninum*, the virulent strain NcLIV is preferred for cyst formation compared to less virulent strains Nc-1 and NcSweB1, which was observed to produce very small amounts of tissue cysts *in vitro* (Vonlaufen et al. 2002).

N. caninum conversion *in vitro* is thought to be more difficult compared to *T. gondii* and is more restricted to both host cell lines used and the type of parasite isolate (Weiss et al. 1999). Another issue related to *N. caninum* bradyzoite detection is the difficulty to distinguish the tachyzoite from bradyzoite stage using haematoxylin and eosin stained sections, due to the thickness of the bradyzoite wall which may be thin and difficult to identify (Dubey et al. 2002). Therefore, in order to differentiate between them in *N. caninum*, immunohistochemical assays were applied through labelling with a bradyzoite specific antibody such as BAG1 (McAllister et al. 1996). NcBAG1 is a small heat shock protein that is expressed during bradyzoite conversion (Vonlaufen et al. 2002).

6.1.5 Aims and objectives

The main aim was to investigate dopamine induction in cells infected with *N. caninum* bradyzoites compared to cells infected with *T. gondii* by measuring dopamine levels using the HPLC.

The involvement/effect of dopamine elevation in *T. gondii* infected cells in the CNS has been clearly investigated. However, the involvement of closely related parasite *N. caninum* in host cell dopamine secretion has not been examined. *N. caninum* also contains two genes in its genome that are involved in the production of tyrosine hydroxylase. The hypothesis is that *N. caninum* does not have any effect on the levels of dopamine secretion in the cells of the CNS compared to *T. gondii* infected cells.

6.2 Materials and Methods

This experiment was done in collaboration with Dr. Glenn Mcconkey's Group at the University of Leeds.

6.2.1 Cell culture

Dopaminergic primary rat cell line PC12 (ECACC, Salisbury) was used in this experiment. PC12 is a cell line derived from a pheochromocytoma of the rat adrenal medulla that has an embryonic origin from the neural crest and has been used to study diseases related to the brain. This cell line has been previously used in the investigation of the dopamine induction measurement during infection with *T. gondii* bradyzoites by Glenn Mcconkeys lab. As this chapter was in collaboration with Glenn's lab and the fact that *T. gondii* and *N. caninum* can infect rodents such as rats, it is a valid model for the investigation. Cells were prepared and maintained by Isra Alsaady; a PhD student at the University of Leeds. In order for the cells to attach, 800 µl poly-L- lysine was added to each well and incubated for 2 hours in the incubator at 37°C and 5 % CO_2 followed by removal of the excess poly-L-Lysine. Then, cells were placed at a density of 5 x 10^3 per well (3ml per well including the RPMI medium) and left to incubate for 24 hours in the incubator. Cells were observed the following day under the microscope for attachment. A total of 600 ng nerve growth factor (NGF) was placed to each well and incubated for 24 hours then replaced by fresh NGF every 24 hours until the cells were ready for the experimental infection. A total of six plates were needed (three biological replicates for each of the *N. caninum* and *T. gondii* infection).

6.2.1.1 Preparation of Alkaline medium

In order for parasites to successfully convert from tachyzoite to bradyzoite stage *in vitro*, an alkaline shock method was executed. IMDM medium was prepared with

10% (v/v) FBS and 1% P/S (v/v), the medium was pH adjusted to 8.2 before filtration.

6.2.1.1.1 Alkaline shocking of tachyzoites

T. gondii Prugniard strain (type II) tachyzoites and *N. caninum* (NcLIV) were maintained in HFF cells, parasites were scraped and host cells were ruptured through flushing them many times in a 20g gauge needle followed by the purification of the parasites through 47mm diameter 3µm pore-sized Nucleopore™ polycarbonate membranes (Whatman). Then, they were washed twice in phosphate-buffered saline (PBS) pH 7.4 by centrifugation at 1500 x g for 10 minutes. The supernatant was discarded and tachyzoites were resuspended in alkaline medium and incubated overnight for 18 hours at 37^{o}C and 5% CO_2. Finally, tachyzoites were centrifuged at 500 x g for 10 minutes and supernatant was discarded where tachyzoite pellet was resuspended in RPMI medium.

6.2.1.2 Infection of PC-12 cells

Parasites were counted using a haemocytometer under a light microscope and the required amount for each well for all three replicates were added to PC-12 cells with *T. gondii* and *N. caninum* as seen in Table 6.1. Parasites were then left five days for bradyzoite conversion in PC-12 cells with daily observation of the cells for intracellular parasites, cells were then ready for the dopamine release assay.

Table 6.1: The total number of parasites inserted per well for both *T. gondii* and *N. caninum*.

Well number	Number of parasites infected/well	
1	Uninfected (0 parasites)	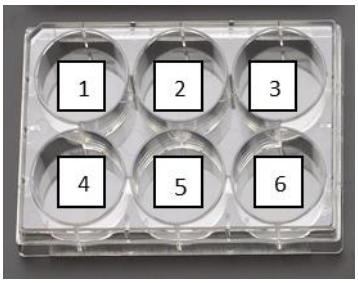
2	0.125 x10^4	
3	0.25 x10^4	
4	0.5 x10^4	
5	1x10^4	
6	2x10^4	

6.2.2 Antibody detection of *N. caninum* conversion

In order to confirm bradyzoite conversion of *N. caninum* tachyzoites, immunofluorescence assay (IFA) was carried out. Cells were grown in chamber slides and infected with alkaline shocked *N. caninum* parasites and left five days for cyst formation. Media from wells were removed and washed three times with PBS, cells were then fixed and permeablised (with PBS, 4% (v/v) formaldehyde and 0.5% (v/v) TritonX-100) and incubated at room temperature for 15 minutes. Slides were then washed three times with PBS and blocked with 5 % (v/v) normal goat serum (NGS) with 5% (v/v) FBS/PBS twice for ten minutes. Then, the slides were rinsed three times with 1 % (v/v) FBS/PBS. Primary antibody for *N. caninum* (BAG-1) polyclonal rabbit antiserum was diluted (1:200) in 1% (v/v) FBS/PBS and was left to incubate at room temperature for one hour and washed six times quickly with PBS. The antibody was kindly provided by Professor Andrew Hemphill at the University of Bern in Switzerland. Secondary antibody (Lectin-Tetramethylrhodamine (TRITC)) as prepared and diluted in 1% (v/v) FBS/PBS and was also incubated at room temperature for one hour. Slides were rinsed briefly in 1% (v/v) FBS /PBS six times. The blue-fluorescent DAPI nucleic acid stain was prepared from stock solution (5mg/ml). The DAPI stock solution was further diluted to 300nM in PBS and applied to the slides for around 5 minutes. Slides were rinsed in PBS followed by six washes with ddH_2O. Slides were mounted with Vectashield and left to dry (Figure 6.1).

6.2.3 Dopamine release assay

For the dopamine release assay, preparation of a low potassium chloride (KCl) containing wash buffer (140 mM NaCl, 4.7 mM KCl, 1.2 mM $MgCl_2$, 2.5 mM $CaCl_2$, 11 mM dextrose, 10 mM HEPES, pH 7.4) and high KCl containing release buffer (40 mM NaCl, 100 mM KCl, 1.2 mM $MgCl_2$, 2.5 mM $CaCl_2$, 11 mM dextrose, 10 mM HEPES, pH 7.4) were needed. Medium from infected cells was first removed and 1 ml of low KCl was added to each well and left to incubate for 30 minutes at 37 ^{o}C. After 2 minutes an aliquot of 250 µl was taken for spontaneous release measurements along with 125 µl 0.1 M PCA (perchloric acid) and filtered with 1ml syringes and 0.2 µm Millipore filters. The samples were then stored in -80^{o}C and later run on HPLC. After 30 minutes, the remaining 750 µl were removed from the wells and the sample was resuspended with 250 µl of the high KCl release buffer followed by 2 minutes incubation at room temperature. The release buffer was collected in Eppendorf tubes containing 125 µl of 0.1M PCA and filtered with 0.2 µm Millipore filters, then stored in -80^{o}C to later run on HPLC.

6.2.4 Harvesting of PC-12 cells

After low KCl and high KCl washing steps, cells were scraped for collection by adding 1ml of RPMI medium to each well and then transferred to Eppendorf tubes, cells were then centrifuged at 400 x g for 5 minutes and the supernatant was discarded and resuspended in 1 ml of PBS. An aliquot of 100µl of the suspension was acquired for CyQUANT™ assay (Life technologies), which accurately determine the number of cells (proliferation assay). Samples were again centrifuged at 400 x g for 5 minutes at 4 ^{o}C, supernatants were discarded and pellets were stored at -80 ^{o}C. The remaining 900 µl of PBS suspensions were centrifuged at 400 x g for 5 minutes, supernatants were discarded and cells were resuspended in 350 µl 0.1 M PCA. Suspensions were then subjected to sonication for 20 seconds using the probe sonicator followed by 14 000 x g centrifugation for 15 minutes at 4^{o}C. The

supernatants were then transferred to fresh Eppendorf tubes and stored at -80 ^{o}C prior to HPLC.

6.2.5 Sample analysis on the HPLC

Samples were run on the reverse phase chromatography coupled with electrochemical detection (HPLC-ED) by Isra Alsaady at the University of Leeds. A brief centrifugation was applied to all the samples, cell homogenates were assayed by HPLC-ED. This was achieved with a Dionex HPLC system consisting of a P580 Pump (Dionex) and Ultimate 3000 Auto sampler Column Compartment with a C18 Acclaim 120 column (5 mm, 4.66150 mm) and an ESA Coulochem III cell, fitted with a glassy carbon electrode used at 700 mV versus Ag/AgCl reference electrode for detection of monoamines. The concentration of compounds was determined using Chromeleon software.

Statistical analysis was done using Excel and Prism software (version 6) (http://www.graphpad.com/scientific-software/prism/).

6.3 Results

For this experiment, PC12 cell line was used as it is known to be a good model of dopaminergic neurons. In order to confirm bradyzoite formation of *N. caninum* in PC12 cells, an immunofluorescence assay was performed. Images taken of the infected cells show staining of parasites with the bradyzoite biomarker BAG-1 and confirm cyst formation of *N. caninum* in PC12 cells using an alkaline shock method (Figure 6.1).

Infected cells of *T. gondii* accumulated higher levels of dopamine which correlated with the infection rate (Figure 6.2). A set of cells were also incubated in high KCl and was measured through HPLC-ED. Dopamine release assays were carried out to assess effects of infection on dopamine signalling. Infected cells with different numbers of alkaline shocked parasites were induced to release dopamine with potassium as K^+ causes discharge of dopamine in vesicles as detected in other studies methods (Yamboliev et al. 2009) (Figure 6.2). As a result, dopamine release increased in infected cultures in a dose-dependent manner with the number of parasites in the culture correlating with the amount of dopamine released in infected PC12 with *T. gondii* (Figure 6.2). An increase in dopamine content and dopamine release were observed in neural cells as a direct response to *T. gondii* infection. On the other hand, the production of total dopamine content measured in PC12 cells were not induced in *N. caninum* infection compared to *T. gondii* infection in both dopamine release assay and total dopamine content. This suggests that there are low significant changes in the dopamine synthesis in the host cells during *N. caninum* cyst formation compared to *T. gondii* infected cells (Figure 6.2). The total dopamine concentrations were compared between cells infected with *T. gondii* and with *N. caninum* (bradyzoite stages) through paired t-test using Prism software (version 6) (Figure 6.3). Results were statistically significant and showed higher dopamine induction in cells infected with *T. gondii* compared to *N. caninum*.

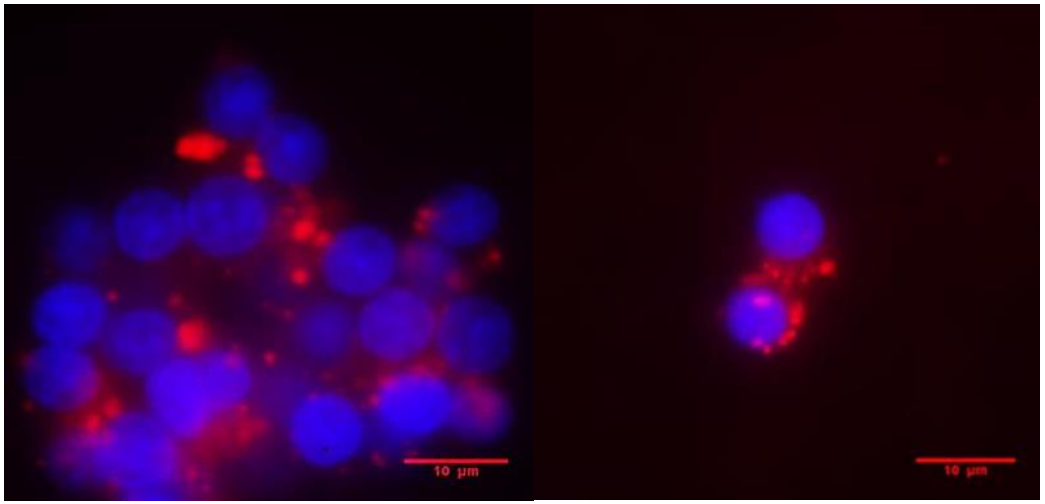

Figure 6.1: Immunofluorescence staining of PC12 cells infected with alkaline induced *N. caninum* parasites. Cells were infected and left for cyst formation, followed by immunostaining with BAG1 antibody for bradyzoite detection (lectin-TRITC red). Cell nuclei are stained with DAPI blue and in red are *N. caninum* bradyzoites.

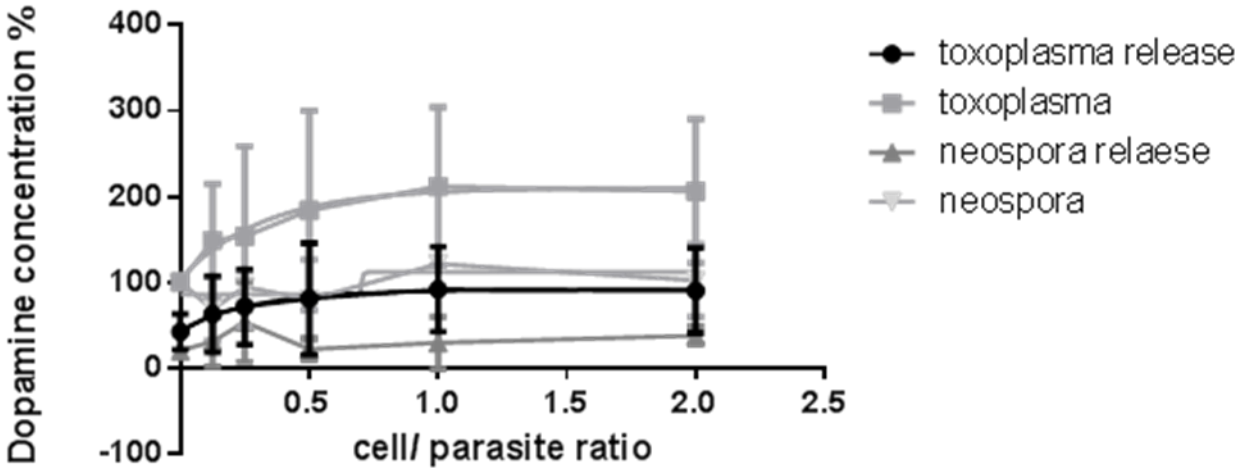

Figure 6.2: Dopamine concentration measurement of PC12 cells infected with *T. gondii* and *N. caninum* parasites using HPLC-ED. Both dopamine release assay and total dopamine content were measured Three replicates were used per infection and different ratios of alkaline shocked parasites were used per well. The x axis shows the cell/ parasite ratio per well, the y axis shows the percentage of dopamine concentration measurements of cells. A standard curve was used to convert HPLC dopamine readings to concentrations. Dopamine induced from KCL release cultures in *T. gondii* infection (black circles), total dopamine measured in *T. gondii* infection is shown in (light grey squares) and increases in correlation with the number of parasites per infection. PC12 cells cell numbers in *N. caninum* infection was also measured according to the infection ratio of cells. Dopamine induced from KCL release cultures in (dark grey triangles) and total dopamine content was measured in *N. caninum* infection (light grey triangles).

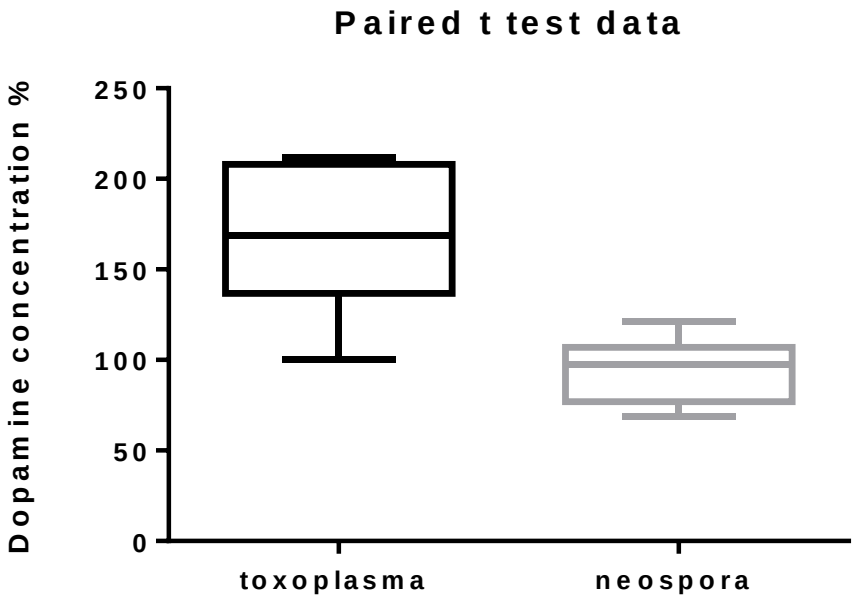

Figure 6.3: Box and whiskers plot of dopamine induction in *T. gondii* infected PC12 cells (bradyzoites) compared *to N. caninum* infected cells (bradyzoites) using Prism software (version 6). The y axis shows the percentage measurement of the dopamine concentrations in infected cells. A standard curve was used to convert HPLC dopamine readings to concentrations. A paired t-test was done to compare total dopamine concentrations of infected cells with *T. gondii* with *N. caninum* (which show a significant correlation).

6.4 Discussion

In this chapter, the main aim was to investigate dopamine induction in cells infected with *N. caninum* compared to cells infected with *T. gondii*. Parasites were first converted to the bradyzoite stage using an alkaline shock procedure. Confirmation of conversion was assessed in cells infected with *N. caninum* using immunostaining with BAG1. Results of dopamine measurements in PC12 cells clearly indicated that *N. caninum* did not induce any distinct changes in dopamine production in infected cells compared to *T. gondii* (Figure 6.2 and 6.3).

Behavioral changes in hosts may be a direct or an indirect effect of *T. gondii* infection. It has already been presented that *T. gondii* increases the dopamine level both *in vivo* and *in vitro* (Prandovsky et al. 2011). The parasite itself was found to contain two genes involved in the dopamine synthesis along with its close relative *N. caninum*; these were not detected in other *Apicomplexa* parasites such as *P. falciparum* or *Eimeria spp*. (McConkey et al. 2013).

In order for the parasite to successfully complete its life cycle, it must modulate and alter its intermediate host responses and behaviour (Barnard 1990). Since the sexual cycle can only take place in the cat, it is crucial for the parasite to evolve ways for its transmission to the definitive host (Webster et al. 2006). Webster, Brunton & MacDonald (1994) demonstrated that *T. gondii* causes an increase activity and also minimizes fear behaviour in rodents.

The cat and mouse cycle has appeared to be successful for the parasites survival and persistence. As proven by many studies, this can be done through alteration of behaviour of the intermediate host during the chronic stage of infection. These interesting findings showed dramatic changes in the behaviour of infected mice towards their predators (the cat); causing them to be attracted to their odour rather than escaping from it (Berdoy, Webster & Macdonald 2000; Kaushik, Lamberton & Webster 2012). It has been speculated that *T. gondii* cysts might be associated with the modulation of dopamine production, or interfere directly with neuronal activity of the host (Gaskell et al. 2009; Prandovszky et al. 2011; Mitra, Sapolsky & Vyas 2013). Furthermore, there have been reports of higher cyst burden found in the amygdalar regions of the brain in the intermediate host, which is associated with innate fear (Vyas et al. 2007).

The findings in this chapter related to *T. gondii* dopamine induction in cells were in agreement with previous findings related to the increase dopamine signaling of neural cells during *T. gondii* infection. Dopamine levels were found increased by 114% comparing to controls, in which no changes were detected in chronically infected mice with *T. gondii* (Stibbs 1985). Prandovsky *et al*. (2011) also found higher concentration of dopamine signalling in an *in vitro* experiment in neural cells infected with *T. gondii*.

On the other hand, cells infected with *N. caninum* did not exhibit any significant changes in dopamine secretion, suggesting that that parasite does not alter dopamine levels in the brain. This may be associated with the successful vertical transmission of *N. caninum* through the vertical route from the mother to the fetus in cattle, therefore does not require the alteration of the behavior of its intermediate hosts such as in rodents. It was suggested that *T. gondii* and *N. caninum* diverged from their common ancestor around 28 million years ago where both genomes and gene expression are conserved (Reid et al. 2012). This could explain why the two genes involved in dopamine synthesis were found in both *N. caninum* and *T. gondii* and not in other apicomplexan parasites. Another explanation to why *N. caninum* does not induce dopamine changes in infected cells could be associated with recent findings related to Rop18 gene which is a virulent gene found in *T. gondii* was discovered to be a pseudo gene in *N. caninum* (Reid et al. 2012).This study has provided new insights in differences between these closely related parasites toward host manipulation and specifically in dopamine secretion in the brain.

Further work can be done to confirm the findings detected *in vitro* through the examination of dopamine induction in mouse models (*in vivo*) during infection with *T. gondii* compared to *N. caninum* along with uninfected (control) models. Another novel approach would be to explore dopamine induction in cattle. There is a lack in the number of studies related to *N. caninum* infections; and specifically in the study of possible behavioral changes in intermediate hosts, which may open new insights in *N. caninum* investigations in the CNS of it hosts.

7 Chapter seven: Discussion and future perspectives

The work presented in this thesis supports the hypothesis that there are differences in human astrocyte responses during infection with *T. gondii* compared to *N. caninum*. The comparative study was achieved through the application of advanced global analysis of the host cells transcriptome, proteome and secretome during infection. The tachyzoite stage for both parasites were used in most of the experiments, as it is known to be the highly invasive stage involved in the pathogenesis outcome in both Toxoplasmosis and Neosporosis, in which both parasites can reach critical sites and tissue of the infected host, such as the CNS.

The basis of the selection of *T. gondii* and *N. caninum* comparative analysis during host cell infection was that these two parasites have very similar histological appearance but behave differently. *N. caninum* was first distinguished from *T. gondii* in 1984 (Bjerkas et al. 1984) along with the high syntenic genome structure (Reid et al. 2012). Another fact is the wide host range that *T. gondii* has in which it can infect many warm blooded animals including humans (Montoya & Liesenfeld 2004), whereas *N. caninum* is mainly successful in cattle and has a more restricted host range (Lindsay et al. 1999; McAllister et al. 1998). The CNS contains different cells and one of the most abundant cell types are astrocytes that also harbour parasites during infection (Hulinska et al. 1990; Halonen et al. 1996). There have been limited transcriptomic and proteomic studies investigating *N. caninum* infection, where no comparative studies in astrocytes during *T. gondii* and *N. caninum* infection have been published.

The main findings associated with this thesis were the identification of transcripts and secreted proteins differentially expressed between the host cells infected with *T. gondii* and those infected with *N. caninum* that were related to cytokines, chemokines and cell adhesion molecules. Previous studies have found that during infection or injury of astrocytes; they result in the migration of leukocytes to the site of infection (Brenier-Pinchart et al. 2004; Strack et al. 2002).

In chapter two, 2D-DIGE followed by LC-MS/MS analysis was used for the comparative study of human astrocytes between two strains of *T. gondii* and *N. caninum*. Although this

technique is believed to be a sensitive, high resolution method for the detection of differentially expressed proteins; it is time consuming, laborious and technical difficulties were present. The number of proteins identified and quantified as differentially expressed were very low. Coupled with the fact that more than one protein was identified under the same protein spot of interest, which made it difficult to distinguish the exact protein found differentially expressed. Proteins have been identified, such as enzyme L-lactate dehydrogenase A chain, that is involved in the glycolysis, as well as Ankyrin3 were found differentially modulated between the infected cells, in which were up-modulated in *T. gondii* infected cells. That may suggest that *T. gondii* modulates proteins for nutritional uptake and regulation of ion transport for the parasites propagation and establishment in cells. While proteins such as Vimentin and Syne2 were up-modulated in *N. caninum* infected cells compared to *T. gondii*, suggesting that *N. caninum* may modify the cytoskeleton of host cells for parasites invasion and entry. In order to understand results obtained from 2D-DIGE, considerations in separation limitations and the frequently observed phenomena of multiple proteins migrating to the same spot must be taken in mind. Therefore, a non-gel based method using label-free quantitative approach was carried out through the application of high resolution tandem mass spectrometry.

In chapter three, changes in the transcriptome of astrocytes during the early stage of parasitic infection was investigated at three different time points, through the application of high resolution RNA-Seq. This has provided valuable insights into the potential biological roles of the expressed mRNA molecules and detection of differences in the host's transcripts between the two infections. These differences were mostly related to metabolic and cell signalling pathways and biological and cellular localization, such as cytokine-cytokine receptor pathway and CAM pathway. Significant differences were observed between HA cells infected with *T. gondii* or *N. caninum* in expressed transcripts, such as CXCL1, CCL2, CXCL2, IL8, VCAM1 and NCAM2. Differences identified in cytokine, chemokine and cell adhesion molecules are key findings in this chapter and may indicate increased cell transmigration across the blood brain barrier (BBB) in HA cells infected with *T. gondii* compared to *N. caninum* infection. CCL2, VCAM1 have been demonstrated to be involved in parasite migration across the BBB and their involvement in toxoplasmic encephalitis (Carruthers & Suzuki 2007; Deckert-Schlüter et al. 1994). In addition, molecules associated

with neutrophil migration were greater in HA cells infected with *N. caninum*, which contradicts other studies that have demonstrated up-regulation of neutrophils in *T. gondii* infection (Kikumura et al. 2012; Denney et al. 1999). Differences with the previous studies could be related to the use of different cell lines (HeLA and Hff cells) and the period of infection incubation (which was higher 24-48 hours p.i.), which may suggest that cells respond differently to parasitic infection with *T. gondii* or *N. caninum*. The validation of the expression of these transcripts *in vivo* will further confirm similarities or differences between *in vivo* and *in vitro* cell transcriptional analysis.. One of the main challenges associated with the RNA-Seq approach was the high cost and difficulties associated with the availability of sufficient amounts of mRNA for sequencing. In this analysis, two replicates were pooled for all three time points and a total of six samples were sequenced and analysed. Although it is recommended to use replicates in transcriptomic analysis, collecting enough mRNA material at each point and the high cost were two of the drawbacks in this investigation. However, many published studies used no replicates in their investigations owing to the use of RNA-Seq deep sequencing (Brawand et al. 2011; Graveley et al. 2011).

In chapter four, global proteomic profiling of human astrocytes during infection (at 0, 4 and 16 hours p.i.) was carried out across the time series for the mRNA analysis using label free quantitative proteomics. This method was more accurate, less time consuming and identified more than 1000 statistically significant proteins in both infected HA cells compared to gel-based quantitative analysis. Cellular localization and metabolic functions were associated with host mitochondria and ER, along with biological processes mainly related to transcription and translational processes. Similarities in the host's proteome profiles were highly observed. This may indicate that at early stages of infection, both parasites modulate the hosts' proteins in a similar matter. Further analysis of early stages of host cell invasion in astrocytes, along with 24-48 hours post infection, may enable the detection of changes that might have only occurred in very early stages or that are in the process of changing between host infections that might have been missed out in the time points chosen for the experiment. Nonetheless, this method has proven to be of higher sensitivity and increased identification and quantification of expressed proteins compared to 2D-DIGE gel based approach.

The secretome has gained the attention of many researchers and is considered to be a biomarker and diagnostic tool for the investigation in many areas of research; including cancer, host-pathogen interactions and vaccine drug development (Ochsenbein 2002; Sibbald et al. 2009; Brey 2005). In addition, studies of parasites excretory secretory antigens (ESA) was found to be a successful tool in diagnostics, as found in a study done on *T. gondii* ESA that enabled to differentiate between active infected and asymptomatic HIV patients with cerebral toxoplasmosis (Meira et al. 2011). Astrocytes are known to secrete cytokines, chemokines and signalling proteins outside the cell during inflammation or injury (Fischer et al. 1997).

In chapter five, expression profiles of secreted proteins were investigated using label-free quantitative proteomics. A comparative analysis of proteins secreted from human astrocytes during *T. gondii* and *N. caninum* infection was performed. This was done through the collection of secreted proteins and were analysed by mass spectrometry LC-MS/MS and bioinformatic analysis. Interestingly, significant differences were noticed between infections, mostly related to cytokines, chemokines, protein kinases and cell adhesion molecules. Molecules associated with the pathogenesis of *T. gondii* in the brain such as CXCL1 and CCL2, were up-regulated in astrocytes infected with this parasite when compared to *N. caninum* infected cells. Researchers have linked the up-regulation of these proteins during infection with *T. gondii* with toxoplasmic encephalitis (Strack et al. 2002; Hunter et al. 1992b). Cell adhesion molecules are associated with many diseases in the brain, especially related to cerebral parasitic infections such as cerebral malaria, toxoplasmosis and trypanasomiasis (Kadl & Leitinger 2005; Coisne et al. 2006). ICAM1 and VCAM1 were up-regulated in astrocytes infected with *T. gondii*, which may be associated with the transmigration of the parasites through the BBB and the ability to successfully reach the brain (Carman & Springer 2004; Ifergan et al. 2006). There were significantly up regulated expressed chemokines in one infection compared to the other. For example; CXCL1, CXCL2 and IL8 are mainly involved in the recruitment of neutrophils. Yet, differences in their secretion during astrocyte infection with *T. gondii* and *N. caninum* were detected. Whereas CXCL1 was up-regulated in astrocytes infected with *T. gondii* (more than 38 fold), CXCL2 and IL8 were up-regulated in *N. caninum* with nearly 60 fold change in CXCL2 and more than 30 fold increase in IL8. It was intriguing that although all these chemokines were mainly

associated with neutrophil migration to sites of inflammation, differences were observed in their secretions. This may suggest that additional functions may be associated with this family of chemokines, or that *T. gondii* is delaying increased induction of these chemokines for its benefit to establish itself in the brain. These key findings in chemokine and CAM protein differences in expression profiles clearly demonstrate the importance in studying the cells secreted proteins, which was not detected in the proteome study of host cells (chapter four).

When comparing transcriptome analysis of infected astrocytes with the secretome analysis, similarities in expression profiles of certain molecules were found. For instance, IL8 and CXCL2 were up-regulated in both the mRNA and the secretome analysis of astrocytes infected with *N. caninum* compared to *T. gondii*. Also, CCL2 and VCAM1 were up regulated in both analysis of astrocytes infected with *T. gondii*. These changes were also not detected in host proteome analysis during infection (chapter four). On the other hand, there were some differences found between both studies; such as CXCL1 that was transcriptionally up-regulated in astrocytes infected with *N. caninum* compared to *T. gondii* infected cells. Whereas CXCL1 in the secretome data was up-regulated in astrocytes infected with *T. gondii* compared to *N. caninum* infection.

Another key investigation in this thesis was the examination of neurotransmitter stimulation through dopamine production in neural cells during infection with both parasites.

In chapter six, the study aimed to compare dopamine induction in neural host cells infected with the *N. caninum* bradyzoite cyst stage to infected cells with *T. gondii* cysts. The results in this chapter supports the hypothesis that *N. caninum* will not induce dopamine production in neural infected cells compared to the findings in cells infected with *T. gondii*. Previous work has already shown the ability of *T. gondii* to increase dopamine production in the brain both *in vivo* and *in vitro* (Gaskell et al. 2009; Prandovszky et al. 2011). This suggested the possible role of dopamine induction in chronically infected mice with *T. gondii* to behavioural changes of the host. This study found that rodents were more attracted to their predator's (the cat) odour for the parasites advantage to continue its life cycle (through the cat mouse cycle) (Berdoy et al. 2000; Kaushik et al. 2012). It has also been linked to other diseases of the CNS in humans such as schizophrenia (Carlsson 1988; Howes & Kapur 2009).

It has been hypothesised that reduced virulence is associated with the evolution of vertical transmission in viruses (Stewart, Logsdon & Kelley 2005). Moreover, speciation of *N. caninum* and *T. gondii* was estimated to have occurred 28 million years ago after the divergence of their respective definitive hosts, the cat and dog. This may be related to findings associated with dopamine induction differences observed between *T. gondii* and *N. caninum*. The identification of ROP18; a secretory gene known to be associated with virulence in *T. gondii* was found to be a pseudo gene in *N. caninum* (Reid *et al*., 2012) may also be associated with host behavioural outcome. The loss of ROP18 function in *N. caninum* may signify the fact that the wide range in intermediate host species are less important to *N. caninum*, and the importance of the cat-mouse cycle in the epidemiology of *T. gondii* may explain the necessity of ROP18-mediated inactivation of immunity-related GTPases (IRG) in mice (Reid et al. 2012). The expansion of antigen proteins in *N. caninum* compared to *T. gondii* may also propose that *N. caninum* has become more specialized in its host range, and is known to be successfully transmitted through the vertical route in cattle. Thus, *N. caninum* does not need to alter or induce dopamine production in host cells in the CNS during infection compared to *T. gondii*.

7.1 Future perspectives

Continuing the research in this thesis, a deeper comparative investigation of astrocyte infection with *T. gondii* and *N. caninum* can be further expanded in many ways. Proteomic analysis between virulent and less virulent strains of *T. gondii* and *N. caninum* in astrocytes will assist in comparative analysis and differences pathogen outcome in host cell responses in association with the parasite strain. Neurons are also important cells of the CNS, the comparison of both transcriptomic and proteomic expression of these cells alongside astrocytes during *T. gondii* and *N. caninum* infection would provide valuable insights in differences related to infection and disease contributions in the CNS. This can be applied through immune studies *in vivo* on mouse model infections alongside the use of primary cell lines *in vitro*.

The latent stage of infection is an important stage to explore as it can be found in both immune competent and immune supressed hosts. In the latter, reactivation of the

bradyzoites to tachyzoites can result in severe TE or even death in *T. gondii* infections (Luft & Chua 2000). Therefore, observations in expression changes *in vivo* in different mouse strains, susceptible and resistant to infection can deliver valuable knowledge to both the biological and clinical aspects of brain infection and pathogenesis.

Further confirmation of the expression of key molecules identified at the transcriptional and proteomic level will enlighten further detailed studies. Functional investigations of key molecule findings in this thesis; such as cytokine and cell adhesion molecules through host RNA-interference (RNAi) silencing of certain molecules (such as VCAM1 and CCL2) in host cells could enable the determination of why changes in these cells occur. The application of knockout genes in tachyzoites; such as ROP18 proteins related to virulence can be applied to compare between *N. caninum* and *T. gondii* in response to the possible involvement of this gene in neural cell modulations or vice versa through knock-in gene of ROP18 in *N. caninum* tachyzoites.

Finally, transmigration adhesion assays involves the migration of cells across the endothelium. This can be applied through the use of BBB *in vitro* models and 3D well models to assist in the validation of infected astrocytes in the migration of leukocytes that can highlight significant changes that may be observed inside the host's brain. Neutrophil assays can be used in astrocyte conditioned media to explore the differences in cytokines associated with neutrophil activation identified between the two infections. As neutrophil activation (such as IL8 and CXCL2) was detected to be up-regulated in host cells infected with *N. caninum* compared to *T. gondii* infected cells in both transcriptome and secretome investigations.

7.2 Conclusions

Overall, this work provided the first large scale transcriptomic and proteomic profiling of human astrocytes infected with *T. gondii* and *N. caninum* tachyzoites and significantly increased the knowledge of host cell response during parasitic infection in the CNS. State of the art techniques in transcriptomic and proteomic approaches identified and quantified

global expression changes occurring in human astrocytes during infection. Two different proteomic techniques have been used; gel-based and non-gel based methods were applied to characterize the proteome of infected host cells. The results have aided the identification of differences in host cell proteins during infection with *T. gondii* compared to *N. caninum* in chemokine and cell adhesion molecules (CCL2, CXCL2, ICAM1 and VCAM1) and the identification of differences in the expression and regulation of molecules related to immune responses and cell signalling processes. Transcriptional analysis identified differences in key molecules in metabolic pathways between infected cells, such as cytokine and CAM metabolic pathways. Changes in dopamine secretion in dopaminergic cells infected with *N. caninum* compared to *T. gondii* showed no significant increase in dopamine production, which may suggest that *N. caninum* does not alter behaviour changes in the intermediate hosts brain. This study has provided new insights in differences between these closely related parasites toward host manipulation and specifically in dopamine secretion in the brain.

References

Abe, C., Tanaka, S., Ihara, F. & Nishikawa, Y. (2014) 'Macrophage depletion prior to Neospora caninum infection results in severe neosporosis in mice', *Clin Vaccine Immunol*, vol. 21, no. 8, pp. 1185-1188.

Adams, D.H. & Lloyd, A.R. (1997) 'Chemokines: leucocyte recruitment and activation cytokines', *Lancet*, vol. 349, no. 9050, pp. 490-495.

Aebersold, R. & Mann, M. (2003) 'Mass spectrometry-based proteomics', *Nature*, vol. 422, no. 6928, pp. 198-207.

Ainscow, E. K. & Brand, M.D. (1999) 'Internal regulation of ATP turnover, glycolysis and oxidative phosphorylation in rat hepatocytes', *Eur J Biochem*, vol. 266, pp. 737-749.

Al-Anouti, F., Tomavo, S., Parmley, S. & Ananvoranich, S. (2004) 'The expression of lactate dehydrogenase is important for the cell cycle of Toxoplasma gondii', *J Biol Chem*, vol. 279, no. 50, pp. 52300-52311.

Alban, A., David, S.O., Bjorkesten, L., Andersson, C., Sloge, E., Lewis, S. & Currie, I. (2003) 'A novel experimental design for comparative two-dimensional gel analysis: two-dimensional difference gel electrophoresis incorporating a pooled internal standard', *Proteomics*, vol. 3, no. 1, pp. 36-44.

AlKurashi, M., Eastick, F.A., Kuchipudi, S.V., Rauch, C., Madouasse, A., Zhu, X.Q. & Elsheikha, H.M. (2011) 'Influence of culture medium pH on internalization, growth and phenotypic plasticity of Neospora caninum', *Vet Parasitol*, vol. 177, no. 3-4, pp. 267-274.

Amichay, D., Gazzinelli, R.T., Karupiah, G., Moench, T.R., Sher, A. & Farber, J.M. (1996) 'Genes for chemokines MuMig and Crg-2 are induced in protozoan and viral infections in response to IFN-gamma with patterns of tissue expression that suggest nonredundant roles in vivo', *J Immunol*, vol. 157, no. 10, pp. 4511-4520.

Amzallag, N., Passer, B.J., Allanic, D., Segura, E., Thery, C., Goud, B., Amson, R. & Telerman, A. (2004) 'TSAP6 facilitates the secretion of translationally controlled tumor protein/histamine-releasing factor via a nonclassical pathway', *J Biol Chem*, vol. 279, no. 44, pp. 46104-46112.

An, E., Sen, S., Park, S.K., Gordish-Dressman, H. & Hathout, Y. (2010) 'Identification of novel substrates for the serine protease HTRA1 in the human RPE secretome', *Invest Ophthalmol Vis Sci*, vol. 51, no. 7, pp. 3379-3386.

Annunen-Rasila, J., Ohlmeier, S., Tuokko, H., Veijola, J. & Majamaa, K. (2007) 'Proteome and cytoskeleton responses in osteosarcoma cells with reduced OXPHOS activity', *Proteomics*, vol. 7, pp. 2189–2200.

Antelmann, H., Tjalsma, H., Voigt, B., Ohlmeier, S., Bron, S., van Dijl, J.M. & Hecker, M. (2001) 'A proteomic view on genome-based signal peptide predictions', *Genome Res*, vol. 11, no. 9, pp. 1484-1502.

Antony, J.M., van Marle, G., Opii, W., Butterfield, D.A., Mallet, F., Yong, V.W., Wallace, J.L., Deacon, R.M., Warren, K. & Power, C. (2004) 'Human endogenous retrovirus glycoprotein-mediated induction of redox reactants causes oligodendrocyte death and demyelination', *Nat Neurosci*, vol. 7, no. 10, pp. 1088-1095.

Arendt, G., von Giesen, H.J., Hefter, H., Neuen-Jacob, E., Roick, H. & Jablonowski, H. (1999) 'Long-term course and outcome in AIDS patients with cerebral toxoplasmosis', *Acta Neurol Scand*, vol. 100, no. 3, pp. 178-184.

Askonas, B.A. (1975) 'Immunoglobulin formation in B lymphoid cells', *J Clin Pathol Suppl (Assoc Clin Pathol)*, vol. 6, pp. 8-12.

Atluri, V.S., Kanthikeel, S.P., Reddy, P.V., Yndart, A. & Nair, M.P. (2013) 'Human synaptic plasticity gene expression profile and dendritic spine density changes in HIV-infected human CNS cells: role in HIV-associated neurocognitive disorders (HAND)', *PLoS One*, vol. 8, no. 4, p. e61399.

Bachoo, R.M., Kim, R.S., Ligon, K.L., Maher, E.A., Brennan, C., Billings, N., Chan, S., Li, C., Rowitch, D.H., Wong, W.H. & DePinho, R.A. (2004) 'Molecular diversity of astrocytes with implications for neurological disorders', *Proc Natl Acad Sci U S A*, vol. 101, no. 22, pp. 8384-8389.

Backman, L., Lindenberger, U., Li, S.C. & Nyberg, L. (2010) 'Linking cognitive aging to alterations in dopamine neurotransmitter functioning: recent data and future avenues', *Neurosci Biobehav Rev*, vol. 34, no. 5, pp. 670-677.

Bajetto, A., Bonavia, R., Barbero, S., Florio, T. & Schettini, G. (2001) 'Chemokines and their receptors in the central nervous system', *Front Neuroendocrinol*, vol. 22, no. 3, pp. 147-184.

Bammler, T., Beyer, R.P., Bhattacharya, S., Boorman, G.A., Boyles, A., Bradford, B.U., Bumgarner, R.E., Bushel, P.R., Chaturvedi, K., Choi, D., Cunningham, M.L., Deng, S., Dressman, H.K., Fannin, R.D., Farin, F.M., Freedman, J.H., Fry, R.C., Harper, A., Humble, M.C., Hurban, P., Kavanagh, T.J., Kaufmann, W.K., Kerr, K.F., Jing, L., Lapidus, J.A., Lasarev, M.R., Li, J., Li, Y.J., Lobenhofer, E.K., Lu, X., Malek, R.L., Milton, S., Nagalla, S.R., O'Malley J, P., Palmer, V.S., Pattee, P., Paules, R.S., Perou, C.M., Phillips, K., Qin, L.X., Qiu, Y., Quigley, S.D., Rodland, M., Rusyn, I., Samson, L.D., Schwartz, D.A., Shi, Y., Shin, J.L., Sieber, S.O., Slifer, S., Speer, M.C., Spencer, P.S., Sproles, D.I., Swenberg, J.A., Suk, W.A., Sullivan, R.C., Tian, R., Tennant, R.W., Todd, S.A., Tucker, C.J., Van Houten, B., Weis, B.K., Xuan, S. & Zarbl, H. (2005) 'Standardizing global gene expression analysis between laboratories and across platforms', *Nat Methods*, vol. 2, no. 5, pp. 351-356.

Banks, W.A., Kastin, A.J. & Gutierrez, E.G. (1994) 'Penetration of interleukin-6 across the murine blood-brain barrier', *Neurosci Lett*, vol. 179, no. 1-2, pp. 53-56.

Bannister, L.H., Hopkins, J.M., Dluzewski, A.R., Margos, G., Williams, I.T., Blackman, M.J., Kocken, C.H., Thomas, A.W. & Mitchell, G.H. (2003) 'Plasmodium falciparum apical membrane antigen 1 (PfAMA-1) is translocated within micronemes along subpellicular microtubules during merozoite development', *J Cell Sci*, vol. 116, no. Pt 18, pp. 3825-3834.

Barber, J.S. & Trees, A.J. (1998) 'Naturally occuring vertical transmission of Neospora caninum in dogs', *International Journal for Parasitology*, vol. 28, pp. 57-64.

Barnard, C. J. (1990) 'Parasitic relationships'. In Parasitism and host behaviour (ed. C. J. Barnard & J. M. Behnke), pp.1–33. London, UK: Taylor & Francis.

Barr, B.C., Anderson, M.L., Dubey, J.P. & Conrad, P.A. (1991a) 'Neospora-like protozoal infections associated with bovine abortions', *Vet Pathol*, vol. 28, no. 2, pp. 110-116.

Barr, B.C., Conrad, P.A., Dubey, J.P. & Anderson, M.L. (1991b) 'Neospora-like encephalomyelitis in a calf: pathology, ultrastructure, and immunoreactivity', *J Vet Diagn Invest*, vol. 3, no. 1, pp. 39-46.

Barragan, A., Brossier, F. & Sibley, L.D. (2005) 'Transepithelial migration of Toxoplasma gondii involves an interaction of intercellular adhesion molecule 1 (ICAM-1) with the parasite adhesin MIC2', *Cell Microbiol*, vol. 7, no. 4, pp. 561-568.

Bartsch, U. (2003) 'Neural CAMS and their role in the development and organization of myelin sheaths', *Front Biosci*, vol. 8, pp. d477-490.

Basch, M.L., Garcia-Castro, M.I. & Bronner-Fraser, M. (2004) 'Molecular mechanisms of neural crest induction', *Birth Defects Res C Embryo Today*, vol. 72, no. 2, pp. 109-123.

Baum J., Papenfuss A. T., Baum B., Speed T. P. & Cowman A. F. (2006) 'Regulation of apicomplexan actin-based motility', *Nat Rev Microbiol*, vol. 4, pp. 621–628.

Beckers, C.J., Dubremetz, J.F., Mercereau-Puijalon, O. & Joiner, K.A. (1994) 'The Toxoplasma gondii rhoptry protein ROP 2 is inserted into the parasitophorous vacuole membrane, surrounding the intracellular parasite, and is exposed to the host cell cytoplasm', *J Cell Biol*, vol. 127, no. 4, pp. 947-961.

Beiting, D.P., Peixoto, L., Akopyants, N.S., Beverley, S.M., Wherry, E.J., Christian, D.A., Hunter, C.A., Brodsky, I.E. & Roos, D.S. (2014) 'Differential induction of TLR3-dependent innate immune signaling by closely related parasite species', *PLoS One*, vol. 9, no. 2, p. e88398.

Bendtsen, J.D., Kiemer, L., Fausboll, A. & Brunak, S. (2005) 'Non-classical protein secretion in bacteria', *BMC Microbiol*, vol. 5, p. 58.

Bennett, S.T., Barnes, C., Cox, A., Davies, L. & Brown, C. (2005) 'Toward the 1,000 dollars human genome', *Pharmacogenomics*, vol. 6, no. 4, pp. 373-382.

Bennuru, S., Meng, Z., Ribeiro, J.M., Semnani, R.T., Ghedin, E., Chan, K., Lucas, D.A., Veenstra, T.D. & Nutman, T.B. (2011) 'Stage-specific proteomic expression patterns of the human filarial parasite Brugia malayi and its endosymbiont Wolbachia', *Proc Natl Acad Sci U S A*, vol. 108, no. 23, pp. 9649-9654.

Bentaib, A., De Tullio, P., Chneiweiss, H., Hermans, E., Junier, M.P. & Leprince, P. (2014) 'Metabolic reprogramming in transformed mouse cortical astrocytes: a proteomic study', *J Proteomics*.

Bentley, D.R., Balasubramanian, S., Swerdlow, H.P., Smith, G.P., Milton, J., Brown, C.G., Hall, K.P., Evers, D.J., Barnes, C.L., Bignell, H.R., Boutell, J.M., Bryant, J., Carter, R.J., Keira Cheetham, R., Cox, A.J., Ellis, D.J., Flatbush, M.R., Gormley, N.A., Humphray, S.J., Irving, L.J., Karbelashvili, M.S., Kirk, S.M., Li, H., Liu, X., Maisinger, K.S., Murray, L.J., Obradovic, B., Ost, T., Parkinson, M.L., Pratt, M.R., Rasolonjatovo, I.M., Reed, M.T., Rigatti, R., Rodighiero, C., Ross, M.T., Sabot, A., Sankar, S.V., Scally, A., Schroth, G.P., Smith, M.E., Smith, V.P., Spiridou, A., Torrance, P.E., Tzonev, S.S., Vermaas, E.H., Walter, K., Wu, X., Zhang, L., Alam, M.D., Anastasi, C., Aniebo, I.C., Bailey, D.M., Bancarz, I.R., Banerjee, S., Barbour, S.G., Baybayan, P.A., Benoit, V.A., Benson, K.F., Bevis, C., Black, P.J., Boodhun, A., Brennan, J.S., Bridgham, J.A., Brown, R.C., Brown, A.A., Buermann, D.H., Bundu, A.A., Burrows, J.C., Carter, N.P., Castillo, N., Chiara, E.C.M., Chang, S., Neil Cooley, R., Crake, N.R., Dada, O.O., Diakoumakos, K.D., Dominguez-Fernandez, B., Earnshaw, D.J., Egbujor, U.C., Elmore, D.W., Etchin, S.S., Ewan, M.R., Fedurco, M., Fraser, L.J., Fuentes Fajardo, K.V., Scott Furey, W., George, D., Gietzen, K.J., Goddard, C.P., Golda, G.S., Granieri, P.A., Green, D.E., Gustafson, D.L., Hansen, N.F., Harnish, K., Haudenschild, C.D., Heyer, N.I., Hims, M.M., Ho, J.T., Horgan, A.M., Hoschler, K., Hurwitz, S., Ivanov, D.V., Johnson, M.Q., James, T., Huw Jones, T.A., Kang, G.D., Kerelska, T.H., Kersey, A.D., Khrebtukova, I., Kindwall, A.P., Kingsbury, Z., Kokko-Gonzales, P.I., Kumar, A., Laurent, M.A., Lawley, C.T., Lee, S.E., Lee, X., Liao, A.K., Loch, J.A., Lok, M., Luo, S., Mammen, R.M., Martin, J.W., McCauley, P.G., McNitt, P., Mehta, P., Moon, K.W., Mullens, J.W., Newington, T., Ning, Z., Ling Ng, B., Novo, S.M., O'Neill, M.J., Osborne, M.A., Osnowski, A., Ostadan, O., Paraschos, L.L., Pickering, L., Pike, A.C., Chris Pinkard, D., Pliskin, D.P., Podhasky, J., Quijano, V.J., Raczy, C., Rae, V.H., Rawlings, S.R., Chiva Rodriguez, A., Roe, P.M., Rogers, J., Rogert Bacigalupo, M.C., Romanov, N., Romieu, A., Roth, R.K., Rourke, N.J., Ruediger, S.T., Rusman, E., Sanches-Kuiper, R.M., Schenker, M.R., Seoane, J.M., Shaw, R.J., Shiver, M.K., Short, S.W., Sizto, N.L., Sluis, J.P., Smith, M.A., Ernest Sohna Sohna, J., Spence, E.J., Stevens, K., Sutton, N., Szajkowski, L., Tregidgo, C.L., Turcatti, G., Vandevondele, S., Verhovsky, Y., Virk, S.M., Wakelin, S., Walcott, G.C., Wang, J., Worsley, G.J., Yan, J., Yau, L., Zuerlein, M., Mullikin, J.C., Hurles, M.E., McCooke, N.J., West, J.S., Oaks, F.L., Lundberg, P.L., Klenerman, D., Durbin, R. & Smith, A.J. (2008) 'Accurate whole human genome sequencing using reversible terminator chemistry', *Nature*, vol. 456, no. 7218, pp. 53-59.

Berdoy, M., Webster, J.P. & Macdonald, D.W. (1995) 'Parasite-altered behaviour: is the effect of Toxoplasma gondii on Rattus norvegicus specific?', *Parasitology*, vol. 111 (Pt 4), pp. 403-409.

Berdoy, M., Webster, J.P. & Macdonald, D.W. (2000) 'Fatal attraction in rats infected with Toxoplasma gondii', *Proc Biol Sci*, vol. 267, no. 1452, pp. 1591-1594.

Berenreiterova, M., Flegr, J., Kubena, A.A. & Nemec, P. (2011) 'The distribution of Toxoplasma gondii cysts in the brain of a mouse with latent toxoplasmosis: implications for the behavioural manipulation hypothesis', *PLoS One*, vol. 6, no. 12, p. e28925.

Besteiro, S., Michelin, A., Poncet, J., Dubremetz, J.F. & Lebrun, M. (2009) 'Export of a Toxoplasma gondii rhoptry neck protein complex at the host cell membrane to form the moving junction during invasion', *PLoS Pathog*, vol. 5, no. 2, p. e1000309.

Bjerkas, I., Mohn, S.F. & Presthus, J. (1984) 'Unidentified cyst-forming sporozoon causing encephalomyelitis and myositis in dogs', *Z Parasitenkd*, vol. 70, no. 2, pp. 271-274.

Blader, I.J. & Saeij, J.P. (2009) 'Communication between Toxoplasma gondii and its host: impact on parasite growth, development, immune evasion, and virulence', *Apmis*, vol. 117, no. 5-6, pp. 458-476.

Blader, I.J., Manger, I.D. & Boothroyd, J.C. (2001) 'Microarray analysis reveals previously unknown changes in Toxoplasma gondii-infected human cells', *J Biol Chem*, vol. 276, no. 26, pp. 24223-24231.

Blasi, E., Barluzzi, R., Mazzolla, R., Pitzurra, L., Puliti, M., Saleppico, S. & Bistoni, F. (1995) 'Biomolecular events involved in anticryptococcal resistance in the brain', *Infect Immun*, vol. 63, no. 4, pp. 1218-1222.

Blume, M., Rodriguez-Contreras, D., Landfear, S., Fleige, T., Soldati-Favre, D., Lucius, R. & Gupta, N. (2009) 'Host-derived glucose and its transporter in the obligate intracellular pathogen Toxoplasma gondii are dispensable by glutaminolysis', *Proc Natl Acad Sci U S A*, vol. 106, no. 31, pp. 12998-13003.

Bohne, W. & Roos, D.S. (1997) 'Stage-specific expression of a selectable marker in Toxoplasma gondii permits selective inhibition of either tachyzoites or bradyzoites', *Mol Biochem Parasitol*, vol. 88, no. 1-2, pp. 115-126.

Bondarenko, P.V., Chelius, D. & Shaler, T.A. (2002) 'Identification and relative quantitation of protein mixtures by enzymatic digestion followed by capillary reversed-phase liquid chromatography-tandem mass spectrometry', *Anal Chem*, vol. 74, no. 18, pp. 4741-4749.

Bradley, P.J., Ward, C., Cheng, S.J., Alexander, D.L., Coller, S., Coombs, G.H., Dunn, J.D., Ferguson, D.J., Sanderson, S.J., Wastling, J.M. & Boothroyd, J.C. (2005) 'Proteomic analysis of rhoptry organelles reveals many novel constituents for host-parasite interactions in Toxoplasma gondii', *J Biol Chem*, vol. 280, no. 40, pp. 34245-34258.

Brawand, D., Soumillon, M., Necsulea, A., Julien, P., Csardi, G., Harrigan, P., Weier, M., Liechti, A., Aximu-Petri, A., Kircher, M., Albert, F.W., Zeller, U., Khaitovich, P., Grutzner, F., Bergmann, S., Nielsen, R., Paabo, S. & Kaessmann, H. (2011) 'The evolution of gene expression levels in mammalian organs', *Nature*, vol. 478, no. 7369, pp. 343-348.

Brenier-Pinchart, M.P., Blanc-Gonnet, E., Marche, P.N., Berger, F., Durand, F., Ambroise-Thomas, P. & Pelloux, H. (2004) 'Infection of human astrocytes and glioblastoma cells with Toxoplasma gondii: monocyte chemotactic protein-1 secretion and chemokine expression in vitro', *Acta Neuropathol*, vol. 107, no. 3, pp. 245-249.

Brenier-Pinchart, M.P., Pelloux, H., Simon, J., Ricard, J., Bosson, J.L. & Ambroise-Thomas, P. (2000) 'Toxoplasma gondii induces the secretion of monocyte chemotactic protein-1 in human fibroblasts, in vitro', *Mol Cell Biochem*, vol. 209, no. 1-2, pp. 79-87.

Brenier-Pinchart, M.P., Vigan, I., Jouvin-Marche, E., Marche, P.N., Pelet, E., Gross, U., Ambroise-Thomas, P. & Pelloux, H. (2002) 'Monocyte chemotactic protein-1 secretion and expression after Toxoplasma gondii infection in vitro depend on the stage of the parasite', *FEMS Microbiol Lett*, vol. 214, no. 1, pp. 45-49.

Brenner, S., Johnson, M., Bridgham, J., Golda, G., Lloyd, D.H., Johnson, D., Luo, S., McCurdy, S., Foy, M., Ewan, M., Roth, R., George, D., Eletr, S., Albrecht, G., Vermaas, E., Williams, S.R., Moon, K., Burcham, T., Pallas, M., DuBridge, R.B., Kirchner, J., Fearon, K., Mao, J. & Corcoran, K. (2000) 'Gene expression analysis by massively parallel signature sequencing (MPSS) on microbead arrays', *Nat Biotechnol*, vol. 18, no. 6, pp. 630-634.

Breviario, F., d'Aniello, E.M., Golay, J., Peri, G., Bottazzi, B., Bairoch, A., Saccone, S., Marzella, R., Predazzi, V., Rocchi, M. & et al. (1992) 'Interleukin-1-inducible genes in endothelial cells. Cloning of a new gene related to C-reactive protein and serum amyloid P component', *J Biol Chem*, vol. 267, no. 31, pp. 22190-22197.

Brey, R.N. (2005) 'Molecular basis for improved anthrax vaccines', *Adv Drug Deliv Rev*, vol. 57, no. 9, pp. 1266-1292.

Brooks, G.A. (2002) 'Lactate shuttles in nature', *Biochem Soc Trans*, vol. 30, no. 2, pp. 258-264.

Brown, K.J., Formolo, C.A., Seol, H., Marathi, R.L., Duguez, S., An, E., Pillai, D., Nazarian, J., Rood, B.R. & Hathout, Y. (2012) 'Advances in the proteomic investigation of the cell secretome', *Expert Rev Proteomics*, vol. 9, no. 3, pp. 337-345.

Brumlik, M.J., Pandeswara, S., Ludwig, S.M., Jeansonne, D.P., Lacey, M.R., Murthy, K., Daniel, B.J., Wang, R.F., Thibodeaux, S.R., Church, K.M., Hurez, V., Kious, M.J., Zhang, B., Alagbala, A., Xia, X. & Curiel, T.J. (2013) 'TgMAPK1 is a Toxoplasma gondii MAP kinase that hijacks host MKK3 signals to regulate virulence and interferon-gamma-mediated nitric oxide production', *Exp Parasitol*, vol. 134, no. 3, pp. 389-399.

Buache, E., Garnotel, R., Aubert, D., Gillery, P. & Villena, I. (2007) 'Reduced secretion and expression of gelatinase profile in Toxoplasma gondii-infected human monocytic cells', *Biochem Biophys Res Commun*, vol. 359, no. 2, pp. 298-303.

Burke, S.M., Issekutz, T.B., Mohan, K., Lee, P.W., Shmulevitz, M. & Marshall, J.S. (2008) 'Human mast cell activation with virus-associated stimuli leads to the selective chemotaxis of natural killer cells by a CXCL8-dependent mechanism', *Blood*, vol. 111, no. 12, pp. 5467-5476.

Buxton, D., McAllister, M.M. & Dubey, J.P. (2002) 'The comparative pathogenesis of neosporosis', *Trends Parasitol*, vol. 18, no. 12, pp. 546-552.

Camoretti-Mercado, B., Forsythe, S.M., LeBeau, M.M., Espinosa, R., 3rd, Vieira, J.E., Halayko, A.J., Willadsen, S., Kurtz, B., Ober, C., Evans, G.A., Thweatt, R., Shapiro, S., Niu, Q., Qin, Y., Padrid, P.A. & Solway, J. (1998) 'Expression and cytogenetic localization of the human SM22 gene (TAGLN)', *Genomics*, vol. 49, no. 3, pp. 452-457.

Carlsson, A. (1988) 'The current status of the dopamine hypothesis of schizophrenia', *Neuropsychopharmacology*, vol. 1, no. 3, pp. 179-186.

Carman, C.V. & Springer, T.A. (2004) 'A transmigratory cup in leukocyte diapedesis both through individual vascular endothelial cells and between them', *J Cell Biol*, vol. 167, no. 2, pp. 377-388.

Carruthers, V.B. & Suzuki, Y. (2007) 'Effects of Toxoplasma gondii infection on the brain', *Schizophr Bull*, vol. 33, no. 3, pp. 745-751.

Carruthers, V.B. (2006) 'Proteolysis and Toxoplasma invasion', *Int J Parasitol*, vol. 36, no. 5, pp. 595-600.

Carter, C.J. (2009) 'Schizophrenia susceptibility genes directly implicated in the life cycles of pathogens: cytomegalovirus, influenza, herpes simplex, rubella, and Toxoplasma gondii', *Schizophr Bull*, vol. 35, no. 6, pp. 1163-1182.

Carvalho, J.V., Alves, C.M., Cardoso, M.R., Mota, C.M., Barbosa, B.F., Ferro, E.A., Silva, N.M., Mineo, T.W., Mineo, J.R. & Silva, D.A. (2010) 'Differential susceptibility of human trophoblastic (BeWo) and uterine cervical (HeLa) cells to Neospora caninum infection', *Int J Parasitol*, vol. 40, no. 14, pp. 1629-1637.

Cassina, P., Pehar, M., Vargas, M.R., Castellanos, R., Barbeito, A.G., Estevez, A.G., Thompson, J.A., Beckman, J.S. & Barbeito, L. (2005) 'Astrocyte activation by fibroblast growth factor-1 and motor neuron apoptosis: implications for amyotrophic lateral sclerosis', *J Neurochem*, vol. 93, no. 1, pp. 38-46.

Catts, V.S., Wong, J., Fillman, S.G., Fung, S.J. & Shannon Weickert, C. (2014) 'Increased expression of astrocyte markers in schizophrenia: Association with neuroinflammation', *Aust N Z J Psychiatry*, vol. 48, no. 8, pp. 722-734.

Charron, A. J. & Sibley, L. D. (2002) 'Host cells: Mobilizable lipid resources for the intracellular parasite Toxoplasma gondii', *Journal of Cell Science*, vol. 115, pp. 3049–3059.

Chaussabel, D., Semnani, R.T., McDowell, M.A., Sacks, D., Sher, A. & Nutman, T.B. (2003) 'Unique gene expression profiles of human macrophages and dendritic cells to phylogenetically distinct parasites', *Blood*, vol. 102, no. 2, pp. 672-681.

Chen, H.L., Seol, H., Brown, K.J., Gordish-Dressman, H., Hill, A., Gallo, V., Packer, R. & Hathout, Y. (2012) 'Secretome Survey of Human Plexiform Neurofibroma Derived Schwann Cells Reveals a Secreted form of the RARRES1 Protein', *Int J Mol Sci*, vol. 13, no. 7, pp. 9380-9399.

Chen, Y., Yu, P., Luo, J. & Jiang, Y. (2003) 'Secreted protein prediction system combining CJ-SPHMM, TMHMM, and PSORT', *Mamm Genome*, vol. 14, no. 12, pp. 859-865.

Chen, Y., Zhang, Y., Yin, Y., Gao, G., Li, S., Jiang, Y., Gu, X. & Luo, J. (2005) 'SPD--a web-based secreted protein database', *Nucleic Acids Res*, vol. 33, no. Database issue, pp. D169-173.

Choi, S.S., Lee, H.J., Lim, I., Satoh, J. & Kim, S.U. (2014) 'Human astrocytes: secretome profiles of cytokines and chemokines', *PLoS One*, vol. 9, no. 4, p. e92325.

Chothia, C. & Jones, E.Y. (1997) 'The molecular structure of cell adhesion molecules', *Annu Rev Biochem*, vol. 66, pp. 823-862.

Christersdottir Bjorklund, T., Reilly, S.J., Gahm, C., Bottazzi, B., Mantovani, A., Tornvall, P. & Halle, M. (2013) 'Increased long-term expression of pentraxin 3 in irradiated human arteries and veins compared to internal controls from free tissue transfers', *J Transl Med*, vol. 11, p. 223.

Clark, H.F., Gurney, A.L., Abaya, E., Baker, K., Baldwin, D., Brush, J., Chen, J., Chow, B., Chui, C., Crowley, C., Currell, B., Deuel, B., Dowd, P., Eaton, D., Foster, J., Grimaldi, C., Gu, Q., Hass, P.E., Heldens, S., Huang, A., Kim, H.S., Klimowski, L., Jin, Y., Johnson, S., Lee, J., Lewis, L., Liao, D., Mark, M., Robbie, E., Sanchez, C., Schoenfeld, J., Seshagiri, S., Simmons, L., Singh, J., Smith, V., Stinson, J., Vagts, A., Vandlen, R., Watanabe, C., Wieand, D., Woods, K., Xie, M.H., Yansura, D., Yi, S., Yu, G., Yuan, J., Zhang, M., Zhang, Z., Goddard, A., Wood, W.I., Godowski, P. & Gray, A. (2003) 'The secreted protein discovery initiative (SPDI), a large-scale effort to identify novel human secreted and transmembrane proteins: a bioinformatics assessment', *Genome Res*, vol. 13, no. 10, pp. 2265-2270.

Clark, R.T., Nance, J.P., Noor, S. & Wilson, E.H. (2011) 'T-cell production of matrix metalloproteinases and inhibition of parasite clearance by TIMP-1 during chronic Toxoplasma infection in the brain', *ASN Neuro*, vol. 3, no. 1, p. e00049.

Cohen-Freue, G., Holzer, T.R., Forney, J.D. & McMaster, W.R. (2007) 'Global gene expression in Leishmania', *Int J Parasitol*, vol. 37, no. 10, pp. 1077-1086.

Coisne, C., Faveeuw, C., Delplace, Y., Dehouck, L., Miller, F., Cecchelli, R. & Dehouck, B. (2006) 'Differential expression of selectins by mouse brain capillary endothelial cells in vitro in response to distinct inflammatory stimuli', *Neurosci Lett*, vol. 392, no. 3, pp. 216-220.

Collantes-Fernandez, E., Arrighi, R.B., Alvarez-Garcia, G., Weidner, J.M., Regidor-Cerrillo, J., Boothroyd, J.C., Ortega-Mora, L.M. & Barragan, A. (2012) 'Infected dendritic cells facilitate systemic dissemination and transplacental passage of the obligate intracellular parasite Neospora caninum in mice', *PLoS One*, vol. 7, no. 3, p. e32123.

Coppens, I., Dunn, J.D., Romano, J.D., Pypaert, M., Zhang, H., Boothroyd, J.C. & Joiner, K.A. (2006) 'Toxoplasma gondii sequesters lysosomes from mammalian hosts in the vacuolar space', *Cell*, vol. 125, no. 2, pp. 261-274.

Courret, N., Darche, S., Sonigo, P., Milon, G., Buzoni-Gatel, D. & Tardieux, I. (2006) 'CD11c- and CD11b-expressing mouse leukocytes transport single Toxoplasma gondii tachyzoites to the brain', *Blood*, vol. 107, no. 1, pp. 309-316.

Craig, R. & Beavis, R.C. (2004) 'TANDEM: matching proteins with tandem mass spectra', *Bioinformatics*, vol. 20, no. 9, pp. 1466-1467.

Craig-Schapiro, R., Perrin, R.J., Roe, C.M., Xiong, C., Carter, D., Cairns, N.J., Mintun, M.A., Peskind, E.R., Li, G., Galasko, D.R., Clark, C.M., Quinn, J.F., D'Angelo, G., Malone, J.P., Townsend, R.R., Morris, J.C., Fagan, A.M. & Holtzman, D.M. (2010) 'YKL-40: a novel prognostic fluid biomarker for preclinical Alzheimer's disease', *Biol Psychiatry*, vol. 68, no. 10, pp. 903-912.

Cravatt, B.F., Simon, G.M. & Yates, J.R., 3rd (2007) 'The biological impact of mass-spectrometry-based proteomics', *Nature*, vol. 450, no. 7172, pp. 991-1000.

Crawford, M.J., Thomsen-Zieger, N., Ray, M., Schachtner, J., Roos, D.S. & Seeber, F. (2006) 'Toxoplasma gondii scavenges host-derived lipoic acid despite its de novo synthesis in the apicoplast', *Embo j*, vol. 25, no. 13, pp. 3214-3222.

Cuervo, P., Fernandes, N. & de Jesus, J.B. (2011) 'A proteomics view of programmed cell death mechanisms during host-parasite interactions', *J Proteomics*, vol. 75, no. 1, pp. 246-256.

Cutillas, P.R. & Vanhaesebroeck, B. (2007) 'Quantitative profile of five murine core proteomes using label-free functional proteomics', *Mol Cell Proteomics*, vol. 6, no. 9, pp. 1560-1573.

Da Gama, L.M., Ribeiro-Gomes, F.L., Guimaraes, U., Jr. & Arnholdt, A.C. (2004) 'Reduction in adhesiveness to extracellular matrix components, modulation of adhesion molecules and in vivo migration of murine macrophages infected with Toxoplasma gondii', *Microbes Infect*, vol. 6, no. 14, pp. 1287-1296.

Dammer, E.B., Duong, D.M., Diner, I., Gearing, M., Feng, Y., Lah, J.J., Levey, A.I. & Seyfried, N.T. (2013) 'Neuron enriched nuclear proteome isolated from human brain', *J Proteome Res*, vol. 12, no. 7, pp. 3193-3206.

de Melo, E.J., de Carvalho, T.U. & de Souza, W. (1992) 'Penetration of Toxoplasma gondii into host cells induces changes in the distribution of the mitochondria and the endoplasmic reticulum', *Cell Struct Funct*, vol. 17, no. 5, pp. 311-317.

DeBarry, J.D. & Kissinger, J.C. (2011) 'Jumbled genomes: missing Apicomplexan synteny', *Mol Biol Evol*, vol. 28, no. 10, pp. 2855-2871.

Deckert-Schluter, M., Schluter, D., Hof, H., Wiestler, O.D. & Lassmann, H. (1994) 'Differential expression of ICAM-1, VCAM-1 and their ligands LFA-1, Mac-1, CD43, VLA-4, and MHC class II antigens in murine Toxoplasma encephalitis: a light microscopic and ultrastructural immunohistochemical study', *J Neuropathol Exp Neurol*, vol. 53, no. 5, pp. 457-468.

Del Carmen, M.G., Mondragon, M., Gonzalez, S. & Mondragon, R. (2009) 'Induction and regulation of conoid extrusion in Toxoplasma gondii', *Cell Microbiol*, vol. 11, no. 6, pp. 967-982.

Delcourt, N., Jouin, P., Poncet, J., Demey, E., Mauger, E., Bockaert, J., Marin, P. & Galeotti, N. (2005) 'Difference in mass analysis using labeled lysines (DIMAL-K): a new, efficient proteomic quantification method applied to the analysis of astrocytic secretomes', *Mol Cell Proteomics*, vol. 4, no. 8, pp. 1085-1094.

Denkers, E.Y., Butcher, B.A., Del Rio, L. & Bennouna, S. (2004) 'Neutrophils, dendritic cells and Toxoplasma', *Int J Parasitology*, vol. 34, no. 3, pp. 411-421.

Denkers, E.Y., Del Rio, L. & Bennouna, S. (2003) 'Neutrophil production of IL-12 and other cytokines during microbial infection', *Chem Immunol Allergy*, vol. 83, pp. 95-114.

Denney, C.F., Eckmann, L. & Reed, S.L. (1999) 'Chemokine secretion of human cells in response to Toxoplasma gondii infection', *Infect Immun*, vol. 67, no. 4, pp. 1547-1552.

Denton, H., Brown, S.M., Roberts, C.W., Alexander, J., McDonald, V., Thong, K.W. & Coombs, G.H. (1996) 'Comparison of the phosphofructokinase and pyruvate kinase activities of Cryptosporidium parvum, Eimeria tenella and Toxoplasma gondii', *Mol Biochem Parasitol*, vol. 76, no. 1-2, pp. 23-29.

Desmonts, G. & Couvreur, J. (1974) 'Congenital toxoplasmosis. A prospective study of 378 pregnancies', *N Engl J Med*, vol. 290, no. 20, pp. 1110-1116.

Dong, C., Davis, R.J. & Flavell, R.A. (2002) 'MAP kinases in the immune response', *Annu Rev Immunol*, vol. 20, pp. 55-72.

Donovan, L.E., Higginbotham, L., Dammer, E.B., Gearing, M., Rees, H.D., Xia, Q., Duong, D.M., Seyfried, N.T., Lah, J.J. & Levey, A.I. (2012) 'Analysis of a membrane-enriched proteome from postmortem human brain tissue in Alzheimer's disease', *Proteomics Clin Appl*, vol. 6, no. 3-4, pp. 201-211.

Dowell, J.A., Johnson, J.A. & Li, L. (2009) 'Identification of astrocyte secreted proteins with a combination of shotgun proteomics and bioinformatics', *J Proteome Res*, vol. 8, no. 8, pp. 4135-4143.

Dowlati, Y., Herrmann, N., Swardfager, W., Liu, H., Sham, L., Reim, E.K. & Lanctot, K.L. (2010) 'A meta-analysis of cytokines in major depression', *Biol Psychiatry*, vol. 67, no. 5, pp. 446-457.

Dowling, P. & Clynes, M. (2011) 'Conditioned media from cell lines: a complementary model to clinical specimens for the discovery of disease-specific biomarkers', *Proteomics*, vol. 11, no. 4, pp. 794-804.

Drogemuller, K., Helmuth, U., Brunn, A., Sakowicz-Burkiewicz, M., Gutmann, D.H., Mueller, W., Deckert, M. & Schluter, D. (2008) 'Astrocyte gp130 expression is critical for the control of Toxoplasma encephalitis', *J Immunol*, vol. 181, no. 4, pp. 2683-2693.

Dubey J. P. (2007) 'The life cycle of Toxoplasma gondii'. In Toxoplasma: molecular and cellular biology (eds Ajioka J. W., Soldati D., editors), pp. 3–16 Norfolk, VA: Horizon Biosciene.

Dubey, J.P. & Jones, J.L. (2008) 'Toxoplasma gondii infection in humans and animals in the United States', *Int J Parasitol*, vol. 38, no. 11, pp. 1257-1278.

Dubey, J.P. & Lindsay, D.S. (1996) 'A review of Neospora caninum and neosporosis', *Vet Parasitol*, vol. 67, no. 1-2, pp. 1-59.

Dubey, J.P. & Schares, G. (2011) 'Neosporosis in animals--the last five years', *Vet Parasitol*, vol. 180, no. 1-2, pp. 90-108.

Dubey, J.P. (2003) 'Review of Neospora caninum and neosporosis in animals', *Korean J Parasitol*, vol. 41, no. 1, pp. 1-16.

Dubey, J.P. (2005) 'Neosporosis in Dogs', 30th World Congress of the WSAVA, Mexico City, Mexico.

Dubey, J.P., Carpenter, J.L., Speer, C.A., Topper, M.J. & Uggla, A. (1988a) 'Newly recognized fatal protozoan disease of dogs', *J Am Vet Med Assoc*, vol. 192, no. 9, pp. 1269-1285.

Dubey, J.P., Hattel, A.L., Lindsay, D.S. & Topper, M.J. (1988b) 'Neonatal Neospora caninum infection in dogs: isolation of the causative agent and experimental transmission', *J Am Vet Med Assoc*, vol. 193, no. 10, pp. 1259-1263.

Dubey, J.P., Lindsay, D.S. & Speer, C.A. (1998) 'Structures of Toxoplasma gondii tachyzoites, bradyzoites, and sporozoites and biology and development of tissue cysts', *Clin Microbiol Rev*, vol. 11, no. 2, pp. 267-299.

Dubey, J.P., Schares, G. & Ortega-Mora, L.M. (2007) 'Epidemiology and control of neosporosis and Neospora caninum', *Clin Microbiol Rev*, vol. 20, no. 2, pp. 323-367.

Dubey, J.P., Sreekumar, C., Knickman, E., Miska, K.B., Vianna, M.C., Kwok, O.C., Hill, D.E., Jenkins, M.C., Lindsay, D.S. & Greene, C.E. (2004) 'Biologic, morphologic, and molecular characterisation of Neospora caninum isolates from littermate dogs', *Int J Parasitol*, vol. 34, no. 10, pp. 1157-1167.

Dubey, J.P., Vianna, M.C., Kwok, O.C., Hill, D.E., Miska, K.B., Tuo, W., Velmurugan, G.V., Conors, M. & Jenkins, M.C. (2007) 'Neosporosis in Beagle dogs: clinical signs, diagnosis, treatment, isolation and genetic characterization of Neospora caninum', *Vet Parasitol*, vol. 149, no. 3-4, pp. 158-166.

Dubremetz, J.F., Garcia-Reguet, N., Conseil, V. & Fourmaux, M.N. (1998) 'Apical organelles and host-cell invasion by Apicomplexa', *Int J Parasitol*, vol. 28, no. 7, pp. 1007-1013.

Dunay, I.R., Fuchs, A. & Sibley, L.D. (2010) 'Inflammatory monocytes but not neutrophils are necessary to control infection with Toxoplasma gondii in mice', *Infect Immun*, vol. 78, no. 4, pp. 1564-1570.

Dustin, M.L., Rothlein, R., Bhan, A.K., Dinarello, C.A. & Springer, T.A. (1986) 'Induction by IL 1 and interferon-gamma: tissue distribution, biochemistry, and function of a natural adherence molecule (ICAM-1)', *J Immunol*, vol. 137, no. 1, pp. 245-254.

Dzierszinski, F., Nishi, M., Ouko, L. & Roos, D.S. (2004) 'Dynamics of Toxoplasma gondii differentiation', *Eukaryot Cell*, vol. 3, no. 4, pp. 992-1003.

Dzierszinski, F., Popescu, O., Toursel, C., Slomianny, C., Yahiaoui, B. & Tomavo, S. (1999) 'The protozoan parasite Toxoplasma gondii expresses two functional plant-like glycolytic enzymes. Implications for evolutionary origin of apicomplexans', *J Biol Chem*, vol. 274, no. 35, pp. 24888-24895.

El Hajj, H., Demey, E., Poncet, J., Lebrun, M., Wu, B., Galeotti, N., Fourmaux, M.N., Mercereau-Puijalon, O., Vial, H., Labesse, G. & Dubremetz, J.F. (2006) 'The ROP2 family of Toxoplasma gondii rhoptry proteins: proteomic and genomic characterization and molecular modelling', *Proteomics*, vol. 6, no. 21, pp. 5773-5784.

Elliott, M.H., Smith, D.S., Parker, C.E. & Borchers, C. (2009) 'Current trends in quantitative proteomics', *J Mass Spectrom*, vol. 44, no. 12, pp. 1637-1660.

Elsheikha, H.M., McKinlay, C.L., Elsaied, N.A. & Smith, P.A. (2013) 'Effects of Neospora caninum infection on brain microvascular endothelial cells bioenergetics', *Parasit Vectors*, vol. 6, p. 24.

Eng, J.K., McCormack, A.L. & Yates, J.R. (1994) 'An approach to correlate tandem mass spectral data of peptides with amino acid sequences in a protein database', *J Am Soc Mass Spectrom*, vol. 5, no. 11, pp. 976-989.

Ethell, I.M. & Ethell, D.W. (2007) 'Matrix metalloproteinases in brain development and remodeling: synaptic functions and targets', *J Neurosci Res*, vol. 85, no. 13, pp. 2813-2823.

Everley, P.A., Krijgsveld, J., Zetter, B.R. & Gygi, S.P. (2004) 'Quantitative cancer proteomics: stable isotope labeling with amino acids in cell culture (SILAC) as a tool for prostate cancer research', *Mol Cell Proteomics*, vol. 3, no. 7, pp. 729-735.

Fagard, R., Van Tan, H., Creuzet, C. & Pelloux, H. (1999) 'Differential development of Toxoplasma gondii in neural cells', *Parasitol Today*, vol. 15, no. 12, pp. 504-507.

Ferguson, D.J. & Dubremetz, J.F. (2007) 'The ultrastructure of Toxoplasma gondii'. In Toxoplasma gondii: the model Apicomplexan: perspectives and methods. First edition. Edited by Weiss LM, Kim K. London: Academic Press.pp. 19-48.

Ferguson, D.J. & Hutchison, W.M. (1987) 'An ultrastructural study of the early development and tissue cyst formation of Toxoplasma gondii in the brains of mice', *Parasitol Res*, vol. 73, no. 6, pp. 483-491.

Fevrier, B., Vilette, D., Archer, F., Loew, D., Faigle, W., Vidal, M., Laude, H. & Raposo, G. (2004) 'Cells release prions in association with exosomes', *Proc Natl Acad Sci U S A*, vol. 101, no. 26, pp. 9683-9688.

Fields, R.D. & Stevens-Graham, B. (2002) 'New insights into neuron-glia communication', *Science*, vol. 298, no. 5593, pp. 556-562.

Findeisen, P. & Neumaier, M. (2009) 'Mass spectrometry-based clinical proteomics profiling: current status and future directions', *Expert Rev Proteomics*, vol. 6, no. 5, pp. 457-459.

Fischer, H.G., Nitzgen, B., Reichmann, G. & Hadding, U. (1997) 'Cytokine responses induced by Toxoplasma gondii in astrocytes and microglial cells', *Eur J Immunol*, vol. 27, no. 6, pp. 1539-1548.

Flegr, J. (2007) 'Effects of toxoplasma on human behavior', *Schizophr Bull*, vol. 33, no. 3, pp. 757-760.

Flegr, J., Preiss, M., Klose, J., Havlicek, J., Vitakova, M. & Kodym, P. (2003) 'Decreased level of psychobiological factor novelty seeking and lower intelligence in men latently infected with the protozoan parasite Toxoplasma gondii Dopamine, a missing link between schizophrenia and toxoplasmosis?', *Biol Psychol*, vol. 63, no. 3, pp. 253-268.

Formolo, C.A., Williams, R., Gordish-Dressman, H., MacDonald, T.J., Lee, N.H. & Hathout, Y. (2011) 'Secretome signature of invasive glioblastoma multiforme', *J Proteome Res*, vol. 10, no. 7, pp. 3149-3159.

Friedman, D.B., Hoving, S. & Westermeier, R. (2009) 'Isoelectric focusing and two-dimensional gel electrophoresis', *Methods Enzymol*, vol. 463, pp. 515-540.

Gail, M., Gross, U. & Bohne, W. (2001) 'Transcriptional profile of Toxoplasma gondii-infected human fibroblasts as revealed by gene-array hybridization', *Mol Genet Genomics*, vol. 265, no. 5, pp. 905-912.

Garnett, J.A., Liu, Y., Leon, E., Allman, S.A., Friedrich, N., Saouros, S., Curry, S., Soldati-Favre, D., Davis, B.G., Feizi, T. & Matthews, S. (2009) 'Detailed insights from microarray and crystallographic studies into carbohydrate recognition by microneme protein 1 (MIC1) of Toxoplasma gondii', *Protein Sci*, vol. 18, no. 9, pp. 1935-1947.

Garrido, C., Schmitt, E., Cande, C., Vahsen, N., Parcellier, A. & Kroemer, G. (2003) 'HSP27 and HSP70: potentially oncogenic apoptosis inhibitors', *Cell Cycle*, vol. 2, no. 6, pp. 579-584.

Gaskell, E.A., Smith, J.E., Pinney, J.W., Westhead, D.R. & McConkey, G.A. (2009) 'A unique dual activity amino acid hydroxylase in Toxoplasma gondii', *PLoS One*, vol. 4, no. 3, p. e4801.

Gatkowska, J., Wieczorek, M., Dziadek, B., Dzitko, K. & Dlugonska, H. (2012) 'Behavioral changes in mice caused by Toxoplasma gondii invasion of brain', *Parasitol Res*, vol. 111, no. 1, pp. 53-58.

Gazzinelli, R.T., Hieny, S., Wynn, T.A., Wolf, S. & Sher, A. (1993) 'Interleukin 12 is required for the T-lymphocyte-independent induction of interferon gamma by an intracellular parasite and induces resistance in T-cell-deficient hosts', *Proc Natl Acad Sci U S A*, vol. 90, no. 13, pp. 6115-6119.

Geng, F. & Tansey, W. P. (2012) 'Similar temporal and spatial recruitment of native 19S and 20S proteasome subunits to transcriptionally active chromatin', *Proc Natl Acad Sci U S A*, vol. 109, pp. 6060–6065.

Gerhard, D.S., Wagner, L., Feingold, E.A., Shenmen, C.M., Grouse, L.H., Schuler, G., Klein, S.L., Old, S., Rasooly, R., Good, P., Guyer, M., Peck, A.M., Derge, J.G., Lipman, D., Collins, F.S., Jang, W., Sherry, S., Feolo, M., Misquitta, L., Lee, E., Rotmistrovsky, K., Greenhut, S.F., Schaefer, C.F., Buetow, K., Bonner, T.I., Haussler, D., Kent, J., Kiekhaus, M., Furey, T., Brent, M., Prange, C., Schreiber, K., Shapiro, N., Bhat, N.K., Hopkins, R.F., Hsie, F., Driscoll, T., Soares, M.B., Casavant, T.L., Scheetz, T.E., Brown-stein, M.J., Usdin, T.B., Toshiyuki, S., Carninci, P., Piao, Y., Dudekula, D.B., Ko, M.S., Kawakami, K., Suzuki, Y., Sugano, S., Gruber, C.E., Smith, M.R., Simmons, B., Moore, T., Waterman, R., Johnson, S.L., Ruan, Y., Wei, C.L., Mathavan, S., Gunaratne, P.H., Wu, J., Garcia, A.M., Hulyk, S.W., Fuh, E., Yuan, Y., Sneed, A., Kowis, C., Hodgson, A., Muzny, D.M., McPherson, J., Gibbs, R.A., Fahey, J., Helton, E.,

Ketteman, M., Madan, A., Rodrigues, S., Sanchez, A., Whiting, M., Madari, A., Young, A.C., Wetherby, K.D., Granite, S.J., Kwong, P.N., Brinkley, C.P., Pearson, R.L., Bouffard, G.G., Blakesly, R.W., Green, E.D., Dickson, M.C., Rodriguez, A.C., Grimwood, J., Schmutz, J., Myers, R.M., Butterfield, Y.S., Griffith, M., Griffith, O.L., Krzywinski, M.I., Liao, N., Morin, R., Palmquist, D., Petrescu, A.S., Skalska, U., Smailus, D.E., Stott, J.M., Schnerch, A., Schein, J.E., Jones, S.J., Holt, R.A., Baross, A., Marra, M.A., Clifton, S., Makowski, K.A., Bosak, S. & Malek, J. (2004) 'The status, quality, and expansion of the NIH full-length cDNA project: the Mammalian Gene Collection (MGC)', *Genome Res*, vol. 14, no. 10b, pp. 2121-2127.

Gibney, E.H., Kipar, A., Rosbottom, A., Guy, C.S., Smith, R.F., Hetzel, U., Trees, A.J. & Williams, D.J.L. (2008) 'The extent of parasite-associated necrosis in the placenta and foetal tissues of cattle following Neospora caninum infection in early and late gestation correlates with foetal death', *Int J Parasitology*, vol. 38, pp. 579-588.

Goda, S., Imai, T., Yoshie, O., Yoneda, O., Inoue, H., Nagano, Y., Okazaki, T., Imai, H., Bloom, E.T., Domae, N. & Umehara, H. (2000) 'CX3C-chemokine, fractalkine-enhanced adhesion of THP-1 cells to endothelial cells through integrin-dependent and -independent mechanisms', *J Immunol*, vol. 164, no. 8, pp. 4313-4320.

Goldman, M., Carver, R.K. & Sulzer, A.J. (1958) 'Reproduction of Toxoplasma gondii by internal budding', *J Parasitol*, vol. 44, no. 2, pp. 161-171.

Gomes, A.F., Guimaraes, E.V., Carvalho, L., Correa, J.R., Mendonca-Lima, L. & Barbosa, H.S. (2011) 'Toxoplasma gondii down modulates cadherin expression in skeletal muscle cells inhibiting myogenesis', *BMC Microbiol*, vol. 11, p. 110.

Gondim, L.F., McAllister, M.M. & Gao, L. (2005) 'Effects of host maturity and prior exposure history on the production of Neospora caninum oocysts by dogs', *Vet Parasitol*, vol. 134, no. 1-2, pp. 33-39.

Graveley, B.R., Brooks, A.N., Carlson, J.W., Duff, M.O., Landolin, J.M., Yang, L., Artieri, C.G., van Baren, M.J., Boley, N., Booth, B.W., Brown, J.B., Cherbas, L., Davis, C.A., Dobin, A., Li, R., Lin, W., Malone, J.H., Mattiuzzo, N.R., Miller, D., Sturgill, D., Tuch, B.B., Zaleski, C., Zhang, D., Blanchette, M., Dudoit, S., Eads, B., Green, R.E., Hammonds, A., Jiang, L., Kapranov, P., Langton, L., Perrimon, N., Sandler, J.E., Wan, K.H., Willingham, A., Zhang, Y., Zou, Y., Andrews, J., Bickel, P.J., Brenner, S.E., Brent, M.R., Cherbas, P., Gingeras, T.R., Hoskins, R.A., Kaufman, T.C., Oliver, B. & Celniker, S.E. (2011) 'The developmental transcriptome of Drosophila melanogaster', *Nature*, vol. 471, no. 7339, pp. 473-479.

Greenbaum, D., Luscombe, N.M., Jansen, R., Qian, J. & Gerstein, M. (2001) 'Interrelating different types of genomic data, from proteome to secretome: 'oming in on function', *Genome Res*, vol. 11, no. 9, pp. 1463-1468.

Guerfali, F.Z., Laouini, D., Guizani-Tabbane, L., Ottones, F., Ben-Aissa, K., Benkahla, A., Manchon, L., Piquemal, D., Smandi, S., Mghirbi, O., Commes, T., Marti, J. & Dellagi, K. (2008) 'Simultaneous gene expression profiling in human macrophages infected with Leishmania major parasites using SAGE', *BMC Genomics*, vol. 9, p. 238.

Gulinello, M., Acquarone, M., Kim, J.H., Spray, D.C., Barbosa, H.S., Sellers, R., Tanowitz, H.B. & Weiss, L.M. (2010) 'Acquired infection with Toxoplasma gondii in adult mice results in sensorimotor deficits but normal cognitive behavior despite widespread brain pathology', *Microbes Infect*, vol. 12, no. 7, pp. 528-537.

Gustafson, P.V., Agar, H.D. & Cramer, D.I. (1954) 'An electron microscope study of Toxoplasma', *Am J Trop Med Hyg*, vol. 3, no. 6, pp. 1008-1022.

Gygi, S.P., Rist, B., Gerber, S.A., Turecek, F., Gelb, M.H. & Aebersold, R. (1999) 'Quantitative analysis of complex protein mixtures using isotope-coded affinity tags', *Nat Biotechnol*, vol. 17, no. 10, pp. 994-999.

Hah, N., Danko, C.G., Core, L., Waterfall, J.J., Siepel, A., Lis, J.T. & Kraus, W.L. (2011) 'A rapid, extensive, and transient transcriptional response to estrogen signaling in breast cancer cells', *Cell*, vol. 145, no. 4, pp. 622-634.

Hall, N. (2007) 'Advanced sequencing technologies and their wider impact in microbiology', *J Exp Biol*, vol. 210, no. Pt 9, pp. 1518-1525.

Halonen, S.K. & Weidner, E. (1994) 'Overcoating of Toxoplasma parasitophorous vacuoles with host cell vimentin type intermediate filaments', *J Eukaryot Microbiol*, vol. 41, no. 1, pp. 65-71.

Halonen, S.K. & Weiss, L.M. (2000) 'Investigation into the mechanism of gamma interferon-mediated inhibition of Toxoplasma gondii in murine astrocytes', *Infect Immun*, vol. 68, no. 6, pp. 3426-3430.

Halonen, S.K., Lyman, W.D. & Chiu, F.C. (1996) 'Growth and development of Toxoplasma gondii in human neurons and astrocytes', *J Neuropathol Exp Neurol*, vol. 55, no. 11, pp. 1150-1156.

Halonen, S.K., Taylor, G.A. & Weiss, L.M. (2001) 'Gamma interferon-induced inhibition of Toxoplasma gondii in astrocytes is mediated by IGTP', *Infect Immun*, vol. 69, no. 9, pp. 5573-5576.

Halonen, S.K., Weiss, L.M. & Chiu, F.C. (1998) 'Association of host cell intermediate filaments with Toxoplasma gondii cysts in murine astrocytes in vitro', *Int J Parasitol*, vol. 28, no. 5, pp. 815-823.

Han, D., Jin, J., Woo, J., Min, H. & Kim, Y. (2014) 'Proteomic analysis of mouse astrocytes and their secretome by a combination of FASP and StageTip-based, high pH, reversed-phase fractionation', *Proteomics*, vol. 14, no. 13-14, pp. 1604-1609.

Harris, T.D., Buzby, P.R., Babcock, H., Beer, E., Bowers, J., Braslavsky, I., Causey, M., Colonell, J., Dimeo, J., Efcavitch, J.W., Giladi, E., Gill, J., Healy, J., Jarosz, M., Lapen, D., Moulton, K., Quake, S.R., Steinmann, K., Thayer, E., Tyurina, A., Ward, R., Weiss, H. & Xie, Z. (2008) 'Single-molecule DNA sequencing of a viral genome', *Science*, vol. 320, no. 5872, pp. 106-109.

Hassan, M.A., Melo, M.B., Haas, B., Jensen, K.D. & Saeij, J.P. (2012) 'De novo reconstruction of the Toxoplasma gondii transcriptome improves on the current genome annotation and reveals alternatively spliced transcripts and putative long non-coding RNAs', *BMC Genomics*, vol. 13, p. 696.

Hathout, Y. (2007) 'Approaches to the study of the cell secretome', *Expert Rev Proteomics*, vol. 4, no. 2, pp. 239-248.

Hatton, G.I. (2002) 'Glial-neuronal interactions in the mammalian brain', *Adv Physiol Educ*, vol. 26, no. 1-4, pp. 225-237.

Hemphill, A. & Gottstein, B. (2000) 'A European perspective on Neospora caninum', *Int J Parasitol*, vol. 30, no. 8, pp. 877-924.

Hemphill, A. (1999) 'The host–parasite relationship in neosporosis', *Adv Parasitol*, vol. 43, pp. 47–104.

Hemphill, A., Gottstein, B. & Kaufmann, H. (1996) 'Adhesion and invasion of bovine endothelial cells by Neospora caninum', *Parasitology*, vol. 112 (Pt 2), pp. 183-197.

Hermes, G., Ajioka, J.W., Kelly, K.A., Mui, E., Roberts, F., Kasza, K., Mayr, T., Kirisits, M.J., Wollmann, R., Ferguson, D.J., Roberts, C.W., Hwang, J.H., Trendler, T., Kennan, R.P., Suzuki, Y., Reardon, C.,

Hickey, W.F., Chen, L. & McLeod, R. (2008) 'Neurological and behavioral abnormalities, ventricular dilatation, altered cellular functions, inflammation, and neuronal injury in brains of mice due to common, persistent, parasitic infection', *J Neuroinflammation*, vol. 5, p. 48.

Hill, D. & Dubey, J.P. (2002) 'Toxoplasma gondii: transmission, diagnosis and prevention', *Clin Microbiol Infect*, vol. 8, no. 10, pp. 634-640.

Hill, D., Coss, C., Dubey, J.P., Wroblewski, K., Sautter, M., Hosten, T., Munoz-Zanzi, C., Mui, E., Withers, S., Boyer, K., Hermes, G., Coyne, J., Jagdis, F., Burnett, A., McLeod, P., Morton, H., Robinson, D. & McLeod, R. (2011) 'Identification of a sporozoite-specific antigen from Toxoplasma gondii', *J Parasitol*, vol. 97, no. 2, pp. 328-337.

Hilt, W. & Wolf, D.H. (1996) 'Proteasomes: destruction as a programme', *Trends Biochem Sci*, vol. 21, no. 3, pp. 96-102.

Hisaeda, H. & Himeno, K. (1997) 'The role of host-derived heat-shock protein in immunity against Toxoplasma gondii infection', *Parasitol Today*, vol. 13, no. 12, pp. 465-468.

Holliman, R.E. (1995) 'Congenital toxoplasmosis: prevention, screening and treatment', *J Hosp Infect*, vol. 30 Suppl, pp. 179-190.

Holt, R.A. & Jones, S.J. (2008) 'The new paradigm of flow cell sequencing', *Genome Res*, vol. 18, no. 6, pp. 839-846.

Honda, H., Barrueto, F.F., Gogusev, J., Im, D.D. & Morin, P.J. (2008) 'Serial analysis of gene expression reveals differential expression between endometriosis and normal endometrium. Possible roles for AXL and SHC1 in the pathogenesis of endometriosis', *Reprod Biol Endocrinol*, vol. 6, p. 59.

Hopf, P.S., Ford, R.S., Zebian, N., Merkx-Jacques, A., Vijayakumar, S., Ratnayake, D., Hayworth, J. & Creuzenet, C. (2011) 'Protein glycosylation in Helicobacter pylori: beyond the flagellins?', *PLoS One*, vol. 6, no. 9, p. e25722.

Howe D. K., Honore S., Derouin F. & Sibley L. D. (1997) 'Determination of genotypes of Toxoplasma gondii strains isolated from patients with toxoplasmosis', *J. Clin. Microbiol*, vol. 35, pp. 1411–1414.

Howe D. K., Summers B. C. & Sibley L. D. (1996) 'Acute virulence in mice is associated with markers on chromosome VIII in Toxoplasma gondii', *Infect. Immun*, vol. 64, pp. 5193–5198.

Howes, O.D. & Kapur, S. (2009) 'The dopamine hypothesis of schizophrenia: version III--the final common pathway', *Schizophr Bull*, vol. 35, no. 3, pp. 549-562.

Huang da, W., Sherman, B.T. & Lempicki, R.A. (2009) 'Systematic and integrative analysis of large gene lists using DAVID bioinformatics resources', *Nat Protoc*, vol. 4, no. 1, pp. 44-57.

Hunter, C.A. & Sibley, L.D. (2012) 'Modulation of innate immunity by Toxoplasma gondii virulence effectors', *Nat Rev Microbiol*, vol. 10, no. 11, pp. 766-778.

Hur, J., Lee, P., Kim, M.J., Kim, Y. & Cho, Y.W. (2010) 'Ischemia-activated microglia induces neuronal injury via activation of gp91phox NADPH oxidase', *Biochem Biophys Res Commun*, vol. 391, no. 3, pp. 1526-1530.

Ifergan, I., Wosik, K., Cayrol, R., Kebir, H., Auger, C., Bernard, M., Bouthillier, A., Moumdjian, R., Duquette, P. & Prat, A. (2006) 'Statins reduce human blood-brain barrier permeability and restrict leukocyte migration: relevance to multiple sclerosis', *Ann Neurol*, vol. 60, no. 1, pp. 45-55.

Innes, E.A., Andrianarivo, A.G., Bjorkman, C., Williams, D.J. & Conrad, P.A. (2002) 'Immune responses to Neospora caninum and prospects for vaccination', *Trends Parasitol*, vol. 18, no. 11, pp. 497-504.

Innes, E.A., Bartley, P.M., Maley, S.W., Wright, S.E. & Buxton, D. (2007) 'Comparative host-parasite relationships in ovine toxoplasmosis and bovine neosporosis and strategies for vaccination', *Vaccine*, vol. 25, no. 30, pp. 5495-5503.

Innes, E.A., Panton, W.R., Marks, J., Trees, A.J., Holmdahl, J. & Buxton, D. (1995) 'Interferon gamma inhibits the intracellular multiplication of Neospora caninum, as shown by incorporation of 3H uracil', *J Comp Pathol*, vol. 113, no. 1, pp. 95-100.

Innes, E.A., Wright, S.E., Maley, S., Rae, A., Schock, A., Kirvar, E., Bartley, P., Hamilton, C., Carey, I.M. & Buxton, D. (2001) 'Protection against vertical transmission in bovine neosporosis', *Int J Parasitology*, vol. 31, pp. 1523-1534.

Jarosinski, K.W. & Massa, P.T. (2002) 'Interferon regulatory factor-1 is required for interferon-gamma-induced MHC class I genes in astrocytes', *J Neuroimmunol*, vol. 122, no. 1-2, pp. 74-84.

Jeon, H., Lee, S., Lee, W.H. & Suk, K. (2010) 'Analysis of glial secretome: the long pentraxin PTX3 modulates phagocytic activity of microglia', *J Neuroimmunol*, vol. 229, no. 1-2, pp. 63-72.

Jesus, E.E., Pinheiro, A.M., Santos, A.B., Freire, S.M., Tardy, M.B., El-Bacha, R.S., Costa, S.L. & Costa, M.F. (2013) 'Effects of IFN-gamma, TNF-alpha, IL-10 and TGF-beta on Neospora caninum infection in rat glial cells', *Exp Parasitol*, vol. 133, no. 3, pp. 269-274.

Jia, B., Lu, H., Liu, Q., Yin, J., Jiang, N. & Chen, Q. (2013) 'Genome-wide comparative analysis revealed significant transcriptome changes in mice after Toxoplasma gondii infection', *Parasit Vectors*, vol. 6, p. 161.

John, B., Weninger, W. & Hunter, C.A. (2010) 'Advances in imaging the innate and adaptive immune response to Toxoplasma gondii', *Future Microbiol*, vol. 5, no. 9, pp. 1321-1328.

Jones, T.C., Bienz, K.A. & Erb, P. (1986) 'In vitro cultivation of Toxoplasma gondii cysts in astrocytes in the presence of gamma interferon', *Infect Immun*, vol. 51, no. 1, pp. 147-156.

Kadl, A. & Leitinger, N. (2005) 'The role of endothelial cells in the resolution of acute inflammation', *Antioxid Redox Signal*, vol. 7, no. 11-12, pp. 1744-1754.

Kapfhamer, D., Miller, D.E., Lambert, S., Bennett, V., Glover, T.W. & Burmeister, M. (1995) 'Chromosomal localization of the ankyrinG gene (ANK3/Ank3) to human 10q21 and mouse 10', *Genomics*, vol. 27, no. 1, pp. 189-191.

Kappe, S.H., Buscaglia, C.A., Bergman, L.W., Coppens, I. & Nussenzweig, V. (2004) 'Apicomplexan gliding motility and host cell invasion: overhauling the motor model', *Trends Parasitol*, vol. 20, no. 1, pp. 13-16.

Kaushik M., Lamberton P. H. & Webster J. P. (2012) 'The role of parasites and pathogens in influencing generalised anxiety and predation-related fear in the mammalian central nervous system', *Horm Behav*, vol. 62, pp. 191–201.

Kavanagh, K.L., Elling, R.A. & Wilson, D.K. (2004) 'Structure of Toxoplasma gondii LDH1: active-site differences from human lactate dehydrogenases and the structural basis for efficient APAD+ use', *Biochemistry*, vol. 43, no. 4, pp. 879-889.

Keene, S.D., Greco, T.M., Parastatidis, I., Lee, S.H., Hughes, E.G., Balice-Gordon, R.J., Speicher, D.W. & Ischiropoulos, H. (2009) 'Mass spectrometric and computational analysis of cytokine-induced alterations in the astrocyte secretome', *Proteomics*, vol. 9, no. 3, pp. 768-782.

Kikumura, A., Ishikawa, T. & Norose, K. (2012) 'Kinetic analysis of cytokines, chemokines, chemokine receptors and adhesion molecules in murine ocular toxoplasmosis', *Br J Ophthalmol*, vol. 96, no. 9, pp. 1259-1267.

Kim, D., Pertea, G., Trapnell, C., Pimentel, H., Kelley, R. & Salzberg, S.L. (2013) 'TopHat2: accurate alignment of transcriptomes in the presence of insertions, deletions and gene fusions', *Genome Biol*, vol. 14, no. 4, p. R36.

Klee, E.W., Carlson, D.F., Fahrenkrug, S.C., Ekker, S.C. & Ellis, L.B. (2004) 'Identifying secretomes in people, pufferfish and pigs', *Nucleic Acids Res*, vol. 32, no. 4, pp. 1414-1421.

Knight, B.C., Brunton, C.L., Modi, N.C., Wallace, G.R. & Stanford, M.R. (2005) 'The effect of Toxoplasma gondii infection on expression of chemokines by rat retinal vascular endothelial cells', *J Neuroimmunol*, vol. 160, no. 1-2, pp. 41-47.

Knight, B.C., Kissane, S., Falciani, F., Salmon, M., Stanford, M.R. & Wallace, G.R. (2006) 'Expression analysis of immune response genes of Muller cells infected with Toxoplasma gondii', *J Neuroimmunol*, vol. 179, no. 1-2, pp. 126-131.

Kobayashi, R., Kubota, T. & Hidaka, H. (1994) 'Purification, characterization, and partial sequence analysis of a new 25-kDa actin-binding protein from bovine aorta: a SM22 homolog', *Biochem Biophys Res Commun*, vol. 198, no. 3, pp. 1275-1280.

Kodzius, R., Kojima, M., Nishiyori, H., Nakamura, M., Fukuda, S., Tagami, M., Sasaki, D., Imamura, K., Kai, C., Harbers, M., Hayashizaki, Y. & Carninci, P. (2006) 'CAGE: cap analysis of gene expression', *Nat Methods*, vol. 3, no. 3, pp. 211-222.

Kondo, T. (2008) 'Tissue proteomics for cancer biomarker development: laser microdissection and 2D-DIGE', *BMB Rep*, vol. 41, no. 9, pp. 626-634.

Koukoulis, G.K., Patriarca, C. & Gould, V.E. (1998) 'Adhesion molecules and tumor metastasis', *Hum Pathol*, vol. 29, no. 9, pp. 889-892.

Kramer, G., Boehringer, D., Ban, N. & Bukau, B. (2009) 'The ribosome as a platform for co-translational processing, folding and targeting of newly synthesized proteins', *Nat Struct Mol Biol*, vol. 16, no. 6, pp. 589-597.

Krause, G., Winkler, L., Mueller, S.L., Haseloff, R.F., Piontek, J. & Blasig, I.E. (2008) 'Structure and function of claudins', *Biochim Biophys Acta*, vol. 1778, no. 3, pp. 631-645.

Krumbholz, M., Theil, D., Cepok, S., Hemmer, B., Kivisakk, P., Ransohoff, R.M., Hofbauer, M., Farina, C., Derfuss, T., Hartle, C., Newcombe, J., Hohlfeld, R. & Meinl, E. (2006) 'Chemokines in multiple sclerosis: CXCL12 and CXCL13 up-regulation is differentially linked to CNS immune cell recruitment', *Brain*, vol. 129, no. Pt 1, pp. 200-211.

Kurys, G., Ambroziak, W. & Pietruszko, R. (1989) 'Human aldehyde dehydrogenase. Purification and characterization of a third isozyme with low Km for gamma-aminobutyraldehyde', *J Biol Chem*, vol. 264, no. 8, pp. 4715-4721.

Lachenmaier, S.M., Deli, M.A., Meissner, M. & Liesenfeld, O. (2011) 'Intracellular transport of Toxoplasma gondii through the blood-brain barrier', *J Neuroimmunol*, vol. 232, no. 1-2, pp. 119-130.

Lambert, H. & Barragan, A. (2010) 'Modelling parasite dissemination: host cell subversion and immune evasion by Toxoplasma gondii', *Cell Microbiol*, vol. 12, no. 3, pp. 292-300.

Lambert, H., Hitziger, N., Dellacasa, I., Svensson, M. & Barragan, A. (2006) 'Induction of dendritic cell migration upon Toxoplasma gondii infection potentiates parasite dissemination', *Cell Microbiol*, vol. 8, no. 10, pp. 1611-1623.

Lambert, H., Vutova, P.P., Adams, W.C., Lore, K. & Barragan, A. (2009) 'The Toxoplasma gondii-shuttling function of dendritic cells is linked to the parasite genotype', *Infect Immun*, vol. 77, no. 4, pp. 1679-1688.

Lee, E.G., Kim, J.H., Shin, Y.S., Shin, G.W., Kim, Y.R., Palaksha, K.J., Kim, D.Y., Yamane, I., Kim, Y.H., Kim, G.S., Suh, M.D. & Jung, T.S. (2005) 'Application of proteomics for comparison of proteome of Neospora caninum and Toxoplasma gondii tachyzoites', *J Chromatogr B Analyt Technol Biomed Life Sci*, vol. 815, no. 1-2, pp. 305-314.

Lee, E.G., Kim, J.H., Shin, Y.S., Shin, G.W., Suh, M.D., Kim, D.Y., Kim, Y.H., Kim, G.S. & Jung, T.S. (2003) 'Establishment of a two-dimensional electrophoresis map for Neospora caninum tachyzoites by proteomics', *Proteomics*, vol. 3, no. 12, pp. 2339-2350.

Li, R.W., Sonstegard, T.S., Van Tassell, C.P. & Gasbarre, L.C. (2007) 'Local inflammation as a possible mechanism of resistance to gastrointestinal nematodes in Angus heifers', *Vet Parasitol*, vol. 145, no. 1-2, pp. 100-107.

Lim, J.W. & Bodnar, A. (2002) 'Proteome analysis of conditioned medium from mouse embryonic fibroblast feeder layers which support the growth of human embryonic stem cells', *Proteomics*, vol. 2, no. 9, pp. 1187-1203.

Lindsay, D.S., Dubey, J.P. & Duncan, R.B. (1999) 'Confirmation that the dog is a definitive host for Neospora caninum', *Vet Parasitol*, vol. 82, no. 4, pp. 327-333.

Lindstrom, M.S. & Zhang, Y. (2008) 'Ribosomal protein S9 is a novel B23/NPM-binding protein required for normal cell proliferation', *J Biol Chem*, vol. 283, no. 23, pp. 15568-15576.

Lister, R., O'Malley, R.C., Tonti-Filippini, J., Gregory, B.D., Berry, C.C., Millar, A.H. & Ecker, J.R. (2008) 'Highly integrated single-base resolution maps of the epigenome in Arabidopsis', *Cell*, vol. 133, no. 3, pp. 523-536.

Liu, F., Hu, W., Cui, S.J., Chi, M., Fang, C.Y., Wang, Z.Q., Yang, P.Y. & Han, Z.G. (2007) 'Insight into the host-parasite interplay by proteomic study of host proteins copurified with the human parasite, Schistosoma japonicum', *Proteomics*, vol. 7, no. 3, pp. 450-462.

Liu, F., Lu, J., Hu, W., Wang, S.Y., Cui, S.J., Chi, M., Yan, Q., Wang, X.R., Song, H.D., Xu, X.N., Wang, J.J., Zhang, X.L., Zhang, X., Wang, Z.Q., Xue, C.L., Brindley, P.J., McManus, D.P., Yang, P.Y., Feng, Z., Chen, Z. & Han, Z.G. (2006) 'New perspectives on host-parasite interplay by comparative transcriptomic and proteomic analyses of Schistosoma japonicum', *PLoS Pathog*, vol. 2, no. 4, p. e29.

Liu, H., Sadygov, R.G. & Yates, J.R., 3rd (2004) 'A model for random sampling and estimation of relative protein abundance in shotgun proteomics', *Anal Chem*, vol. 76, no. 14, pp. 4193-4201.

Liu, J., Hong, Z., Ding, J., Liu, J., Zhang, J. & Chen, S. (2008) 'Predominant release of lysosomal enzymes by newborn rat microglia after LPS treatment revealed by proteomic studies', *J Proteome Res*, vol. 7, no. 5, pp. 2033-2049.

Liu, Y., Zhou, J. & White, K.P. (2014) 'RNA-seq differential expression studies: more sequence or more replication?', *Bioinformatics*, vol. 30, no. 3, pp. 301-304.

Lu, C.Y. & Lai, S.C. (2013a) 'Induction of matrix metalloproteinase-2 and -9 via Erk1/2-NF-kappaB pathway in human astroglia infected with Toxoplasma gondii', *Acta Trop*, vol. 127, no. 1, pp. 14-20.

Lu, C.Y. & Lai, S.C. (2013b) 'Matrix metalloproteinase-2 and -9 lead to fibronectin degradation in astroglia infected with Toxoplasma gondii', *Acta Trop*, vol. 125, no. 3, pp. 320-329.

Luft, B.J. & Castro, K.G. (1991) 'An overview of the problem of toxoplasmosis and pneumocystosis in AIDS in the USA: implication for future therapeutic trials', *Eur J Clin Microbiol Infect Dis*, vol. 10, no. 3, pp. 178-181.

Luft, B.J. & Chua, A. (2000) 'Central Nervous System Toxoplasmosis in HIV Pathogenesis, Diagnosis, and Therapy', *Curr Infect Dis Rep*, vol. 2, no. 4, pp. 358-362.

Lundgren, D.H., Hwang, S.I., Wu, L. & Han, D.K. (2010) 'Role of spectral counting in quantitative proteomics', *Expert Rev Proteomics*, vol. 7, no. 1, pp. 39-53.

Luther, S.A. & Cyster, J.G. (2001) 'Chemokines as regulators of T cell differentiation', *Nat Immunol*, vol. 2, no. 2, pp. 102-107.

Mackintosh, C.L., Beeson, J.G. & Marsh, K. (2004) 'Clinical features and pathogenesis of severe malaria', *Trends Parasitol*, vol. 20, no. 12, pp. 597-603.

Makarov, A. (2000) 'Electrostatic axially harmonic orbital trapping: a high-performance technique of mass analysis', *Anal Chem*, vol. 72, no. 6, pp. 1156-1162.

Makridakis, M. & Vlahou, A. (2010) 'Secretome proteomics for discovery of cancer biomarkers', *J Proteomics*, vol. 73, no. 12, pp. 2291-2305.

Mallick, P. & Kuster, B. (2010) 'Proteomics: a pragmatic perspective', *Nat Biotechnol*, vol. 28, no. 7, pp. 695-709.

Mammari, N., Vignoles, P., Halabi, M.A., Darde, M.L. & Courtioux, B. (2014) 'In vitro infection of human nervous cells by two strains of Toxoplasma gondii: a kinetic analysis of immune mediators and parasite multiplication', *PLoS One*, vol. 9, no. 6, p. e98491.

Margulies, M., Egholm, M., Altman, W.E., Attiya, S., Bader, J.S., Bemben, L.A., Berka, J., Braverman, M.S., Chen, Y.J., Chen, Z., Dewell, S.B., Du, L., Fierro, J.M., Gomes, X.V., Godwin, B.C., He, W., Helgesen, S., Ho, C.H., Irzyk, G.P., Jando, S.C., Alenquer, M.L., Jarvie, T.P., Jirage, K.B., Kim, J.B., Knight, J.R., Lanza, J.R., Leamon, J.H., Lefkowitz, S.M., Lei, M., Li, J., Lohman, K.L., Lu, H., Makhijani, V.B., McDade, K.E., McKenna, M.P., Myers, E.W., Nickerson, E., Nobile, J.R., Plant, R., Puc, B.P., Ronan, M.T., Roth, G.T., Sarkis, G.J., Simons, J.F., Simpson, J.W., Srinivasan, M., Tartaro, K.R., Tomasz, A., Vogt, K.A., Volkmer, G.A., Wang, S.H., Wang, Y., Weiner, M.P., Yu, P., Begley, R.F. & Rothberg, J.M. (2005) 'Genome sequencing in microfabricated high-density picolitre reactors', *Nature*, vol. 437, no. 7057, pp. 376-380.

Martin, J.A. & Wang, Z. (2011) 'Next-generation transcriptome assembly', *Nat Rev Genet*, vol. 12, no. 10, pp. 671-682.

Massaro, A.R. (2002) 'The role of NCAM in remyelination', *Neurol Sci*, vol. 22, no. 6, pp. 429-435.

Mazzolla, R., Barluzzi, R., Puliti, M., Saleppico, S., Mosci, P., Bistoni, F. & Blasi, E. (1996) 'Biomolecular events involved in the establishment of brain anticandidal resistance', *J Neuroimmunol*, vol. 64, no. 1, pp. 9-17.

McAllister, M.M., Dubey, J.P., Lindsay, D.S., Jolley, W.R., Wills, R.A. & McGuire, A.M. (1998) 'Dogs are definitive hosts of Neospora caninum', *Int J Parasitology*, vol. 28, pp. 1473-1478.

McAllister, M.M., Parmley, S.F., Weiss, L.M., Welch, V.J. & McGuire, A.M. (1996) 'An immunohistochemical method for detecting bradyzoite antigen (BAG5) in Toxoplasma gondii-infected tissues cross-reacts with a Neospora caninum bradyzoite antigen', *J Parasitol*, vol. 82, no. 2, pp. 354-355.

McAuley, J., Boyer, K.M., Patel, D., Mets, M., Swisher, C., Roizen, N., Wolters, C., Stein, L., Stein, M., Schey, W. & et al. (1994) 'Early and longitudinal evaluations of treated infants and children and untreated historical patients with congenital toxoplasmosis: the Chicago Collaborative Treatment Trial', *Clin Infect Dis*, vol. 18, no. 1, pp. 38-72.

McConkey, G.A., Martin, H.L., Bristow, G.C. & Webster, J.P. (2013) 'Toxoplasma gondii infection and behaviour - location, location, location?', *J Exp Biol*, vol. 216, no. Pt 1, pp. 113-119.

McNeil, P.L. & Steinhardt, R.A. (2003) 'Plasma membrane disruption: repair, prevention, adaptation', *Annu Rev Cell Dev Biol*, vol. 19, pp. 697-731.

McNicoll, F., Drummelsmith, J., Muller, M., Madore, E., Boilard, N., Ouellette, M. & Papadopoulou, B. (2006) 'A combined proteomic and transcriptomic approach to the study of stage differentiation in Leishmania infantum', *Proteomics*, vol. 6, no. 12, pp. 3567-3581.

Meira, C.S., Vidal, J.E., Costa-Silva, T.A., Frazatti-Gallina, N. & Pereira-Chioccola, V.L. (2011) 'Immunodiagnosis in cerebrospinal fluid of cerebral toxoplasmosis and HIV-infected patients using Toxoplasma gondii excreted/secreted antigens', *Diagn Microbiol Infect Dis*, vol. 71, no. 3, pp. 279-285.

Mellman, I. & Warren, G. (2000) 'The road taken: past and future foundations of membrane traffic', *Cell*, vol. 100, no. 1, pp. 99-112.

Mills, J.D., Nalpathamkalam, T., Jacobs, H.I., Janitz, C., Merico, D., Hu, P. & Janitz, M. (2013) 'RNA-Seq analysis of the parietal cortex in Alzheimer's disease reveals alternatively spliced isoforms related to lipid metabolism', *Neurosci Lett*, vol. 536, pp. 90-95.

Miman, O., Kusbeci, O.Y., Aktepe, O.C. & Cetinkaya, Z. (2010) 'The probable relation between Toxoplasma gondii and Parkinson's disease', *Neurosci Lett*, vol. 475, no. 3, pp. 129-131.

Mitra, R., Sapolsky, R.M. & Vyas, A. (2013) 'Toxoplasma gondii infection induces dendritic retraction in basolateral amygdala accompanied by reduced corticosterone secretion', *Dis Model Mech*, vol. 6, no. 2, pp. 516-520.

Molofsky, A.V., Krencik, R., Ullian, E.M., Tsai, H.H., Deneen, B., Richardson, W.D., Barres, B.A. & Rowitch, D.H. (2012) 'Astrocytes and disease: a neurodevelopmental perspective', *Genes Dev*, vol. 26, no. 9, pp. 891-907.

Monopoli, M.P., Raghnaill, M.N., Loscher, J.S., O'Sullivan, N.C., Pangalos, M.N., Ring, R.H., von Schack, D., Dunn, M.J., Regan, C.M., Pennington, S. & Murphy, K.J. (2011) 'Temporal proteomic profile of memory consolidation in the rat hippocampal dentate gyrus', *Proteomics*, vol. 11, no. 21, pp. 4189-4201.

Montoya, J.G. & Liesenfeld, O. (2004) 'Toxoplasmosis', *The Lancet*, vol. 363, no. 9425, pp. 1965-1976.

Moore, N.H., Costa, L.G., Shaffer, S.A., Goodlett, D.R. & Guizzetti, M. (2009) 'Shotgun proteomics implicates extracellular matrix proteins and protease systems in neuronal development induced by astrocyte cholinergic stimulation', *J Neurochem*, vol. 108, no. 4, pp. 891-908.

Mordue, D.G., Desai, N., Dustin, M. & Sibley, L.D. (1999) 'Invasion by Toxoplasma gondii establishes a moving junction that selectively excludes host cell plasma membrane proteins on the basis of their membrane anchoring', *J Exp Med*, vol. 190, no. 12, pp. 1783-1792.

Mortazavi, A., Williams, B.A., McCue, K., Schaeffer, L. & Wold, B. (2008) 'Mapping and quantifying mammalian transcriptomes by RNA-Seq', *Nat Methods*, vol. 5, no. 7, pp. 621-628.

Murakami, T., Nakajima, M., Nakamura, T., Hara, A., Uyama, E., Mita, S., Matsushita, S. & Uchino, M. (2000) 'Parkinsonian symptoms as an initial manifestation in a Japanese patient with acquired immunodeficiency syndrome and Toxoplasma infection', *Intern Med*, vol. 39, no. 12, pp. 1111-1114.

Murdoch, C. & Finn, A. (2000) 'Chemokine receptors and their role in inflammation and infectious diseases', *Blood*, vol. 95, no. 10, pp. 3032-3043.

Muzny, D.M., Scherer, S.E., Kaul, R., Wang, J., Yu, J., Sudbrak, R., Buhay, C.J., Chen, R., Cree, A., Ding, Y., Dugan-Rocha, S., Gill, R., Gunaratne, P., Harris, R.A., Hawes, A.C., Hernandez, J., Hodgson, A.V., Hume, J., Jackson, A., Khan, Z.M., Kovar-Smith, C., Lewis, L.R., Lozado, R.J., Metzker, M.L., Milosavljevic, A., Miner, G.R., Morgan, M.B., Nazareth, L.V., Scott, G., Sodergren, E., Song, X.Z., Steffen, D., Wei, S., Wheeler, D.A., Wright, M.W., Worley, K.C., Yuan, Y., Zhang, Z., Adams, C.Q., Ansari-Lari, M.A., Ayele, M., Brown, M.J., Chen, G., Chen, Z., Clendenning, J., Clerc-Blankenburg, K.P., Chen, R., Chen, Z., Davis, C., Delgado, O., Dinh, H.H., Dong, W., Draper, H., Ernst, S., Fu, G., Gonzalez-Garay, M.L., Garcia, D.K., Gillett, W., Gu, J., Hao, B., Haugen, E., Havlak, P., He, X., Hennig, S., Hu, S., Huang, W., Jackson, L.R., Jacob, L.S., Kelly, S.H., Kube, M., Levy, R., Li, Z., Liu, B., Liu, J., Liu, W., Lu, J., Maheshwari, M., Nguyen, B.V., Okwuonu, G.O., Palmeiri, A., Pasternak, S., Perez, L.M., Phelps, K.A., Plopper, F.J., Qiang, B., Raymond, C., Rodriguez, R., Saenphimmachak, C., Santibanez, J., Shen, H., Shen, Y., Subramanian, S., Tabor, P.E., Verduzco, D., Waldron, L., Wang, J., Wang, J., Wang, Q., Williams, G.A., Wong, G.K., Yao, Z., Zhang, J., Zhang, X., Zhao, G., Zhou, J., Zhou, Y., Nelson, D., Lehrach, H., Reinhardt, R., Naylor, S.L., Yang, H., Olson, M., Weinstock, G. & Gibbs, R.A. (2006) 'The DNA sequence, annotation and analysis of human chromosome 3', *Nature*, vol. 440, no. 7088, pp. 1194-1198.

Nagalakshmi, U., Wang, Z., Waern, K., Shou, C., Raha, D., Gerstein, M. & Snyder, M. (2008) 'The transcriptional landscape of the yeast genome defined by RNA sequencing', *Science*, vol. 320, no. 5881, pp. 1344-1349.

Nath, A. & Sinai, A.P. (2003) 'Cerebral Toxoplasmosis', *Curr Treat Options Neurol*, vol. 5, no. 1, pp. 3-12.

Nedergaard, M., Rodriguez, J.J. & Verkhratsky, A. (2010) 'Glial calcium and diseases of the nervous system', *Cell Calcium*, vol. 47, no. 2, pp. 140-149.

Nelson, M.M., Jones, A.R., Carmen, J.C., Sinai, A.P., Burchmore, R. & Wastling, J.M. (2008) 'Modulation of the host cell proteome by the intracellular apicomplexan parasite Toxoplasma gondii', *Infect Immun*, vol. 76, no. 2, pp. 828-844.

Nichols, B.A., Chiappino, M.L. & O'Connor, G.R. (1983) 'Secretion from the rhoptries of Toxoplasma gondii during host-cell invasion', *J Ultrastruct Res*, vol. 83, no. 1, pp. 85-98.

Nickel, W. & Seedorf, M. (2008) 'Unconventional mechanisms of protein transport to the cell surface of eukaryotic cells', *Annu Rev Cell Dev Biol*, vol. 24, pp. 287-308.

Nikolov, M., Schmidt, C. & Urlaub, H. (2012) 'Quantitative mass spectrometry-based proteomics: an overview', *Methods Mol Biol*, vol. 893, pp. 85-100.

Norenberg, M.D. (1994) 'Astrocyte responses to CNS injury', *J Neuropathol Exp Neurol*, vol. 53, no. 3, pp. 213-220.

Norose, K., Naoi, K., Fang, H. & Yano, A. (2008) 'In vivo study of toxoplasmic parasitemia using interferon-gamma-deficient mice: absolute cell number of leukocytes, parasite load and cell susceptibility', *Parasitol Int*, vol. 57, no. 4, pp. 447-453.

O'Brien, T.W. (2003) 'Properties of human mitochondrial ribosomes', *IUBMB Life* , vol. 55, no. 9, pp. 505–513.

Ochsenbein, A.F. (2002) 'Principles of tumor immunosurveillance and implications for immunotherapy', *Cancer Gene Ther*, vol. 9, no. 12, pp. 1043-1055.

O'Farrell, P.H. (1975) 'High resolution two-dimensional electrophoresis of proteins', *J Biol Chem*, vol. 250, no. 10, pp. 4007-4021.

Ohtsuki, S., Yamaguchi, H., Katsukura, Y., Asashima, T. & Terasaki, T. (2008) 'mRNA expression levels of tight junction protein genes in mouse brain capillary endothelial cells highly purified by magnetic cell sorting', *J Neurochem*, vol. 104, no. 1, pp. 147-154.

Okeoma, C.M., Williamson, N.B., Pomroy, W.E., Stowell, K.M. & Gillespie, L.M. (2004) 'Isolation and molecular characterisation of Neospora caninum in cattle in New Zealand', *N Z Vet J*, vol. 52, no. 6, pp. 364-370.

Old, W.M., Meyer-Arendt, K., Aveline-Wolf, L., Pierce, K.G., Mendoza, A., Sevinsky, J.R., Resing, K.A. & Ahn, N.G. (2005) 'Comparison of label-free methods for quantifying human proteins by shotgun proteomics', *Mol Cell Proteomics*, vol. 4, no. 10, pp. 1487-1502.

Oppermann, F.S., Gnad, F., Olsen, J.V., Hornberger, R., Greff, Z., Keri, G., Mann, M. & Daub, H. (2009) 'Large-scale proteomics analysis of the human kinome', *Mol Cell Proteomics*, vol. 8, no. 7, pp. 1751-1764.

Otten, U., Marz, P., Heese, K., Hock, C., Kunz, D. & Rose-John, S. (2000) 'Cytokines and neurotrophins interact in normal and diseased states', *Ann N Y Acad Sci*, vol. 917, pp. 322-330.

Pan, B.T. & Johnstone, R.M. (1983) 'Fate of the transferrin receptor during maturation of sheep reticulocytes in vitro: selective externalization of the receptor', *Cell*, vol. 33, no. 3, pp. 967-978.

Panchaud, A., Affolter, M., Moreillon, P. & Kussmann, M. (2008) 'Experimental and computational approaches to quantitative proteomics: status quo and outlook', *J Proteomics*, vol. 71, no. 1, pp. 19-33.

Pandey, A. & Mann, M. (2000) 'Proteomics to study genes and genomes', *Nature*, vol. 405, no. 6788, pp. 837-846.

Paoloni-Giacobino, A., Chen, H. & Antonarakis, S.E. (1997) 'Cloning of a novel human neural cell adhesion molecule gene (NCAM2) that maps to chromosome region 21q21 and is potentially involved in Down syndrome', *Genomics*, vol. 43, no. 1, pp. 43-51.

Patel, V.J., Thalassinos, K., Slade, S.E., Connolly, J.B., Crombie, A., Murrell, J.C. & Scrivens, J.H. (2009) 'A comparison of labeling and label-free mass spectrometry-based proteomics approaches', *J Proteome Res*, vol. 8, no. 7, pp. 3752-3759.

Paul, D., Kumar, A., Gajbhiye, A., Santra, M.K. & Srikanth, R. (2013) 'Mass spectrometry-based proteomics in molecular diagnostics: discovery of cancer biomarkers using tissue culture', *Biomed Res Int*, vol. 2013, p. 783131.

Pavlou, M.P. & Diamandis, E.P. (2010) 'The cancer cell secretome: a good source for discovering biomarkers?', *J Proteomics*, vol. 73, no. 10, pp. 1896-1906.

Peixoto, L., Chen, F., Harb, O.S., Davis, P.H., Beiting, D.P., Brownback, C.S., Ouloguem, D. & Roos, D.S. (2010) 'Integrative genomic approaches highlight a family of parasite-specific kinases that regulate host responses', *Cell Host Microbe*, vol. 8, no. 2, pp. 208-218.

Pekny, M. & Nilsson, M. (2005) 'Astrocyte activation and reactive gliosis', *Glia*, vol. 50, no. 4, pp. 427-434.

Pel, H. J. & Grivell, L. A. (1994) 'Protein synthesis in mitochondria', *Mol Biol Rep*, vol. 19, no. 3, pp.183–194.

Pelloux, H., Pernod, G., Polack, B., Coursange, E., Ricard, J., Verna, J.M. & Ambroise-Thomas, P. (1996) 'Influence of cytokines on Toxoplasma gondii growth in human astrocytoma-derived cells', *Parasitol Res*, vol. 82, no. 7, pp. 598-603.

Perera, C.N., Spalding, H.S., Mohammed, S.I. & Camarillo, I.G. (2008) 'Identification of proteins secreted from leptin stimulated MCF-7 breast cancer cells: a dual proteomic approach', *Exp Biol Med (Maywood)*, vol. 233, no. 6, pp. 708-720.

Perkins, D.N., Pappin, D.J., Creasy, D.M. & Cottrell, J.S. (1999) 'Probability-based protein identification by searching sequence databases using mass spectrometry data', *Electrophoresis*, vol. 20, no. 18, pp. 3551-3567.

Peters, M., Lutkefels, E., Heckeroth, A.R. & Schares, G. (2001) 'Immunohistochemical and ultrastructural evidence for Neospora caninum tissue cysts in skeletal muscles of naturally infected dogs and cattle', *Int J Parasitol*, vol. 31, no. 10, pp. 1144-1148.

Petersen, T.N., Brunak, S., von Heijne, G. & Nielsen, H. (2011) 'SignalP 4.0: discriminating signal peptides from transmembrane regions', *Nat Methods*, vol. 8, no. 10, pp. 785-786.

Peterson, P.K., Gekker, G., Hu, S. & Chao, C.C. (1993) 'Intracellular survival and multiplication of Toxoplasma gondii in astrocytes', *J Infect Dis*, vol. 168, no. 6, pp. 1472-1478.

Petrak, J., Ivanek, R., Toman, O., Cmejla, R., Cmejlova, J., Vyoral, D., Zivny, J. & Vulpe, C.D. (2008) 'Deja vu in proteomics. A hit parade of repeatedly identified differentially expressed proteins', *Proteomics*, vol. 8, no. 9, pp. 1744-1749.

Pinheiro, A.M., Costa, S.L., Freire, S.M., Almeida, M.A., Tardy, M., El Bacha, R. & Costa, M.F. (2006) 'Astroglial cells in primary culture: a valid model to study Neospora caninum infection in the CNS', *Vet Immunol Immunopathol*, vol. 113, no. 1-2, pp. 243-247.

Pinheiro, A.M., Costa, S.L., Freire, S.M., Ribeiro, C.S., Tardy, M., El-Bacha, R.S. & Costa, M.F. (2010) 'Neospora caninum: early immune response of rat mixed glial cultures after tachyzoites infection', *Exp Parasitol*, vol. 124, no. 4, pp. 442-447.

Planque, C., Kulasingam, V., Smith, C.R., Reckamp, K., Goodglick, L. & Diamandis, E.P. (2009) 'Identification of five candidate lung cancer biomarkers by proteomics analysis of conditioned media of four lung cancer cell lines', *Mol Cell Proteomics*, vol. 8, no. 12, pp. 2746-2758.

Pockley, A. G. (2001) 'Heat shock proteins in health and disease: therapeutic targets or therapeutic agents?', *Exp. Rev. Mol. Med*, vol. 3, pp. 1–21.

Polonais, V. & Soldati-Favre, D. (2010) 'Versatility in the acquisition of energy and carbon sources by the Apicomplexa', *Biol Cell*, vol. 102, pp. 435–445.

Pomel, S., Luk, F.C. & Beckers, C.J. (2008) 'Host cell egress and invasion induce marked relocations of glycolytic enzymes in Toxoplasma gondii tachyzoites', *PLoS Pathog*, vol. 4, no. 10, p. e1000188.

Potolicchio, I., Carven, G.J., Xu, X., Stipp, C., Riese, R.J., Stern, L.J. & Santambrogio, L. (2005) 'Proteomic analysis of microglia-derived exosomes: metabolic role of the aminopeptidase CD13 in neuropeptide catabolism', *J Immunol*, vol. 175, no. 4, pp. 2237-2243.

Prandovszky, E., Gaskell, E., Martin, H., Dubey, J.P., Webster, J.P. & McConkey, G.A. (2011) 'The neurotropic parasite Toxoplasma gondii increases dopamine metabolism', *PLoS One*, vol. 6, no. 9, p. e23866.

Proost, P., Wuyts, A., Conings, R., Lenaerts, J.P., Billiau, A., Opdenakker, G. & Van Damme, J. (1993) 'Human and bovine granulocyte chemotactic protein-2: complete amino acid sequence and functional characterization as chemokines', *Biochemistry*, vol. 32, no. 38, pp. 10170-10177.

Quinn, H.E., Ellis, J.T. & Smith, N.C. (2002) 'Neospora caninum: a cause of immune-mediated failure of pregnancy?', *Trends Parasitol*, vol. 18, no. 9, pp. 391-394.

Quinn, H.E., Miller, C.M. & Ellis, J.T. (2004) 'The cell-mediated immune response to Neospora caninum during pregnancy in the mouse is associated with a bias towards production of interleukin-4', *Int J Parasitol*, vol. 34, no. 6, pp. 723-732.

Rabilloud, T. (1996) 'Solubilization of proteins for electrophoretic analyses', *Electrophoresis*, vol. 17, no. 5, pp. 813-829.

Rahman, A. & Fazal, F. (2009) 'Hug tightly and say goodbye: role of endothelial ICAM-1 in leukocyte transmigration', *Antioxid Redox Signal*, vol. 11, no. 4, pp. 823-839.

Reese, M.L. & Boothroyd, J.C. (2011) 'A conserved non-canonical motif in the pseudoactive site of the ROP5 pseudokinase domain mediates its effect on Toxoplasma virulence', *J Biol Chem*, vol. 286, no. 33, pp. 29366-29375.

Reese, M.L., Zeiner, G.M., Saeij, J.P., Boothroyd, J.C. & Boyle, J.P. (2011) 'Polymorphic family of injected pseudokinases is paramount in Toxoplasma virulence', *Proc Natl Acad Sci U S A*, vol. 108, no. 23, pp. 9625-9630.

Reid, A.J., Vermont, S.J., Cotton, J.A., Harris, D., Hill-Cawthorne, G.A., Konen-Waisman, S., Latham, S.M., Mourier, T., Norton, R., Quail, M.A., Sanders, M., Shanmugam, D., Sohal, A., Wasmuth, J.D., Brunk, B., Grigg, M.E., Howard, J.C., Parkinson, J., Roos, D.S., Trees, A.J., Berriman, M., Pain, A. & Wastling, J.M. (2012) 'Comparative genomics of the apicomplexan parasites Toxoplasma gondii and Neospora caninum: Coccidia differing in host range and transmission strategy', *PLoS Pathog*, vol. 8, no. 3, p. e1002567.

Reiss, M., Viebig, N., Brecht, S., Fourmaux, M.N., Soete, M., Di Cristina, M., Dubremetz, J.F. & Soldati, D. (2001) 'Identification and characterization of an escorter for two secretory adhesins in Toxoplasma gondii', *J Cell Biol*, vol. 152, no. 3, pp. 563-578.

Rigbolt, K.T., Vanselow, J.T. & Blagoev, B. (2011) 'GProX, a user-friendly platform for bioinformatics analysis and visualization of quantitative proteomics data', *Mol Cell Proteomics*, vol. 10, no. 8, p. O110.007450.

Ringman, J.M., Schulman, H., Becker, C., Jones, T., Bai, Y., Immermann, F., Cole, G., Sokolow, S., Gylys, K., Geschwind, D.H., Cummings, J.L. & Wan, H.I. (2012) 'Proteomic changes in cerebrospinal fluid of presymptomatic and affected persons carrying familial Alzheimer disease mutations', *Arch Neurol*, vol. 69, no. 1, pp. 96-104.

Robert-Gangneux, F. & Klein, F. (2009) 'Serologic screening for Neospora caninum, France', *Emerg Infect Dis*, vol. 15, no. 6, pp. 987-989.

Ross, P.L., Huang, Y.N., Marchese, J.N., Williamson, B., Parker, K., Hattan, S., Khainovski, N., Pillai, S., Dey, S., Daniels, S., Purkayastha, S., Juhasz, P., Martin, S., Bartlet-Jones, M., He, F., Jacobson, A. & Pappin, D.J. (2004) 'Multiplexed protein quantitation in Saccharomyces cerevisiae using amine-reactive isobaric tagging reagents', *Mol Cell Proteomics*, vol. 3, no. 12, pp. 1154-1169.

Rothlein, R., Dustin, M.L., Marlin, S.D. & Springer, T.A. (1986) 'A human intercellular adhesion molecule (ICAM-1) distinct from LFA-1', *J Immunol*, vol. 137, no. 4, pp. 1270-1274.

Rovere, P., Peri, G., Fazzini, F., Bottazzi, B., Doni, A., Bondanza, A., Zimmermann, V.S., Garlanda, C., Fascio, U., Sabbadini, M.G., Rugarli, C., Mantovani, A. & Manfredi, A.A. (2000) 'The long pentraxin PTX3 binds to apoptotic cells and regulates their clearance by antigen-presenting dendritic cells', *Blood*, vol. 96, no. 13, pp. 4300-4306.

Saeij, J.P., Boyle, J.P., Coller, S., Taylor, S., Sibley, L.D., Brooke-Powell, E.T., Ajioka, J.W. & Boothroyd, J.C. (2006) 'Polymorphic secreted kinases are key virulence factors in toxoplasmosis', *Science*, vol. 314, no. 5806, pp. 1780-1783.

Saeij, J.P., Coller, S., Boyle, J.P., Jerome, M.E., White, M.W. & Boothroyd, J.C. (2007) 'Toxoplasma co-opts host gene expression by injection of a polymorphic kinase homologue', *Nature*, vol. 445, no. 7125, pp. 324-327.

Sanger, F., Nicklen, S. & Coulson, A.R. (1977) 'DNA sequencing with chain-terminating inhibitors', *Proc Natl Acad Sci U S A*, vol. 74, no. 12, pp. 5463-5467.

Sawada, M., Kondo, H., Tomioka, Y., Park, C., Morita, T., Shimada, A. & Umemura, T. (2000) 'Isolation of Neospora caninum from the brain of a naturally infected adult dairy cow', *Vet Parasitol*, vol. 90, no. 3, pp. 247-252.

Sayles, P.C. & Johnson, L.L. (1996) 'Exacerbation of toxoplasmosis in neutrophil-depleted mice', *Nat Immun*, vol. 15, no. 5, pp. 249-258.

Schluter, D., Deckert, M., Hof, H. & Frei, K. (2001) 'Toxoplasma gondii infection of neurons induces neuronal cytokine and chemokine production, but gamma interferon- and tumor necrosis factor-stimulated neurons fail to inhibit the invasion and growth of T. gondii', *Infect Immun*, vol. 69, no. 12, pp. 7889-7893.

Schluter, D., Lohler, J., Deckert, M., Hof, H. & Schwendemann, G. (1991) 'Toxoplasma encephalitis of immunocompetent and nude mice: immunohistochemical characterisation of Toxoplasma antigen,

infiltrates and major histocompatibility complex gene products', *J Neuroimmunol*, vol. 31, no. 3, pp. 185-198.

Schmitz, B., Vischer, P., Brand, E., Schmidt-Petersen, K., Korb-Pap, A., Guske, K., Nedele, J., Schelleckes, M., Hillen, J., Rotrige, A., Simmet, T., Paul, M., Cambien, F. & Brand, S.M. (2013) 'Increased monocyte adhesion by endothelial expression of VCAM-1 missense variation in vitro', *Atherosclerosis*, vol. 230, no. 2, pp. 185-190.

Schrader, W. & Klein, H.W. (2004) 'Liquid chromatography/Fourier transform ion cyclotron resonance mass spectrometry (LC-FTICR MS): an early overview', *Anal Bioanal Chem*, vol. 379, no. 7-8, pp. 1013-1024.

Schrimpf, S.P., Weiss, M., Reiter, L., Ahrens, C.H., Jovanovic, M., Malmstrom, J., Brunner, E., Mohanty, S., Lercher, M.J., Hunziker, P.E., Aebersold, R., von Mering, C. & Hengartner, M.O. (2009) 'Comparative functional analysis of the Caenorhabditis elegans and Drosophila melanogaster proteomes', *PLoS Biol*, vol. 7, no. 3, p. e48.

Schwab, J. C., Beckers, C. J. M. & Joiner, K. A. (1994) 'The parasitophorous vacuole membrane surrounding intracellular Toxoplasma gondii functions as a molecular seive', *Proc Natl Acad Sci U S A*, vol. 91, pp. 509-513.

Schweitzer, S. C. & Evans, R. M. (1998) 'Vimentin and lipid metabolism', *Subcell. Biochem*, vol. 31, pp. 437–462.

Scigelova, M. & Makarov, A. (2006) 'Orbitrap mass analyzer--overview and applications in proteomics', *Proteomics*, vol. 6 Suppl 2, pp. 16-21.

Shapiro, A.L., Vinuela, E. & Maizel, J.V., Jr. (1967) 'Molecular weight estimation of polypeptide chains by electrophoresis in SDS-polyacrylamide gels', *Biochem Biophys Res Commun*, vol. 28, no. 5, pp. 815-820.

Sheffield, H.G. & Melton, M.L. (1968) 'The fine structure and reproduction of Toxoplasma gondii', *J Parasitol*, vol. 54, no. 2, pp. 209-226.

Shendure, J., Porreca, G.J., Reppas, N.B., Lin, X., McCutcheon, J.P., Rosenbaum, A.M., Wang, M.D., Zhang, K., Mitra, R.D. & Church, G.M. (2005) 'Accurate multiplex polony sequencing of an evolved bacterial genome', *Science*, vol. 309, no. 5741, pp. 1728-1732.

Shin, Y.S., Shin, G.W., Kim, Y.R., Lee, E.Y., Yang, H.H., Palaksha, K.J., Youn, H.J., Kim, J.H., Kim, D.Y., Marsh, A.E., Lakritz, J. & Jung, T.S. (2005) 'Comparison of proteome and antigenic proteome between two Neospora caninum isolates', *Vet Parasitol*, vol. 134, no. 1-2, pp. 41-52.

Sibbald, M.J., Ziebandt, A.K., Engelmann, S., Hecker, M., de Jong, A., Harmsen, H.J., Raangs, G.C., Stokroos, I., Arends, J.P., Dubois, J.Y. & van Dijl, J.M. (2006) 'Mapping the pathways to staphylococcal pathogenesis by comparative secretomics', *Microbiol Mol Biol Rev*, vol. 70, no. 3, pp. 755-788.

Sibley L. D. & Boothroyd J. C. (1992) ' Virulent strains of Toxoplasma gondii comprise a single clonal lineage', *Nature*, vol. 359, pp. 82–85.

Sibley L. D., Mordue D. G., Su C., Robben P. M. & Howe D. K. (2002) 'Genetic approaches to studying virulence and pathogenesis in Toxoplasma gondii', Philos. *Trans. R. Soc. B*, vol. 357, pp. 81–88.

Sibley, L.D. (2003)'Toxoplasma gondii: perfecting an intracellular life style', *Traffic*, vol. 4, pp. 581–586.

Siegel, S.E., Lunde, M.N., Gelderman, A.H., Halterman, R.H., Brown, J.A., Levine, A.S. & Graw, R.G., Jr. (1971) 'Transmission of toxoplasmosis by leukocyte transfusion', *Blood*, vol. 37, no. 4, pp. 388-394.

Silva, N.M., Manzan, R.M., Carneiro, W.P., Milanezi, C.M., Silva, J.S., Ferro, E.A. & Mineo, J.R. (2010) 'Toxoplasma gondii: the severity of toxoplasmic encephalitis in C57BL/6 mice is associated with increased ALCAM and VCAM-1 expression in the central nervous system and higher blood-brain barrier permeability', *Exp Parasitol*, vol. 126, no. 2, pp. 167-177.

Silvestrini, F., Lasonder, E., Olivieri, A., Camarda, G., van Schaijk, B., Sanchez, M., Younis Younis, S., Sauerwein, R. & Alano, P. (2010) 'Protein export marks the early phase of gametocytogenesis of the human malaria parasite Plasmodium falciparum', *Mol Cell Proteomics*, vol. 9, no. 7, pp. 1437-1448.

Simpson, R.J. (ed.) (2003) Proteins and Proteomics, Cold Spring Harbour Laboratory Press, New York.

Sinai, A. P. & Joiner, K. A. (2001) 'The Toxoplasma gondii protein ROP2 mediates host organelle association with the parasitophorous vacuole membrane', *J. Cell Biol*, vol. 154, pp. 95-108.

Sinai, A.P., Webster, P. & Joiner, K.A. (1997) 'Association of host cell endoplasmic reticulum and mitochondria with the Toxoplasma gondii parasitophorous vacuole membrane: a high affinity interaction', *J Cell Sci*, vol. 110 (Pt 17), pp. 2117-2128.

Skariah, S., McIntyre, M.K. & Mordue, D.G. (2010) 'Toxoplasma gondii: determinants of tachyzoite to bradyzoite conversion', *Parasitol. Res*, vol. 107, pp. 253–260.

Skorupa, A., Urbach, S., Vigy, O., King, M.A., Chaumont-Dubel, S., Prehn, J.H. & Marin, P. (2013) 'Angiogenin induces modifications in the astrocyte secretome: relevance to amyotrophic lateral sclerosis', *J Proteomics*, vol. 91, pp. 274-285.

Smolka, M.B., Zhou, H., Purkayastha, S. & Aebersold, R. (2001) 'Optimization of the isotope-coded affinity tag-labeling procedure for quantitative proteome analysis', *Anal Biochem*, vol. 297, no. 1, pp. 25-31.

Sodeik, B. (2000) 'Mechanisms of viral transport in the cytoplasm', *Trends Microbiol*, vol. 8, no. 10, pp. 465-472.

Soete, M., Camus, D. & Dubremetz, J.F. (1994) 'Experimental induction of bradyzoite-specific antigen expression and cyst formation by the RH strain of Toxoplasma gondii in vitro', *Exp Parasitol*, vol. 78, no. 4, pp. 361-370.

Sofroniew, M.V. & Vinters, H.V. (2010) 'Astrocytes: biology and pathology', *Acta Neuropathol*, vol. 119, no. 1, pp. 7-35.

Sorber, K., Dimon, M.T. & DeRisi, J.L. (2011) 'RNA-Seq analysis of splicing in Plasmodium falciparum uncovers new splice junctions, alternative splicing and splicing of antisense transcripts', *Nucleic Acids Res*, vol. 39, no. 9, pp. 3820-3835.

Sotelo, J.R. (1959) 'An electron microscope study on the cytoplasmic and nuclear components of rat primary oocytes', *Z Zellforsch Mikrosk Anat*, vol. 50, pp. 749-765.

Spear, W., Chan, D., Coppens, I., Johnson, R.S., Giaccia, A. & Blader, I.J. (2006) 'The host cell transcription factor hypoxia-inducible factor 1 is required for Toxoplasma gondii growth and survival at physiological oxygen levels', *Cell Microbiol*, vol. 8, no. 2, pp. 339-352.

Speer, C.A. & Dubey, J.P. (1989) 'Ultrastructure of tachyzoites, bradyzoites and tissue cysts of Neospora caninum', *J Protozool*, vol. 36, no. 5, pp. 458-463.

Sprong, H., van der Sluijs, P. & van Meer, G. (2001) 'How proteins move lipids and lipids move proteins', *Nat Rev Mol Cell Biol*, vol. 2, no. 7, pp. 504-513.

Stein, J.V. & Nombela-Arrieta, C. (2005) 'Chemokine control of lymphocyte trafficking: a general overview', *Immunology*, vol. 116, no. 1, pp. 1-12

Stewart, A.D., Logsdon, J.M., Jr. & Kelley, S.E. (2005) 'An empirical study of the evolution of virulence under both horizontal and vertical transmission', *Evolution*, vol. 59, no. 4, pp. 730-739.

Stibbs, H.H. (1985) 'Changes in brain concentrations of catecholamines and indoleamines in Toxoplasma gondii infected mice', *Ann Trop Med Parasitol*, vol. 79, no. 2, pp. 153-157.

Stone, M., Hartmann-Petersen, R., Seeger, M., Bech-Otschir, D., Wallace, M. & Gordon, C. (2004) 'Uch2/Uch37 is the major deubiquitinating enzyme associated with the 26S proteasome in fission yeast', *J Mol Biol*, vol. 344, no. 3, pp. 697-706.

Strack, A., Schluter, D., Asensio, V.C., Campbell, I.L. & Deckert, M. (2002) 'Regulation of the kinetics of intracerebral chemokine gene expression in murine Toxoplasma encephalitis: impact of host genetic factors', *Glia*, vol. 40, no. 3, pp. 372-377.

Sukhumavasi, W., Egan, C.E. & Denkers, E.Y. (2007) 'Mouse neutrophils require JNK2 MAPK for Toxoplasma gondii-induced IL-12p40 and CCL2/MCP-1 release', *J Immunol*, vol. 179, no. 6, pp. 3570-3577.

Sultan, M., Schulz, M.H., Richard, H., Magen, A., Klingenhoff, A., Scherf, M., Seifert, M., Borodina, T., Soldatov, A., Parkhomchuk, D., Schmidt, D., O'Keeffe, S., Haas, S., Vingron, M., Lehrach, H. & Yaspo, M.L. (2008) 'A global view of gene activity and alternative splicing by deep sequencing of the human transcriptome', *Science*, vol. 321, no. 5891, pp. 956-960.

Sutherland, R.J., Whishaw, I.Q. & Kolb, B. (1988) 'Contributions of cingulate cortex to two forms of spatial learning and memory', *J Neurosci*, vol. 8, no. 6, pp. 1863-1872.

Suzuki, Y. & Joh, K. (1994) 'Effect of the strain of Toxoplasma gondii on the development of toxoplasmic encephalitis in mice treated with antibody to interferon-gamma', *Parasitol Res*, vol. 80, no. 2, pp. 125-130.

Suzuki, Y. & Remington, J.S. (1993) 'Toxoplasmic encephalitis in AIDS patients and experimental models for study of the disease and its treatment', *Res Immunol*, vol. 144, no. 1, pp. 66-67.

Suzuki, Y., Orellana, M.A., Schreiber, R.D. & Remington, J.S. (1988) 'Interferon-gamma: the major mediator of resistance against Toxoplasma gondii', *Science*, vol. 240, no. 4851, pp. 516-518.

Swardfager, W., Lanctot, K., Rothenburg, L., Wong, A., Cappell, J. & Herrmann, N. (2010) 'A meta-analysis of cytokines in Alzheimer's disease', *Biol Psychiatry*, vol. 68, no. 10, pp. 930-941.

Tanaka, S., Nishimura, M., Ihara, F., Yamagishi, J., Suzuki, Y. & Nishikawa, Y. (2013) 'Transcriptome analysis of mouse brain infected with Toxoplasma gondii', *Infect Immun*, vol. 81, no. 10, pp. 3609-3619.

Tannu, N.S. & Hemby, S.E. (2006) 'Two-dimensional fluorescence difference gel electrophoresis for comparative proteomics profiling', *Nat Protoc*, vol. 1, no. 4, pp. 1732-1742.

Tarassishin, L., Lim, J., Weatherly, D.B., Angeletti, R.H. & Lee, S.C. (2014) 'Interleukin-1-induced changes in the glioblastoma secretome suggest its role in tumor progression', *J Proteomics*, vol. 99, pp. 152-168.

Tessier-Lavigne, M. & Goodman, C.S. (1996) 'The molecular biology of axon guidance', *Science*, vol. 274, no. 5290, pp. 1123-1133.

Thompson, A., Schafer, J., Kuhn, K., Kienle, S., Schwarz, J., Schmidt, G., Neumann, T., Johnstone, R., Mohammed, A.K. & Hamon, C. (2003) 'Tandem mass tags: a novel quantification strategy for comparative analysis of complex protein mixtures by MS/MS', *Anal Chem*, vol. 75, no. 8, pp. 1895-1904.

Thouvenot, E., Lafon-Cazal, M., Demettre, E., Jouin, P., Bockaert, J. & Marin, P. (2006) 'The proteomic analysis of mouse choroid plexus secretome reveals a high protein secretion capacity of choroidal epithelial cells', *Proteomics*, vol. 6, no. 22, pp. 5941-5952.

Tjalsma, H., Bolhuis, A., Jongbloed, J.D., Bron, S. & van Dijl, J.M. (2000) 'Signal peptide-dependent protein transport in Bacillus subtilis: a genome-based survey of the secretome', *Microbiol Mol Biol Rev*, vol. 64, no. 3, pp. 515-547.

Tobin, C., Pollard, A. & Knoll, L. (2010) 'Toxoplasma gondii cyst wall formation in activated bone marrow-derived macrophages and bradyzoite conditions', *J Vis Exp*, no. 42.

Torrey, E.F. & Yolken, R.H. (2003) 'Toxoplasma gondii and schizophrenia', *Emerg Infect Dis*, vol. 9, no. 11, pp. 1375-1380.

Tranas, J., Heinzen, R.A., Weiss, L.M. & McAllister, M.M. (1999) 'Serological evidence of human infection with the protozoan Neospora caninum', *Clin Diagn Lab Immunol*, vol. 6, no. 5, pp. 765-767.

Trapnell, C., Williams, B.A., Pertea, G., Mortazavi, A., Kwan, G., van Baren, M.J., Salzberg, S.L., Wold, B.J. & Pachter, L. (2010) 'Transcript assembly and quantification by RNA-Seq reveals unannotated transcripts and isoform switching during cell differentiation', Nat Biotechnol, vol. 28, no. 5, pp. 511-515.

Trees, A.J. & Williams, D.J. (2005) 'Endogenous and exogenous transplacental infection in Neospora caninum and Toxoplasma gondii', *Trends Parasitol*, vol. 21, no. 12, pp. 558-561.

Trees, A.J., Davison, H.C., Innes, E.A. & Wastling, J.M. (1999) 'Towards evaluating the economic impact of bovine neosporosis', *Int J Parasitol*, vol. 29, no. 8, pp. 1195-1200.

Tsai, H.H., Frost, E., To, V., Robinson, S., Ffrench-Constant, C., Geertman, R., Ransohoff, R.M. & Miller, R.H. (2002) 'The chemokine receptor CXCR2 controls positioning of oligodendrocyte precursors in developing spinal cord by arresting their migration', *Cell*, vol. 110, no. 3, pp. 373-383.

Turner, G.D., Morrison, H., Jones, M., Davis, T.M., Looareesuwan, S., Buley, I.D., Gatter, K.C., Newbold, C.I., Pukritayakamee, S., Nagachinta, B. & et al. (1994) 'An immunohistochemical study of the pathology of fatal malaria. Evidence for widespread endothelial activation and a potential role for intercellular adhesion molecule-1 in cerebral sequestration', *Am J Pathol*, vol. 145, no. 5, pp. 1057-1069.

Unlu, M., Morgan, M.E. & Minden, J.S. (1997) 'Difference gel electrophoresis: a single gel method for detecting changes in protein extracts', *Electrophoresis*, vol. 18, no. 11, pp. 2071-2077.

Valadi, H., Ekstrom, K., Bossios, A., Sjostrand, M., Lee, J.J. & Lotvall, J.O. (2007) 'Exosome-mediated transfer of mRNAs and microRNAs is a novel mechanism of genetic exchange between cells', *Nat Cell Biol*, vol. 9, no. 6, pp. 654-659.

Van Damme, J., Wuyts, A., Froyen, G., Van Coillie, E., Struyf, S., Billiau, A., Proost, P., Wang, J.M. & Opdenakker, G. (1997) 'Granulocyte chemotactic protein-2 and related CXC chemokines: from gene regulation to receptor usage', *J Leukoc Biol*, vol. 62, no. 5, pp. 563-569.

Van den Bergh, G., Clerens, S., Vandesande, F. & Arckens, L. (2003) 'Reversed-phase high-performance liquid chromatography prefractionation prior to two-dimensional difference gel electrophoresis and mass spectrometry identifies new differentially expressed proteins between striate cortex of kitten and adult cat', *Electrophoresis*, vol. 24, no. 9, pp. 1471-1481.

van der Poll, T., Keogh, C.V., Guirao, X., Buurman, W.A., Kopf, M. & Lowry, S.F. (1997) 'Interleukin-6 gene-deficient mice show impaired defense against pneumococcal pneumonia', *J Infect Dis*, vol. 176, no. 2, pp. 439-444.

Vaz, F.M., Fouchier, S.W., Ofman, R., Sommer, M. & Wanders, R.J. (2000) 'Molecular and biochemical characterization of rat gamma-trimethylaminobutyraldehyde dehydrogenase and evidence for the involvement of human aldehyde dehydrogenase 9 in carnitine biosynthesis', *J Biol Chem*, vol. 275, no. 10, pp. 7390-7394.

Velculescu, V.E., Zhang, L., Vogelstein, B. & Kinzler, K.W. (1995) 'Serial analysis of gene expression', *Science*, vol. 270, no. 5235, pp. 484-487.

Veszelka, S., Pasztoi, M., Farkas, A.E., Krizbai, I., Ngo, T.K., Niwa, M., Abraham, C.S. & Deli, M.A. (2007) 'Pentosan polysulfate protects brain endothelial cells against bacterial lipopolysaccharide-induced damages', *Neurochem Int*, vol. 50, no. 1, pp. 219-228.

Vinters, H.V., Kwok, M.K., Ho, H.W., Anders, K.H., Tomiyasu, U., Wolfson, W.L. & Robert, F. (1989) 'Cytomegalovirus in the nervous system of patients with the acquired immune deficiency syndrome', *Brain*, vol. 112 (Pt 1), pp. 245-268.

Viola, A. & Luster, A.D. (2008) 'Chemokines and their receptors: drug targets in immunity and inflammation', *Annu Rev Pharmacol Toxicol*, vol. 48, pp. 171-197.

Vleminckx, K. & Kemler, R. (1999) 'Cadherins and tissue formation: integrating adhesion and signaling', *Bioessays*, vol. 21, no. 3, pp. 211-220.

Voges, D., Zwickl, P. & Baumeister, W. (1999) 'The 26S proteasome: a molecular machine designed for controlled proteolysis', Annu Rev Biochem, vol. 68, pp. 1015–1068.

Volarevic, S., Stewart, M.J., Ledermann, B., Zilberman, F., Terracciano, L., Montini, E., Grompe, M., Kozma, S.C. & Thomas, G. (2000) 'Proliferation, but not growth, blocked by conditional deletion of 40S ribosomal protein S6', *Science*, vol. 288, no. 5473, pp. 2045-2047.

Vonlaufen, N., Guetg, N., Naguleswaran, A., Muller, N., Bjorkman, C., Schares, G., von Blumroeder, D., Ellis, J. & Hemphill, A. (2004) 'In vitro induction of Neospora caninum bradyzoites in vero cells reveals differential antigen expression, localization, and host-cell recognition of tachyzoites and bradyzoites', *Infect Immun*, vol. 72, no. 1, pp. 576-583.

Vonlaufen, N., Muller, N., Keller, N., Naguleswaran, A., Bohne, W., McAllister, M.M., Bjorkman, C., Muller, E., Caldelari, R. & Hemphill, A. (2002) 'Exogenous nitric oxide triggers Neospora caninum tachyzoite-to-bradyzoite stage conversion in murine epidermal keratinocyte cell cultures', *Int J Parasitol*, vol. 32, no. 10, pp. 1253-1265.

Vyas, A., Kim, S.K., Giacomini, N., Boothroyd, J.C. & Sapolsky, R.M. (2007) 'Behavioral changes induced by Toxoplasma infection of rodents are highly specific to aversion of cat odors', *Proc Natl Acad Sci U S A*, vol. 104, no. 15, pp. 6442-6447.

Walther, T.C. & Mann, M. (2010) 'Mass spectrometry-based proteomics in cell biology', *J Cell Biol*, vol. 190, no. 4, pp. 491-500.

Wang, D.D. & Bordey, A. (2008) 'The astrocyte odyssey', *Prog Neurobiol*, vol. 86, no. 4, pp. 342-367.

Wang, N. & Stamenovic, D. (2002) 'Mechanics of vimentin intermediate filaments', *J. Muscle Res*. Cell. Motil, vol. 23, pp. 535–540.

Wang, W., Nag, S., Zhang, X., Wang, M.H., Wang, H., Zhou, J. & Zhang, R. (2014) 'Ribosomal Proteins and Human Diseases: Pathogenesis, Molecular Mechanisms, and Therapeutic Implications', *Med Res Rev*.

Wang, Z., Gerstein, M. & Snyder, M. (2009) 'RNA-Seq: a revolutionary tool for transcriptomics', *Nat Rev Genet*, vol. 10, no. 1, pp. 57-63.

Wasmuth, J., Daub, J., Peregrin-Alvarez, J.M., Finney, C.A. & Parkinson, J. (2009) 'The origins of apicomplexan sequence innovation', *Genome Res*, vol. 19, no. 7, pp. 1202-1213.

Wastling, J.M., Armstrong, S.D., Krishna, R. & Xia, D. (2012) 'Parasites, proteomes and systems: has Descartes' clock run out of time?', *Parasitology*, vol. 139, no. 9, pp. 1103-1118.

Webster, J.P. (2007) 'The effect of Toxoplasma gondii on animal behavior: playing cat and mouse', *Schizophr Bull*, vol. 33, no. 3, pp. 752-756.

Webster, J.P., Brunton, C.F. & MacDonald, D.W. (1994) 'Effect of Toxoplasma gondii upon neophobic behaviour in wild brown rats, Rattus norvegicus', *Parasitology*, vol. 109 (Pt 1), pp. 37-43.

Webster, J.P., Lamberton, P.H., Donnelly, C.A. & Torrey, E.F. (2006) 'Parasites as causative agents of human affective disorders? The impact of anti-psychotic, mood-stabilizer and anti-parasite medication on Toxoplasma gondii's ability to alter host behaviour', *Proc Biol Sci*, vol. 273, no. 1589, pp. 1023-1030.

Weiss, J.M., Downie, S.A., Lyman, W.D. & Berman, J.W. (1998) 'Astrocyte-derived monocyte-chemoattractant protein-1 directs the transmigration of leukocytes across a model of the human blood-brain barrier', *J Immunol*, vol. 161, no. 12, pp. 6896-6903.

Weiss, L.M., Ma, Y.F., Halonen, S., McAllister, M.M. & Zhang, Y.W. (1999) 'The in vitro development of Neospora caninum bradyzoites', *Int J Parasitol*, vol. 29, no. 10, pp. 1713-1723.

Welzl, H. & Stork, O. (2003) 'Cell adhesion molecules: key players in memory consolidation?', *News Physiol Sci*, vol. 18, pp. 147-150.

Wen, X., Kudo, T., Payne, L., Wang, X., Rodgers, L. & Suzuki, Y. (2010) 'Predominant interferon-gamma-mediated expression of CXCL9, CXCL10, and CCL5 proteins in the brain during chronic infection with Toxoplasma gondii in BALB/c mice resistant to development of toxoplasmic encephalitis', *J Interferon Cytokine Res*, vol. 30, no. 9, pp. 653-660.

Werner, H., Masihi, K.N. & Senk, U. (1981) 'Latent toxoplasma-infection as a possible risk factor for CNS-disorders', *Zentralbl Bakteriol Mikrobiol Hyg A*, vol. 250, no. 3, pp. 368-375.

Westermann, A.J., Gorski, S.A. & Vogel, J. (2012) 'Dual RNA-seq of pathogen and host', *Nat Rev Microbiol*, vol. 10, no. 9, pp. 618-630.

Westermeier, R. & Gorg, A. (2011) 'Two-dimensional electrophoresis in proteomics', *Methods Biochem Anal*, vol. 54, pp. 411-439.

Williams, D.J., Guy, C.S., McGarry, J.W., Guy, F., Tasker, L., Smith, R.F., MacEachern, K., Cripps, P.J., Kelly, D.F. & Trees, A.J. (2000) 'Neospora caninum-associated abortion in cattle: the time of experimentally-induced parasitaemia during gestation determines foetal survival', *Parasitology*, vol. 121 (Pt 4), pp. 347-358.

Williams, D.J., Hartley, C.S., Bjorkman, C. & Trees, A.J. (2009) 'Endogenous and exogenous transplacental transmission of Neospora caninum - how the route of transmission impacts on epidemiology and control of disease', *Parasitology*, pp. 1-6.

Wilson, C.B., Remington, J.S., Stagno, S. & Reynolds, D.W. (1980) 'Development of adverse sequelae in children born with subclinical congenital Toxoplasma infection', *Pediatrics*, vol. 66, no. 5, pp. 767-774.

Wilson, D.N. & Beckmann, R. (2011) 'The ribosomal tunnel as a functional environment for nascent polypeptide folding and translational stalling', Curr Opin Struct Biol, vol. 21, no. 2, pp. 274-282.

Wilson, E.H. & Hunter, C.A. (2004) 'The role of astrocytes in the immunopathogenesis of toxoplasmic encephalitis', *Int J Parasitol*, vol. 34, no. 5, pp. 543-548.

Wolf, M., Delgado, M.B., Jones, S.A., Dewald, B., Clark-Lewis, I. & Baggiolini, M. (1998) 'Granulocyte chemotactic protein 2 acts via both IL-8 receptors, CXCR1 and CXCR2', *Eur J Immunol*, vol. 28, no. 1, pp. 164-170.

Wozniak, M.A., Modzelewska, K., Kwong, L. & Keely, P.J. (2004) 'Focal adhesion regulation of cell behavior', *Biochim Biophys Acta*, vol. 1692, no. 2-3, pp. 103-119.

Wu, C. (1995) 'Heat shock transcription factors: structure and regulation', *Annual review of cell and developmental biology*, vol. 11, pp. 441–469.

Wuyts, A., Proost, P., Lenaerts, J.P., Ben-Baruch, A., Van Damme, J. & Wang, J.M. (1998) 'Differential usage of the CXC chemokine receptors 1 and 2 by interleukin-8, granulocyte chemotactic protein-2 and epithelial-cell-derived neutrophil attractant-78', *Eur J Biochem*, vol. 255, no. 1, pp. 67-73.

Xi, L., Zhu, S.G., Hobbs, D.C. & Kukreja, R.C. (2011) 'Identification of protein targets underlying dietary nitrate-induced protection against doxorubicin cardiotoxicity', *J Cell Mol Med*, vol. 15, no. 11, pp. 2512-2524.

Xia, D., Sanderson, S.J., Jones, A.R., Prieto, J.H., Yates, J.R., Bromley, E., Tomley, F.M., Lal, K., Sinden, R.E., Brunk, B.P., Roos, D.S. & Wastling, J.M. (2008) 'The proteome of Toxoplasma gondii: integration with the genome provides novel insights into gene expression and annotation', *Genome Biol*, vol. 9, no. 7, p. R116.

Yamada, S., Nagai, T., Nakai, T., Ibi, D., Nakajima, A. & Yamada, K. (2014) 'Matrix metalloproteinase-3 is a possible mediator of neurodevelopmental impairment due to polyI:C-induced innate immune activation of astrocytes', *Brain Behav Immun*, vol. 38, pp. 272-282.

Yang, J.W., Suder, P., Silberring, J. & Lubec, G. (2005) 'Proteome analysis of mouse primary astrocytes', *Neurochem Int*, vol. 47, no. 3, pp. 159-172.

Yin, P., Knolhoff, A.M., Rosenberg, H.J., Millet, L.J., Gillette, M.U. & Sweedler, J.V. (2012) 'Peptidomic analyses of mouse astrocytic cell lines and rat primary cultured astrocytes', *J Proteome Res*, vol. 11, no. 8, pp. 3965-3973.

Zhang, H., Li, X.J., Martin, D.B. & Aebersold, R. (2003) 'Identification and quantification of N-linked glycoproteins using hydrazide chemistry, stable isotope labeling and mass spectrometry', *Nat Biotechnol*, vol. 21, no. 6, pp. 660-666.

Zhang, J., Xin, L., Shan, B., Chen, W., Xie, M., Yuen, D., Zhang, W., Zhang, Z., Lajoie, G.A. & Ma, B. (2012) 'PEAKS DB: de novo sequencing assisted database search for sensitive and accurate peptide identification', *Mol Cell Proteomics*, vol. 11, no. 4, p. M111.010587.

Zhang, Y.W., Halonen, S.K., Ma, Y.F., Wittner, M. & Weiss, L.M. (2001) 'Initial characterization of CST1, a Toxoplasma gondii cyst wall glycoprotein', *Infect Immun*, vol. 69, no. 1, pp. 501-507.

Zhou, D.H., Zhao, F.R., Nisbet, A.J., Xu, M.J., Song, H.Q., Lin, R.Q., Huang, S.Y. & Zhu, X.Q. (2014) 'Comparative proteomic analysis of different Toxoplasma gondii genotypes by two-dimensional fluorescence difference gel electrophoresis combined with mass spectrometry', *Electrophoresis*, vol. 35, no. 4, pp. 533-545.

Zhou, G., Li, H., DeCamp, D., Chen, S., Shu, H., Gong, Y., Flaig, M., Gillespie, J.W., Hu, N., Taylor, P.R., Emmert-Buck, M.R., Liotta, L.A., Petricoin, E.F., 3rd & Zhao, Y. (2002) '2D differential in-gel electrophoresis for the identification of esophageal scans cell cancer-specific protein markers', *Mol Cell Proteomics*, vol. 1, no. 2, pp. 117-124.

Zhou, H., Zhao, Q., Das Singla, L., Min, J., He, S., Cong, H., Li, Y. & Su, C. (2013) 'Differential proteomic profiles from distinct Toxoplasma gondii strains revealed by 2D-difference gel electrophoresis', *Exp Parasitol*, vol. 133, no. 4, pp. 376-382.

Zhu, G., Marchewka, M.J. & Keithly, J.S. (2000) 'Cryptosporidium parvum appears to lack a plastid genome', *Microbiology*, vol. 146 (Pt 2), pp. 315-321.

Zhu, S. (2009) 'Psychosis may be associated with toxoplasmosis', *Med Hypotheses*, vol. 73, no. 5, pp. 799-801.

Zhu, W., Smith, J.W. & Huang, C.M. (2010) 'Mass spectrometry-based label-free quantitative proteomics', *J Biomed Biotechnol*, vol. 2010, p. 840518.

Zhu, Y.M., Bagstaff, S.M. & Woll, P.J. (2006) 'Production and upregulation of granulocyte chemotactic protein-2/CXCL6 by IL-1beta and hypoxia in small cell lung cancer', *Br J Cancer*, vol. 94, no. 12, pp. 1936-1941.

Zlokovic, B.V. (2008) 'The blood-brain barrier in health and chronic neurodegenerative disorders', *Neuron*, vol. 57, no. 2, pp. 178-201.

Zlotnik, A. & Yoshie, O. (2000) 'Chemokines: a new classification system and their role in immunity', *Immunity*, vol. 12, no. 2, pp. 121-127.

Zybailov, B., Coleman, M.K., Florens, L. & Washburn, M.P. (2005) 'Correlation of relative abundance ratios derived from peptide ion chromatograms and spectrum counting for quantitative proteomic analysis using stable isotope labeling', *Anal Chem*, vol. 77, no. 19, pp. 6218-6224.

List of Appendices

Appendix I- Differentially expressed host cell proteins identified using 2D-DIGE.

Appendix II- Differentially expressed host cells transcripts during infection (Appendix IIa and IIb on disc).

Appendix III- Host cells proteome proteins identified using label-free proteomics (Appendix IIIa and IIIb on disc).

Appendix IV- Differentially expressed secreted proteins of host cells during infection.

Appendix V- Host cell secreted proteins identified during infection (Appendix Va and Vb on disc)

Appendix I: Differentially expressed proteins of host cells using 2D-DIGE approach (total of 26 proteins)

Table I: Protein spots differentially expressed in 2D-DIGE pick gel, the top five hits (according to the protein score and protein matches) for each pot were selected, The spot number (Spot no), protein hit number (prot hit num), name (Prot name), description (prot desc), score (prot score), match (prot match), t-test and fold change (FC) were identified. Fold changes highlighted in red indicate up-regulated proteins and fold changes highlighted in green indicate down-regulated proteins.

Spot no	Prot hit num	Pro acc	Prot name	Prot desc	Prot score	Prot mass	Prot match	Prot sequence	Prot cover	Prot pi	t-test	FC
2418	1	Q8WZ42	TITIN_HUMAN	Titin	133	3843119	75	61	2.3	6.01	0.045	-4.57
	2	Q12955	ANK3_HUMAN	Ankyrin-3	67	482394	19	16	4.7	6.07		
	3	Q9UPN3	MACF1_HUMAN	Microtubule-actin cross-linking factor 1, isoforms 1/2/3/5	62	623626	17	15	3	5.27		
	4	Q12789	TF3C1_HUMAN	General transcription factor 3C polypeptide 1	56	241062	9	9	4.1	7.01		
	5	Q5VST9	OBSCN_HUMAN	Obscurin	51	879630	10	10	1.6	5.69		
4436	1	P00338	LDHA_HUMAN	L-lactate dehydrogenase A chain	225	37061	6	4	19.8	8.44	0.026	-2.39
	2	P12277	KCRB_HUMAN	Creatine kinase B-type	222	43013	5	4	13.4	5.34		
	3	P06733	ENOA_HUMAN	Alpha-enolase	181	47592	9	6	21.8	7.01		
	4		GSTA1_HUMAN	; TOPep_Count=14	170	25652	25	3	30.6	8.92		
	5	P08670	VIME_HUMAN	Vimentin	165	53787	5	4	9.2	5.05		
2638	1		TRYP_PIG	; TOPep_Count=12	111	25189	24	23	3	7	0.0047	-1.77
	2		K1C10_HUMAN	; TOPep_Count=27	86	59822	2	1	2	5.13		
	3		K2C1_HUMAN	; TOPep_Count=35	72	66129	3	2	3	8.16		
	4	Q969S9	RRF2M_HUMAN	Ribosome-releasing factor 2	58	87512	4	2	1	6.08		

	5	P08670	VIME_HUMAN	Vimentin	43	53787	3	1	3	5.05		
3534	1	P25705	ATPA_HUMAN	ATP synthase subunit alpha, mitochondrial	658	59939	16	15	30.1	9.16	0.036	-1.51
	2	P10809	CH60_HUMAN	60 kDa heat shock protein, mitochondrial	488	61298	20	13	38.7	5.7		
	3	P06733	ENOA_HUMAN	Alpha-enolase	475	47592	16	9	30.8	7.01		
	4	P60709	ACTB_HUMAN	Actin, cytoplasmic 1	462	42163	18	10	39.1	5.29		
	5		K1C10_HUMAN	; TOPep_Count=27	429	59822	11	10	18.5	5.13		
2293	1		K2C1_HUMAN	; TOPep_Count=35	844	66281	22	22	32.1	8.15	0.026	-1.51
	2	Q01995	TAGL_HUMAN	Transgelin	348	22764	14	10	45	8.87		
	3	P37802	TAGL2_HUMAN	Transgelin-2	336	22659	11	9	48.5	8.41		
	4	P48047	ATPO_HUMAN	ATP synthase subunit O, mitochondrial	287	23488	6	6	27.6	9.97		
	5	P40926	MDHM_HUMAN	Malate dehydrogenase, mitochondrial	216	36048	6	6	16.8	8.92		
2125	1	P10809	CH60_HUMAN	60 kDa heat shock protein, mitochondrial	366	61298	13	8	25.8	5.7	0.045	1.53
	2	O43707	ACTN4_HUMAN	Alpha-actinin-4	349	105356	7	6	10.1	5.27		
	3	P12277	KCRB_HUMAN	Creatine kinase B-type	341	43013	5	5	31.2	5.34		
	4	P00338	LDHA_HUMAN	L-lactate dehydrogenase A chain	299	37061	8	5	23.1	8.44		
	5	P60709	ACTB_HUMAN	Actin, cytoplasmic 1	270	42163	9	6	29	5.29		
3070	1	P12277	KCRB_HUMAN	Creatine kinase B-type	319	43013	8	6	31.2	5.34	0.021	2.03
	2	P06733	ENOA_HUMAN	Alpha-enolase	298	47592	13	6	21.8	7.01		
	3	P10809	CH60_HUMAN	60 kDa heat shock protein, mitochondrial	280	61298	9	6	19.5	5.7		
	4	P05023	AT1A1_HUMAN	Sodium/potassium-transporting ATPase subunit alpha-1	254	114246	6	5	6.5	5.33		

	5	O43707	ACTN4_HUMAN	Alpha-actinin-4	254	105356	7	6	10.1	5.27		
2620	1	P05023	AT1A1_HUMAN	Sodium/potassium-transporting ATPase subunit alpha-1	353	114246	6	5	6.5	5.33	0.027	2.54
	2	O43707	ACTN4_HUMAN	Alpha-actinin-4	352	105356	7	6	10.1	5.27		
	3	P10809	CH60_HUMAN	60 kDa heat shock protein, mitochondrial	337	61298	14	9	25.1	5.7		
	4	P60709	ACTB_HUMAN	Actin, cytoplasmic 1	321	42163	32	10	33.5	5.29		
	5	P13929	ENOB_HUMAN	Beta-enolase	289	47410	8	4	16.1	7.59		
2227	1	Q8WZ42	TITIN_HUMAN	Titin	85	3843119	61	48	1.8	6.01	0.013	2.67
	2	Q8WXH0	SYNE2_HUMAN	Nesprin-2	72	801817	18	13	2	5.26		
	3	O94833	BPAEA_HUMAN	Bullous pemphigoid antigen 1, isoforms 6/9/10	71	593763	17	11	2.6	5.49		
	4	A7E2Y1	MYH7B_HUMAN	Myosin-7B	62	222393	8	8	5.3	5.73		
	5	Q9P2D7	DYH1_HUMAN	Dynein heavy chain 1, axonemal	60	497704	9	8	2.8	5.66		
2023	1		TRYP_PIG	; TOPep_Count=12	129	25189	25	4	19	7	0.00063	2.07
	2	P11021	GRP78_HUMAN	78 kDa glucose-regulated protein	90	72513	3	3	6.7	5.06		
	3	P60709	ACTB_HUMAN	Actin, cytoplasmic 1	58	42163	3	3	10.4	5.29		
	4		K2C1_HUMAN	; TOPep_Count=35	43	66129	1	1	3.1	8.16		
	5	Q8TF72	SHRM3_HUMAN	Protein Shroom3	40	218432	1	1	0.5	7.87		
2307	1	P60709	ACTB_HUMAN	Actin, cytoplasmic 1	221	42163	6	4	15.2	5.29	0.028	1.89
	2	Q6UWP8	SBSN_HUMAN	Suprabasin	200	60673	7	4	8.5	6.5		
	3	P00338	LDHA_HUMAN	L-lactate dehydrogenase A chain	162	37061	5	3	14.4	8.44		
	4	P07148	FABPL_HUMAN	Fatty acid-binding protein, liver	141	14367	5	3	44.5	6.6		
	5	P31946	1433B_HUMAN	14-3-3 protein beta/alpha	117	28290	3	2	13	4.76		

2782	1	P08670	VIME_HUMAN	Vimentin	639	53787	16	16	31.3	5.05	0.02	-1.68
	2		K1C10_HUMAN	; TOPep_Count=27	402	59822	11	11	20.2	5.13		
	3		K2C1_HUMAN	; TOPep_Count=35	305	66129	11	11	15.2	8.16		
	4		K22E_HUMAN	; TOPep_Count=41	232	66222	8	8	12.8	8.07		
	5	P67936	TPM4_HUMAN	Tropomyosin alpha-4 chain	230	28730	10	10	28.9	4.67		
4081	1	P08670	VIME_HUMAN	Vimentin	980	53787	29	24	48.4	5.05	0.045	-1.54
	2	Q04695	K1C17_HUMAN	Keratin, type I cytoskeletal 17	478	48472	14	14	29.6	4.97		
	3	Q9P2E9	RRBP1_HUMAN	Ribosome-binding protein 1	478	152891	14	14	10.4	8.69		
	4	Q9BRK5	CAB45_HUMAN	45 kDa calcium-binding protein	357	42006	11	10	28.1	4.76		
	5	P02533	K1C14_HUMAN	Keratin, type I cytoskeletal 14	305	51983	9	9	16.3	5.09		
2023	1	P06733	ENOA_HUMAN	Alpha-enolase	376	47592	14	8	26.2	7.01	0.0002	2.44
	2	P60709	ACTB_HUMAN	Actin, cytoplasmic 1	309	42163	15	9	36.7	5.29		
	3	P10809	CH60_HUMAN	60 kDa heat shock protein, mitochondrial	289	61298	10	6	19.5	5.7		
	4	P09104	ENOG_HUMAN	Gamma-enolase	238	47692	6	4	15.6	4.91		
	5	P12277	KCRB_HUMAN	Creatine kinase B-type	216	43013	7	5	17.8	5.34		
3608	1	P06733	ENOA_HUMAN	Alpha-enolase	489	47592	20	8	28.3	7.01	0.045	-1.54
	2	P10809	CH60_HUMAN	60 kDa heat shock protein, mitochondrial	477	61298	15	10	28.9	5.7		
	3	P60709	ACTB_HUMAN	Actin, cytoplasmic 1	428	42163	24	14	46	5.29		
	4	O43707	ACTN4_HUMAN	Alpha-actinin-4	363	105356	8	6	10.1	5.27		
	5	Q9BQE3	TBA1C_HUMAN	Tubulin alpha-1C chain	334	50659	9	5	21.3	4.96		

3608	1	P25705	ATPA_HUMAN	ATP synthase subunit alpha, mitochondrial	658	59939	16	15	30.1	9.16	0.045	-1.54
	2	P10809	CH60_HUMAN	60 kDa heat shock protein, mitochondrial	488	61298	20	13	38.7	5.7		
	3	P06733	ENOA_HUMAN	Alpha-enolase	475	47592	16	9	30.8	7.01		
	4	P60709	ACTB_HUMAN	Actin, cytoplasmic 1	462	42163	18	10	39.1	5.29		
	5		K1C10_HUMAN	; TOPep_Count=27	429	59822	11	10	18.5	5.13		
1301	1	P60709	ACTB_HUMAN	Actin, cytoplasmic 1	488	42163	25	10	33.5	5.29	0.0085	-1.96
	2	P06733	ENOA_HUMAN	Alpha-enolase	461	47592	14	6	23.4	7.01		
	3	O43707	ACTN4_HUMAN	Alpha-actinin-4	360	105356	7	6	10.1	5.27		
	4	P10809	CH60_HUMAN	60 kDa heat shock protein, mitochondrial	358	61298	13	9	28.2	5.7		
	5	P09104	ENOG_HUMAN	Gamma-enolase	342	47692	8	4	15.6	4.91		
2029	1	P60709	ACTB_HUMAN	Actin, cytoplasmic 1	213	42163	7	5	23.7	5.29	0.015	-2.3
	2	P00338	LDHA_HUMAN	L-lactate dehydrogenase A chain	200	37061	6	4	18.3	8.44		
	3	P06733	ENOA_HUMAN	Alpha-enolase	182	47592	10	6	21.8	7.01		
	4	P12277	KCRB_HUMAN	Creatine kinase B-type	156	43013	6	4	13.4	5.34		
	5	P00558	PGK1_HUMAN	Phosphoglycerate kinase 1	149	45096	5	4	13.6	8.3		
4473	1	P07237	PDIA1_HUMAN	Protein disulfide-isomerase	229	57591	10	8	15.5	4.76	0.019	-2.57
	2		TRYP_PIG	; TOPep_Count=12	113	25189	42	4	19	7		
	3	P43243	MATR3_HUMAN	Matrin-3	41	95189	2	2	2.7	5.87		
	4		ALBU_HUMAN	; TOPep_Count=42	35	71428	1	1	2.8	5.92		
	5		K2C1_HUMAN	; TOPep_Count=35	32	66129	1	1	3.1	8.16		
2069	1	Q8WZ42	TITIN_HUMAN	Titin OS	155	3843119	83	64	2.5	6.01	0.046	-2.46

	2	Q8TF72	SHRM3_HUMAN	Protein Shroom3	85	218125	12	12	7.3	7.75		
	3	Q8NF91	SYNE1_HUMAN	Nesprin-1	83	1017069	21	21	3.3	5.38		
	4	Q09666	AHNK_HUMAN	Neuroblast differentiation-associated protein AHNAK	77	629213	28	22	4.4	5.8		
	5	Q9NU22	MDN1_HUMAN	Midasin	65	638008	16	13	3.7	5.46		
1674	1	P60709	ACTB_HUMAN	Actin, cytoplasmic 1	392	42163	22	10	35.9	5.29	0.028	-1.69
	2	P06733	ENOA_HUMAN	Alpha-enolase	347	47592	14	7	24.8	7.01		
	3	P07148	FABPL_HUMAN	Fatty acid-binding protein, liver	309	14367	14	5	57	6.6		
	4	P10809	CH60_HUMAN	60 kDa heat shock protein, mitochondrial	302	61298	11	7	19.5	5.7		
	5	O43707	ACTN4_HUMAN	Alpha-actinin-4	290	105356	7	6	10.1	5.27		
1379	1	P06733	ENOA_HUMAN	Alpha-enolase	275	47592	12	7	28.7	7.01	0.033	1.71
	2	P10809	CH60_HUMAN	60 kDa heat shock protein, mitochondrial	233	61298	7	5	14.3	5.7		
	3	P60709	ACTB_HUMAN	Actin, cytoplasmic 1	185	42163	11	5	21	5.29		
	4	P00338	LDHA_HUMAN	L-lactate dehydrogenase A chain	180	37061	6	4	19.8	8.44		
	5	P12277	KCRB_HUMAN	Creatine kinase B-type	174	43013	6	4	13.4	5.34		
3070	1	P60709	ACTB_HUMAN	Actin, cytoplasmic 1	284	42163	16	9	5	5.29	0.012	-1.73
	2	P06733	ENOA_HUMAN	Alpha-enolase	263	47592	14	9	4	7.01		
	3	P10809	CH60_HUMAN	60 kDa heat shock protein, mitochondrial	258	61298	10	8	6	5.7		
	4	P00558	PGK1_HUMAN	Phosphoglycerate kinase 1	236	45096	7	5	4	8.3		
	5	P08727	K1C19_HUMAN	Keratin, type I cytoskeletal 19	231	44190	6	5	3	5.04		
2759	1	P06733	ENOA_HUMAN	Alpha-enolase	218	47592	10	6	21.8	7.01	0.028	1.52

	2	P00338	LDHA_HUMAN	L-lactate dehydrogenase A chain	186	37061	5	3	15	8.44		
	3	P10809	CH60_HUMAN	60 kDa heat shock protein, mitochondrial	181	61298	6	5	17.4	5.7		
	4	P60709	ACTB_HUMAN	Actin, cytoplasmic 1	167	42163	8	5	26.1	5.29		
	5		GSTA1_HUMAN	; TOPep_Count=14	163	25652	24	3	30.6	8.92		
4321	1	P06733	ENOA_HUMAN	Alpha-enolase	333	47592	11	6	21.8	7.01	0.023	1.71
	2	P60709	ACTB_HUMAN	Actin, cytoplasmic 1	276	42163	12	8	34.6	5.29		
	3	P12277	KCRB_HUMAN	Creatine kinase B-type	235	43013	7	5	17.8	5.34		
	4	P00338	LDHA_HUMAN	L-lactate dehydrogenase A chain	226	37061	6	4	19.8	8.44		
	5	P00558	PGK1_HUMAN	Phosphoglycerate kinase 1	202	45096	6	4	13.6	8.3		
1833	1	P06733	ENOA_HUMAN	Alpha-enolase	262	47592	12	6	21.8	7.01	0.04	2.87
	2	P60709	ACTB_HUMAN	Actin, cytoplasmic 1	213	42163	9	6	27.7	5.29		
	3	P00338	LDHA_HUMAN	L-lactate dehydrogenase A chain	186	37061	6	4	16.8	8.44		
	4	O43707	ACTN4_HUMAN	Alpha-actinin-4	167	105356	3	3	5.4	5.27		
	5		GSTA1_HUMAN	; TOPep_Count=14	167	25652	26	4	34.2	8.92		

Appendix IV: Statistically significant secreted proteins of human astrocytes during infection with *T. gondii* compared to secreted host cells infected with *N. caninum*.

Table IV: Statistically significant human astrocyte proteins during *T. gondii* infection. Up-regulated secreted proteins are highlighted in red and down-regulated proteins are highlighted in green. Predicted proteins identified as secreted (Pred secr) (SecretomeP, SignalP or SPD) are labelled with 'Yes' and secreted proteins predicted not to be secreted are labelled with 'No'.

Accession no	Protein	Description	Anova (p)	Log2 Cont	Log2 Toxo	Pred secr
P09341	GROA_HUMAN	Growth-regulated alpha protein	0.000108	0	5.257845	Yes
P09238	MMP10_HUMAN	Stromelysin-2	0.000263	0	4.624676	Yes
P05362	ICAM1_HUMAN	Intercellular adhesion molecule 1	0.000103	0	4.19749	YES
P13500	CCL2_HUMAN	C-C motif chemokine 2	4.31E-05	0	3.654107	Yes
P15121	ALDR_HUMAN	Aldose reductase	0.008836	0	3.361175	No
Q08397	LOXL1_HUMAN	Lysyl oxidase homolog 1	0.002837	0	2.726979	Yes
P19320	VCAM1_HUMAN	Vascular cell adhesion protein 1	0.002893	0	2.365301	Yes
P25786	PSA1_HUMAN	Proteasome subunit alpha type-1	0.004337	0	2.211186	No
P06454	PTMA_HUMAN	Prothymosin alpha	0.046505	0	2.013212	No
P05231	IL6_HUMAN	Interleukin-6	0.016789	0	1.999948	Yes
P26022	PTX3_HUMAN	Pentraxin-related protein PTX3	0.001155	0	1.977178	Yes
P31153	METK2_HUMAN	S-adenosylmethionine synthase isoform type-2	0.001737	0	1.915867	Yes
P61163	ACTZ_HUMAN	Alpha-centractin	0.033373	0	1.883014	No
O14818	PSA7_HUMAN	Proteasome subunit alpha type-7	0.048428	0	1.403476	No
P17987	TCPA_HUMAN	T-complex protein 1 subunit alpha	0.017136	0	1.346837	Yes
O43493	TGON2_HUMAN	Trans-Golgi network integral membrane protein 2	0.017583	0	1.307799	No
P59998	ARPC4_HUMAN	Actin-related protein 2/3 complex subunit 4	0.008322	0	1.291607	Yes
P38646	GRP75_HUMAN	Stress-70 protein, mitochondrial OS	0.000697	0	1.260346	No
P28074	PSB5_HUMAN	Proteasome subunit beta type-5	0.001689	0	1.252413	Yes
P50990	TCPQ_HUMAN	T-complex protein 1 subunit theta	0.00156	0	1.236334	No
P21291	CSRP1_HUMAN	Cysteine and glycine-rich protein 1	0.011696	0	1.017476	No
Q14767	LTBP2_HUMAN	Latent-transforming growth factor beta-binding protein 2	0.02889	0	1.017025	Yes
P07900	HS90A_HUMAN	Heat shock protein HSP 90-alpha	0.010883	0	1.008597	No
O15511	ARPC5_HUMAN	Actin-related protein 2/3 complex subunit 5	0.003562	0	0.992675	Yes
Q14974	IMB1_HUMAN	Importin subunit beta-1	0.025356	0	0.988888	Yes

P63313	TYB10_HUMAN	Thymosin beta-10	0.021646	0	0.961515	Yes
P14550	AK1A1_HUMAN	Alcohol dehydrogenase [NADP(+)]	0.002491	0	0.957828	No
P07437	TBB5_HUMAN	Tubulin beta chain	0.009428	0	0.947041	No
O76003	GLRX3_HUMAN	Glutaredoxin-3	0.047604	0	0.936697	Yes
P03956	MMP1_HUMAN	Interstitial collagenase	0.036559	0	0.930272	Yes
P11021	GRP78_HUMAN	78 kDa glucose-regulated protein	0.000481	0	0.927743	Yes
P25788	PSA3_HUMAN	Proteasome subunit alpha type-3	0.008862	0	0.897865	No
P09972	ALDOC_HUMAN	Fructose-bisphosphate aldolase C	0.01806	0	0.88451	No
P14314	GLU2B_HUMAN	Glucosidase 2 subunit beta	0.003944	0	0.866184	Yes
Q01082	SPTB2_HUMAN	Spectrin beta chain, non-erythrocytic 1	0.027778	0	0.861815	No
P30050	RL12_HUMAN	60S ribosomal protein L12	0.005206	0	0.8578	Yes
P30086	PEBP1_HUMAN	Phosphatidylethanolamine-binding protein 1	0.004218	0	0.856006	Yes
P80723	BASP1_HUMAN	Brain acid soluble protein 1	0.043949	0	0.849623	No
P08238	HS90B_HUMAN	Heat shock protein HSP 90-beta	0.01094	0	0.837652	No
P53396	ACLY_HUMAN	ATP-citrate synthase	0.016232	0	0.83065	Yes
P27797	CALR_HUMAN	Calreticulin	0.017732	0	0.823313	No
P49588	SYAC_HUMAN	Alanine--tRNA ligase, cytoplasmic	0.02464	0	0.820437	No
A6NMY6	AXA2L_HUMAN	Putative annexin A2-like protein	0.000404	0	0.801217	Yes
Q16527	CSRP2_HUMAN	Cysteine and glycine-rich protein 2	0.029279	0	0.800834	Yes
P62328	TYB4_HUMAN	Thymosin beta-4	0.011207	0	0.795066	Yes
P23381	SYWC_HUMAN	Tryptophan--tRNA ligase, cytoplasmic	0.010216	0	0.788698	No
P07195	LDHB_HUMAN	L-lactate dehydrogenase B chain	0.004474	0	0.780505	Yes
P02795	MT2_HUMAN	Metallothionein-2	0.003684	0	0.773442	Yes
Q71U36	TBA1A_HUMAN	Tubulin alpha-1A chain	0.01182	0	0.763696	No
P34931	HS71L_HUMAN	Heat shock 70 kDa protein 1-like	0.018605	0	0.757331	No
Q9NQR4	NIT2_HUMAN	Omega-amidase NIT2 OS	0.034322	0	0.744647	Yes
P62805	H4_HUMAN	Histone H4 OS	0.047206	0	0.743187	No
Q14315	FLNC_HUMAN	Filamin-C OS	0.021335	0	0.733525	No
Q15365	PCBP1_HUMAN	Poly(rC)-binding protein 1	0.031335	0	0.730129	Yes
Q9BRA2	TXD17_HUMAN	Thioredoxin domain-containing protein 17	0.000712	0	0.721117	No
P55209	NP1L1_HUMAN	Nucleosome assembly protein 1-like 1	0.029703	0	0.714747	No
P60842	IF4A1_HUMAN	Eukaryotic initiation factor 4A-I	0.013077	0	0.711941	Yes
P02760	AMBP_HUMAN	Protein AMBP	0.030574	0	0.709603	Yes
P04075	ALDOA_HUMAN	Fructose-bisphosphate aldolase A	0.005546	0	0.705727	No
P60983	GMFB_HUMAN	Glia maturation factor beta	0.014842	0	0.677299	Yes
P37837	TALDO_HUMAN	Transaldolase	0.014305	0	0.653274	No

P14625	ENPL_HUMAN	Endoplasmin	0.008421	0	0.648768	No
P14174	MIF_HUMAN	Macrophage migration inhibitory factor	0.001703	0	0.647196	Yes
P18669	PGAM1_HUMAN	Phosphoglycerate mutase 1	0.038812	0	0.636581	No
P54727	RD23B_HUMAN	UV excision repair protein RAD23 homolog B	0.038491	0	0.615021	No
P07355	ANXA2_HUMAN	Annexin A2	0.025654	0	0.612429	Yes
P04004	VTNC_HUMAN	Vitronectin	0.005287	0	0.610916	Yes
P68104	EF1A1_HUMAN	Elongation factor 1-alpha 1	0.022367	0	0.603369	No
P23284	PPIB_HUMAN	Peptidyl-prolyl cis-trans isomerase B	0.011181	0	0.59286	Yes
P09486	SPRC_HUMAN	SPARC	0.029222	0	-0.64863	Yes
P09493	TPM1_HUMAN	Tropomyosin alpha-1 chain	0.004885	0	-0.66525	Yes
O00391	QSOX1_HUMAN	Sulfhydryl oxidase 1	0.016832	0	-0.72541	Yes
P35555	FBN1_HUMAN	Fibrillin-1	0.011265	0	-0.73377	Yes
P18065	IBP2_HUMAN	Insulin-like growth factor-binding protein 2	0.015588	0	-0.75658	Yes
Q92743	HTRA1_HUMAN	Serine protease HTRA1	0.032223	0	-0.85143	Yes
Q96IZ0	PAWR_HUMAN	PRKC apoptosis WT1 regulator protein	0.041202	0	-0.8957	Yes
Q16610	ECM1_HUMAN	Extracellular matrix protein 1	0.038878	0	-0.91286	Yes
P12107	COBA1_HUMAN	Collagen alpha-1(XI) chain	0.049795	0	-0.91288	Yes
P24593	IBP5_HUMAN	Insulin-like growth factor-binding protein 5	0.018139	0	-0.91306	Yes
P63261	ACTG_HUMAN	Actin, cytoplasmic 2	0.033869	0	-0.93031	No
P55285	CADH6_HUMAN	Cadherin-6	0.027749	0	-0.93272	No
P48061	SDF1_HUMAN	Stromal cell-derived factor 1	0.01213	0	-0.93275	Yes
P17936	IBP3_HUMAN	Insulin-like growth factor-binding protein 3	0.008403	0	-0.95564	Yes
P24534	EF1B_HUMAN	Elongation factor 1-beta	0.005794	0	-0.96469	Yes
P61978	HNRPK_HUMAN	Heterogeneous nuclear ribonucleoprotein K	0.010264	0	-0.99162	No
Q9UBP4	DKK3_HUMAN	Dickkopf-related protein 3	0.003557	0	-1.03339	Yes
P27658	CO8A1_HUMAN	Collagen alpha-1(VIII) chain	0.026119	0	-1.036	Yes
P68032	ACTC_HUMAN	Actin, alpha cardiac muscle 1	0.049451	0	-1.07526	No
Q05682	CALD1_HUMAN	Caldesmon	0.008266	0	-1.08126	No
O60565	GREM1_HUMAN	Gremlin-1	0.008403	0	-1.08995	Yes
P08476	INHBA_HUMAN	Inhibin beta A chain	0.041069	0	-1.09314	Yes
P28300	LYOX_HUMAN	Protein-lysine 6-oxidase	0.0088	0	-1.12782	Yes
O95633	FSTL3_HUMAN	Follistatin-related protein 3	0.0369	0	-1.1306	Yes
P02545	LMNA_HUMAN	Prelamin-A/C	0.009051	0	-1.1379	No
P24844	MYL9_HUMAN	Myosin regulatory light polypeptide 9	0.043409	0	-1.14577	Yes
P25940	CO5A3_HUMAN	Collagen alpha-3(V) chain	0.041054	0	-1.20935	Yes
P25398	RS12_HUMAN	40S ribosomal protein S12	0.034829	0	-1.23693	Yes
P16949	STMN1_HUMAN	Stathmin	0.028402	0	-1.27325	Yes
Q9UI42	CBPA4_HUMAN	Carboxypeptidase A4	0.013366	0	-1.37723	Yes
P27816	MAP4_HUMAN	Microtubule-associated protein 4	0.012288	0	-1.37819	No

Q02818	NUCB1_HUMAN	Nucleobindin-1	0.00856	0	-1.51679	No
P41219	PERI_HUMAN	Peripherin	0.001806	0	-1.51762	Yes
Q15056	IF4H_HUMAN	Eukaryotic translation initiation factor 4H	0.001988	0	-1.52172	Yes
O43852	CALU_HUMAN	Calumenin	0.000302	0	-1.65663	Yes
P55058	PLTP_HUMAN	Phospholipid transfer protein	0.002739	0	-1.66905	Yes
Q02952	AKA12_HUMAN	A-kinase anchor protein 12	0.027524	0	-1.7027	No
P38159	RBMX_HUMAN	RNA-binding motif protein, X chromosome	0.002406	0	-1.75489	No
Q13443	ADAM9_HUMAN	Disintegrin and metalloproteinase domain-containing protein 9	0.007574	0	-1.7928	Yes
O14979	HNRDL_HUMAN	Heterogeneous nuclear ribonucleoprotein D-like	0.049791	0	-1.84856	Yes
Q16643	DREB_HUMAN	Drebrin	0.004587	0	-1.89107	No
Q96TA1	NIBL1_HUMAN	Niban-like protein 1	0.033447	0	-1.91785	No
P17661	DESM_HUMAN	Desmin	0.001407	0	-1.95785	Yes
P08670	VIME_HUMAN	Vimentin	3.39E-05	0	-1.95913	Yes
P62857	RS28_HUMAN	40S ribosomal protein S28	6.79E-05	0	-2.1068	Yes
P07602	SAP_HUMAN	Prosaposin	0.005073	0	-2.11668	Yes
O43390	HNRPR_HUMAN	Heterogeneous nuclear ribonucleoprotein R	0.040803	0	-2.36523	No
O43399	TPD54_HUMAN	Tumor protein D54	0.005077	0	-2.38273	Yes
P13497	BMP1_HUMAN	Bone morphogenetic protein 1	0.004657	0	-2.47727	Yes
Q8NC51	PAIRB_HUMAN	Plasminogen activator inhibitor 1 RNA-binding protein	0.000374	0	-2.71477	No
Q68BL8	OLM2B_HUMAN	Olfactomedin-like protein 2B	0.004609	0	-2.71667	No
Q00688	FKBP3_HUMAN	Peptidyl-prolyl cis-trans isomerase FKBP3	0.001	0	-2.77179	Yes
O95084	PRS23_HUMAN	Serine protease 23	0.001414	0	-2.81696	Yes
Q9H4D0	CSTN2_HUMAN	Calsyntenin-2	0.020465	0	-3.01607	No
P62701	RS4X_HUMAN	40S ribosomal protein S4, X isoform	0.013136	0	-3.05041	Yes
Q15233	NONO_HUMAN	Non-POU domain-containing octamer-binding protein	0.018906	0	-3.06885	No
P53999	TCP4_HUMAN	Activated RNA polymerase II transcriptional coactivator p15	0.021747	0	-3.50275	Yes
P35637	FUS_HUMAN	RNA-binding protein FUS	0.034132	0	-3.54684	No
Q6NZI2	PTRF_HUMAN	Polymerase I and transcript release factor	0.00886	0	-3.73683	Yes
P62854	RS26_HUMAN	40S ribosomal protein S26	0.029222	0	-3.84154	No
Q93063	EXT2_HUMAN	Exostosin-2	0.009943	0	-3.85753	Yes
P15502	ELN_HUMAN	Elastin	0.001098	0	-4.2452	Yes
O75787	RENR_HUMAN	Renin receptor	0.001684	0	-4.29192	Yes

Table V: Statistically significant human astrocyte proteins during *N. caninum* infection. Up-regulated secreted proteins are highlighted in red and down-regulated proteins are highlighted in green. Predicted proteins identified as secreted (Pred secr) (SecretomeP, SignalP or SPD) are labelled with 'Yes' and secreted proteins predicted not to be secreted are labelled with 'No'.

Accession no	Protein	Description	Anova (p)	Log2 Cont	Log2 Neo	Pred secr
P19875	CXCL2_HUMAN	C-X-C motif chemokine 2	0.004193	0	5.896856	Yes
P10145	IL8_HUMAN	Interleukin-8	7.23E-05	0	4.932294	Yes
P05231	IL6_HUMAN	Interleukin-6	0.003763	0	4.547647	Yes
Q9Y5K6	CD2AP_HUMAN	CD2-associated protein	0.001248	0	3.855305	No
Q08397	LOXL1_HUMAN	Lysyl oxidase homolog 1	2.02E-05	0	3.327341	Yes
P09341	GROA_HUMAN	Growth-regulated alpha protein	0.048183	0	2.317003	Yes
P13500	CCL2_HUMAN	C-C motif chemokine 2	0.016222	0	2.116471	Yes
Q14767	LTBP2_HUMAN	Latent-transforming growth factor beta-binding protein 2	8.47E-05	0	1.999367	Yes
P30048	PRDX3_HUMAN	Thioredoxin-dependent peroxide reductase, mitochondrial	0.005613	0	1.987092	Yes
P68431	H31_HUMAN	Histone H3.1	0.011383	0	1.344802	Yes
P05556	ITB1_HUMAN	Integrin beta-1	0.013207	0	1.343346	No
Q14624	ITIH4_HUMAN	Inter-alpha-trypsin inhibitor heavy chain H4	0.006484	0	1.317681	Yes
P04114	APOB_HUMAN	Apolipoprotein B-100	0.00136	0	1.298246	Yes
P48307	TFPI2_HUMAN	Tissue factor pathway inhibitor 2	0.000265	0	1.270384	Yes
O95373	IPO7_HUMAN	Importin-7	0.014602	0	1.260445	Yes
P04278	SHBG_HUMAN	Sex hormone-binding globulin	0.002403	0	1.190953	Yes
P08697	A2AP_HUMAN	Alpha-2-antiplasmin	0.004238	0	1.189347	Yes
P00734	THRB_HUMAN	Prothrombin	0.015799	0	1.147557	Yes
P02774	VTDB_HUMAN	Vitamin D-binding protein	0.013655	0	1.124911	Yes
P09871	C1S_HUMAN	Complement C1s subcomponent	0.001142	0	1.12364	Yes
P13611	CSPG2_HUMAN	Versican core protein	0.005848	0	1.119053	Yes
P01042	KNG1_HUMAN	Kininogen-1	0.022292	0	1.109376	Yes
P05155	IC1_HUMAN	Plasma protease C1 inhibitor	0.002318	0	1.078543	Yes
P62888	RL30_HUMAN	60S ribosomal protein L30	0.007565	0	1.054243	No
O95445	APOM_HUMAN	Apolipoprotein M	0.005913	0	1.027931	Yes
P02765	FETUA_HUMAN	Alpha-2-HS-glycoprotein	0.003949	0	0.964087	Yes
P60033	CD81_HUMAN	CD81 antigen	0.019602	0	0.963493	No
P05156	CFAI_HUMAN	Complement factor I	0.041823	0	0.95824	Yes
P43652	AFAM_HUMAN	Afamin	0.021232	0	0.88913	Yes
P07355	ANXA2_HUMAN	Annexin A2	0.045594	0	0.884813	Yes
Q9UBQ6	EXTL2_HUMAN	Exostosin-like 2	0.043217	0	0.876997	Yes
P01024	CO3_HUMAN	Complement C3	0.01306	0	0.851629	Yes

P02787	TRFE_HUMAN	Serotransferrin	0.003646	0	0.849204	Yes
P02753	RET4_HUMAN	Retinol-binding protein 4	0.027072	0	0.841751	Yes
P07942	LAMB1_HUMAN	Laminin subunit beta-1	0.019793	0	0.813016	Yes
P04217	A1BG_HUMAN	Alpha-1B-glycoprotein	0.044014	0	0.809553	Yes
Q2TAA2	IAH1_HUMAN	Isoamyl acetate-hydrolyzing esterase 1 homolog	0.033829	0	0.79734	No
P02788	TRFL_HUMAN	Lactotransferrin	0.004901	0	0.7829	Yes
P01008	ANT3_HUMAN	Antithrombin-III	0.009356	0	0.767951	Yes
Q06033	ITIH3_HUMAN	Inter-alpha-trypsin inhibitor heavy chain H3	0.016263	0	0.758894	Yes
O14773	TPP1_HUMAN	Tripeptidyl-peptidase 1	0.009003	0	0.751712	Yes
Q96RW7	HMCN1_HUMAN	Hemicentin-1	0.015014	0	0.735199	Yes
Q9UJ70	NAGK_HUMAN	N-acetyl-D-glucosamine kinase	0.020945	0	0.728763	Yes
P07602	SAP_HUMAN	Prosaposin	0.041079	0	0.722354	Yes
P05543	THBG_HUMAN	Thyroxine-binding globulin	0.034971	0	0.692797	Yes
O75095	MEGF6_HUMAN	Multiple epidermal growth factor-like domains protein 6	0.006864	0	0.625488	No
P02790	HEMO_HUMAN	Hemopexin	0.041066	0	0.607574	Yes
O76061	STC2_HUMAN	Stanniocalcin-2	0.044448	0	0.60245	Yes
P69905	HBA_HUMAN	Hemoglobin subunit alpha	0.004738	0	0.585297	No
Q01955	CO4A3_HUMAN	Collagen alpha-3(IV) chain	0.02057	0	-0.59476	No
Q16658	FSCN1_HUMAN	Fascin	0.014835	0	-0.60687	No
Q93063	EXT2_HUMAN	Exostosin-2	0.009555	0	-0.60711	Yes
O15131	IMA6_HUMAN	Importin subunit alpha-6	0.045424	0	-0.63944	No
P52565	GDIR1_HUMAN	Rho GDP-dissociation inhibitor 1	0.001439	0	-0.65415	No
P21399	ACOC_HUMAN	Cytoplasmic aconitate hydratase	0.0083	0	-0.66004	No
Q9Y4L1	HYOU1_HUMAN	Hypoxia up-regulated protein 1	0.042532	0	-0.67882	No
Q9Y3B8	ORN_HUMAN	Oligoribonuclease, mitochondrial	0.032857	0	-0.6852	Yes
P21333	FLNA_HUMAN	Filamin-A	0.036551	0	-0.70203	No
Q9Y696	CLIC4_HUMAN	Chloride intracellular channel protein 4	0.039115	0	-0.70242	Yes
Q13643	FHL3_HUMAN	Four and a half LIM domains protein 3	0.030363	0	-0.71357	Yes
Q15366	PCBP2_HUMAN	Poly(rC)-binding protein 2	0.041669	0	-0.73183	Yes
P29692	EF1D_HUMAN	Elongation factor 1-delta	0.037069	0	-0.74074	Yes
Crap_sp	IGF2_HUMAN	; TOPep_Count	0.015622	0	-0.74341	No
Q00610	CLH1_HUMAN	Clathrin heavy chain 1	0.044838	0	-0.74668	No
P26038	MOES_HUMAN	Moesin	0.036645	0	-0.74743	No
P61081	UBC12_HUMAN	NEDD8-conjugating enzyme Ubc12	0.039068	0	-0.75347	Yes
P34931	HS71L_HUMAN	Heat shock 70 kDa protein 1-like	0.031944	0	-0.75646	No
P68104	EF1A1_HUMAN	Elongation factor 1-alpha 1	0.03463	0	-0.76633	No
Q15185	TEBP_HUMAN	Prostaglandin E synthase 3	0.034712	0	-0.7838	Yes
P07814	SYEP_HUMAN	Bifunctional glutamate/proline--tRNA ligase	0.010643	0	-0.79573	No
Q92598	HS105_HUMAN	Heat shock protein 105 kDa	0.016439	0	-0.79828	No
Q99436	PSB7_HUMAN	Proteasome subunit beta type-7	0.007606	0	-0.80392	No

Q9H4M9	EHD1_HUMAN	EH domain-containing protein 1	0.042251	0	-0.80582	No
Q15393	SF3B3_HUMAN	Splicing factor 3B subunit 3	0.032923	0	-0.80858	Yes
P37108	SRP14_HUMAN	Signal recognition particle 14 kDa protein	0.018586	0	-0.81516	No
P11940	PABP1_HUMAN	Polyadenylate-binding protein 1	0.029906	0	-0.82132	No
P62244	RS15A_HUMAN	40S ribosomal protein S15a	0.00922	0	-0.82468	Yes
Q9BR76	COR1B_HUMAN	Coronin-1B	0.049361	0	-0.82815	No
P54652	HSP72_HUMAN	Heat shock-related 70 kDa protein 2	0.013418	0	-0.84171	No
Q15435	PP1R7_HUMAN	Protein phosphatase 1 regulatory subunit 7	0.003406	0	-0.8575	Yes
Q86V81	THOC4_HUMAN	THO complex subunit 4	0.016018	0	-0.8585	No
Q14103	HNRPD_HUMAN	Heterogeneous nuclear ribonucleoprotein D0	0.008204	0	-0.8608	No
P05198	IF2A_HUMAN	Eukaryotic translation initiation factor 2 subunit 1	0.01074	0	-0.87124	No
P14735	IDE_HUMAN	Insulin-degrading enzyme	0.049522	0	-0.87584	No
P28300	LYOX_HUMAN	Protein-lysine 6-oxidase	0.042412	0	-0.87822	Yes
Q9BXS5	AP1M1_HUMAN	AP-1 complex subunit mu-1	0.035891	0	-0.88176	Yes
Q9Y5S9	RBM8A_HUMAN	RNA-binding protein 8A	0.033068	0	-0.8931	No
P62633	CNBP_HUMAN	Cellular nucleic acid-binding protein	0.021278	0	-0.89334	Yes
Q15262	PTPRK_HUMAN	Receptor-type tyrosine-protein phosphatase kappa	0.041837	0	-0.89497	No
P54577	SYYC_HUMAN	Tyrosine--tRNA ligase, cytoplasmic	0.00479	0	-0.89745	No
P35579	MYH9_HUMAN	Myosin-9	0.033139	0	-0.8984	No
P11142	HSP7C_HUMAN	Heat shock cognate 71 kDa protein	0.032782	0	-0.92003	No
P14618	KPYM_HUMAN	Pyruvate kinase PKM	0.027482	0	-0.9419	No
P10124	SRGN_HUMAN	Serglycin	0.036848	0	-0.95154	Yes
P63241	IF5A1_HUMAN	Eukaryotic translation initiation factor 5A-1	0.018876	0	-0.95814	No
P60709	ACTB_HUMAN	Actin, cytoplasmic 1	0.015704	0	-0.96231	No
Q14847	LASP1_HUMAN	LIM and SH3 domain protein 1	0.003552	0	-0.96854	Yes
P30740	ILEU_HUMAN	Leukocyte elastase inhibitor	0.045763	0	-0.97168	Yes
Q15637	SF01_HUMAN	Splicing factor 1	0.008246	0	-0.9757	No
Q13200	PSMD2_HUMAN	26S proteasome non-ATPase regulatory subunit 2	0.025768	0	-0.98281	Yes
P00568	KAD1_HUMAN	Adenylate kinase isoenzyme 1	0.039498	0	-0.99018	Yes
P54920	SNAA_HUMAN	Alpha-soluble NSF attachment protein	0.031812	0	-0.99161	Yes
Q13283	G3BP1_HUMAN	Ras GTPase-activating protein-binding protein 1	0.003941	0	-0.99459	No
P09651	ROA1_HUMAN	Heterogeneous nuclear ribonucleoprotein A1	0.020638	0	-0.99541	No
Q96AE4	FUBP1_HUMAN	Far upstream element-binding protein 1	0.00298	0	-1.00105	No
P08133	ANXA6_HUMAN	Annexin A6	0.047675	0	-1.02685	No
Q14194	DPYL1_HUMAN	Dihydropyrimidinase-related protein 1	0.015702	0	-1.03726	No

P67936	TPM4_HUMAN	Tropomyosin alpha-4 chain	0.0373	0	-1.03846	No
P41271	NBL1_HUMAN	Neuroblastoma suppressor of tumorigenicity 1	0.001165	0	-1.03862	Yes
Q14240	IF4A2_HUMAN	Eukaryotic initiation factor 4A-II	0.039348	0	-1.04089	No
O94979	SC31A_HUMAN	Protein transport protein Sec31A	0.025219	0	-1.04899	No
P10909	CLUS_HUMAN	Clusterin	0.004155	0	-1.0523	Yes
P49773	HINT1_HUMAN	Histidine triad nucleotide-binding protein 1	0.015388	0	-1.05364	Yes
P38919	IF4A3_HUMAN	Eukaryotic initiation factor 4A-III	0.015378	0	-1.05515	Yes
P62258	1433E_HUMAN	14-3-3 protein epsilon	0.002343	0	-1.06284	No
Q13813	SPTN1_HUMAN	Spectrin alpha chain, non-erythrocytic 1	0.036168	0	-1.06936	No
P46940	IQGA1_HUMAN	Ras GTPase-activating-like protein IQGAP1	0.041896	0	-1.0743	No
Q9UHD8	SEPT9_HUMAN	Septin-9	0.014838	0	-1.08365	Yes
P24666	PPAC_HUMAN	Low molecular weight phosphotyrosine protein phosphatase	0.021208	0	-1.08722	Yes
Q16401	PSMD5_HUMAN	26S proteasome non-ATPase regulatory subunit 5	0.0138	0	-1.12616	Yes
O60701	UGDH_HUMAN	UDP-glucose 6-dehydrogenase	0.003653	0	-1.13156	No
O60506	HNRPQ_HUMAN	Heterogeneous nuclear ribonucleoprotein Q	0.02246	0	-1.1368	No
P23381	SYWC_HUMAN	Tryptophan--tRNA ligase, cytoplasmic	0.046107	0	-1.15377	No
Q9UJU6	DBNL_HUMAN	Drebrin-like protein	0.000765	0	-1.16386	Yes
P24844	MYL9_HUMAN	Myosin regulatory light polypeptide 9	0.000598	0	-1.16553	Yes
P63313	TYB10_HUMAN	Thymosin beta-10	0.020687	0	-1.16915	Yes
P42167	LAP2B_HUMAN	Lamina-associated polypeptide 2, isoforms beta/gamma	0.006612	0	-1.17114	Yes
Q92945	FUBP2_HUMAN	Far upstream element-binding protein 2	0.02796	0	-1.17772	No
P62906	RL10A_HUMAN	60S ribosomal protein L10a	0.001456	0	-1.18222	Yes
P35052	GPC1_HUMAN	Glypican-1	0.024022	0	-1.18866	No
P33176	KINH_HUMAN	Kinesin-1 heavy chain	0.023291	0	-1.19117	No
P16989	YBOX3_HUMAN	Y-box-binding protein 3	0.022127	0	-1.19516	Yes
P08107	HSP71_HUMAN	Heat shock 70 kDa protein 1A/1B	0.004045	0	-1.20094	No
P45974	UBP5_HUMAN	Ubiquitin carboxyl-terminal hydrolase 5	0.04381	0	-1.20349	No
P54727	RD23B_HUMAN	UV excision repair protein RAD23 homolog B	0.010912	0	-1.20387	No
Q8WX93	PALLD_HUMAN	Palladin	0.03477	0	-1.21397	No
O75326	SEM7A_HUMAN	Semaphorin-7A	0.021852	0	-1.21938	No
P46782	RS5_HUMAN	40S ribosomal protein S5	0.016778	0	-1.25287	Yes
P55285	CADH6_HUMAN	Cadherin-6	0.023758	0	-1.25478	No
P23396	RS3_HUMAN	40S ribosomal protein S3	0.013884	0	-1.25842	No
P22626	ROA2_HUMAN	Heterogeneous nuclear ribonucleoproteins A2/B1	0.015464	0	-1.25845	No

Q00688	FKBP3_HUMAN	Peptidyl-prolyl cis-trans isomerase FKBP3	0.004527	0	-1.30994	Yes
O76003	GLRX3_HUMAN	Glutaredoxin-3	0.045414	0	-1.34226	Yes
Q13509	TBB3_HUMAN	Tubulin beta-3 chain	0.009444	0	-1.35281	No
P10155	RO60_HUMAN	60 kDa SS-A/Ro ribonucleoprotein	0.008415	0	-1.3574	No
O43294	TGFI1_HUMAN	Transforming growth factor beta-1-induced transcript 1 protein	0.044062	0	-1.36843	Yes
O95881	TXD12_HUMAN	Thioredoxin domain-containing protein 12	0.041023	0	-1.38816	Yes
Q9NP97	DLRB1_HUMAN	Dynein light chain roadblock-type 1	0.018618	0	-1.38957	Yes
Q9BZZ5	API5_HUMAN	Apoptosis inhibitor 5	0.008709	0	-1.39758	No
O95965	ITGBL_HUMAN	Integrin beta-like protein 1	8.34E-05	0	-1.39909	No
O00231	PSD11_HUMAN	26S proteasome non-ATPase regulatory subunit 11	0.000507	0	-1.42558	No
P27348	1433T_HUMAN	14-3-3 protein theta	0.006331	0	-1.44988	No
Q15019	SEPT2_HUMAN	Septin-2	0.025432	0	-1.45669	No
P62306	RUXF_HUMAN	Small nuclear ribonucleoprotein F	0.028542	0	-1.47478	No
P05783	K1C18_HUMAN	Keratin, type I cytoskeletal 18	0.021737	0	-1.50003	Yes
O43852	CALU_HUMAN	Calumenin	0.034527	0	-1.52271	Yes
Q02952	AKA12_HUMAN	A-kinase anchor protein 12	0.042422	0	-1.52444	No
P62269	RS18_HUMAN	40S ribosomal protein S18	0.0027	0	-1.54025	No
P62318	SMD3_HUMAN	Small nuclear ribonucleoprotein Sm D3	0.008013	0	-1.54544	Yes
P41219	PERI_HUMAN	Peripherin	0.009195	0	-1.55543	Yes
P62736	ACTA_HUMAN	Actin, aortic smooth muscle	0.000454	0	-1.56497	Yes
P30044	PRDX5_HUMAN	Peroxiredoxin-5, mitochondrial	0.021234	0	-1.57146	Yes
P31939	PUR9_HUMAN	Bifunctional purine biosynthesis protein PURH	0.044877	0	-1.57366	No
P08865	RSSA_HUMAN	40S ribosomal protein SA	0.024006	0	-1.57425	Yes
P49591	SYSC_HUMAN	Serine--tRNA ligase, cytoplasmic	0.018958	0	-1.57632	No
P49588	SYAC_HUMAN	Alanine--tRNA ligase, cytoplasmic	0.02883	0	-1.58136	No
P51911	CNN1_HUMAN	Calponin-1	0.00661	0	-1.59187	No
Q9BUD6	SPON2_HUMAN	Spondin-2	0.000497	0	-1.59547	Yes
Q99729	ROAA_HUMAN	Heterogeneous nuclear ribonucleoprotein A/B	0.031058	0	-1.59563	No
Q15459	SF3A1_HUMAN	Splicing factor 3A subunit 1	0.042717	0	-1.60287	No
O00571	DDX3X_HUMAN	ATP-dependent RNA helicase DDX3X	0.007926	0	-1.6109	No
P13798	ACPH_HUMAN	Acylamino-acid-releasing enzyme	0.03596	0	-1.61794	Yes
P15502	ELN_HUMAN	Elastin	0.004973	0	-1.62306	Yes
O00151	PDLI1_HUMAN	PDZ and LIM domain protein 1	0.00981	0	-1.62617	No
P61978	HNRPK_HUMAN	Heterogeneous nuclear ribonucleoprotein K	0.005452	0	-1.62981	No
Q9Y3F4	STRAP_HUMAN	Serine-threonine kinase receptor-associated protein	0.010655	0	-1.63505	No

Q13561	DCTN2_HUMAN	Dynactin subunit 2	0.00216	0	-1.63838	No
P62314	SMD1_HUMAN	Small nuclear ribonucleoprotein Sm D1	0.001305	0	-1.67436	No
P05455	LA_HUMAN	Lupus La protein	0.002483	0	-1.67533	No
P62277	RS13_HUMAN	40S ribosomal protein S13	0.007612	0	-1.70047	Yes
P68371	TBB4B_HUMAN	Tubulin beta-4B chain	0.010022	0	-1.71608	No
Q93052	LPP_HUMAN	Lipoma-preferred partner	0.001422	0	-1.73791	Yes
P27816	MAP4_HUMAN	Microtubule-associated protein 4	0.001732	0	-1.77733	No
P07951	TPM2_HUMAN	Tropomyosin beta chain	0.003692	0	-1.78386	No
Q04760	LGUL_HUMAN	Lactoylglutathione lyase	0.026019	0	-1.78637	No
P17661	DESM_HUMAN	Desmin	0.001798	0	-1.822	Yes
P84103	SRSF3_HUMAN	Serine/arginine-rich splicing factor 3	0.00309	0	-1.82652	No
Q08211	DHX9_HUMAN	ATP-dependent RNA helicase A	0.010212	0	-1.8393	No
P62081	RS7_HUMAN	40S ribosomal protein S7	0.038395	0	-1.84632	Yes
Q04917	1433F_HUMAN	14-3-3 protein eta	0.000823	0	-1.84766	No
Q01813	K6PP_HUMAN	6-phosphofructokinase type C	0.015171	0	-1.84783	Yes
P36578	RL4_HUMAN	60S ribosomal protein L4	0.007506	0	-1.85836	Yes
O14979	HNRDL_HUMAN	Heterogeneous nuclear ribonucleoprotein D-like	0.005679	0	-1.86971	Yes
P62249	RS16_HUMAN	40S ribosomal protein S16	0.004815	0	-1.87635	Yes
P04632	CPNS1_HUMAN	Calpain small subunit 1	0.017777	0	-1.87763	Yes
P63104	1433Z_HUMAN	14-3-3 protein zeta/delta	0.013334	0	-1.88233	No
P13497	BMP1_HUMAN	Bone morphogenetic protein 1	0.013535	0	-1.90514	Yes
P47897	SYQ_HUMAN	Glutamine--tRNA ligase	0.036949	0	-1.91789	No
Q92499	DDX1_HUMAN	ATP-dependent RNA helicase DDX1	0.010153	0	-1.93879	No
P19623	SPEE_HUMAN	Spermidine synthase	0.007623	0	-1.94363	Yes
Q15056	IF4H_HUMAN	Eukaryotic translation initiation factor 4H	0.001071	0	-1.94396	Yes
Q05682	CALD1_HUMAN	Caldesmon	7.27E-05	0	-1.94973	No
Q8NC51	PAIRB_HUMAN	Plasminogen activator inhibitor 1 RNA-binding protein	0.000227	0	-1.95547	No
P15880	RS2_HUMAN	40S ribosomal protein S2	0.004499	0	-1.95736	Yes
O75718	CRTAP_HUMAN	Cartilage-associated protein	0.00256	0	-1.9648	Yes
P62913	RL11_HUMAN	60S ribosomal protein L11	0.018074	0	-1.9698	No
Q07960	RHG01_HUMAN	Rho GTPase-activating protein 1	0.025769	0	-1.97224	No
P42766	RL35_HUMAN	60S ribosomal protein L35	0.006697	0	-1.98016	Yes
Q15121	PEA15_HUMAN	Astrocytic phosphoprotein PEA-15	0.002919	0	-2.04093	Yes
Q07020	RL18_HUMAN	60S ribosomal protein L18	0.033874	0	-2.05112	No
Q9C005	DPY30_HUMAN	Protein dpy-30 homolog	0.011988	0	-2.06845	Yes
P63261	ACTG_HUMAN	Actin, cytoplasmic 2	0.015889	0	-2.10928	Yes
P62266	RS23_HUMAN	40S ribosomal protein S23	0.019676	0	-2.12442	No
P04792	HSPB1_HUMAN	Heat shock protein beta-1	0.004511	0	-2.13719	Yes
P09493	TPM1_HUMAN	Tropomyosin alpha-1 chain	0.001922	0	-2.28312	Yes
Q6NZI2	PTRF_HUMAN	Polymerase I and transcript	0.002841	0	-2.28601	Yes

		release factor				
P26373	RL13_HUMAN	60S ribosomal protein L13	0.005806	0	-2.30247	No
P39019	RS19_HUMAN	40S ribosomal protein S19	0.004364	0	-2.3049	Yes
O60869	EDF1_HUMAN	Endothelial differentiation-related factor 1	0.023983	0	-2.32426	Yes
Q8IZ52	CHSS2_HUMAN	Chondroitin sulfate synthase 2	0.004349	0	-2.32674	Yes
P24534	EF1B_HUMAN	Elongation factor 1-beta	0.003253	0	-2.3382	Yes
P62899	RL31_HUMAN	60S ribosomal protein L31	0.015291	0	-2.37841	No
P13521	SCG2_HUMAN	Secretogranin-2	0.020326	0	-2.38983	Yes
P09496	CLCA_HUMAN	Clathrin light chain A	0.007042	0	-2.40165	Yes
Q15942	ZYX_HUMAN	Zyxin	0.000604	0	-2.41406	Yes
P08670	VIME_HUMAN	Vimentin	0.00306	0	-2.42918	Yes
P46776	RL27A_HUMAN	60S ribosomal protein L27a	0.008284	0	-2.47581	Yes
Q15233	NONO_HUMAN	Non-POU domain-containing octamer-binding protein	0.003396	0	-2.54724	No
Q15102	PA1B3_HUMAN	Platelet-activating factor acetylhydrolase IB subunit gamma	0.03026	0	-2.54927	No
P63220	RS21_HUMAN	40S ribosomal protein S21	0.003423	0	-2.64639	Yes
Q02878	RL6_HUMAN	60S ribosomal protein L6	0.002151	0	-2.65525	No
P18124	RL7_HUMAN	60S ribosomal protein L7	0.004936	0	-2.73801	No
O14737	PDCD5_HUMAN	Programmed cell death protein 5	0.008235	0	-2.83988	Yes
P06703	S10A6_HUMAN	Protein S100-A6	0.032342	0	-2.85647	Yes
P83731	RL24_HUMAN	60S ribosomal protein L24	0.000666	0	-2.97196	Yes
O95084	PRS23_HUMAN	Serine protease 23	0.00026	0	-3.02317	Yes
P61313	RL15_HUMAN	60S ribosomal protein L15	0.021332	0	-3.09594	No
Q09666	AHNK_HUMAN	Neuroblast differentiation-associated protein AHNAK	0.00081	0	-3.15672	No
P98179	RBM3_HUMAN	Putative RNA-binding protein 3	0.004183	0	-3.17134	Yes
P16949	STMN1_HUMAN	Stathmin	0.000838	0	-3.27402	Yes
P50281	MMP14_HUMAN	Matrix metalloproteinase-14	0.003786	0	-3.60015	No
P08621	RU17_HUMAN	U1 small nuclear ribonucleoprotein 70 kDa	0.000379	0	-3.67991	No
P51991	ROA3_HUMAN	Heterogeneous nuclear ribonucleoprotein A3	0.000101	0	-3.68613	No
Q96L21	RL10L_HUMAN	60S ribosomal protein L10-like	0.001621	0	-3.76404	Yes
P40429	RL13A_HUMAN	60S ribosomal protein L13a	0.016176	0	-3.83481	Yes
O75787	RENR_HUMAN	Renin receptor	0.015457	0	-3.8551	Yes
P62241	RS8_HUMAN	40S ribosomal protein S8	0.011054	0	-3.8942	No
P82979	SARNP_HUMAN	SAP domain-containing ribonucleoprotein	0.000827	0	-4.25378	No
Q13443	ADAM9_HUMAN	Disintegrin and metalloproteinase domain-containing protein 9	0.001098	0	-5.16985	Yes
O95450	ATS2_HUMAN	A disintegrin and metalloproteinase with thrombospondin motifs 2	0.001968	0	-5.24947	Yes